VOLUME 28 (1961) No. 1

NUCLEAR PHYSICS

JOURNAL DEVOTED TO THE EXPERIMENTAL AND THEORETICAL STUDY OF THE FUNDAMENTAL CONSTITUENTS OF MATTER AND THEIR INTERACTIONS

EDITOR: L. ROSENFELD · COPENHAGEN

L. A. KÖNIG, J. H. E. MATTAUCH and A. H. WAPSTRA, Adjustment of relative nuclidic masses (II) $70 < A < 200$ 1

A. H. WAPSTRA, Adjustment of relative nuclidic masses (III) $A \geqq 200$ . . . 29

D. R. BÈS and Z. SZYMAŃSKI, The ground-state equilibrium deformation in rare-earth nuclei 42

ZDZISŁAW SZYMAŃSKI, Equilibrium deformations of nuclei in the transuranic region 63

W. KRÓLIKOWSKI, On single-strange mesons 81

SAMI CUPERMAN, Search for pseudoscalar interaction in $\frac{1}{2}+ \rightarrow \frac{1}{2}-$ β-decay transitions. (I) Measurement of the longitudinal polarization of the β^--particles emitted in the transition $_{81}Tl^{207} \rightarrow _{82}Pb^{207}$ 84

F. C. BARKER, Positive parity states of Be^9 and C^{13} 96

BIBHUTI BHUSAN DEO, Electromagnetic interactions of charged pions 122

BIBHUTI BHUSAN DEO, On masses and mass-shifts of elementary particles . . 135

O. HANSEN, Energy levels in the stable isotopes of titanium 140

H. G. DEVARE, On the decay of I^{133} 148

YUKIO TOMOZAWA, Higher resonances in pion-nucleon reactions and the isobar model 160

J. BURDE and M. RAKAVY, Determination of the lifetime of the 283 keV excited level of Dy^{160} 172

November 1961

NORTH-HOLLAND PUBLISHING COMPANY-AMSTERDAM

EDITORIAL BOARD

AUSTRALIA & NEW ZEALAND:	H. Messel (Sydney), M. L. Oliphant (Canberra)
AUSTRIA:	B. Karlik (Vienna), H. Thirring (Vienna)
BELGIUM:	M. de Hemptinne (Louvain), J. Verhaeghe (Ghent)
CANADA:	G. Volkoff (Vancouver)
DENMARK:	C. Møller (Copenhagen), S. Rozental (Copenhagen), G. E. Brown (Copenhagen)
FINLAND:	L. Simons (Helsinki)
FRANCE:	A. Berthelot (Saclay), S. Gorodetzky (Strasbourg)
GERMANY (DEM. REP.):	G. Hertz (Leipzig)
GERMANY (FED. REP.):	W. Gentner (Freiburg i. B.), J. H. D. Jensen (Heidelberg)
GREAT BRITAIN:	W. E. Burcham (Birmingham), R. J. Blin-Stoyle (Brighton)
HUNGARY:	L. Janossy (Budapest)
INDIA:	H. Bhabha (Bombay), R. Ramanna (Trombay)
IRISH REPUBLIC:	J. McConnell (Maynooth)
ISRAEL:	G. Racah (Jerusalem)
ITALY:	E. Amaldi (Rome)
JAPAN:	S. Kikuchi (Tokay), S. Tomonaga (Tokyo)
MEXICO:	M. Moshinsky (Mexico)
NETHERLANDS:	H. Brinkman (Groningen), S. R. de Groot (Leiden)
NORWAY:	E. Hylleraas (Oslo), A. Lundby (Oslo), H. Wergeland (Trondheim)
POLAND:	L. Infeld (Warsaw), J. Werle (Warsaw)
PORTUGAL:	J. M. Araújo (Porto), J. R. de Almeida Santos (Coimbra)
SOUTH AMERICA:	G. Beck (Rio de Janeiro), J. Leite Lopes (Rio de Janeiro)
SOUTH-EAST ASIA:	T. H. R. Skyrme (Kuala Lumpur)
SPAIN:	J. M. Otero (Madrid), C. Sanchez del Rio (Madrid)
SWEDEN:	O. Klein (Stockholm), K. Siegbahn (Uppsala), I. Waller (Uppsala)
SWITZERLAND:	P. Huber (Basel), P. Scherrer (Zürich)
U.A.R. & ARAB COUNTRIES:	F. El Bedewi (Cairo), M. G. Nooh (Cairo)
U.S.A.:	H. H. Barschall (Madison, Wisconsin), S. Devons (New York), G. C. Wick (Brookhaven), D. Inglis (Argonne)
U.S.S.R.:	M. A. Markov (Moscow), I. S. Shapiro (Moscow), D. V. Skobeltzyn (Moscow)
YUGOSLAVIA:	I. Supek (Zagreb)

CONTRIBUTIONS may be sent to the Editor, Professor L. Rosenfeld, NORDITA, Blegdamsvej 17, Copenhagen Ø, either directly, or preferably through the intermediary of one of the members of the Editorial Board of the country or region in which the author is working. They may be written in English, French or German.

NUCLEAR PHYSICS is published in fortnightly issues. The subscription price per volume of 700 pages is fl 57.00; 114s; $ 15.00. Post-free.

SUBSCRIPTIONS should be sent to the publishers, NORTH-HOLLAND PUBLISHING COMPANY P.O. Box 103, Amsterdam or to any subscription-agent.

BOOKS FOR REVIEW should be sent to Professor Rosenfeld.

No part of this issue may be reproduced in any form, by print, photoprint, microfilm or any other means without permission from the publisher.

Printed in the Netherlands

NUCLEAR PHYSICS 1962

Personal subscription scheme

Only to be used for new personal subscriptions, not for renewals

When Nuclear Physics was started at the end of 1955, the intention was to publish one or two volumes a year of 700 pages each. Neither the publisher nor the editor could envisage that the influx of papers would make it necessary to publish eight such volumes a year, as were in 1961.

Although since 1955 the guilder has been revaluated with 4 %, the production costs of mathematical composition have risen by approximately 25% and the number of words per page has been increased by 20% since the first volume, the subscription price per volume has been maintained at $ 15.00 (108s.).

Moreover Nuclear Physics does not impose any page charge, in order to make it easier for scientists from countries with a weak currency to contribute to the journal.

It is difficult to compare subscription prices, but per page Nuclear Physics is undoubtedly one of the less expensive journals in the field of physics.

However, we realize that a total subscription price per year of $ 120.00 for eight volumes is prohibitive for a private subscriber and the suggestion has been made that Nuclear Physics could fix a special price for personal subscriptions.

Indeed, there are a number of scientific journals which give a certain discount to private subscribers. In the case of Nuclear Physics a discount of 30% or even 50% would not be sufficient to attract private subscriptions.

personal subscription scheme ▶

Now it is known that for technical publications the composition of the type is the most expensive part of the production and that as soon as the break-even point is reached, the run-on costs are comparatively low.

Accordingly, we decided early 1961 to make Nuclear Physics available to personal subscribers at the run-on costs. This meant that starting with 1961 individual physicists could subscribe for their own use to the eight volumes (approx. 5600 pages) of Nuclear Physics scheduled for 1961 at a total price of $ 20.00 or the equivalent in other currency (postage included).

Should you want to join this personal subscription scheme for 1962, please return the order-form.

It has to be understood that the publisher has the right to refuse a personal subscription or its renewal. In case of refusal, the publisher will return the cheque.

We were glad to see that this new arrangement appealed to many nuclear physicists and that it did not lead to any misunderstanding about the extremely complicated way of fixing subscription prices for learned journals.

THE EDITOR
L. Rosenfeld

THE PUBLISHER
M. D. Frank

How to act: Write a letter to the Subscription Department of North-Holland Publishing Company, P.O. Box 103, Amsterdam, Netherlands, asking for a personal subscription.

This letter should contain:

- **a cheque or banknotes for $ 20.00**

  (£ 7.4.0-; DM 80; N.Frs. 100)

- **a statement running as follows:**

"This subscription is for personal use only and will not replace an existing library subscription, nor will it be put at the disposal of any library now or in the future.

My position is: _____"

(Mention should be made of the institution to which you are attached.)

Any enquiry or communication concerning the personal subscription scheme should be addressed to the publisher, North-Holland Publishing Company, P.O. Box 103, Amsterdam, Netherlands.

Only to be used for NEW personal subscriptions, not for renewals

SUBSCRIPTION FORM

NORTH-HOLLAND PUBLISHING COMPANY
P.O. BOX 103
AMSTERDAM - NETHERLANDS

Date _____

Please enter my personal subscription to

NUCLEAR PHYSICS 1962

(VOLUMES 29—36)

at the total subscription price of $ 20.00

(£ 7.4.0.; DM. 80; N. Frs. 100)

I declare that this subscription is for my personal use only and that it will not replace an existing library subscription, nor will it be put at the disposal of any library now or in the future.

I enclose ☐ banknotes

☐ cheque

My position is _____

(mention should be made of the institution to which you are attached)

Name (please print) _____

_____

Address _____

_____

City, Zone, State _____

Signature

_____

(tear off here)

1.E.2:
6.D

Nuclear Physics **28** (1961) 1—28; © *North-Holland Publishing Co., Amsterdam*
Not to be reproduced by photoprint or microfilm without written permission from the publisher

ADJUSTMENT OF RELATIVE NUCLIDIC MASSES (II)
$70 < A < 200$

L. A. KÖNIG and J. H. E. MATTAUCH
Max-Planck-Institut für Chemie (Otto-Hahn-Institut) Mainz
and
A. H. WAPSTRA
Instituut voor Kernphysisch Onderzoek, Amsterdam

Received 1 May 1961

Abstract: This paper describes the second part of the least squares computation of nuclidic massses from all available data. A compilation of all measurements relevant to the mass range $70 < A < 200$ is given.

1. Introduction

Masses in the present region were computed earlier by one of us [1]) by fitting reaction data and microwave results to mass spectroscopic ones by a somewhat intuitive procedure guided by experience in least squares computations but not based on exact methods. (Some values computed from more recent data were published by Kravtsov [2])). This procedure has the advantage that in the course of the computation one can correct, in a somewhat inexact way, for localized apparent errors in the initial data; but it is rather difficult to assign errors to the results or to their combinations (e.g. reaction energies derived from these masses). Now, both the quantity and the quality of the experimental material has increased considerably. We therefore decided to use for this region the more exact methods outlined in the first part [3]) of the present work. The approximately 430 masses in this region for which data are known are grouped, as in part I, in primary masses computed by least squares adjustments and in secondary masses computed afterwards.

The primary data contain masses of nuclides with $A \leqq 70$ computed in part I; in the present calculation, the values for these masses are treated as auxiliary constants (without errors), which is permitted since their accuracy is considerably better than that of almost all data used here. In this way correlations with masses of part I are avoided. Also within the present mass range the following simplifications of this sort have been made: as will be seen in sect. 2 mass doublets sometimes connect two nuclides of rather different mass numbers A. In essentially all these cases, the doublet measurement is considerably less precise than our knowledge of the mass of the light nuclide.

It is, therefore, permissible to treat the latter as auxiliary constant in the computation of the heavy doublet mass. In this way the primary data can be grouped in 17 independent sets, which for convenience of the calculation were combined in eight groups [4]) adjusted separately by application of the least squares method, using an electronic computer.

Before making these adjustments, one has to satisfy oneself as far as possible that the input data are consistent to a sufficient degree. We therefore first discuss the rules accepted as a guide in selecting the input data. Mass excesses M mentioned in the discussion are always given in the new scale of atomic masses [5]) in which the mass excess of ^{12}C is taken exactly equal to zero.

2. Mass Spectroscopic Data

These data are collected in the tables 1a and 1b. (Tables 1a, 1b, 2a, 2b, 3 and 4 follow the text of this paper). In the first part [3]) of this computation, errors in the results of the Minnesota group have been multiplied with the consistency factor 2.65 of a large, strongly interconnected group of their results. The same factor will be applied to their present data since, as will be apparent later (sect. 6), the agreement with other data is not so good that one could consider to omit this multiplication factor.

Not all doublets measured by the Minnesota group in the present range have been used. A few earlier measurements on Kr and Xe isotopes have been far surpassed by recent results. The former have therefore been omitted, though no serious discrepancies existed between them and the later values.

Duckworth and his collaborators assigned errors to their results which, for nuclides also measured by the Minnesota group, were considerably larger. Their doublets for these cases therefore carry almost no weight and have been omitted. These cases are, however, useful for estimating the dependability of Duckworth's results. The root of the mean square of the differences between Duckworth's doublets and the values computed from the Minnesota results, each divided by the error assigned by Duckworth, is 4.0. This does not necessarily mean that Duckworth *et al.* underestimated their errors by this factor, since part of the difference will be due to the uncertainties in the Minnesota doublets; yet, very probably the assigned errors are considerably too low. We have therefore, rather arbitrarily, applied the correction factor 2.65 also to the errors in Duckworth's results.

3. Nuclear Data

Contrary to the procedure used in the first part [3]) of the present computation, our policy in this part is to give only one value for each reaction energy or decay energy. If several values are known, only their weighted mean has been given.

The values of the adjusted masses do not depend on whether such pre-averaging has been applied or not, provided that in the first case internal errors have been assigned to all means. However, the values of χ^2 differ in both cases; the value χ_t^2 of a total adjustment using all observed input data without pre-averaging is given by the sum of the value χ_m^2 of an adjustment after pre-averaging plus the values χ_i^2 belonging to the separate weighted means. With a homogeneous group of data, e.g. the mass doublets, one should (in an adjustment after pre-averaging) assign internal errors to the weighted means, even in cases when the external error is significantly larger than the internal one; if then χ_i^2 should come out larger than the corresponding sum of degrees of freedom, all errors should be corrected. In the present mass range, however, there is no homogeneous group of measured ground state reaction energies. Even where possibly homogeneous groups of reaction energies exist (e.g. in the case of (γ, n) reactions) there is often doubt whether these values refer to ground state transitions. Thus, discrepancies between such groups of data can be of only a local character. We therefore adopted the policy to assign external errors to the means of different values for the same reaction in cases where these errors are larger than the corresponding internal errors.

The nuclear data used are collected in tables 2a and 2b. We have found it advantageous to refer wherever possible to the large data collection of the Nuclear Data Sheets. In many cases the adopted values agree with the average values given in these Sheets, but in some we had to deviate. Some disintegration or reaction energies recommended in the Sheets are obtained using also mass spectroscopical results; since the latter results are used here as such, we could not accept the above values of the Sheets. Then, in a few cases values for important electron capture disintegration energies not given in the Sheets were derived from data on L/K capture ratios, or limits on the occurrence of positons. A few reaction energies have been corrected for the change in calibration discussed in the first part [3]) of the present work. Other values deviate from those in the indicated Sheets since the latter contain information more recent than the date of our data collecting. Such deviating values have been marked with an asterisk attached to the reference number.

4. Microwave Measurements

A few amazingly accurate measurements of ratios of nuclear masses or mass differences have been made by microwave measurements [6]). In the range $A \leqq 70$ these measurements do not really compete with the results of the present mass adjustment, as is shown in table A. Yet, the agreement is surprisingly good. Thus, it appears reasonable to accept the results of this type of experiments in the present mass range, where they might make a contribution, with the errors indicated by their authors. These ratios are collected in table 3,

TABLE A

Mass ratios from microwave measurements with nuclides with $A < 70$, compared with values computed from our mass adjustment

Ratio	From mass adjustment	Experimental
$^{3}H/^{2}H$	1.497 465 92 ± 8	1.497 467 ± 7
		470 ± 8
		467 ± 12
		448 ± 60
$^{6}Li/^{7}Li$	0.857 343 46 ± 16	0.857 342 3 ± 20
$^{12}C/^{13}C$	0.922 838 81 ± 5	0.922 838 81 ± 25
		844 7 ± 20
$^{14}C/^{12}C$	1.166 936 83 ± 3	1.166 937 43 ± 23
$^{17}O/^{16}O$	1.062 783 61 ± 6	1.062 784 72 ± 105
$^{18}O/^{16}O$	1.125 305 13 ± 2	1.125 304 71 ± 28
$^{32}S/^{33}S$	0.969 689 34 ± 9	0.969 690 9 ± 32
		688 4 ± 32
$^{32}S/^{34}S$	0.941 244 74 ± 9	0.941 246 2 ± 23
		243 5 ± 25
$^{35}Cl/^{37}Cl$	0.945 976 11 ± 9	0.945 980 1 ± 50
		977 5 ± 40
		978 1 ± 30
		980 3 ± 15
$^{39}K/^{41}K$	0.951 219 93 ± 13	0.951 225 0 ± 70
		218 9 ± 15

From S. Geschwind, Encycl. of Physics **38**, 1 (1958) 38—59, with ref. g replaced by B. Rosenblum, A. H. Nethercot, Jr., and C. H. Townes, Phys. Rev. **109** (1958) 400

together with their observed and their adjusted values. For use in the present computation they were linearized in the way proposed earlier [1]) by one of us.

5. Consistency Checks

In the region $A \leqq 70$, most of the important nuclear reactions or decays have been studied so thoroughly that there is not much doubt about the correctness of the assignment to ground state transitions. Moreover, the distance between the ground states and the first excited states is so large that a faulty assignment immediately results in a large discrepancy. In both respects, the situation is different in the present mass range. It is therefore necessary to check that no important discrepancies occur between the present input data. This is done by making a rough adjustment using the method sketched in an earlier paper by one of us [1]).

Essentially, this method starts with adopting an initial nuclidic mass and then uses chains of nuclear reaction energies and microwave results to derive other masses, making rough adjustments in the course of this procedure. Thereafter, the obtained masses are compared with mass spectroscopic results. In this way discrepancies are located, studied and eliminated in order to assure that the final more or less automatic adjustment will give reasonable results.

In cases in which discrepancies occurred, the data were compared with systematics of beta decay energies and last neutron and proton binding energies. When such comparison added to the doubts about the correctness of one of the disagreeing data, this one was omitted or its error was increased; these cases are mentioned in table B. In other cases, such a decision is not possible. The

TABLE B

Some unused reaction and decay energies

Reaction	Reported value (keV)	Ref.	Adjusted value (keV)
^{74}Se(n, γ)^{75}Se	7 950± 20	59-1-48 [a])	8 015± 29
^{76}As(β^+)^{76}Ge	1 692± 30	54Ma [b])	980± 90
^{84}Sr(d, p)^{85}Sr	5 250±300	60-3-42	6 290± 60
^{84}Kr(d, p)^{85}Kr	3 720± 50	60-3-40	4 980± 50
^{86}Sr(γ, n)^{85}Sr	− 9 500±200	60-3-52 [a])	−11 460± 90
^{92}Mo(n, 2n)^{91}Mo	−12 350±100	60-5-88	−13 140± 80
^{93}Nb(d, p)^{94}Nb	5 030±100	58-9-37	4 965± 30
^{94}Mo(p, n)^{94}Tc	− 5 050±100	58-9-38	− 5 102± 30
^{96}Zr(p, n)^{96}Nb	− 2 580±200	58-7-29 [b])	− 500± 700
^{103}Rh(p, n)^{103}Pd	− 1 530	58-10-60	− 1 343± 30
^{114}Cd(d, p)^{115}Cd	3 520±150	60-3-109	3 929± 35
^{137}Ba(n, γ)^{138}Ba	9 230± 70	53K [a])	8 580± 140
^{144}Sm(γ, n)^{143}Sm	− 9 600± 50	59-1-116 [d])	−10 780± 340
^{152}Gd(α)^{148}Sm	1 748±200	59-4-89 [c])	2 080± 330
^{186}W(n, γ)^{187}W	7 100±300	49Ka [a])	3 400±1 500
^{194}Pt(γ, n)^{193}Pt	− 9 500±200	58-9-94 [a])	− 8 030± 250
^{195}Ir(β^-)^{195}Pt	2 100±100	54Ba [b])	
^{198}Ir(β^-)^{198}Pt	4 100±300	58-12-40 [b])	
^{199}Hg(n, γ)^{200}Hg	8 030± 30	58-8-70	7 989± 23

[a]) Target uncertain
[b]) Disagrees with β-systematics
[c]) Disagrees with α-systematics.
[d]) See footnote below table 2b.

The first column contains the reaction, the second one the reported value, and the last one the adjusted value following from our adjustment. The references are given in the third column. Wherever possible we have referred to the Nuclear Data Sheets. The deviating references are:

49Ka H. E. Kubitschek and S. M. Dancoff, Phys. Rev. **76** (1949) 531
53Ka B. B. Kinsey and G. A. Bartholomew, Can. J. Phys. **31** (1953) 1051
54Ba F. D. S. Butement and A. J. Poë, Phil. Mag. **45** (1954) 31
54Ma B. B. Murray and J. D. Kurbatov, Phys. Rev. **94** (1954) 780

reactions ^{107}Ag (n, γ) ^{108}Ag and ^{107}Ag (d, p) ^{108}Ag yield for ^{108}Ag neutron binding energies of (7270±20) keV and (7189±10) keV, respectively; neutron binding energy systematics cannot decide between these two values. Such cases have been left unchanged since only a few of them are present which will not spoil the χ^2 tests too much †).

† If, in future, more such cases might turn up, one might treat them as "parallel" reactions (see sect. 3) and pre-average them, assigning the external error to the mean value.

In some cases we were forced to use sometimes peculiar measurements such as accepting estimated values for some reaction or decay energies in order to eliminate contradictory results. This happens when an experimental result yields a limit to a reaction energy, which limit is violated by the combination of other input values. Thus, the mass doublets for ^{198}Pt and ^{198}Hg together with the β^- decay energy of ^{198}Au yield an electron capture decay energy of (3200$\pm$ 800) keV for the last nuclide. Yet, already a decay energy of 660 keV combined with the experimental lower limit for the electron capture halflife [7]) would mean that the transition to the 403 keV 2^+ state in ^{198}Pt has a reduced halflife a hundred times larger than that to the 412 keV 2^+ state in ^{198}Hg. Therefore, an estimated input value (360$\pm$300) keV for this decay energy was accepted among the input data. We have tried to keep the number of these cases a minimum, and where possible to obtain them from experimental data (e.g. limits on log ft values or on the occurrence of positon branches in electron capture decay). These cases are mentioned explicitly in table 2a and 2b.

It should be said that the above procedures of testing for consistency have not been applied to the whole of the input material. Between the screening of the main body of input data and the computation, some series of new data came to our notice, notably a series of (γ, n) reaction energies [8]) and a few new mass doublets of high precision [9]). They have been added to the input data without this check and also without the pre-averaging described in sect. 3, since their importance was deemed greater than that of avoiding a few large contributions to the χ^2 test. Thus, contributions > 3 are caused for (γ, n) reactions on ^{93}Nb, ^{103}Rh, ^{107}Ag, ^{141}Pr and ^{179}Hf.

6. Results

The adjusted values of the nuclidic masses obtained in the present computation are given in a separately published table [10]) combined with the results for other parts of the periodic system and with the secondary masses. Here, we only discuss the dependability of the present results. Table 4 shows the degree of consistency in the present computation. In most cases, the value of the consistency factor $R_e/R_1 = \{\chi^2/f\}^{\frac{1}{2}}$ is sufficiently near to 1. It is worthwhile to inspect the distributions of the contributions of the different input data [4]) to the sum χ^2 (see table 4). Most of the data are comparatively only very little changed by the adjustment; the rest of the contributions then evidently must spread out rather much to make up the sums χ^2.

Since the consistency factors never deviate more than three times the standard deviation from 1, we did not think it necessary to multiply the errors to the adjusted values by these factors. On the other hand, one may suspect that large contributions to χ^2 point to the existence of local errors which could profit by further study. Below, we therefore make some comments on the largest single contributions to χ^2.

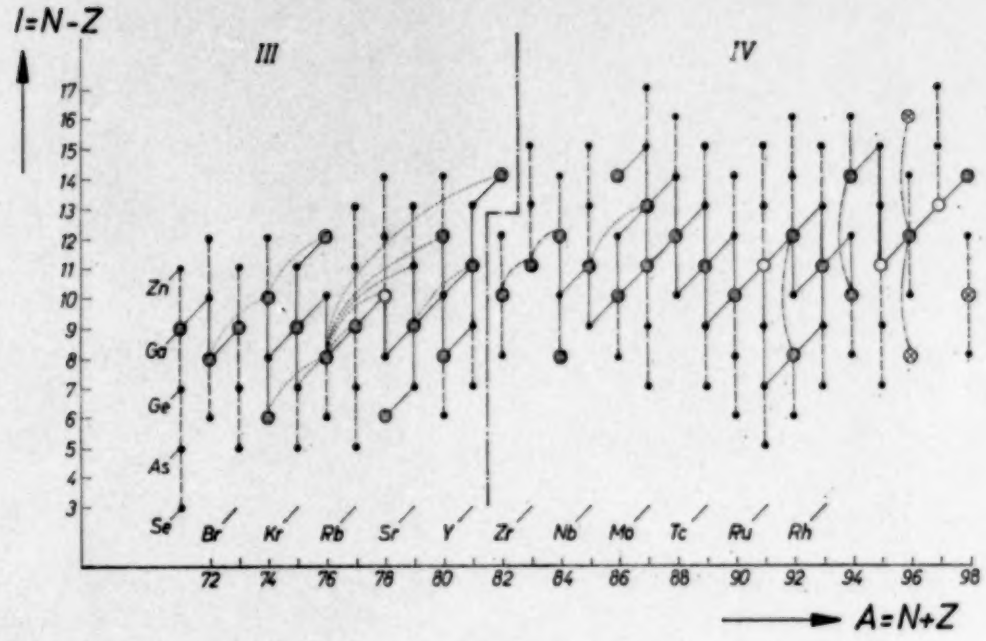

Fig. 1. Survey of the input data of the third (^{71}Zn—^{82}Se) and fourth adjustment (^{82}Br—^{98}Rh).
Legend:

○ nuclides occurring in nature,

● artificially produced nuclides,

/|/ the shading designates primary nuclides determined by mass spectroscopic doublets,

× designation of secondary nuclides determined by mass spectroscopic doublets,

——— reactions or decays connecting primary nuclides (primary reactions),

– – – secondary reactions or decays (at least one of the two nuclides connected thus is a secondary mass),

connections by microwave data,

connections by isotopic doublets,

—·—·—boundary between two groups of nuclides occurring in separate adjustments (see table 4).

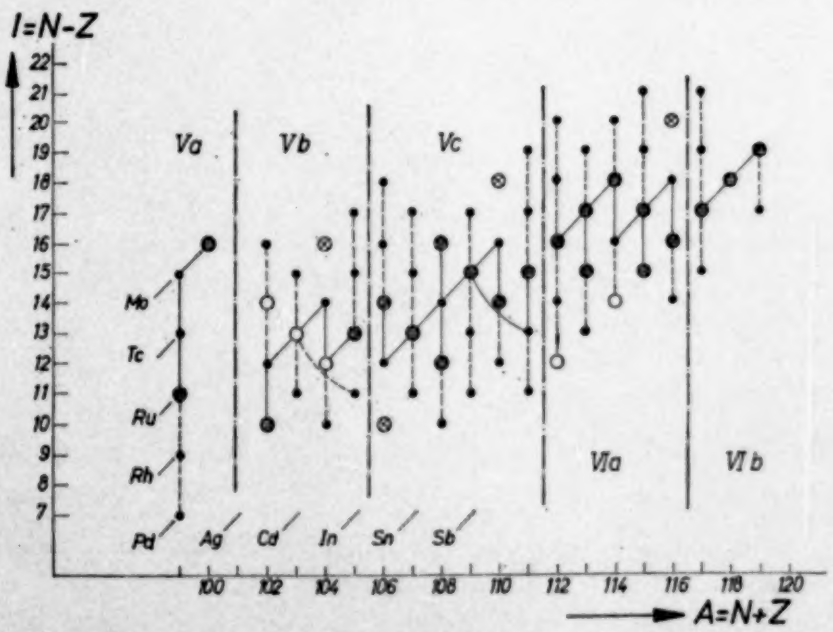

Fig. 2. Survey of the input data of the fifth (^{99}Mo—^{111}Sn) and sixth adjustment (^{112}Pd—^{119}Sb).
Legend as in fig. 1.

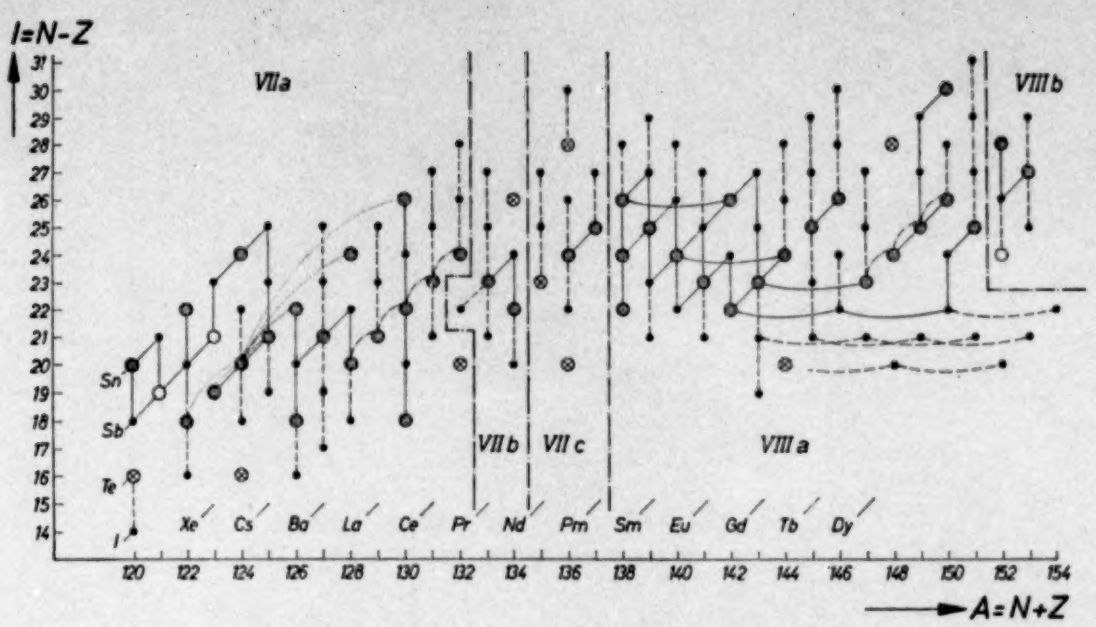

Fig. 3. Survey of the input data of the seventh (^{120}Sn—^{137}Ba) and eight adjustment (^{133}Cs—^{154}Dy). Legend as in fig. 1.

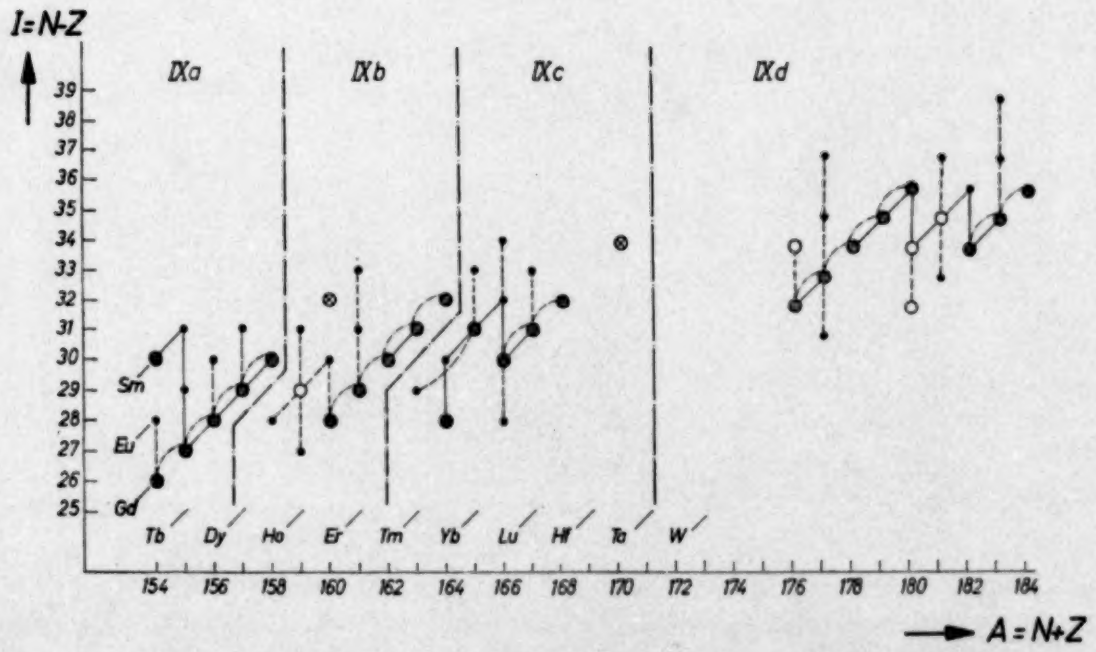

Fig. 4. Survey of the input data of the ninth adjustment (^{154}Sm—^{184}W). Legend as in fig. 1.

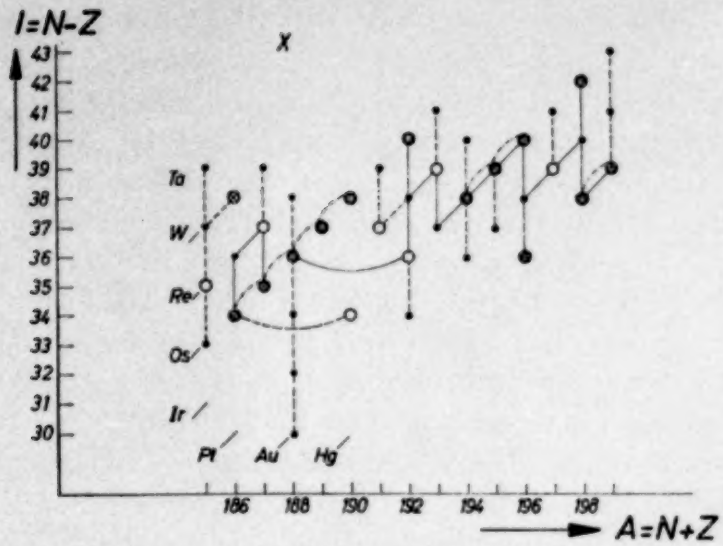

Fig. 5. Survey of the input data of the tenth adjustment (^{185}Ta—^{199}Hg). Legend as in fig. 1.

Some of the largest single contributions to χ^2 have already been removed by further work. Geller *et al.* [8]) showed that the ^{89}Y(γ, n) reaction energy is smaller than (11590±80)keV, and newer ^{88}Sr(p, n) measurements [11]) indicate that the ^{88}Y(β^+) energy in table 2a is probably somewhat low. This explains the large contributions (16.6 and 7.2) to χ^2 for the range ^{82}Kr—^{98}Mo due to the ^{88}Sr(d, p) and ^{89}Y(γ, n) reactions.

The value for the ^{155}Gd(n, γ) reactions in table 2a has to be replaced by the new value [12]) (8522±10)keV, by which the discrepancy with the mass doublet ^{156}Gd—^{155}Gd contributing 16.5 to χ^2 for the range ^{154}Sm—^{158}Gd would be removed.

Large contributions 16.00 and 7.19 to χ^2 for the range ^{120}Sn—^{132}Xe are due to the mass doublets $C_{10}H_6$—^{126}Te and $C_{10}H_8$—^{128}Te. These doublets belong to the oldest group of mass doublets accepted in the present computation; it is perhaps not surprising that they should disagree somewhat. The fact that they were allowed to influence χ^2 by these amounts is due to the last minute, additions of new Xe-doublets mentioned in sect. 5; just because of the accuracy of these new data, the Te-doublets have scarcely influenced the results of the present computation.

Other large contributions are due to disagreement between (n, γ) and (d, p) reaction energies on ^{107}Ag(7.3) and ^{127}I(6.9); to the somewhat unfortunate ^{198}Pt doublet (6.8); to the last minute additions of (γ, n) reactions (6.9 for ^{196}Pt, 4.4 for ^{183}W and 4.3 for ^{179}Hf) and of Kr doublets (6.4 for ^{78}Kr(d, p) and 4.3 for C_6H_{13}—^{85}Rb), all of which are mentioned in sect. 5. The only other contribution larger than 4 occurred for the microwave ratio containing ^{70}Ge, ^{72}Ge and ^{74}Ge (7.3); the influence of this deviating value on our results is, however, rather small.

We can now decide afterwards whether it was correct that the errors assigned

to the mass doublets were multiplied with the consistency factor 2.65 as mentioned in sect. 2. The first thing seen is that the average consistency factor 1.21 of all adjustments is slightly large; evidently, this would have been worse if a factor smaller than 2.65 had been applied to the doublet errors. The magnitude of the average consistency factor is determined, however, both by mass doublets and by the other data; one could imagine that not the first group is mainly responsible for the discrepancies. An exact answer to this question is not possible; one can, however, get an idea how sensitive the consistency factor depends on the errors assigned to the two groups of data by looking at the average contributions to χ^2 for different groups of data. This quantity is 0.63 for all data, 0.90 for the Minnesota mass doublets (with the exception of the most recent very accurate values [9]) which are not checked by other data of comparable precision), 0.81 for Duckworth *et al.*'s mass doublets and 0.86 for microwave data, compared with the value 0.51 for the reaction and decay energies. Thus, it appears that the contributions of the mass doublets to χ^2 are already rather large compared with those of the reaction and decay energies (the relatively few microwave data do not play a significant role). We think that these results justify our decision to use the above mentioned correction factor to the doublet errors.

Yet, even now the errors following from our adjustment should be used with some caution. In the earlier adjustment [1]), where the errors in the final results were only estimated, one could easily make allowance for the possibility that part of each error was systematic. This cannot easily be done in the present automatic computation. As a result, we feel that some errors may be somewhat low, especially in the region $150 < A < 196$. Indeed, new Minnesota [13]) and Russian [14]) measurements in this region indicate that the masses in this part of our table may be about 1 MeV low, as compared with assigned errors of about 0.5 MeV.

7. Rejected Data

No reasons need to be given for experimental data not used in the present computation wherever better experimental data are available (see ref. [3])). Borderline cases and cases rejected on the basis of comparisons as discussed in sect. 5 are shown in table B.

The authors are much indebted to Mr. W. Thiele for his collaboration with the programming and the numerical calculations on Siemens digital computers type 2002. One of us (L.A.K.) wishes to thank the Instituut voor Kernphysisch Onderzoek, Amsterdam, especially Professor Dr. A. H. Wapstra, for a grant and for the hospitality extended to him. The work of another of us (A.H.W.) is part of the research program of the "Stichting voor Fundamenteel Onderzoek der Materie (F.O.M.)", which is financially supported by the "Nederlandse Organisatie voor Zuiver Wetenschappelijk Onderzoek (Z.W.O.)".

References

1) A. H. Wapstra, Physica **21** (1955) 385
2) V. A. Kravtsov, Uspekhi Fiz. Nauk. **65** (1958) 452
3) F. Everling, L. A. König, J. H. E. Mattauch and A. H. Wapstra, Nuclear Physics **25** (1961) 177
4) J. H. E. Mattauch, Proc. Int. Conf. Nuclidic Masses, Hamilton (University of Toronto Press, Toronto 1960) **3**
5) T. P. Kohman, J. H. E. Mattauch and A. H. Wapstra, Naturwiss. **45** (1958) 174; J. Chimie Physique **55** (1958) **393**, Science **127** (1958) **1431**; Physics Today **12** (1959) 30; J. Mattauch, Z. Naturf. **13a** (1958) 572
6) S. Geschwind, Encyclopedia of Physics **38/1** (Spinger Verlag, Berlin, 1958)
7) A. A. Bashilov, Nuclear Physics **1** (1956) 629
8) K. N. Geller, J. Halpern and E. G. Muirhead, Phys. Rev. **118** (1960) 1302
9) J. L. Benson, R. A. Damerow and R. R. Ries, Phys. Rev. **113** (1959) 1105; and A. O. Nier, private communication (Kr, Xe and Ag)
10) F. Everling, L. A. König, J. H. E. Mattauch and A. H. Wapstra, Nuclear Physics **18** (1960) 529
11) J. W. Nelson, H. S. Adams, R. H. Davis, J. D. Fox, N. P. Heydenburg, H. S. Plendl, R. K. Sheline, and G. M. Temmer, Bull. Amer. Phys. Soc. **5** (1960) 424
12) J. K. Knowles, G. Manning, G. A. Bartholomew and P. J. Campion, Proc. Conf. Kingston, 1960, ed. by D. A. Bromley and E. W. Vogt (North-Holland Publ. Co., Amsterdam 1960) p. 576
13) V. B. Bhanot, W. H. Johnson Jr. and A. O. Nier, Phys. Rev. **120** (1960) 235
14) R. A. Demirkhanov, T. I. Gutkin and V. V. Dorokhov, JETP **37** (1960) 866; V. Kravtsov, private communication

TABLE 1a

Primary mass spectroscopical data

Doublet	Measured value μMU ($^{16}O = 16$)		Lab.	Adopted value μu		Adjusted value μu		$\frac{v}{\sigma}$
$^{12}C_5{}^1H_{11} - {}^{71}Ga$	161 300 ±	80	M8	161 250 ±	210	161 240 ±	50	0.0561
$^{12}C_5{}^1H_{12} - {}^{72}Ge$	172 350	50	*	172 300	130	172 160	50	0.9943
$^{12}C_6{}^1H - {}^{73}Ge$	84 510	30	*	84 480	80	84 470	70	0.1994
$^{12}C_6{}^1H_2 - {}^{74}Ge$	94 680	60	*	94 650	160	94 500	60	0.9346
$^{12}C_6{}^1H_4 - {}^{76}Ge$	110 050	40	*	110 020	110	109 940	90	0.6655
$^{12}C_6{}^1H_3 - {}^{75}As$	101 790	40	*	101 760	110	101 900	50	-1.3527
$^{12}C_6{}^1H_2 - {}^{74}Se$	93 140	70	*	93 110	190	93 200	60	-0.4671
$^{12}C_6{}^1H_4 - {}^{76}Se$	112 060	40	*	112 020	110	112 073	48	-0.4629
$^{12}C_6{}^1H_5 - {}^{77}Se$	119 085	125	H8*	119 050	330	119 194	48	-0.4432
$^{12}C_6{}^1H_8 - {}^{80}Se$	146 170	40	M8	146 120	110	146 092	17	0.2974
$^{12}C_6{}^1H_{10} - {}^{82}Se$	161 660	40	*	161 610	110	161 600	70	0.0464
$^{12}C_6{}^1H_7 - {}^{79}Br$	136 420	50	*	136 380	130	136 431	19	-0.4114
$^{12}C_6{}^1H_9 - {}^{81}Br$	154 050	50	*	154 000	130	154 086	37	-0.6387
$^{12}C_6{}^1H_6 - {}^{78}Kr$	126 624	2	M12	126 584	5	126 585	5	-0.2695
$^{12}C_6{}^1H_8 - {}^{80}Kr$	146 272	5	*	146 226	13	146 217	13	0.6367
$^{12}C_6{}^1H_{10} - {}^{82}Kr$	164 822	3	*	164 770	8	164 770	8	0.0048
$^{83}Kr - {}^{82}Kr$	966	12	*	966	32	966	10	-0.0193
$^{12}C_6{}^1H_{11} - {}^{83}Kr$	172 001	3	*	171 946	8	171 946	8	0.0027
$^{84}Kr - {}^{83}Kr$	-2 311	12	*	-2 310	32	-2 309	9	-0.0302
$^{12}C_6{}^1H_{12} - {}^{84}Kr$	182 457	2	*	182 399	5	182 399	5	0.0664
$^{12}C_6{}^1H_{14} - {}^{86}Kr$	199 000	3	*	198 937	8	198 936	8	0.1060
$^{12}C_6{}^1H_{13} - {}^{85}Rb$	189 750	60	M8	189 690	160	190 020	60	-2.0823
$^{12}C_5{}^{16}O{}^1H_{11} - {}^{87}Rb$	171 730	170	*	171 680	450	171 810	80	-0.3036
$^{12}C_6{}^1H_{12} - {}^{84}Sr$	180 700	150	*	180 640	400	180 527	11	0.2909
$^{12}C_6{}^1H_{14} - {}^{86}Sr$	200 250	100	*	200 190	260	200 290	80	-0.4007
$^{12}C_5{}^{16}O{}^1H_{11} - {}^{87}Sr$	172 050	60	*	172 000	160	172 100	80	-0.6865
$^{12}C_4{}^{16}O_2{}^1H_8 - {}^{88}Sr$	146 460	110	*	146 410	290	146 820	90	-1.4007
$^{12}C_8{}^1H_9 - {}^{89}Y{}^{16}O$	169 840	110	*	169 790	290	170 080	90	-1.0155
$^{12}C_7{}^1H_6 - {}^{90}Zr$	142 660	250	*	142 600	700	142 630	90	-0.0271
$^{12}C_7{}^1H_8 - {}^{92}Zr$	158 979	460	H4*	158 900	1 200	158 010	110	0.7539
$^{92}Mo - {}^{92}Zr$	1 340	260	H7*	1 300	700	1 700	80	-0.5269
$^{12}C_7{}^1H_9 - {}^{93}Nb$	164 810	80	M8	164 760	210	164 410	110	1.6369
$^{94}Zr - {}^{94}Mo$	1 220	200	H7*	1 200	500	1 400	360	-0.3348
$^{12}C_8 - {}^{96}Mo$	95 067	204	H2,H4*	95 000	500	95 450	360	-0.7631
$^{12}C_7{}^1H_{14} - {}^{98}Mo$	204 719	336	H5*	204 700	900	204 040	410	0.6888
$^{12}C_8{}^1H_4 - {}^{100}Mo$	124 812	240	H2,H4*	124 800	600	123 730	490	1.6438
$^{12}C_7{}^1H_{15} - {}^{99}Ru$	210 172	257	H10*	210 100	700	211 300	490	-1.7595
$^{12}C_8{}^1H_6 - {}^{102}Pd$	142 120	80	M7	142 070	210	142 010	190	0.2933
$^{12}C_8{}^1H_9 - {}^{105}Pd$	165 650	140	*	165 600	370	165 790	270	-0.5133
$^{12}C_8{}^1H_{10} - {}^{106}Pd$	175 385	127	*	175 330	340	175 050	120	0.8218
$^{12}C_8{}^1H_{12} - {}^{108}Pd$	190 480	100	M7	190 420	260	189 980	120	1.6538
$^{12}C_8{}^1H_{11} - {}^{107}Ag$	181 130	100	M13	181 070	260	181 110	110	-0.1276

TABLE 1a

(Continued)

Doublet	Measured value μMU ($^{16}O = 16$)		Lab.	Adopted value μu		Adjusted value μu		$\frac{v}{\sigma}$
$^{12}C_8\,^{1}H_{13} - {}^{109}Ag$	197 140	± 100	M13	197 080	± 260	197 030	± 110	0.1967
$^{12}C_8\,^{1}H_{12} - {}^{108}Cd$	189 880	100	M7	189 820	260	189 900	120	-0.3221
$^{12}C_8\,^{1}H_{14} - {}^{110}Cd$	206 200	120	*	206 130	320	206 590	110	-1.4271
$^{12}C_8\,^{1}H_{15} - {}^{111}Cd$	213 150	80	*	213 080	210	213 230	190	-0.6847
$^{12}C_8\,^{1}H_{16} - {}^{112}Cd$	222 220	67	*	222 150	180	222 370	110	-1.2341
$^{12}C_8\,^{1}H_{17} - {}^{113}Cd$	228 610	90	*	228 540	240	228 420	100	0.5076
$^{12}C_8\,^{1}H_{18} - {}^{114}Cd$	237 320	140	*	237 240	370	237 290	100	-0.1184
$^{12}C_6\,^{16}O_2\,^{1}H_{10} - {}^{114}Cd$	164 600	120	*	164 550	320	164 520	100	0.0980
$^{12}C_8\,^{1}H_{17} - {}^{113}In$	228 770	100	*	228 700	260	228 750	100	-0.1959
$^{12}C_9\,^{1}H_7 - {}^{115}In$	151 200	100	*	151 150	260	150 710	100	1.6692
$^{12}C_9\,^{1}H_7 - {}^{115}Sn$	151 460	250	*	151 400	700	151 240	110	0.2490
$^{12}C_9\,^{1}H_8 - {}^{116}Sn$	160 470	140	*	160 420	370	160 490	190	-0.1990
$^{12}C_6\,^{16}O_2\,^{1}H_{12} - {}^{116}Sn$	181 560	180	*	181 500	480	181 620	190	-0.2544
$^{12}C_9\,^{1}H_9 - {}^{117}Sn$	167 370	90	*	167 320	240	167 370	190	-0.2109
$^{12}C_9\,^{1}H_{10} - {}^{118}Sn$	176 290	190	*	176 200	500	176 460	190	-0.4477
$^{12}C_6\,^{16}O_2\,^{1}H_{14} - {}^{118}Sn$	197 260	260	*	197 200	700	197 590	190	-0.5705
$^{12}C_9\,^{1}H_{11} - {}^{119}Sn$	182 970	110	*	182 910	290	182 690	200	0.7583
$^{12}C_{10} - {}^{120}Sn$	97 840	140	*	97 810	370	97 870	140	-0.1580
$^{12}C_{10}\,^{1}H_2 - {}^{122}Sn$	112 220	140	*	112 180	370	112 240	140	-0.1484
$^{12}C_{10}\,^{1}H_4 - {}^{124}Sn$	126 100	100	*	126 060	260	126 060	130	0.0014
$^{12}C_{10}\,^{1}H_2 - {}^{122}Te$	112 780	80	*	112 740	210	112 650	130	0.4502
$^{123}Te - {}^{12}C_{10}\,^{1}H_2$	888 980	400	*	888 700	1 100	888 530	130	0.1556
$^{12}C_{10}\,^{1}H_4 - {}^{124}Te$	128 220	100	*	128 180	260	128 540	130	-1.3796
$^{125}Te - {}^{12}C_{10}\,^{1}H_4$	873 600	320	*	873 300	800	873 120	130	0.2387
$^{12}C_{10}\,^{1}H_6 - {}^{126}Te$	143 120	60	*	143 070	160	143 710	37	-4.0008
$^{12}C_{10}\,^{1}H_8 - {}^{128}Te$	157 090	120	*	157 040	320	157 890	140	-2.6828
$^{12}C_{10}\,^{1}H_{10} - {}^{130}Te$	171 340	80	*	171 290	210	171 550	140	-1.2691
$^{12}C_{10}\,^{1}H_7 - {}^{127}I$	150 160	120	*	150 110	320	150 424	23	-0.9833
$^{12}C_{10}\,^{1}H_6 - {}^{126}Xe$	142 540	140	*	142 490	370	142 782	32	-0.7760
$^{12}C_{10}\,^{1}H_8 - {}^{128}Xe$	159 119	4	M12	159 068	11	159 064	10	0.3759
$^{129}Xe - {}^{128}Xe$	1 571	12	*	1 571	32	1 565	13	0.1885
$^{12}C_{10}\,^{1}H_9 - {}^{129}Xe$	165 696	4	*	165 643	11	165 643	10	0.0343
$^{130}Xe - {}^{129}Xe$	- 954	12	*	- 954	32	- 956	13	0.0881
$^{12}C_{10}\,^{1}H_{10} - {}^{130}Xe$	174 799	4	*	174 743	11	174 740	90	0.0882
$^{131}Xe - {}^{130}Xe$	1 898	11	*	1 897	29	1 894	12	0.1052
$^{12}C_{10}\,^{1}H_{11} - {}^{131}Xe$	181 049	3	*	180 991	8	180 991	7	0.0300
$^{132}Xe - {}^{131}Xe$	- 607	11	*	- 607	29	- 607	10	-0.0092
$^{12}C_{10}\,^{1}H_{12} - {}^{132}Xe$	189 801	3	*	189 741	8	189 741	8	-0.0157
$^{12}C_3\,^{16}O_6 - {}^{132}Xe$	65 400	150	M7	65 380	400	65 328	8	0.1297
$^{12}C_{10}\,^{1}H_{13} - {}^{133}Cs$	196 660	70	M10	196 600	190	196 640	150	-0.2278
$^{12}C_6\,^{16}O_3\,^{1}H_{10} - {}^{130}Ba$	156 240	200	*	156 200	500	156 751	24	-1.0586
$^{12}C_{10}\,^{1}H_{14} - {}^{134}Ba$	205 360	80	*	205 290	210	205 240	150	0.2603

TABLE 1a
(Continued)

Doublet	Measured value μMU ($^{16}O = 16$)	Lab.	Adopted value μu	Adjusted value μu	$\frac{v}{\sigma}$
$^{12}C_{10}{}^{1}H_{16} - {}^{136}Ba$	220 890 ± 90	M10	220 820 ± 240	220 850 ± 140	-0.1138
$^{12}C_{9}{}^{13}C{}^{1}H_{16} - {}^{137}Ba$	223 080 60	"	223 010 160	223 000 130	0.0759
$^{12}C_{10}{}^{1}H_{18} - {}^{138}Ba$	236 030 80	"	235 950 210	235 840 80	0.5406
$^{12}C_{10}{}^{1}H_{18} - {}^{138}La$	234 170 200	"	234 100 500	234 040 80	0.1036
$^{12}C_{9}{}^{13}C{}^{1}H_{18} - {}^{139}La$	238 230 60	"	238 150 160	238 150 80	0.0091
$^{12}C_{10}{}^{1}H_{18} - {}^{138}Ce$	234 890 200	"	234 820 500	235 130 80	-0.5946
$^{12}C_{10}{}^{1}H_{20} - {}^{140}Ce$	251 290 60	"	251 210 160	251 220 50	-0.0740
$^{12}C_{10}{}^{1}H_{22} - {}^{142}Ce$	262 930 70	"	262 850 190	263 120 80	-1.4676
$^{12}C_{11}{}^{1}H_{9} - {}^{141}Pr$	163 000 30	"	162 950 80	163 038 46	-1.1249
$^{12}C_{10}{}^{1}H_{22} - {}^{142}Nd$	264 740 30	"	264 660 80	264 677 47	-0.2669
$^{12}C_{10}{}^{13}C{}^{1}H_{10} - {}^{143}Nd$	172 080 100	"	172 030 260	171 980 50	0.1609
$^{12}C_{10}{}^{19}F{}^{1}H_{5} - {}^{144}Nd$	127 770 70	"	127 730 190	127 630 50	0.5331
$^{12}C_{10}{}^{19}F{}^{1}H_{6} - {}^{145}Nd$	133 330 190	"	133 300 500	133 200 150	0.1807
$^{12}C_{10}{}^{19}F{}^{1}H_{7} - {}^{146}Nd$	140 530 60	"	140 490 160	140 490 150	-0.0571
$^{12}C_{9}{}^{16}O_{2}{}^{1}H_{10} - {}^{150}Nd$	147 300 70	"	147 250 190	147 370 150	-0.6447
$^{12}C_{9}{}^{13}C{}^{19}F{}^{1}H_{7} - {}^{147}Sm$	142 090 30	"	142 040 80	141 920 50	1.6166
$^{148}Sm - {}^{147}Sm$	1 000 250 60	"	999 930 160	999 940 130	-0.0555
$^{149}Sm - {}^{148}Sm$	1 002 710 60	"	1 002 390 160	1 002 370 100	0.1135
$^{150}Sm - {}^{149}Sm$	1 000 420 60	"	1 000 100 160	1 000 074 31	0.1736
$^{12}C_{9}{}^{16}O_{2}{}^{1}H_{10} - {}^{150}Sm$	151 230 70	"	151 180 190	151 070 130	0.5799
$^{12}C_{12}{}^{1}H_{8} - {}^{152}Sm$	143 290 130	"	143 240 340	143 260 330	-0.0364
$^{12}C_{12}{}^{1}H_{10} - {}^{154}Sm$	156 370 150	"	156 320 400	156 580 300	-0.6604
$^{12}C_{12}{}^{1}H_{7} - {}^{151}Eu$	135 260 170	"	135 220 450	135 150 180	0.1521
$^{12}C_{13}{}^{1}H_{11} - {}^{151}Eu{}^{16}O$	171 690 190	"	171 600 500	171 530 180	0.2006
$^{12}C_{12}{}^{13}C{}^{1}H_{12} - {}^{153}Eu{}^{16}O$	181 800 400	"	181 700 1 100	181 620 350	0.1120
$^{154}Gd - {}^{77}Se_{2}$	81 000 200	HB	81 000 500	80 360 280	1.1523
$^{155}Gd - {}^{154}Gd$	1 002 150 60	M9	1 001 830 160	1 001 780 150	0.3457
$^{156}Gd - {}^{52}Cr_{3}$	100 400 400	HB	100 400 1 100	100 690 260	-0.3085
$^{156}Gd - {}^{78}Se_{2}$	87 500 200	"	87 500 500	87 540 260	-0.1300
$^{156}Gd - {}^{155}Gd$	999 900 60	M9	999 580 160	999 136 50	-4.0657
$^{157}Gd - {}^{156}Gd$	1 002 200 60	"	1 001 880 160	1 002 120 90	0.4965
$^{158}Gd - {}^{79}Br_{2}$	86 600 200	HB	86 600 500	87 500 270	-1.7486
$^{158}Gd - {}^{157}Gd$	1 000 530 60	M9	1 000 210 160	1 000 156 9	0.3530
$^{160}Dy - {}^{80}Se_{2}$	91 000 800	HB	91 000 2 100	91 000 1 000	-0.0156
$^{161}Dy - {}^{160}Dy$	1 002 100 60	M9	1 001 780 160	1 001 780 160	-0.0012
$^{162}Dy - {}^{81}Br_{2}$	92 900 500	HB	92 900 1 300	93 000 1 000	-0.1088
$^{162}Dy - {}^{161}Dy$	1 000 210 60	M9	999 890 160	999 890 160	-0.0012
$^{163}Dy - {}^{162}Dy$	1 002 260 60	"	1 001 940 160	1 001 900 90	0.2431
$^{164}Dy - {}^{82}Se_{2}$	95 200 800	HB	95 200 2 100	94 800 1 000	0.1897
$^{164}Dy - {}^{163}Dy$	1 000 800 60	M9	1 000 480 160	1 000 480 160	-0.0142
$^{165}Ho - {}^{55}Mn_{3}$	114 800 800	HB	114 800 2 100	115 400 700	-0.3013
$^{164}Er - {}^{82}Se_{2}$	96 500 400	"	96 500 1 100	95 200 700	1.1702

TABLE 1a

(Continued)

Doublet	Measured value μMU ($^{12}C = 16$)	Lab.	Adopted value μu	Adjusted value μu	$\frac{v}{\sigma}$
$^{167}Er - {}^{166}Er$	1 002 060 ± 60	M9	1 001 740 ± 160	1 001 640 ± 80	0.6141
$^{168}Er - {}^{56}Fe_3$	126 000 300	H8	126 000 800	126 600 600	-0.7646
$^{168}Er - {}^{167}Er$	1 000 650 60	M9	1 000 330 160	1 000 310 160	0.1529
$^{176}Hf - {}^{88}Sr_2$	128 700 600	H8	128 700 1 600	129 120 460	-0.2920
$^{177}Hf - {}^{176}Hf$	1 002 250 60	M9	1 001 930 160	1 001 577 33	2.2306
$^{178}Hf - {}^{89}Y_2$	131 600 600	H8	131 600 1 600	131 630 440	-0.0431
$^{178}Hf - {}^{177}Hf$	1 000 880 60	M9	1 000 560 160	1 000 570 160	-0.0292
$^{179}Hf - {}^{178}Hf$	1 002 360 60	"	1 002 040 160	1 001 930 60	0.6835
$^{180}Hf - {}^{60}Ni_3$	154 260 540	H4	154 200 1 400	152 770 430	1.0065
$^{180}Hf - {}^{90}Zr_2$	137 100 300	H8	137 100 800	136 480 430	0.7228
$^{180}Hf - {}^{179}Hf$	1 001 130 60	M9	1 000 810 160	1 000 700 90	0.7056
$^{182}W - {}^{91}Zr_2$	135 500 300	H8	135 500 800	135 970 380	-0.6444
$^{183}W - {}^{61}Ni_3$	155 367 366	H1	155 300 1 000	155 340 380	-0.0263
$^{183}W - {}^{182}W$	1 002 230 60	M9	1 001 910 160	1 002 025 8	-0.7156
$^{184}W - {}^{92}Zr_2$	139 580 280	H7	139 500 700	139 970 390	-0.5800
$^{184}W - {}^{92}Mo_2$	136 900 440	"	136 900 1 200	136 560 390	0.2536
$^{184}W - {}^{183}W$	1 000 990 60	M9	1 000 670 160	1 000 660 160	0.0897
$^{187}Os - {}^{186}Os$	1 002 140 60	"	1 001 820 160	1 002 040 80	-1.3469
$^{188}Os - {}^{94}Zr_2$	142 680 240	H7	142 600 600	142 710 300	-0.1118
$^{188}Os - {}^{94}Mo_2$	145 120 320	"	145 100 800	145 500 300	-0.5023
$^{188}Os - {}^{187}Os$	1 000 330 60	M9	1 000 010 160	1 000 010 160	0
$^{189}Os - {}^{63}Cu_3$	169 800 900	H10	169 700 2 400	168 440 330	0.5487
$^{189}Os - {}^{188}Os$	1 002 550 60	M9	1 002 230 160	1 002 240 160	-0.0325
$^{190}Os - {}^{95}Mo_2$	146 000 400	H8	146 000 1 100	145 980 360	-0.0272
$^{190}Os - {}^{189}Os$	1 000 520 60	M9	1 000 200 160	1 000 200 160	0.0041
$^{192}Os - {}^{64}Ni_3$	179 700 720	H10	179 600 1 900	176 640 340	1.5772
$^{192}Os - {}^{96}Zr_2$	143 660 480	H7	143 600 1 300	144 150 340	-0.4248
$^{192}Os - {}^{96}Mo_2$	150 920 280	"	150 900 700	151 410 340	-0.7282
$^{192}Os - {}^{96}Ru_2$	144 880 340	"	144 800 900	145 370 340	-0.5997
$^{194}Pt - {}^{97}Mo_2$	150 932 388	H5	150 900 1 000	150 930 240	-0.0464
$C_{15}H_{15} - {}^{195}Pt$	153 270 585	H_3	153 200 1 500	152 910 240	0.1982
$^{195}Pt - {}^{65}Cu_3$	179 985 292	"	179 900 800	181 110 240	-1.5234
$^{195}Pt - {}^{194}Pt$	1 002 450 60	M9	1 002 130 160	1 002 033 42	0.6219
$^{196}Pt - {}^{98}Mo_2$	155 232 568	H5	155 200 1 600	153 600 240	1.0164
$^{196}Pt - {}^{98}Ru_2$	154 060 500	H10	154 000 1 300	153 650 240	0.2696
$^{196}Pt - {}^{195}Pt$	1 000 490 60	M9	1 000 170 160	1 000 160 13	0.0739
$^{198}Pt - {}^{66}Zn_3$	186 714 792	H1	186 700 2 100	189 390 310	-1.3048
$^{198}Pt - {}^{99}Ru_2$	152 660 400	H10	152 600 1 100	155 380 310	-2.6164
$^{12}C_{14}H_{28} - {}^{196}Hg$	253 346 8.0	M11	253 265 21	253 288 18	-1.0643
$^{12}C_{14}H_{30} - {}^{198}Hg$	268 080 6.6	"	267 995 17	267 988 15	0.3679
$^{199}Hg - {}^{12}C_{14}H_{30}$	733 716 10.0	"	733 483 26	733 499 20	-0.6115
$^{199}Hg - {}^{198}Hg$	1 001 816 11.0	"	1 001 498 29	1 001 487 21	0.3514

In the above table the first column denotes the mass-spectroscopic doublet. The second one gives the measured value and its error in μMU($^{16}O = 16$). The fourth column gives in μu the input datum and its error multiplied with the consistency factor (see sect. 2). In the fifth column the adjusted values of the mass spectroscopic doublets and their errors are to be found, both again expressed in μu. The last column gives the ratio of the difference v between the two preceding columns divided by the error σ in the adopted input value (fourth column). As to the indication of the laboratory in the third column the following abbreviations are used:

M7 R. E. Halsted, Phys. Rev. **88** (1952) 666
M8 T. L. Collins, W. H. Johnson, Jr. and A. O. Nier, Phys. Rev. **94** (1954) 398
M9 W. H. Johnson, Jr. and V. B. Bhanot, Phys. Rev. **107** (1957) 1669
M10 W. H. Johnson, Jr. and A. O. Nier, Phys. Rev. **105** (1957) 1014
M11 J. L. Benson, R. A. Damerow, and R. R. Ries, Phys. Rev. **113** (1959) 1105
M12 W. H. Johnson, Jr., private communication (1959)
M13 W. H. Johnson, jr., private communication (1960)
H1 H. E. Duckworth, H. A. Johnson, R. S. Preston and R. F. Woodcock, Phys. Rev. **78** (1950) 386
H2 H. E. Duckworth, R. S. Preston and K. S. Woodcock, Phys. Rev. **79** (1950) 188
H3 H. E. Duckworth, K. S. Woodcock and R. S. Preston, Phys. Rev. **78** (1950) 479
H4 H. E. Duckworth, C. L. Kegley, J. M. Olson and G. S. Stanford, Phys. Rev. **83** (1951) 1114
H5 H. E. Duckworth and R. S. Preston, Phys. Rev. **82** (1951) 468
H6 B. G. Hogg and H. E. Duckworth, Can. J. Phys **30** (1952) 637
H7 J. S. Geiger, B. G. Hogg, H. E. Duckworth and J. W. Dedwney, Phys. Rev. **89** (1953) 621
H8 B. G. Hogg and H. E. Duckworth, Can. J. Phys. **32** (1954) 65
H9 J. T. Kerr, unpublished
H10 E. M. Pennington, unpublished

* Asterisks added to the reference numbers indicate that the doublet shown is the combination of two measured doublets, e.g. $(^{94}Mo - ^{94}Zr) = (^{188}Os^{++} - ^{94}Zr) - (^{188}Os^{++} - ^{94}Mo)$.

TABLE 1b

Secondary mass spectroscopical data

Doublet	Measured value μMU ($^{16}O = 16$)	Lab.	Adopted value μu
$^{96}Zr - {}^{96}Mo$	3 630 ± 280	H7*	3 600 ± 700
$^{96}Ru - {}^{96}Mo$	3 020 210	"	3 000 600
$^{12}C_7{}^{1}H_{14} - {}^{98}Ru$	204 133 297	H10*	204 100 800
$^{12}C_8{}^{1}H_8 - {}^{104}Ru$	157 126 150	H6	157 080 400
$^{12}C_8{}^{1}H_{14} - {}^{110}Pd$	205 120 120	M7	205 050 320
$^{12}C_8{}^{1}H_{10} - {}^{106}Cd$	172 360 140	"	172 310 370
$^{12}C_6{}^{16}O_2{}^{1}H_{12} - {}^{116}Cd$	178 780 120	"	178 720 320
$^{12}C_9{}^{1}H_{12} - {}^{120}Te$	189 450 150	"	189 390 400
$^{12}C_{10}{}^{1}H_4 - {}^{124}Xe$	125 220 60	"	125 180 160
$^{12}C_{10}{}^{1}H_{14} - {}^{134}Xe$	204 220 3	M12	204 155 8
$^{12}C_{10}{}^{1}H_{16} - {}^{136}Xe$	218 051 4	"	217 982 11
$^{12}C_{10}{}^{1}H_{12} - {}^{132}Ba$	188 840 120	M10	188 780 320
$^{12}C_9{}^{13}C{}^{1}H_{14} - {}^{135}Ba$	207 400 100	"	207 330 260
$^{12}C_{10}{}^{1}H_{16} - {}^{136}Ce$	218 190 200	"	218 100 500
$^{12}C_8{}^{13}C_2{}^{19}F{}^{1}H_7 - {}^{148}Nd$	143 460 60	"	143 410 160
$^{12}C_{10}{}^{19}F{}^{1}H_5 - {}^{144}Sm$	125 920 90	"	125 880 240
$^{160}Gd - {}^{80}Se_2$	94 300 200	H8	94 300 500
$^{170}Er - {}^{85}Rb_2$	111 700 800	"	111 700 2 100
$^{186}W - {}^{93}Nb_2$	139 400 600	H9	139 400 1 600

In the above table the first column denotes the mass-spectroscopic doublet. The second one gives the measured value and its error in μMU ($^{16}O = 16$). As to the indication of the laboratory in the third column see the text below table 1a. The fourth column contains in μu the adopted value and its error.

TABLE 2a

Primary Reaction and Decay Energies

Nuclear reaction or decay	Measured value keV	Ref.	Adjusted value keV	$\frac{v}{\sigma}$
$^{71}Ga(\gamma,n)^{70}Ga$	−9 240 ± 60	59-2-42,60Ge1	−9 195 ± 47	−0.7615
$^{71}Ga(n,\gamma)^{72}Ga$	6 971 17	57C28	6 967 17	0.2206
$^{72}Ga\ (\beta^-)^{72}Ge$	3 990 10	59-1-28*	3 989 10	0.1298
$^{73}Ge(\gamma,n)^{72}Ge$	−6 500 160	59-1-31*	−6 570 80	0.4314
$^{75}Ge(\beta^-)^{75}As$	1 180 20	59-1-41*	1 178 20	0.0754
$^{76}Ge(\gamma,n)^{75}Ge$	−9 300 200	55Da	−9 450 90	0.7536
$^{74}As(\beta^+)^{74}Ge$	2 562 10	59-4-71*	2 564 10	−0.2266
$^{74}As(\beta^-)^{74}Se$	1 360 10	59-4-71	1 360 10	0.0327
$^{75}As(\gamma,n)^{74}As$	−10 257 29	59-1-46,60Ge1	−10 240 27	−0.5751
$^{75}As(n,\gamma)^{76}As$	7 300 40	59-5-41	7 290 34	0.2422
$^{75}As(p,n)^{75}Se$	−1 648 2	59-1-48	−1 648.0 2.0	0.0068
$^{76}As(\beta^-)^{76}Se$	2 970 10	59-5-39	2 969 10	0.0605
$^{76}Se(n,\gamma)^{77}Se$	7 416 9	59-3-48	7 415 9	0.1470
$^{77}Se(n,\gamma)^{78}Se$	10 483 14	59-5-51	10 480 14	0.2277
$^{78}Se(p,n)^{78}Br$	−4 450 200	59-5-52*	−4 250 70	−1.0130
$^{79}Se(\beta^-)^{79}Br$	160 5	59-2-50	161 5	−0.1218
$^{81}Se(\beta^-)^{81}Br$	1 400 50	59-1-64	1 410 49	−0.2047
$^{82}Se(\gamma,n)^{81}Se$	−9 350 200	59-1-69	−9 190 80	−0.8188
$^{78}Br(\beta^+)^{78}Se$	3 420 80	59-5-52*	3 470 70	−0.5676
$^{79}Br(\gamma,n)^{78}Br$	−10 650 150	59-2-51*	−10 600 80	−0.3045
$^{79}Br(n,\gamma)^{80}Br$	7 879 13	59-1-58	7 892 12	−0.9860
$^{80}Br(\beta^+)^{80}Se$	1 888 6	59-1-56	1 889 6	−0.2026
$^{80}Br(\beta^-)^{80}Kr$	2 000 10	59-1-56	2 005 10	−0.5278
$^{81}Br(\gamma,n)^{80}Br$	−10 130 35	60Ge1	−10 117 32	−0.3745
$^{78}Kr(d,p)^{79}Kr$	5 980 50	59-2-53	6 106 19	−2.5241
$^{79}Kr(\beta^+)^{79}Br$	1 620 5	59-2-52	1 621 5	−0.2524
$^{80}Kr(d,p)^{81}Kr$	5 630 100	58-1-39*	5 640 90	−0.1132
$^{81}Kr(\varepsilon)^{81}Br$	200 200	a	250 90	−0.2265
$^{86}Kr(d,p)^{87}Kr$	3 300 50	60-3-60	3 281 49	0.3706
$^{87}Kr(\beta^-)^{87}Rb$	4 200 200	60-3-60*	3 900 90	1.4824
$^{84}Rb(\beta^+)^{84}Kr$	2 652 5	58-3-38	2 652 5	−0.0677
$^{84}Rb(\beta^-)^{84}Sr$	909 8	58-3-38	909 8	−0.0063
$^{85}Rb(\gamma,n)^{84}Rb$	−10 580 57	60-3-41	−10 530 50	−0.8040
$^{85}Rb(p,n)^{85}Sr$	−1 890 30	60-3-42	−1 890 30	0.0139
$^{86}Rb(\beta^-)^{86}Sr$	1 772 5	60-3-50*	1 772 5	−0.0167
$^{87}Rb(\beta^-)^{87}Sr$	272 2	60-3-61*	272.3 2.4	−0.1356
$^{87}Rb(\gamma,n)^{86}Rb$	−9 924 41	60-3-61	−9 918 17	−0.1398

TABLE 2a
(Continued)

Nuclear reaction or decay	Measured value, keV		Ref.	Adjusted value keV		$\frac{v}{\sigma}$
$^{87}Rb(d,p)^{88}Rb$	3 750	± 200	60-3-71	3 970	± 80	-1.1219
$^{88}Rb(\beta^-)^{88}Sr$	5 170	70	60-3-71*	5 200	70	-0.3927
$^{86}Sr(\gamma,n)^{85}Sr$	-11 500	300	60-3-52*	-11 460	90	-0.1394
$^{86}Sr\ (n,\gamma)^{87}Sr$	8 417	18	60-3-62*	8 418	16	-0.0809
$^{87}Sr(n,\gamma)^{88}Sr$	11 140	50	60-3-72	11 124	47	0.3139
$^{88}Sr(d,p)^{89}Sr$	4 260	70	60-3-83*	4 545	41	-4.0781
$^{89}Sr(\beta^-)^{89}Y$	1 463	10	60-3-83	1 469	10	-0.5826
$^{88}Y(\beta^+)^{88}Sr$	3 442	10	60-3-73*	3 447	10	-0.4589
$^{89}Y(\gamma,n)^{88}Y$	-11 820	50	60-3-84*	-11 686	40	-2.6881
$^{89}Y(n,\gamma)^{90}Y$	6 849	9	60-4-35	6 848	9	0.1133
$^{90}Y(\beta^-)^{90}Zr$	2 260	10	60-4-34*	2 259	10	0.1259
$^{89}Zr(\beta^+)^{89}Y$	2 843	7	60-3-85*	2 842	7	0.1458
$^{90}Zr(\gamma,n)^{89}Zr$	-11 780	90	60-4-36	-11 949	15	1.8745
$^{90}Zr(d,p)^{91}Zr$	4 960	50	T	4 981	49	-0.4142
$^{91}Zr(n,\gamma)^{92}Zr$	8 660	40	T	8 683	36	-0.5835
$^{91}Zr(d,p)^{92}Zr$	6 500	100	T	6 459	36	0.4137
$^{92}Zr(p,n)^{92}Nb$	-2 500	200	T	-2 860	50	1.7833
$^{92}Zr(d,p)^{93}Zr$	4 430	40	58-9-23	4 457	37	-0.6637
$^{93}Zr(\beta^-)^{93}Nb$	63	2	58-9-23	63.1	2.0	-0.0332
$^{94}Zr(d,p)^{95}Zr$	4 190	50	58-7-24	4 190	50	0.0339
$^{95}Zr(\beta^-)^{95}Nb$	1 122	5	58-7-23*	1 122	5	0.0034
$^{91}Nb(\varepsilon)^{91}Zr$	1 400	300	55Ha	1 590	110	-0.6496
$^{92}Nb(\beta^+)^{92}Zr$	2 140	150	59W30	2 070	50	0.4396
$^{93}Nb(\gamma,n)^{92}Nb$	-8 827	38	58-9-24,60Ge1	-8 818	37	-0.2268
$^{93}Nb(n,\gamma)^{94}Nb$	7 190	30	58-9-37	7 189	30	0.0204
$^{93}Nb(p,n)^{93}Mo$	-1 270	40	58-9-26	-1 265	40	-0.1195
$^{94}Nb(\beta^-)^{94}Mo$	2 070	50	58-9-35	2 070	50	0.0339
$^{95}Nb(\beta^-)^{95}Mo$	927	4	58-2-27*	927.0	4.0	0.0027
$^{91}Mo(\beta^+)^{91}Nb$	4 440	40	58-1-44	4 443	40	-0.0866
$^{92}Mo(\gamma,n)^{91}Mo$	-13 150	80	T	-13 140	80	-0.1732
$^{92}Mo(d,p)^{93}Mo$	5 630	50	58-9-26	5 623	49	0.1494
$^{95}Mo(n,\gamma)^{96}Mo$	9 160	10	58-5-26	9 160	10	0.0068
$^{96}Mo(d,p)^{97}Mo$	4 510	300	58-9-49	4 730	210	-0.7335
$^{97}Mo(\gamma,n)^{96}Mo$	- 7 100	300	58-9-49	-6 950	210	-0.4841
$^{97}Mo(d,p)^{98}Mo$	6 060	100	58-7-35	6 070	100	-0.0831
$^{99}Mo(\beta^-)^{99}Tc$	1 380	10	58-3-43	1 380	10	0.0278
$^{100}Mo(\gamma,n)^{99}Mo$	-8 100	300	58-7-48	-8 350	280	0.8330
$^{99}Tc(\beta^-)^{99}Ru$	293	2	58-3-45	293.0	2.0	0.0056

TABLE 2a
(Continued)

Nuclear reaction or decay	Measured value keV	Ref.	Adjusted value keV	$\frac{v}{\sigma}$
$^{102}Rh(\beta^-)^{102}Pd$	1 130 ± 20	58-10-50*	1 131 ± 20	-0.0297
$^{103}Rh(\gamma,n)^{102}Rh$	-9 328 30	58-10-59,60Ge1	-9 327 30	-0.0403
$^{103}Rh(n,\gamma)^{104}Rh$	6 792 14	58-9-64	6 792 14	0.0208
$^{104}Rh(\beta^-)^{104}Pd$	2 440 30	58-9-62	2 439 30	0.0446
$^{105}Pd(\gamma,n)^{104}Pd$	-7 200 300	58-11-61	-7 070 240	-0.4461
$^{106}Ag(\beta^+)^{106}Pd$	2 970 10	60-4-52*	2 970 10	-0.0261
$^{107}Ag(\gamma,n)^{106}Ag$	-9 393 28	58-5-46*,60Ge1	-9 391 28	-0.0682
$^{107}Ag(n,\gamma)^{108}Ag$	7 270 20	58-3-53	7 213 9	2.8600
$^{107}Ag(d,p)^{108}Ag$	4 974 10	58-3-53*	4 988 9	-1.4090
$^{108}Ag(\beta^+)^{108}Pd$	1 820 50	58-3-51	1 837 49	-0.3354
$^{108}Ag(\beta^-)^{108}Cd$	1 770 60	58-3-51	1 770 60	0.0784
$^{109}Ag(\gamma,n)^{108}Ag$	-9 184 23	60-2-55*	-9 180 23	-0.1699
$^{109}Ag(d,p)^{110}Ag$	4 591 5	60-2-69*	4 591 5	0.0241
$^{109}Ag(\alpha,2n)^{111}In$	-14 300 200	53Ba	-14 440 180	0.6942
$^{110}Ag(\beta^-)^{110}Cd$	2 875 15	60-2-65*	2 874 15	0.0723
$^{111}Cd(p,n)^{111}In$	-2 330 300	51Ga, b	-2 020 210	-1.0413
$^{112}Cd(d,p)^{113}Cd$	4 100 90	60-2-104	4 190 70	-1.0156
$^{113}Cd(\beta^-)^{113}In$	310 10	60-2-103	310 10	0.0079
$^{113}Cd(\gamma,n)^{112}Cd$	-6 480 130	60-2-104	-6 420 70	-0.4914
$^{113}Cd(n,\gamma)^{114}Cd$	9 046 8	60-3-94	9 046 8	-0.0481
$^{114}In(\beta^+)^{114}Cd$	1 420 20	60-3-96*	1 420 20	-0.0105
$^{115}In(\beta^-)^{115}Sn$	500 20	60-3-110	500 20	-0.0081
$^{115}In(\gamma,n)^{114}In$	-9 025 28	60-3-111	-9 025 27	-0.0007
$^{115}In(d,p)^{116}In$	4 430 200	60-3-124*	4 380 170	0.2300
$^{116}In(\beta^-)^{116}Sn$	3 290 60	60-3-121	3 290 60	0.0690
$^{117}Sn(d,p)^{118}Sn$	7 140 200	60-3-144	7 030 130	0.5667
$^{118}Sn(\gamma,n)^{117}Sn$	-9 100 200	60-3-144	-9 250 130	0.7568
$^{119}Sn(\gamma,n)^{118}Sn$	-6 540 130	60-4-61	-6 590 120	0.3635
$^{120}Sn(d,p)^{121}Sn$	3 920 70	60-4-78	3 954 46	-0.4789
$^{121}Sn(\beta^-)^{121}Sb$	383 5	60-4-78	383 5	-0.0342
$^{123}Sn(\beta^-)^{123}Sb$	1 420 10	58-7-57	1 420 10	-0.0125
$^{124}Sn(\gamma,n)^{123}Sn$	-8 500 150	58-6-22	-8 470 120	-0.1878
$^{124}Sn(d,p)^{125}Sn$	3 520 70	58-7-63	3 510 70	0.0881
$^{125}Sn(\beta^-)^{125}Sb$	2 340 10	58-7-63	2 340 10	0.0126
$^{120}Sb(\beta^+)^{120}Sn$	2 720 20	60-4-70	2 723 20	-0.1277
$^{121}Sb(\gamma,n)^{120}Sb$	-9 305 57	60-4-79	-9 284 45	-0.3691
$^{121}Sb(n,\gamma)^{122}Sb$	6 800 40	60-4-90*	6 801 40	-0.0183
$^{122}Sb(\beta^+)^{122}Sn$	1 590 30	60-4-88	1 590 30	0.0129
$^{122}Sb(\beta^-)^{122}Te$	1 971 4	60-4-88	1 971.0 4.0	-0.0086

TABLE 2a

(Continued)

Nuclear reaction or decay	Measured value keV	Ref.	Adjusted value keV	$\frac{v}{\sigma}$
$^{123}Sb(\gamma,n)^{122}Sb$	−8 980 ± 50	60Ge1	−8 976 ± 48	−0.0833
$^{125}Sb(\beta^-)^{125}Te$	757 6	58-7-65	757 6	0.0075
$^{123}Te(n,\gamma)^{124}Te$	9 400 10	59Ba	9 400 10	−0.0272
$^{124}Te(d,p)^{125}Te$	4 250 70	58-7-67	4 296 43	−0.6589
$^{125}Te(\gamma,n)^{124}Te$	−6 560 60	60Ge1	−6 521 43	−0.6527
$^{126}I(\beta^+)^{126}Te$	2 130 20	58-6-29	2 115 20	0.7504
$^{126}I(\beta^-)^{126}Xe$	1 251 5	58-6-29	1 251 5	0.0112
$^{127}I(\gamma,n)^{126}I$	−9 136 20	58-8-5,60Ge1	−9 152 20	0.7968
$^{127}I(n,\gamma)^{128}I$	6 710 20	59B05	6 706 18	0.1901
$^{127}I(d,p)^{128}I$	4 350 50	58-8-13	4 481 18	−2.6298
$^{128}I(\beta^-)^{128}Xe$	2 121 8	58-2-44	2 124 8	−0.3596
$^{130}I(\varepsilon)^{130}Te$	300 200	59-3-53*, c	−10 130	1.5630
$^{130}I(\beta^-)^{130}Xe$	2 950 30	59-3-53	2 957 30	−0.2344
$^{130}Cs(\beta^+)^{130}Xe$	2 990 20	58-6-36	2 991 20	−0.0429
$^{130}Cs(\beta^-)^{130}Ba$	442 4	58-6-36	442.0 4.0	0.0086
$^{133}Cs(d,p)^{134}Cs$	4 500 100	58-8-37	4 510 90	−0.1320
$^{134}Cs(\beta^-)^{134}Ba$	2 055 2	58-8-34	2 055.0 2.0	−0.0026
$^{137}Ba(\gamma,n)^{136}Ba$	−6 949 38	60Ge1	−6 950 38	0.0195
$^{138}Ba(d,p)^{139}Ba$	2 495 10	58-10-71*	2 495 10	−0.0224
$^{139}Ba(\beta^-)^{139}La$	2 380 20	58-10-70	2 381 19	−0.0449
$^{138}La(\varepsilon)^{138}Ba$	1 650 50	58-8-63*, d	1 676 27	−0.5278
$^{138}La(\beta^-)^{138}Ce$	1 015 15	58-8-63	1 015 15	0.0181
$^{139}La(\gamma,n)^{138}La$	−8 782 22	58-10-72,60Ge1	−8 777 21	−0.2173
$^{139}La(d,p)^{140}La$	2 870 100	59-1-92	2 790 70	0.7659
$^{140}La(\beta^-)^{140}Ce$	3 780 30	59-1-89*	3 773 29	0.2298
$^{139}Ce(\varepsilon)^{139}La$	270 6	58-10-73	270 6	0.0017
$^{140}Ce(\gamma,n)^{139}Ce$	−9 050 200	59-1-93	−9 060 70	0.0561
$^{140}Ce(d,p)^{141}Ce$	3 170 100	58-10-82	3 304 27	−1.3383
$^{141}Ce(\beta^-)^{141}Pr$	580 5	58-10-81	580 5	−0.0710
$^{142}Ce(\gamma,n)^{141}Ce$	−7 150 200	59-1-100	−7 120 70	−0.1623
$^{142}Ce(d,p)^{143}Ce$	2 860 70	58-11-71	2 920 60	−0.9284
$^{142}Ce(\alpha)^{138}Ba$	1 545 200	59-1-100	1 320 90	1.1144
$^{143}Ce(\beta^-)^{143}Pr$	1 440 10	58-11-70	1 441 10	−0.1326
$^{140}Pr(\beta^+)^{140}Ce$	3 250 20	59-1-94	3 259 19	−0.4636
$^{141}Pr(\gamma,n)^{140}Pr$	−9 378 21	58-10-83,60Ge1	−9 368 20	−0.4682
$^{141}Pr(n,\gamma)^{142}Pr$	5 830 30	59-1-102	5 836 28	−0.1866
$^{142}Pr(\beta^-)^{142}Nd$	2 153 8	59-1-101	2 153 8	−0.0498
$^{143}Pr(\beta^-)^{143}Nd$	933 5	58-11-72	933 5	−0.0663
$^{142}Nd(d,p)^{143}Nd$	3 790 80	58-11-73	3 850 50	−0.7230

TABLE 2a
(Continued)

Nuclear reaction or decay	Measured value keV	Ref.	Adjusted value keV	$\frac{v}{\sigma}$
$^{143}Nd(n,\gamma)^{144}Nd$	7 814 ± 8	59Ba	7 814 ± 8	-0.0014
$^{144}Nd(\alpha)^{140}Ce$	1 905 100	59-1-114	1 880 50	0.2920
$^{145}Nd(n,\gamma)^{146}Nd$	7 580 10	59Ba	7 580 10	0.0039
$^{149}Nd(\beta^-)^{149}Pm$	1 600 100	58-12-9	1 640 90	-0.3735
$^{150}Nd(\gamma,n)^{149}Nd$	-7 400 200	59-2-57	-7 250 150	-0.7470
$^{149}Pm(\beta^-)^{149}Sm$	1 050 50	58-12-10	1 059 49	-0.1868
$^{146}Sm(\alpha)^{142}Nd$	2 625 50	59-1-130	2 620 50	0.0396
$^{147}Sm(\alpha)^{143}Nd$	2 241 25	59-1-139	2 228 24	0.5370
$^{149}Sm(\gamma,n)^{148}Sm$	-5 890 160	60Ge1	-5 860 100	-0.1828
$^{149}Sm(n,\gamma)^{150}Sm$	8 000 30	59-2-63	8 002 29	-0.0656
$^{154}Sm(d,p)^{155}Sm$	3 360 300	54We	3 520 250	-0.5357
$^{155}Sm(\beta^-)^{155}Eu$	1 750 100	59-3-77	1 770 100	-0.1786
$^{150}Eu(\beta^-)^{150}Gd$	1 070 10	59-2-61	1 070 10	0.0079
$^{151}Eu(\gamma,n)^{150}Eu$	-8 040 110	60Ge1	-8 050 110	0.0870
$^{152}Eu(\beta^+)^{152}Sm$	1 860 7	59-4-82	1 860 7	0.0008
$^{153}Eu(\gamma,n)^{152}Eu$	-8 650 130	60Ge1	-8 650 130	0.0148
$^{155}Eu(\beta^-)^{155}Gd$	243 4	59-3-78*	243.0 4.0	-0.0071
$^{150}Gd(\alpha)^{146}Sm$	2 770 150	59-2-62	2 750 140	0.1187
$^{155}Gd(n,\gamma)^{156}Gd$	7 780 50	59-5-60	7 859 47	-1.5802
$^{157}Gd(\gamma,n)^{156}Gd$	-6 390 110	60Ge1	-6 390 90	0.0209
$^{157}Gd(n,\gamma)^{158}Gd$	7 926 8	59Ba, 59-3-85	7 926 8	-0.0093
$^{163}Dy(\gamma,n)^{162}Dy$	-6 320 110	60Ge1	-6 300 90	-0.1914
$^{164}Ho(\beta^-)^{164}Er$	990 30	59-5-129	989 30	0.0356
$^{165}Ho(\gamma,n)^{164}Ho$	-8 117 42	59-6-106	-8 119 42	0.0473
$^{165}Ho(n,\gamma)^{166}Ho$	6 200 400	59N20	6 370 380	-0.4135
$^{166}Ho(\beta^-)^{166}Er$	1 847 5	58-9-82	1 847 5	-0.0052
$^{167}Er(\gamma,n)^{166}Er$	-6 560 80	60Ge1	-6 540 70	-0.2494
$^{177}Hf(\gamma,n)^{176}Hf$	-6 618 32	60-1-112*	-6 602 31	-0.4910
$^{179}Hf(\gamma,n)^{178}Hf$	-6 289 60	60-1-112*	-6 270 60	-0.3002
$^{180}Hf(\gamma,n)^{179}Hf$	-7 480 110	60-1-120*	-7 420 90	-0.5495
$^{180}Ta(\varepsilon)^{180}Hf$	800 400	e	560 350	0.6027
$^{181}Ta(\gamma,n)^{180}Ta$	-7 644 22	60-2-116	-7 645 22	0.0342
$^{181}Ta(n,\gamma)^{182}Ta$	6 070 30	60-1-133*	6 071 30	-0.0452
$^{182}Ta(\beta^-)^{182}W$	1 732 10	60-1-129*	1 732 10	-0.0151
$^{182}W(n,\gamma)^{183}W$	6 182 8	59-6-119*	6 185 8	-0.3797
$^{183}W(\gamma,n)^{182}W$	-6 290 50	59-6-118	-6 185 8	-2.0993
$^{186}Re(\beta^-)^{186}Os$	1 067 2	59-5-136*	1 067.0 2.0	0.0182
$^{187}Re(\beta^-)^{187}Os$	4 4	59-2-105	4.1 4.0	-0.0364
$^{187}Re(\gamma,n)^{186}Re$	-7 180 80	60Ge1	-7 240 70	0.7284

TABLE 2a

(Continued)

Nuclear reaction or decay	Measured value keV	Ref.	Adjusted value keV	$\frac{v}{\sigma}$
$^{192}Ir(\varepsilon)^{192}Os$	1 300 ± 300	59-2-121*, f	1 410 ± 260	-0.3722
$^{192}Ir(\beta^-)^{192}Pt$	1 453 5	59-2-121	1 453 5	-0.0030
$^{193}Ir(\gamma,n)^{192}Ir$	-7 791 49	51Sa, 60Ge1	-7 786 48	-0.0971
$^{192}Pt(\alpha)^{188}Os$	2 660 200	59-2-127	2 680 190	-0.1212
$^{193}Pt(\varepsilon)^{193}Ir$	50 30	58-2-59*	52 30	-0.0554
$^{194}Pt(\gamma,n)^{193}Pt$	-8 200 300	g	-8 030 250	-0.5540
$^{195}Pt(\gamma,n)^{194}Pt$	-6 188 40	58-12-31,60Ge1	-6 178 39	-0.2481
$^{195}Pt(n,\gamma)^{196}Pt$	7 920 12	58-2-60	7 922 12	-0.1695
$^{196}Pt(\gamma,n)^{195}Pt$	-8 290 140	60Ge1	-7 922 12	-2.6283
$^{196}Au(\varepsilon)^{196}Pt$	1 500 300	h	1 790 220	-0.9686
$^{196}Au(\beta^-)^{196}Hg$	700 20	58-1-76	678 17	1.0791
$^{197}Au(\gamma,n)^{196}Au$	-8 046 20	58-10-97,60Ge1	-8 067 17	1.0351
$^{197}Au(n,\gamma)^{198}Au$	6 494 8	58-12-46	6 497 8	-0.4058
$^{198}Au(\varepsilon)^{198}Pt$	360 300	58-12-46, i	660 280	-0.9963
$^{198}Au(\beta^-)^{198}Hg$	1 372 2	58-12-42*	1 372.2 2.0	-0.0948
$^{199}Hg(\gamma,n)^{198}Hg$	-6 590 90	60Ge1	-6 686 19	1.0660

In the above table, the first column indicates the nuclear reaction or decay, the second gives the adopted reaction or decay energy and its error. The fourth column gives the value following from the final adjustment, the fifth one the ratio of the difference between the two preceding values divided by the error in the adopted value (second column). References in the third column have preferably been given to the year, the set and the page numbers of the Nuclear Data Sheets (Nuclear Data Sheets, Nuclear Data Group, Washington D.C., 1958—1960), according to a key number 58—3—27. In cases where the given values do not agree numerically with values given in the sheets for reasons as discussed in the text, an asterisk has been added to this number. More recent references are given below, using where possible the reference key numbers given in the list of "Recent References" of the "Nuclear Data Sheets", and otherwise similar symbols but with a letter instead of the last number. These new references are the following:

51Ga C. L. McGinnis, Phys. Rev. **81** (1951) 734

51Sa R. Sher, J. Halpern and A. K. Mann, Phys. Rev. **84** (1951) 387

53Ba E. Bleuler, A. K. Stebbins and D. J. Tendam, Phys. Rev. **90** (1953) 460

54Wa N. S. Wall, Ph. D. thesis, Massachusetts Institute of Technology (1953) and private communication

55Da de Sousa Santos, Goldenberg, Pieroni, Silva, Borello, Villaca and Lopes, Proc. Int. Conf. on Peaceful Uses of Atomic Energy, Geneva 1955 (United Nations, New York, 1956) vol. II, p. 169

55Ha R. W. Hayward, D. D. Hoppes and H. Ernst, Phys. Rev. **98** (1955) 231

57C28 P. J. Campion and G. A. Bartholomew, Can. J. Phys. **35** (1957) 1361

59Ba G. A. Bartholomew, private communication

59B05 R. Balzer, H. Knoepfel, J. Lang, R. Müller and P. Stoll, Nuovo Cim. **11** (1959) 609

59N20 J. H. Neiler, R. L. Macklin, J. H. Gibbons and P. D. Miller, Bull. Am. Phys. Soc. **4** (1959) 43R9

59W30 H. I. West, Jr., L. G. Mann and G. M. Iddings, Phys. Rev. **113** (1959) 881

60Ge1 K. N. Geller, J. Halpern and E. G. Muirhead, Phys. Rev. **118** (1960) 1302

T K. Way, R. W. King, C. L. McGinnis and R. van Lieshout, Nuclear Level Schemes $A = 40$ to 92, TID 5 300 (1955)

59-8-43 K. Way, G. Anderson, F. Everling, G. H. Fuller, N. B. Gove, R. Levesque, J. B. Marion, C. L. McGinnis, R. Nakasima, and M. Yamada, Nuclear Data Sheets, National Academy of Sciences-National Research Council, Washington 25 D.C. (1958—1960), indicated by year, set and page numbers.

a $\log \frac{1}{12} q^2 ft = 8.5$ yields $Q_K = 200$ keV. The error given is very liberal (200 ± 200).

b Value given by 51Ga not corrected for recoil.

c Value estimated from β-decay systematics. Not adopting this value would make ^{130}Te β^--instable by about 1 MeV.

d Value computed from percentage K-capture making a correction for capture in the M, N . . . shells not made by the author.

e Not adding this value would make Q negative.

f Estimated from log ft value.

g Estimated from neutron binding energy systematics instead of reported value $9\,500 \pm 200$ which is much to high.

h The reported value 911^{+55}_{-25} (G. K. Gupta, Proc. Phys. Soc. **71** (1958) 330) has not been corrected for capture in the M, N . . . shells. After such a correction it would become $1050 \pm ^{180}_{80}$ keV. Even this value looks quite low in the β-decay energy systematics. Therefore the value in the table has been adopted.

i Estimated from lower limit of partial halflife for electron capture.

TABLE 2b

Secondary Reaction and Decay Energies

Nuclear reaction or decay	Measured value keV	Ref.	Nuclear reaction or decay	Measured value keV	Ref.
$^{71}Zn\ (\beta^-)\ ^{71}Ga$	2 910 ± 200	59-2-41*	$^{95}Ru\ (\beta^+)\ ^{95}Tc$	2 200 100	58-7-26
$^{72}Zn\ (\beta^-)\ ^{72}Ga$	1 600 200	59-1-27	$^{103}Ru\ (\beta^-)\ ^{103}Rh$	750 10	58-10-56*
$^{73}Ga\ (\beta^-)\ ^{73}Ge$	1 552 40	59-1-37	$^{105}Ru\ (\beta^-)\ ^{105}Rh$	1 905 15	60B13,58-11-59
$^{74}Ga\ (\beta^-)\ ^{74}Ge$	5 600 50	59-4-69	$^{106}Ru\ (\beta^-)\ ^{106}Rh$	38 1	60-4-47
$^{71}Ge\ (\varepsilon)\ ^{71}Ga$	233 3	59-2-43	$^{98}Rh\ (\beta^+)\ ^{98}Ru$	4 200 300	58-7-38
$^{73}Ge\ (p,n)\ ^{73}As$	-1 154 30	59-1-40*	$^{99}Rh\ (\beta^+)\ ^{99}Ru$	2 100 20	58-7-44
$^{77}Ge\ (\beta^-)\ ^{77}As$	2 750 50	59-3-44	$^{102}Rh\ (\beta^+)\ ^{102}Ru$	2 270 20	58-10-50
$^{78}Ge\ (\beta^-)\ ^{78}As$	900 100	59-5-49*	$^{103}Rh\ (\alpha,2n)\ ^{105}Ag$	-15 600 500	58-11-63
$^{71}As\ (\beta^+)\ ^{71}Ge$	2 009 7	59-2-45	$^{105}Rh\ (\beta^-)\ ^{105}Pd$	565 3	58-11-60*
$^{72}As\ (\beta^+)\ ^{72}Ge$	4 360 30	59-1-32*	$^{106}Rh\ (\beta^-)\ ^{106}Pd$	3 530 10	60-4-48
$^{77}As\ (\beta^-)\ ^{77}Se$	684 9	59-3-46	$^{107}Rh\ (\beta^-)\ ^{107}Pd$	1 500 50	58-5-44
$^{78}As\ (\beta^-)\ ^{78}Se$	4 100 100	59-5-50*	$^{99}Pd\ (\beta^+)\ ^{99}Rh$	3 800 200	58-7-46
$^{79}As\ (\beta^-)\ ^{79}Se$	2 300 100	59-2-49	$^{103}Pd\ (\varepsilon)\ ^{103}Rh$	560 30	58-10-60
$^{80}As\ (\beta^-)\ ^{80}Se$	6 000 200	59I a	$^{107}Pd\ (\beta^-)\ ^{107}Ag$	35 1	58-1-45
$^{71}Se\ (\beta^+)\ ^{71}As$	4 400 300	59-2-46	$^{109}Pd\ (\beta^-)\ ^{109}Ag$	1 113 5	60-2-52
$^{73}Se\ (\beta^+)\ ^{73}As$	2 750 10	59-1-41	$^{111}Pd\ (\beta^-)\ ^{111}Ag$	2 200 40	60-2-81*
$^{77}Se\ (p,n)\ ^{77}Br$	-2 147 4	59-3-49	$^{112}Pd\ (\beta^-)\ ^{112}Ag$	300 20	60-2-92
$^{83}Se\ (\beta^-)\ ^{83}Br$	3 450 90	59C51	$^{104}Ag\ (\beta^+)\ ^{104}Pd$	4 280 10	58-5-32
$^{75}Br\ (\beta^+)\ ^{75}Se$	2 722 20	59-1-51*	$^{111}Ag\ (\beta^-)\ ^{111}Cd$	1 050 10	60-2-82
$^{76}Br\ (\beta^+)\ ^{76}Se$	4 590 10	59-5-43*	$^{112}Ag\ (\beta^-)\ ^{112}Cd$	4 040 30	60-2-93
$^{82}Br\ (\beta^-)\ ^{82}Kr$	3 092 2	59-1-70	$^{113}Ag\ (\beta^-)\ ^{113}Cd$	2 000 40	60-2-102
$^{83}Br\ (\beta^-)\ ^{83}Kr$	1 000 20	59-1-80	$^{114}Ag\ (\beta^-)\ ^{114}Cd$	4 600 ± 400	60-3-92*
$^{84}Br\ (\beta^-)\ ^{84}Kr$	4 700 50	58-3-37*	$^{115}Ag\ (\beta^-)\ ^{115}Cd$	2 900 300	60-3-107
$^{85}Br\ (\beta^-)\ ^{85}Kr$	2 800 100	60-3-39	$^{107}Cd\ (\beta^+)\ ^{107}Ag$	1 440 10	58-5-47
$^{87}Br\ (\beta^-)\ ^{87}Kr$	8 000 400	60-3-59	$^{109}Cd\ (\varepsilon)\ ^{109}Ag$	158 4	60-2-56
$^{77}Kr\ (\beta^+)\ ^{77}Br$	2 880 20	59-3-51*	$^{112}Cd\ (p,n)\ ^{112}In$	-3 410 20	60-2-95*
$^{85}Kr\ (\beta^-)\ ^{85}Rb$	675 7	60-3-40*	$^{115}Cd\ (\beta^-)\ ^{115}In$	1 450 10	60-3-108
$^{88}Kr\ (\beta^-)\ ^{88}Rb$	2 800 200	60-3-70	$^{117}Cd\ (\beta^-)\ ^{117}In$	2 540 300	60-3-134*
$^{80}Rb\ (\beta^+)\ ^{80}Kr$	5 100 500	59-1-59	$^{108}In\ (\beta^+)\ ^{108}Cd$	5 100 100	58-3-55
$^{81}Rb\ (\beta^+)\ ^{81}Kr$	2 240 30	58-1-40	$^{109}In\ (\beta^+)\ ^{109}Cd$	2 020 10	60-2-57
$^{82}Rb\ (\beta^+)\ ^{82}Kr$	4 170 30	59-1-74	$^{110}In\ (\beta^+)\ ^{110}Cd$	3 960 40	60-2-75
$^{89}Rb\ (\beta^-)\ ^{89}Sr$	3 920 50	60-3-82	$^{112}In\ (\beta^+)\ ^{112}Cd$	2 540 50	60-2-95
$^{87}Sr\ (p,n)\ ^{87}Y$	-2 470 200	60-3-63*	$^{112}In\ (\beta^-)\ ^{112}Sn$	656 6	60-2-95
$^{90}Sr\ (\beta^-)\ ^{90}Y$	535 7	T	$^{114}In\ (\beta^-)\ ^{114}Sn$	1 985 4	60-3-96*
$^{91}Sr\ (\beta^-)\ ^{91}Y$	2 670 10	T	$^{117}In\ (\beta^-)\ ^{117}Sn$	1 470 10	60-3-135
$^{92}Sr\ (\beta^-)\ ^{92}Y$	1 920 40	57H a	$^{111}Sn\ (\beta^+)\ ^{111}In$	2 520 30	60-2-86*
$^{86}Y\ (\beta^+)\ ^{86}Sr$	6 010 50	60-3-53*	$^{113}Sn\ (\varepsilon)\ ^{113}In$	684 4	60-2-106
$^{91}Y\ (\beta^-)\ ^{91}Zr$	1 549 4	T	$^{116}Sb\ (\beta^+)\ ^{116}Sn$	4 700 300	60-3-127
$^{92}Y\ (\beta^-)\ ^{92}Zr$	3 600 50	T	$^{117}Sb\ (\beta^+)\ ^{117}Sn$	1 820 30	60-3-137
$^{93}Y\ (\beta^-)\ ^{93}Zr$	2 890 ± 20	58-9-22	$^{119}Sb\ (\varepsilon)\ ^{119}Sn$	579 20	60-4-62
$^{94}Y\ (\beta^-)\ ^{94}Zr$	5 000 200	58-9-33	$^{124}Sb\ (\beta^-)\ ^{124}Te$	2 916 3	58-6-23
$^{87}Zr\ (\beta^+)\ ^{87}Y$	3 510 20	60-3-64*	$^{127}Sb\ (\beta^-)\ ^{127}Te$	1 600 50	58-8-3*
$^{97}Zr\ (\beta^-)\ ^{97}Nb$	2 660 30	58-9-47	$^{127}Te\ (\beta^-)\ ^{127}I$	689 7	58-8-4
$^{89}Nb\ (\beta^+)\ ^{89}Zr$	3 880 100	60-3-86*	$^{129}Te\ (\beta^-)\ ^{129}I$	1 480 5	58-8-19
$^{90}Nb\ (\beta^+)\ ^{90}Zr$	6 117 30	60-4-37*	$^{131}Te\ (\beta^-)\ ^{131}I$	2 280 20	58-2-45
$^{96}Nb\ (\beta^-)\ ^{96}Mo$	3 130 30	58-7-29	$^{132}Te\ (\beta^-)\ ^{132}I$	505 15	58-8-27*
$^{97}Nb\ (\beta^-)\ ^{97}Mo$	1 932 7	58-9-48	$^{120}I\ (\beta^+)\ ^{120}Te$	5 000 200	60-4-72*
$^{90}Mo\ (\beta^+)\ ^{90}Nb$	2 540 100	60-4-40*	$^{122}I\ (\beta^+)\ ^{122}Te$	4 140 40	60-4-92
$^{96}Mo\ (p,n)\ ^{96}Tc$	-3 760 300	58-7-31*	$^{124}I\ (\beta^+)\ ^{124}Te$	3 190 40	59M122,59B161
$^{91}Tc\ (\beta^+)\ ^{91}Mo$	2 540 100	+	$^{125}I\ (\varepsilon)\ ^{125}Te$	150 30	58-7-68
$^{92}Tc\ (\beta^+)\ ^{92}Mo$	6 400 600	T	$^{129}I\ (\beta^-)\ ^{129}Xe$	189 5	58-4-18
$^{93}Tc\ (\beta^+)\ ^{93}Mo$	3 160 30	58-9-27	$^{131}I\ (\beta^-)\ ^{131}Xe$	970 1	58-6-40
$^{94}Tc\ (\beta^+)\ ^{94}Mo$	4 320 30	58-9-38*	$^{132}I\ (\beta^-)\ ^{132}Xe$	3 570 40	58-4-23
$^{95}Tc\ (\beta^+)\ ^{95}Mo$	1 656 20	58-2-29*	$^{133}I\ (\beta^-)\ ^{133}Xe$	1 900 70	58-6-48
$^{98}Tc\ (\beta^-)\ ^{98}Ru$	1 700 200	58-7-36	$^{136}I\ (\beta^-)\ ^{136}Xe$	7 000 100	58-8-51
$^{102}Tc\ (\beta^-)\ ^{102}Ru$	4 100 300	58-5-28	$^{127}Xe\ (\varepsilon)\ ^{127}I$	700 350	58-8-6,a

TABLE 2b

(Continued)

Nuclear reaction or decay	Measured value keV		Ref.
^{133}Xe (β^-) ^{133}Cs	428	4	58-6-49
^{135}Xe (β^-) ^{135}Cs	1 160	10	58-8-45
^{126}Cs (β^+) ^{126}Xe	4 800	400	58-7-75*
^{127}Cs (β^+) ^{127}Xe	2 085	± 10	58-8-7
^{128}Cs (β^+) ^{128}Xe	4 000	100	58-8-15
^{131}Cs (ε) ^{131}Xe	355	6	58-6-44
^{133}Cs (γ,n) ^{132}Cs	-9 025	28	58-4-25,60Ge1
^{135}Cs (β^-) ^{135}Ba	210	5	58-4-27
^{136}Cs (β^-) ^{136}Ba	2 580	20	59G50
^{137}Cs (β^-) ^{137}Ba	1 176	3	58-6-56
^{138}Cs (β^-) ^{138}Ba	4 830	50	58-8-60*
^{139}Cs (β^-) ^{139}Ba	4 300	200	58-10-69
^{133}Ba (ε) ^{133}Cs	490	3	58G123 b
^{140}Ba (β^-) ^{140}La	1 050	10	59-1-87
^{134}La (β^+) ^{134}Ba	3 700	200	58-8-39
^{136}La (β^+) ^{136}Ba	3 000	200	58-8-55*
^{141}La (β^-) ^{141}Ce	2 430	30	58-10-80
^{144}Ce (β^-) ^{144}Pr	310	4	59-1-111*
^{145}Ce (β^-) ^{145}Pr	2 000	100	59-1-119
^{146}Ce (β^-) ^{146}Pr	1 000	100	59-1-126
^{139}Pr (β^+) ^{139}Ce	2 000	100	58-10-74
^{144}Pr (β^-) ^{144}Nd	2 980	10	59-1-113
^{145}Pr (β^-) ^{145}Nd	1 805	10	59-1-120*
^{146}Pr (β^-) ^{146}Nd	4 200	200	59-1-127
^{141}Nd (β^+) ^{141}Pr	1 800	10	58-10-84
^{147}Nd (β^-) ^{147}Pm	900	10	59-1-136
^{151}Nd (β^-) ^{151}Pm	2 400	100	58-12-17
^{143}Pm (ε) ^{143}Nd	1 100	150	58-11-74 c
^{145}Pm (ε) ^{145}Nd	140	10	59-1-122
^{146}Pm (β^-) ^{146}Sm	750	100	59-1-129
^{147}Pm (β^-) ^{147}Sm	225	3	59-1-138
^{150}Pm (β^-) ^{150}Sm	3 800	400	59-2-58
^{151}Pm (β^-) ^{151}Sm	1 800	100	58-12-18
^{143}Sm (β^+) ^{143}Pm	3 500	200	58-11-75 c
^{145}Sm (ε) ^{145}Pm	645	15	59-1-123
^{151}Sm (β^-) ^{151}Eu	76	1	58-12-19*
^{153}Sm (β^-) ^{153}Eu	803	5	59-3-57
^{147}Eu (α) ^{143}Pm	2 960	100	59-1-140*
^{152}Eu (β^-) ^{152}Gd	1 810	10	59-4-82
^{154}Eu (β^-) ^{154}Gd	1 970	20	59-3-67
^{156}Eu (β^-) ^{156}Gd	2 540	50	59-5-59*
^{157}Eu (β^-) ^{157}Gd	1 700	100	59-3-84
^{148}Gd (α) ^{144}Sm	3 250	100	58-12-6*
^{149}Gd (α) ^{145}Sm	3 090	± 150	58-12-12*
^{153}Gd (ε) ^{153}Eu	210	20	59-3-60*
^{159}Gd (β^-) ^{159}Tb	944	7	59-5-71*
^{161}Gd (β^-) ^{161}Tb	2 000	70	59-5-101
^{151}Tb (α) ^{147}Eu	3 530	100	58-12-22
^{159}Tb (γ,n) ^{158}Tb	-8 148	31	60Ge1,59-5-72
^{159}Tb (n,γ) ^{160}Tb	6 500	400	59-5-89
^{160}Tb (β^-) ^{160}Dy	1 820	10	59-5-83*
^{161}Tb (β^-) ^{161}Dy	580	20	59-5-102
^{152}Dy (α) ^{148}Gd	3 760	80	59-4-91*
^{153}Dy (α) ^{149}Gd	3 577	50	59-3-62
^{154}Dy (α) ^{150}Gd	3 464	40	59-3-73
^{159}Dy (ε) ^{159}Tb	380	20	59K28
^{165}Dy (β^-) ^{165}Ho	1 250	20	59-6-103*
^{166}Dy (β^-) ^{166}Ho	500	5	59H48
^{165}Ho (γ,2n) ^{163}Ho	-15 900	500	59-6-106
^{167}Ho (β^-) ^{167}Er	1 000	100	59-2-66
^{166}Tm (β^+) ^{166}Er	3 100	300	58-9-87
^{177}Yb (β^-) ^{177}Lu	1 380	50	59-3-101
^{176}Lu (β^-) ^{176}Hf	1 020	20	58-2-49
^{177}Lu (β^-) ^{177}Hf	497	2	59-3-102
^{181}Hf (β^-) ^{181}Ta	1 025	3	60-2-113*
^{183}Hf (β^-) ^{183}Ta	2 200	200	59-6-116*
^{177}Ta (ε) ^{177}Hf	1 150	50	59-3-106
^{180}Ta (β^-) ^{180}W	700	20	60-1-121+
^{183}Ta (β^-) ^{183}W	1 068	10	59-6-117
^{185}Ta (β^-) ^{185}W	1 700	100	59-6-129*
^{181}W (ε) ^{181}Ta	200	40	60-2-118*
^{185}W (β^-) ^{185}Re	430	2	59-6-130*
^{186}W (γ,n) ^{185}W	-7 280	60	59-5-135
^{187}W (β^-) ^{187}Re	1 315	10	59-2-103
^{188}Re (β^-) ^{188}Os	2 116	2	59-3-123
^{185}Os (ε) ^{185}Re	985	7	59-6-134*
^{191}Os (β^-) ^{191}Ir	314	2	60-4-98
^{193}Os (β^-) ^{193}Ir	1 136	5	58-2-57
^{188}Ir (β^+) ^{188}Os	3 000	200	59-3-128
^{191}Ir (n,γ) ^{192}Ir	6 085	15	59B05
^{194}Ir (β^-) ^{194}Pt	2 236	10	58-9-92
^{188}Pt (ε) ^{188}Ir	523	± 50	59-3-129
^{190}Pt (α) ^{186}Os	3 380	200	59-4-102
^{197}Pt (β^-) ^{197}Au	750	10	58-10-94
^{199}Pt (β^-) ^{199}Au	1 780	100	58-2-61*
^{188}Au (β^+) ^{188}Pt	5 180	100	59-3-130+
^{192}Au (β^+) ^{192}Pt	3 240	50	58-1-71
^{194}Au (β^+) ^{194}Pt	2 566	14	58-1-74
^{195}Au (ε) ^{195}Pt	270	20	58-12-32
^{199}Au (β^-) ^{199}Hg	455	5	58-9-98*

In the above table, the first column indicates the nuclear reaction or decay, the second one gives the adopted reaction or decay energy and its error. As to the references in the third column see the text below table 2a. Below follow new references and a few remarks:

57Ha R. L. Heath, Phys. Rev. **105** (1957) 1011

58G123 R. K. Gupta, S. Jha, M. C. Joshi and B. K. Madan, Nuovo Cim. **8** (1958) 48

59B05 R. Balzer, H. Knoepfel, J. Lang, R. Müller and P. Stoll, Nuovo Cim. **11** (1959) 609

59C51 R. G. Cochran and W. W. Pratt, Phys. Rev. **113** (1959) 852

59G50 R. K. Girgis and R. van Lieshout, Nuclear Physics **12** (1959) 204

59H48 R. G. Helmer and S. B. Burson, Bull. Amer. Phys. Soc. **4** (1959) 427

59K28 B. H. Ketelle and A. R. Brosi, Phys. Rev. **116** (1959) 98

59Ia G. L. G. Ildowie, private communication to R. van Lieshout

59M122 A. C. G. Mitchell, J. O. Juliano, C. B. Creager and C. W. Kocher, Phys. Rev. **113** (1959) 628

59S161 K. Sugiyama, H. Ikegami, T. Yamazaki and M. Sakai, J. Phys. Soc. Japan **14** (1959) 986

60Ge1 K. N. Geller, J. Halpern and E. G. Muirhead, Phys. Rev. **118** (1960) 1302

60Ri3 R. A. Ricci, S. Monaro and R. van Lieshout, Nuclear Physics **16** (1960) 339

T K. Way, R. W. King, C. L. McGinnis and R. van Lieshout, Nuclear Level Schemes $A = 40$ to 92, TID 5300 (1955)

59-8-43 K. Way, G. Andersson, F. Everling, G. H. Fuller, N. B. Gove, R. Levesque, J. B. Marion, C. L. McGinnis, R. Nakasima and M. Yamada, Nuclear Data Sheets, National Academy of Sciences — National Research Council, Washington 25, D.C. (1958—1960)

a Value computed for $\log ft \approx 6$.

b Value corrected for the occurrence of M, N . . . capture.

c The $^{143}Pm(\varepsilon)$ decay energy was computed from putting $\log ft \approx 7$, in order to compute independently the $^{144}Sm(\gamma, n)$ reaction energy. The value was retained (but the error in the $^{143}Sm(\beta^+)$ decay energy increased somewhat) in order to be able to show (in table B) the disagreement with the directly measured value of the reaction energy.

† In the cases marked thus, the given value is incorrect, because of the following reasons:

$^{91}Tc(\beta^+)$. The origin of the given value is lost; it disagrees badly with beta systematics.

$^{180}Ta(\beta^-)$. Erroneously, the decay energy of the isomeric state has been used here; the correct value is 500 ± 30 keV (60 Gel). As a result, the mass of ^{180}W in the tables is slightly in error.

$^{188}Au(\beta^+)$. Erroneously, the α disintegration energy has been used as β^+ decay energy.

TABLE 3

Microwave results

Ratio	Measured value ($\times 10^6$)	Adjusted value ($\times 10^6$)	$\frac{v}{\sigma}$
$^{79}Br/^{81}Br$	975 307.8 ± 1.8	975 307.88 ± 0.44	-0.0456
$^{85}Rb/^{87}Rb$	977 016.4 2.8	977 016.5 1.1	-0.0532
$(^{72}Ge - ^{70}Ge)/(^{74}Ge - ^{70}Ge)$	499 852 35	499 757 15	2.7141
$(^{76}Ge - ^{74}Ge)/(^{76}Ge - ^{72}Ge)$	500 127 35	500 100 17	0.7794
$(^{74}Se - ^{76}Se)/(^{74}Se - ^{80}Se)$	333 125 18	333 126 6	-0.0768
$(^{75}Se - ^{76}Se)/(^{75}Se - ^{80}Se)$	199 566 30	199 583 7	-0.5812
$(^{77}Se - ^{76}Se)/(^{80}Se - ^{77}Se)$	333 947 23	333 949 6	-0.0895
$(^{78}Se - ^{76}Se)/(^{80}Se - ^{78}Se)$	999 510 50	999 477 27	0.6671
$(^{79}Se - ^{76}Se)/(^{80}Se - ^{79}Se)$	3 005 570 210	3 005 330 70	1.1555
$(^{82}Se - ^{76}Se)/(^{82}Se - ^{80}Se)$	2 998 441 110	2 998 490 70	-0.4751
$(^{128}Te - ^{122}Te)/(^{124}Te - ^{122}Te)$	3 001 270 600	3 001 220 200	0.0802
$(^{128}Te - ^{123}Te)/(^{124}Te - ^{123}Te)$	5 008 260 1 000	5 007 670 190	0.5890
$(^{128}Te - ^{125}Te)/(^{125}Te - ^{124}Te)$	2 995 090 600	2 995 300 240	-0.3539
$(^{128}Te - ^{126}Te)/(^{126}Te - ^{124}Te)$	1 000 300 140	1 000 490 90	-1.3676
$(^{129}Te - ^{130}Te)/(^{124}Te - ^{130}Te)$	333 460 35	333 446 25	0.4088

In the above table, the first column gives the mass ratio measured and the second one its experimental value. The adjusted value following from the present mass adjustment is given in the third column. All these input data are to be found in S. Geschwind, Encycl. of Physics **38**, I (1958) 38—59 and are used as primary data. The last column gives the difference v between the measured and the adjusted value divided by the standard deviation σ of the second column.

TABLE 4

Consistency data

Adj. no.	Mass range	N	n	$\sqrt{\chi^2/(N-n)}$	χ^2	0– 0.2	0.2– 0.4	0.4– 0.8	0.8– 1.2	1.2– 1.6	1.6– 2.0	2– 4	>4
III	$^{71}Ga - ^{82}Se$	52	27	1.07	28.4	29	7	8	4	1	1	0	2
IV	$^{82}Kr - ^{98}Mo$	65	39	1.40	51.2	42	5	8	1	1	1	4	3
V a	$^{99}Mo - ^{100}Mo$	5	4	2.55	6.5	2	0	1	0	0	0	2	0
V b	$^{102}Rh - ^{105}Pd$	7	6	0.74	0.6	6	1	0	0	0	0	0	0
V c	$^{106}Pd - ^{111}In$	18	11	1.60	18.0	10	0	3	1	0	1	2	1
VI a	$^{112}Cd - ^{116}Sn$	18	9	0.83	6.1	13	2	0	1	1	0	1	0
VI b	$^{117}Sn - ^{119}Sn$	7	3	0.74	2.2	2	3	2	0	0	0	0	0
VII a	$^{120}Sn - ^{132}Xe$	55	30	1.33	44.9	37	4	5	2	0	3	1	3
VII b	$^{133}Cs - ^{134}Ba$	4	3	0.37	0.1	4	0	0	0	0	0	0	0
VII c	$^{136}Ba - ^{137}Ba$	3	2	0.14	0.02	3	0	0	0	0	0	0	0
VIII a	$^{138}Ba - ^{151}Eu$	54	31	0.81	15.1	36	8	4	1	2	1	2	0
VIII b	$^{152}Sm - ^{153}Eu$	4	3	0.12	0.01	4	0	0	0	0	0	0	0
IX a	$^{154}Sm - ^{158}Gd$	15	8	1.88	24.8	8	2	1	0	1	0	2	1
IX b	$^{160}Dy - ^{164}Dy$	8	5	0.22	0.1	8	0	0	0	0	0	0	0
IX c	$^{164}Ho - ^{168}Er$	10	7	0.95	2.7	7	1	1	0	1	0	0	0
IX d	$^{176}Hf - ^{184}W$	23	11	1.10	14.5	11	4	5	1	0	0	0	2
X	$^{186}Re - ^{199}Hg$	44	22	1.24	33.6	23	6	2	7	0	2	2	2
Total		392	221	1.21	248.8								

The first column gives the numbers of the adjustments. These numbers are also mentioned in the figures (following this table). For practical reasons independent subgroups (marked a, b, c, and d in the first column) were adjusted in one operation, which does not influence the result. The second column indicates the mass range. The numbers of the equations (N) and of the variables (n) are given in the third and fourth column. The fifth column contains the consistency factor $\sqrt{\chi^2/(N-n)}$, the sixth one the value of χ^2. The columns 7 to 14 show the numbers of contributions to χ^2 counted in the interval given in the heading of the table. The bottom row refers to the total values of the entire mass adjustment of part II.

1.E.2:
6.D

Nuclear Physics **28** (1961) 29—41; © *North-Holland Publishing Co., Amsterdam*
Not to be reproduced by photoprint or microfilm without written permission from the publisher

ADJUSTMENT OF RELATIVE NUCLIDIC MASSES (III) $A \geqq 200$

A. H. WAPSTRA

Instituut voor Kernfysisch Onderzoek, Amsterdam

Received 17 May 1961

Abstract: This paper describes the procedure used in computing nuclidic masses for $A \geqq 200$ from tabulated experimental data, and gives a list of all reaction energies of some types of reactions calculated from the mass list.

1. Introduction

In the region above $A = 200$, series of nuclides are connected by alpha decay chains. Many alpha particle energies have been determined very accurately by magnetic spectrometer, or with moderate precision by proportional counters. The differences in mass of nuclides in the four alpha radioactive series (Th series $A = 4n$; Np series $A = 4n+1$, U series $A = 4n+2$ and Ac series $A = 4n+3$) can therefore be determined accurately.

The adjustment of the masses in the four series relative to one another was first made with the use of assumptions about the relative masses of even, odd mass and odd nuclides [1]). Later, some nuclear reaction measurements allowed a purely empirical relative adjustment. The relative masses determined in this way were correct within some tens of kilovolts [2, 3]). The absolute masses had to be derived using a few mass spectrometric results; their errors were of the order of 1 MeV.

Recently, some extremely accurate mass spectrometer results on Hg and Pb isotopes were reported by Benson *et al.* [4]). They have the same order of precision as the nuclear reaction measurements and allow, therefore, the computation of absolute nuclidic masses with the same order of precision as the relative masses mentioned above. This paper describes such a computation which completes a recalculation of all nuclidic masses determined by experimental data [5, 6]); the complete results of this calculation are given elsewhere [7]).

2. Initial Data

Table 1 gives Benson *et al.*'s mass doublets [4]) used in the present computation. The same group has made many important measurements in the low mass region. A least squares adjustment of their results [5]) showed that their reported errors are somewhat low: $R_e/R_t = 2.65$. Nearly identical correc-

tion factors to the errors are found for all groups of mass spectrometer measurements used in the new mass computation [6]). The same correction factor is, therefore, applied in table 3 to the errors as given by the authors.

We have limited ourselves to the mass spectroscopic measurements by Benson *et al.*, though recent measurements with a precision of $\approx 80\mu$MU have been reported by Kerr and Duckworth [8]) and such of $\approx 40\ \mu$MU by Demirkhanov, Gutkin and Doroknov [9]). The last ones differ in the average by 5.5 times their probable error from the values given by Benson *et al.* (where necessary, recomputed using the results of the first part [5]) of the present mass computation). A comparison with eight independent combinations of reaction energies shows that Benson's values agree quite well with the reaction measurements whereas the results of Demirkhanov's experiments again disagree by about five times the probable error, in the average. The errors given by the Russian authors are, therefore, about a factor five low. Then, their results would carry no weight in the present computation. The same is true for Kerr and Duckworth's results, certainly after applying the correction factor found necessary in the second part of this computation [6]).

Most nuclear data used in the present work are alpha and beta decay energies, but also a few reaction energies have been used. The last ones and the alpha and beta decay energies that suffered a change in the present mass adjustment, are given in table 2a. The beta decay energies that have not been changed in the course of the adjustment are presented in table 2b.

Initial alpha decays unchanged in the present adjustment are given in table 3. They are distinguished from the other data in this table (reaction energies as computed from the present mass adjustment) by adding an asterisk. All these values are obtained from reports by Asaro and Perlman [10]) and Wapstra [11]). They deviate slightly from the energies given by the authors. Most alpha energies are determined essentially with respect to one calibration energy, which is somewhat in doubt. Elsewhere [11]) we have given reasons for the choice of the calibration energy adopted here and worked out the necessary changes for magnetically determined alpha particle energies. The conversion to alpha decay energies has been made using actual masses, not by multiplying with $A/(A-4)$. Alpha energies determined with proportional counters have been treated in the same way except that a correction for the adopted calibration was made only in those cases where there were indications that this correction is necessary. Usually, the correction is small compared with the reported errors; it was only done to avoid piling up of systematic errors.

3. Adjustments

Fig. 1, giving schematically the experimental data accepted in the present computation, shows that the number of interconnections is low. Very accurate

connections exist between ^{204}Hg—^{204}Tl—^{204}Pb and between ^{206}Pb—^{207}Pb—^{208}Pb. They are so much more accurate than connections involving other nuclei that the masses of these nuclei are not influenced by the other connections. These masses were therefore obtained by simple least squares adjustments of

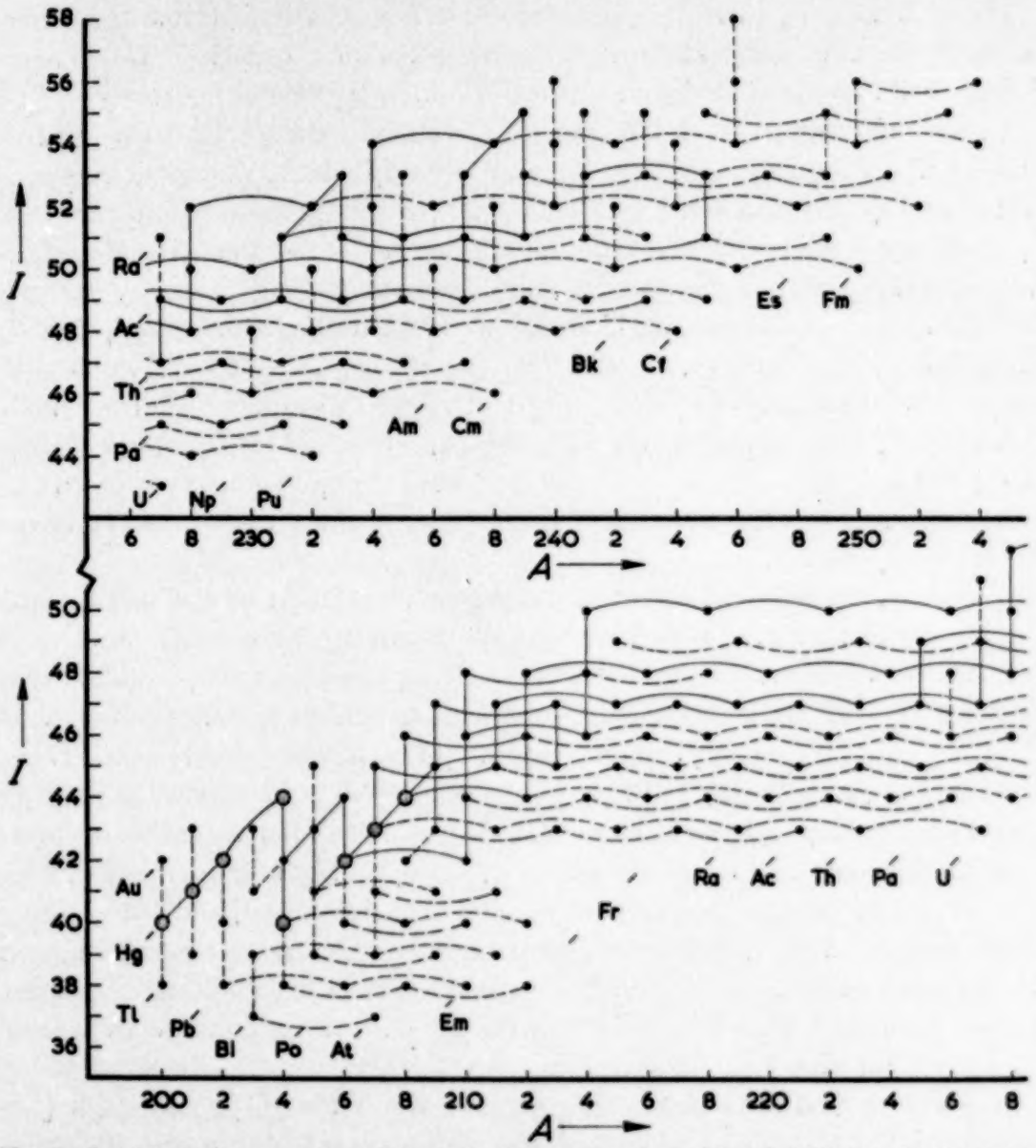

Fig. 1. Graphical representation of the experimental results used as initial data in the present mass computation. Vertical lines represent beta decays, upward curved arcs alpha decays between even-proton elements, downwards ones between odd-proton elements. Oblique lines represent reaction energies. Mass spectroscopic data are represented by open circles. Drawn lines represent data involved in some adjustment (see sect. 3); other data are represented by dotted lines.

mass spectroscopic data (using $^{1}H = 1.007\ 288\ 73$ u as an exact number) and the beta decay and neutron capture energies between these nuclei. The consistency factors in these two adjustments, $R_e/R_1 = 0.65$ and 1.00, are satisfactory.

Some cycles consisting of two alpha and two beta decay energies are easily adjusted in a way described earlier [1]). In the ^{241}Am—^{241}Pu—^{245}Cm—^{245}Bk cycle there is a closure error of 160±60 keV which is very probably due to either ^{245}Cm (α) or ^{245}Bk (ε) or both; for want of a better solution, the error has been divided equally over these two reactions and their errors have been raised to 80 keV. The 172±6 keV closure error in the cycle ^{237}U—^{237}Np—^{241}Am—^{241}Pu has been assigned to the least-known ^{241}Pu alpha decay.

Another closure error of 207±45 keV occurs in the cycle ^{209}Pb—^{209}Tl—^{213}Bi—^{213}Po. Probably the ^{213}Po (α) and ^{213}Bi (β) decay energies, measured by two groups each, are correct; and it is quite improbable that the ^{213}Bi alpha energy should be 207 keV high. On the other hand, the original authors did not assign errors to the beta endpoints and the three gamma ray energies in ^{209} Tl. The error estimates by Lidofsky may very well be somewhat optimistic Furthermore, the ^{232}Th (n, γ) and ^{238}U (γ, n) energies 5030 and 6080 keV, computed with the help of the data above, decay chains and the ^{209}Pb—^{213}Po—^{213}Bi branch, agree much better with the experimental values 5110±50 and 5870±100 keV than the values 4813 and 6287 computed using the ^{209}Pb—^{209}Tl—^{213}Bi branch. The reported ^{209}Tl beta energy is therefore not used in the present computation.

Apparently rather complex interconnections are caused by the five nuclear reaction measurements on ^{232}Th and ^{238}U. Studying these interconnections somewhat more closely with the help of fig. 1, it appears that an adjustment of the decay energies involved in these interconnections will alter only the following deday energies to an appreciable extent (they having the largest errors, mentioned in parentheses): ^{211}Pb β^+ (± 70 keV); ^{228}Ac β^- (±40 keV); ^{214}Pb β^- (±60 keV); ^{234}Pa β^- (± 60 keV and^{239} U β^- (± 50 keV). The system of interconnections is therefore treated as a least squares problem in these five variables all other decay energies are treated as constants in the adjustment of these decay energies. Ten equations are available for determining these variables: the above-mentioned reaction energies and five direct determinations; a least squares adjustment of these data with a satisfactory consistency factor ($R_e/R_i = 0.86$) yields our final results.

The above adjustment yields ^{209}Bi through the ^{208}Pb (d, p) and ^{209}Pb (β^-) reactions; it is worth mentioning that the result agrees very well with the value obtained from the ^{204}Pb mass and the ^{208}Po (α) and ^{209}Bi (p, 2n) reactions.

The masses of isotopes with $A = 200$, 201 and 202 are obtained by simple adjustments from the data in tables 1 and 2. The mass of Tl^{205} can be derived from the ^{205}Tl (γ, n), the ^{206}Pb (γ, n) and the ^{206})Pb (d, t) reactions; the results − 23 764±36, −23771±60 and −23770±149 keV agree quite well. Assuming the highest energy thermal neutron capture gamma ray [13]) in Tl to be due to ^{205}Tl this reaction yields a fourth value −23811±34 keV. The adopted value is an average of these results.

The mass of ^{203}Tl is computed from the assumption that the 6200$\pm$ 30 keV capture gamma ray [13]) in Tl leads to the 419$\pm$5 keV state of ^{204}Tl. Any other combination of known data would lead to a neutron binding energy in ^{204}Tl which would not lie between the corresponding quantities in ^{202}Tl and ^{206}Tl 6790$\pm$200 and 6581$\pm$48 keV respectively. Accepting e.g. the reported ^{203}Tl (γ, n) reaction energy in table 1 (itself almost 1 MeV low if compared with neutron binding energy systematics) would yield a ^{204}Tl neutron binding energy of 5710 keV. Demirkhanov *et al's* [12]) mass spectroscopic result deviates about as much in the opposite direction. Furthermore, it is very plausible that the 6200 keV capture gamma ray belongs to ^{204}Tl; its intensity is about 0.08 quants per capture whereas the total intensity of capture in the mass 205 isotopes is only 0.14 per capture in Tl, of which 0.04 should be assigned to the 6540 keV ground state transition in ^{206}Tl mentioned above.

As a check on the values obtained as mentioned above, the corresponding alpha decay and proton and neutron binding energies were plotted. The alpha decay energies of ^{251}Fm and ^{253}Fm were found to be somewhat low, possibly due to the reported transitions not going to the ground states of the daughter nuclei. These decay energies were therefore not used in our final computation.

4. Results

The masses obtained in the present computation are given elsewhere [7]) in combination with the results of part I and II of this recalculation of nuclear masses. A very complete list of reaction energies obtained from the adjustments in those earlier parts is published elsewhere [14]); it is not the intention to do the same for the present mass range since only few likely target isotopes are present here. For the purpose of various systematics, however, table 3 gives the binding energies of the last proton, neutron, two protons and two neutrons, the (d, α) reaction energy (which is equal to 23 846 keV minus the binding energy of the last proton and neutron) and the alpha decay energy, all these data as derived from the present computation. In using them, it should be kept in mind that a considerable part of the errors may be systematic: e.g. a systematic error of 50 keV due to the averaged influence of the ^{214}Pb—^{214}Bi—^{214}Po chain and the ^{238}U—^{234}Tb—^{234}Pa—^{234}U chain together with the ^{238}U(γ, n) reaction is present in the binding energies of all alpha decay descendents of ^{250}Fm down to ^{226}Ra, as will be clear from fig. 1.

This work is part of the research program of the "Stichting voor Fundamenteel Onderzoek der Materie" which is financially supported by the "Nederlandse Organisatie voor Zuiver Wetenschappelijk Onderzoek". It was carried out for a considerable part during a temporary stay at Argonne National Laboratory. Dr. J. T. Huizenga has critically reviewed the initial data. I thank him and Dr. T. B. Novey for their interest in this work.

References

1) A. J. Berthelot, J. Phys. Radium **3** (1942) 17;
M. O. Stern, Rev. Mod. Phys. **21** (1949) 402;
A. H. Wapstra, Physica **16** (1950) 33
2) A. H. Wapstra, Thesis, Amsterdam (1953)
3) J. R. Huizenga, Physica **21** (1955) 410;
B. M. Foreman and G. T. Seaborg, J. Inorg. Nucl. Chem. **7** (1958) 305
4) J. L. Benson, R. A. Damerov and R. R. Ries, Phys. Rev. **113** (1959) 1105
5) F. Everling, L. König, J. Mattauch and A. H. Wapstra, Nuclear Physics **15** (1960) 348; **25** (1961) 177
6) L. König, J. Mattauch and A. H. Wapstra, Nuclear Physics **28** (1961) 1
7) F. Everling, L. König, J. Mattauch and A. H. Wapstra, Nuclear Physics **18** (1960) 529
8) J. Kerr and K. E. Duckworth, Can. J. Phys. **36** (1958) 986
9) R. A. Demirkhanov, I. I. Gutkin and V. V. Doroknov, JETP (USSR) **35** (1959) 639
10) F. Asaro and I. Perlman, Rev. mod. Phys. **26** (1954) 456, **29** (1957) 831
11) A. H. Wapstra, Nuclear Physics **18** (1960) 587
12) A. H. Wapstra, Physica **21** (1955) 367
13) G. A. Bartholomew and B. B. Kinsey, J. Phys. **31** (1953) 1025
14) F. Everling, L. König, J. Mattauch and A. H. Wapstra, 1960 Nuclear Data Tables, parts I and II (U.S. Government Printing Office, Washington)

TABLE 1

Mass Spectroscopic Initial Data

Doublet	Measured value μMU(^{16}O = 16)	Adopted value μu	Adjusted value μu	$\frac{v}{\sigma}$
$C_{14}H_{32}$ - ^{200}Hg	282 150 ± 5	282 060 ± 14	282 063 ± 13	-0.21
^{201}Hg - ^{200}Hg	1 002 298 11	1 001 979 30	1 001 971 20	0.27
$C_{14}H_{32}$ - ^{201}Hg	- 720 130 9	- 719 901 23	- 719 907 17	0.26
$C_{16}H_{10}$ - ^{202}Hg	107 656 8	107 622 22	107 622 20	0.00
$C_{16}H_{12}$ - ^{204}Hg	120 462 8	120 424 22	120 421 18	0.17
^{204}Hg - ^{202}Hg	2 003 488 12	2 002 851 32	2 002 842 26	0.28
$C_{16}H_{12}$ - ^{204}Pb	120 856 14	120 818 36	120 834 23	-0.45
$C_{16}H_{14}$ - ^{206}Pb	135 152 6	135 109 17	135 094 11	0.88
$C_{16}H_{14}$ - ^{207}Pb	- 866 614 10	- 866 339 28	- 866 345 11	0.21
$C_{16}H_{16}$ - ^{208}Pb	148 592 6	148 545 16	148 560 11	-0.94

The second column gives the original value (ref. [4])); the third one the same value expressed in the new mass scale (^{12}C = 12) and the error multiplied with 2.65, as explained in sect. 2. The fourth column gives the same doublet as computed from the final mass table; the last column the difference with the third column divided by the adopted error in the latter one.

TABLE 2a

Initial reaction energies and alpha and beta decay energies changed in the mass adjustment

Reaction	Adopted value (keV)	Ref.	Adjusted value (keV)	$\frac{v}{\sigma}$
$^{201}Hg\ (\gamma,n)\ ^{200}Hg$	−6 230 ± 70	60Ge	−6 237 ± 14	0.10
$^{202}Hg\ (\gamma,n)\ ^{201}Hg$	−7 600 130	60Ge	−7 777 25	1.36
$^{203}Tl\ (\gamma,n)\ ^{202}Tl$	−8 800 200	59-2-135	−7 890 200	+
$^{203}Tl\ (n,\gamma)\ ^{204}Tl$	6 619 30	53Ba	6 619 30	0
$^{204}Tl\ (\varepsilon)\ ^{204}Hg$	376 20	58-12-58	380 18	−0.20
$^{205}Tl\ (\gamma,n)\ ^{204}Tl$	−7 515 29	60Ge	−7 538 25	0.79
$^{205}Tl\ (n,\gamma)\ ^{206}Tl$	6 540 30	53Ba	6 564 13	−0.80
$^{206}Pb\ (\gamma,n)\ ^{205}Pb$	−8 140 60	60Ge	−8 124 35	−0.27
$^{206}Pb\ (d,t)\ ^{205}Pb$	−1 830 100	58-10-106	−1 866 35	0.36
$^{206}Pb\ (n,\gamma)\ ^{207}Pb$	6 734 8	58-2-67	6 731 8	0.38
$^{207}Pb\ (n,\gamma)\ ^{208}Pb$	7 380 8	58-4-67	7 376 8	0.50
$^{208}Tl\ (\beta^-)\ ^{208}Pb$	4 993 6	58-10-112	4 995 6	−0.33
$^{208}Pb\ (d,p)\ ^{209}Pb$	1 700 20	59-3-134	1 701 20	−0.05
$^{209}Tl\ (\beta^-)\ ^{209}Pb$	4 120 30	57L	3 913 35	+
$^{209}Bi\ (\gamma,n)\ ^{208}Bi$	−7 432 10	60Ge	−7 432 10	0
$^{210}Tl\ (\beta^-)\ ^{210}Pb$	5 400 100	58-2-69	5 425 30	−0.25
$^{211}Pb\ (\beta^-)\ ^{211}Bi$	1 390 70	59-4-108	1 406 34	−0.23
$^{212}Bi\ (\beta^-)\ ^{212}Po$	2 253 10	59-4-120	2 247 6	0.60
$^{214}Pb\ (\beta^-)\ ^{214}Bi$	1 030 60	57L	1 050 50	−0.16
$^{214}Bi\ (\beta^-)\ ^{214}Po$	3 210 30	57L	3 206 30	0.13
$^{228}Ac\ (\beta^-)\ ^{228}Th$	2 210 40	54K	2 254 36	−1.10
$^{232}Th\ (\gamma,n)\ ^{231}Th$	−6 350 40	54V	−6 338 35	−0.30
$^{232}Th\ (n,\gamma)\ ^{233}Th$	5 110 50	58-4-71	5 074 36	0.72
$^{235}Np\ (\alpha)\ ^{231}Pa$	5 153 20	57A, 58Gi	5 151 16	0.10
$^{234}Pa\ (\beta-)\ ^{234}U$	2 280 60	57L	2 300 50	−0.33
$^{235}Np\ (\varepsilon)\ ^{235}U$	125 20	57L, 58Gi	127 20	−0.10
$^{237}Pu\ (\varepsilon)\ ^{237}U$	210 50	58-4-73	230 21	−0.40
$^{238}U\ (\gamma,n)\ ^{237}U$	−5 860 100	58-6-71	−6 040 60	1.80
$^{238}U\ (d,t)\ ^{237}U$	400 200	54V	218 60	0.96
$^{238}U\ (d,p)\ ^{239}U$	2 400 150	54V	2 435 90	−0.23
$^{239}U\ (\beta^-)\ ^{239}Np$	1 240 50	54K	1 280 50	0.80
$^{241}Pu\ (\alpha)\ ^{237}U$	4 976 5	57A	5 148 4	+
$^{245}Cm\ (\alpha)\ ^{241}Pu$	5 625 50	57A	5 700 80	−1.50
$^{245}Bk\ (\varepsilon)\ ^{245}Cm$	660 30	57L	750 80	−3.00
$^{251}Fm\ (\alpha)\ ^{247}Cf$	7 000 50	57A	−	+
$^{253}Fm\ (\alpha)\ ^{249}Cf$	7 050 50	57A	−	+

For the meaning of the last two columns, see table 1. Reference collections:

58-2-69 K. Way *et al.*, Nuclear Data Sheets, indicated by year, set and page number

54A, 57A See ref. [19])

54K R. W. King, Rev. Mod. Phys. **26** (1954) 327

57L L. J. Lidofski, Rev. Mod. Phys. **29** (1956) 773

Other references:

53Ba See ref. [13]) and the discussion in the text

58Gi J. E. Gindler, J. R. Huizenga and D. W. Engelkemeir, Phys. Rev. **109** (1958) 1263

60Ge K. N. Geller, J. Halpern and E. G. Muirhead, Phys. Rev. **118** (1960) 1304

+ Adopted value not used in final computation, for reasons stated in the text.

TABLE 2b

Initial beta decay energies not changed in mass adjustment.

Reaction	Adopted value (keV)		
^{200}Au (β^-) ^{200}Hg	2 300	± 100	58-8-68
^{200}Tl (ε) ^{200}Hg	2 450	10	58-4-60
^{201}Au (β^-) ^{201}Hg	1 500	100	58-2-64
^{201}Tl (ε) ^{201}Hg	410	60	60Gu
^{202}Tl (ε) ^{202}Hg	1 400	200	58-12-53 a
^{202}Pb (ε) ^{202}Tl	50	35	58-1-81*
^{203}Hg (β^-) ^{203}Tl	486	3	59-2-133*
^{203}Bi (ε) ^{203}Pb	3 190	50	59-2-138
^{204}Tl (β^-) ^{204}Pb	765	2	58-12-58*
^{204}Bi (ε) ^{204}Pb	4 300	500	b
^{205}Hg (β^-) ^{205}Tl	1 650	100	58-10-104*
^{205}Pb (ε) ^{205}Tl	50	35	58-10-106
^{205}Bi (β^+) ^{205}Pb	2 650	30	58-10-107
^{206}Tl (β^-) ^{206}Pb	1 510	10	58-6-62
^{206}Bi (ε) ^{206}Pb	3 600	150	58-4-65*
^{207}Tl (β^-) ^{207}Pb	1 442	8	58-12-69
^{207}Bi (ε) ^{207}Pb	2 400	40	58-4-66
^{207}Po (β^+) ^{207}Bi	2 906	8	58-9-107
^{209}Pb (β^-) ^{209}Bi	630	10	59-3-134*
^{210}Pb (β^-) ^{210}Bi	63	1	58-10-117
^{210}Bi (β^-) ^{210}Po	1 158	6	58-10-119
^{212}Pb (β^-) ^{212}Bi	582	7	59-4-118
^{213}Bi (β^-) ^{213}Po	1 390	10	54K
^{225}Ra (β^-) ^{225}Ac	350	10	57L
^{226}Ac (β^-) ^{226}Th	1 200	100	54K
^{227}Ra (β^-) ^{227}Ac	1 310	10	54K
^{227}Ac (β^-) ^{227}Th	43	2	57L
^{228}Ra (β^-) ^{228}Ac	55	3	58Go
^{230}Pa (β^-) ^{230}U	410	2	57L
^{231}Th (β^-) ^{231}Pa	386	3	57L
^{232}Pa (β^-) ^{232}U	1 250	20	57L
^{233}Th (β^-) ^{233}Pa	1 230	10	58-4-71
^{233}Pa (β^-) ^{233}U	568	4	57L
^{234}Th (β^-) ^{234}Pa	192	1	57L
^{234}Np (β^+) ^{234}U	1 800	100	57L
^{235}Pa (β^-) ^{235}U	1 400	100	54K
^{236}Np (β^-) ^{236}Pu	515	± 7	57L
^{237}U (β^-) ^{237}Np	513	3	57L
^{238}Np (β^-) ^{238}Pu	1 305	8	57L
^{239}Np (β^-) ^{239}Pu	724	10	57L
^{240}U (β^-) ^{240}Np	360	20	54K
^{240}Np (β^-) ^{240}Pu	2 050	60	57L
^{241}Np (β^-) ^{241}Pu	1 630	100	59Va
^{241}Pu (β^-) ^{241}Am	21	1	58-6-74
^{242}Am (β^-) ^{242}Cm	633	5	57L
^{243}Pu (β^-) ^{243}Am	570	30	54K
^{244}Am (β^-) ^{244}Cm	1 500	100	57L
^{246}Pu (β^-) ^{246}Am	375	30	57L
^{246}Am (β^-) ^{246}Cm	2 290	50	57L
^{249}Bk (β^-) ^{249}Cf	125	2	58-2-71,59Vb
^{250}Bk (β^-) ^{250}Cf	1 800	100	57L

Reference collections:

54K R. W. King, Rev. Mod. Phys. **26** (1954) 327

57L L. J. Lidofsky, Rev. Mod. Phys. **29** (1954) 1957

58-4-68 K. Way *et al.*, Nuclear Data Sheets, indicated by year, set and page number.

Remarks and References:

58Go Goetze and Huster, Z.Naturforsch. **13a** (1958) 796

59Va Vandenbosch, Phys. Rev. **113** (1959) 259

59Vb Vandenbosch *et al.* Phys. Rev. **115** (1959) 115

60Gu Gupta, Ark. Fys. **26** (1960) 69

a Combination in α-β-decay-cycles makes the estimate in **58-12-53** more probable than the experimental values, that have moreover partly shown to be incorrect (see 60Gu).

b Estimated value, chosen to yield acceptable decay energies for ^{208}At and ^{213}Fr.

TABLE 3

Binding energies of the last one or (two) protons or neutrons, alpha decay energies and (d, α) reaction energies.

A El Z	B_n	B_p	Q_α	B_{2n}	B_{2p}	$Q_{d\alpha}$
200 Au 79	6 140 ± 100	7 140 ± 140	-	13 750 ± 100	-	13 760 ± 300
Hg 80	7 989 23	7 661 24	1 040 ± 220	14 676 18	13 820 ± 280	10 805 19
Tl 81	-	4 756 25	1 699 25	-	12 032 21	14 627 21
201 Au 79	7 040 140	-	-	13 180 100	-	11 890 140
Hg 80	6 237 19	7 750 100	330 25	14 226 26	14 900 100	12 172 27
Tl 81	8 280 60	5 040 60	1 490 60	-	12 710 70	13 040 70
202 Hg 80	7 777 25	8 490 100	460 290	14 013 22		10 540 100
Tl 81	6 790 210	5 590 200	1 200 200	15 060 100	13 350 220	14 240 200
Pb 82	-	5 950 210	2 620 200	-	11 000 200	11 840 200
203 Hg 80	6 001 41	-	- 380 110	13 779 41	-	11 570 110
Tl 81	7 890 200	5 705 41	915 42	14 680 70	14 200 110	12 588 41
Pb 82	6 940 210	6 110 200	2 370 50	-	11 700 50	13 180 70
Bi 83	-	2 970 220	-	-	8 920 90	-
204 Hg 80	7 485 35	-	-	13 487 23	-	-
Tl 81	6 619 30	6 323 30	440 100	14 510 200	-	13 746 27
Pb 82	8 380 50	6 602 30	1 976 25	15 320 200	12 306 27	11 580 200
Bi 83	7 300 500	3 300 500	3 800 500	-	9 400 500	15 800 500
205 Hg 80	5 510 100	-	-	12 990 110	-	-
Tl 81	7 538 25	6 376 32	- 60 100	14 158 39	-	12 209 39
Pb 82	6 723 40	6 706 40	1 488 41	15 100 60	13 030 50	12 750 50
Bi 83	8 400 500	3 290 50	3 730 80	15 650 80	9 870 60	14 400 70
206 Tl 81	6 564 23	7 430 100	-	14 103 26	-	13 130 23
Pb 82	8 124 35	7 292 27	1 141 21	14 848 24	13 667 21	11 240 24
Bi 83	7 170 160	3 740 150	3 340 250	15 500 500	10 450 150	15 600 150
Po 84	-	4 360 210	5 322 10*	-	7 650 200	13 300 500
207 Tl 81	6 799 15	-	-	13 364 28	-	11 840 100
Pb 82	6 731 8	7 459 12	411 39	14 856 36	14 890 100	12 047 26
Bi 83	7 930 160	3 549 41	3 300 60	15 110 60	10 840 48	14 400 60
Po 84	7 060 210	4 240 150	5 206 20*	-	7 980 60	14 650 60
At 85	-	2 430 220	5 863 30*	-	6 790 90	-
208 Tl 81	3 823 13	-	-	10 623 16	-	-
Pb 82	7 376 8	8 036 11	520 21	14 108 11	-	11 235 15
Bi 83	6 900 48	3 718 26	3 016 35	14 830 150	11 176 29	15 621 27
Po 84	8 378 48	4 690 48	5 209 8*	15 430 210	8 238 26	13 450 150
At 85	7 400 500	2 700 500	5 765 20*	-	7 000 500	16 300 500
209 Tl 81	5 008 41	-	-	8 832 42	-	-
Pb 82	3 926 20	8 139 21	2 100 100	11 303 21	-	14 108 23
Bi 83	7 432 10	3 774 22	3 122 34	14 332 46	11 809 25	14 920 24
Po 84	6 960 44	4 750 46	4 972 8*	15 340 60	8 467 39	14 420 60
At 85	8 400 500	2 740 50	5 756 4*	15 770 90	7 430 60	14 950 60
210 Tl 81	3 690 50	-	-	8 696 32	-	-
Pb 82	5 199 24	8 330 42	-	9 126 13	-	12 732 14
Bi 83	4 632 26	4 480 24	5 054 12	12 065 28	12 618 14	17 664 13
Po 84	7 690 36	5 008 25	5 406 1*	14 651 26	8 781 11	13 630 27
At 85	7 300 150	3 080 160	5 630 4*	15 700 500	7 830 150	16 030 150
Em 86	-	3 960 210	6 157 3*	-	6 700 200	13 700 500

TABLE 3 (Continued)

A El Z	B_n	B_p	Q_α	B_{2n}	B_{2p}	$Q_{d\alpha}$
211 Pb 82	3 762 ± 36	8 405 ± 46	-	8 962 ± 41	-	13 980 ± 50
Bi 83	5 105 13	4 386 13	6 748 4#	9 738 25	12 715 ± 41	16 485 23
Po 84	4 548 17	4 924 18	7 589 15#	12 239 40	9 403 26	16 514 28
At 85	7 580 160	2 977 41	5 978 3#	14 880 60	7 984 47	15 400 50
Rn 86	7 250 210	3 910 160	5 963 3#	-	6 990 60	14 860 60
212 Pb 82	5 190 37	-	-	8 953 16	-	12 475 32
Bi 83	4 367 13	4 991 36	6 205 2#	9 472 14	13 394 31	17 318 14
Po 84	6 012 17	5 829 12	8 953 3#	10 561 11	10 216 13	15 134 13
At 85	-	-	-	-	-	-
Rn 86	7 953 49	4 280 48	6 388 5#	15 200 200	7 256 26	14 210 150
Fr 87	-	2 200 500	6 537 9#	-	6 100 500	16 700 500
213 Bi 83	5 223 28	5 022 29	5 990 30	9 590 29	-	15 857 45
Po 84	4 367 25	5 830 26	8 513 15#	10 379 30	10 820 43	15 873 28
At 85	-	3 350 200	9 380 200#	10 930 210	9 180 200	16 710 200
214 Pb 82	-	-	-	8 820 60	-	-
Bi 83	4 062 41	-	5 615 3#	9 286 31	-	16 985 32
Po 84	5 878 28	6 486 30	7 834 2#	10 245 13	11 508 16	14 361 14
At 85	5 060 200	4 040 60	8 960 50#	-	9 870 50	17 670 50
215 Bi 83	5 030 120	5 300 130	-	9 090 120	-	-
Po 84	4 088 38	6 511 47	7 509 10#	9 966 45	-	15 497 46
At 85	5 900 60	4 060 24	8 160 20#	10 960 200	10 545 36	16 132 34
Rn 86	-	5 110 110	8 770 100#	-	9 150 100	15 900 230
216 Po 84	5 790 36	7 270 120	6 909 2#	9 878 16	12 570 60	13 769 32
At 85	4 581 39	4 554 48	7 945 30#	10 480 60	11 064 44	17 429 33
Rn 86	6 610 110	5 821 38	8 170 30#	-	9 880 33	14 350 60
217 At 85	5 983 44	4 747 30	7 185 10#	10 565 37	12 020 120	15 533 47
Rn 86	4 641 49	5 880 50	7 895 30#	11 250 110	10 430 50	15 608 46
Fr 87	-	3 060 290	8 460 200#	-	8 880 280	16 400 300
218 Po 84	-	-	6 112 3#	9 610 60	-	-
At 85	4 431 43	-	6 816 4#	10 415 40	-	16 892 33
Rn 86	6 510 43	6 408 33	7 263 10#	11 152 13	11 154 19	13 679 35
Fr 87	5 510 290	3 930 80	8 000 50#	-	9 810 80	17 500 80
219 At 85	5 460 110	5 020 120	6 390 50#	9 890 110	-	-
Rn 86	4 410 39	6 387 48	6 940 5#	10 920 50	-	15 252 47
Fr 87	6 470 80	3 883 33	7 440 20#	11 980 290	10 290 42	15 680 50
Ra 88	-	4 950 160	8 160 100#	-	8 880 150	15 600 320
220 Rn 86	6 326 35	7 250 110	6 404 2#	10 737 19	12 280 60	13 357 33
Fr 87	5 200 50	4 670 60	6 820 30#	11 670 80	11 060 50	16 986 46
Ra 88	7 200 150	5 684 48	7 577 20#	-	9 566 40	13 920 80
221 Fr 87	6 350 50	4 700 32	6 451 10#	11 554 43	11 950 110	15 044 47
Ra 88	5 380 60	5 860 70	6 840 30#	12 570 150	10 530 60	15 010 60
Ac 89	-	2 890 300	7 740 100#	-	8 580 300	15 980 330
222 Rn 86	-	-	5 584 3#	10 430 60	-	-
Fr 87	-	-	-	-	-	-
Ra 88	6 670 50	6 181 36	6 678 10#	12 051 41	10 880 21	13 537 47
Ac 89	6 160 310	3 670 100	7 100 50#	-	9 530 100	17 020 90

TABLE 3 (Continued)

A El Z	B_n	B_p	Q_α	B_{2n}	B_{2p}	$Q_{d\alpha}$
223 Pr 87	-	5 170 ± 70	5 440 ± 100*	10 903 ± 47	-	-
Ra 88	5 091 ± 41	-	5 977 4*	11 760 60	-	14 798 ± 47
Ac 89	6 790 90	3 793 40	6 768 20*	12 950 300	9 973 ± 48	15 600 60
Th 90	-	4 360 190	7 690 100*	-	8 030 180	15 550 350
224 Ra 88	6 533 35	6 903 35	5 790 2*	11 625 22	12 070 60	-
Ac 89	5 680 60	4 380 60	6 289 30*	12 470 100	-	16 600 60
Th 90	7 620 180	5 180 60	7 268 20*	-	8 976 46	14 090 100
225 Ra 88	4 995 35	-	-	11 529 44	-	14 172 44
Ac 89	6 710 60	4 563 34	5 927 5*	12 395 49	11 465 46	14 974 46
Th 90	5 950 70	5 450 80	6 696 30*	13 570 180	9 830 70	14 940 70
226 Ra 88	6 360 50	-	4 868 3*	11 360 60	-	-
Ac 89	5 240 110	4 810 110	-	11 960 120	-	16 260 100
Th 90	6 920 60	5 661 39	6 447 10*	12 872 47	10 223 24	13 700 60
Pa 91	-	3 430 120	6 940 50*	-	8 880 110	16 690 110
227 Ra 88	4 470 70	-	-	10 832 48	-	-
Ac 89	6 550 110	5 000 70	5 038 5*	11 792 46	-	14 711 44
Th 90	5 391 42	5 810 110	6 147 3*	12 310 70	11 619 44	15 018 46
Pa 91	7 150 110	3 658 46	6 582 20*	-	9 320 50	15 490 70
U 92	-	4 380 220	6 920 100*	-	7 810 210	-
228 Ra 88	6 201 40	-	-	10 670 70	-	-
Ac 89	4 946 35	5 470 40	-	11 500 110	-	16 120 70
Th 90	7 157 35	6 417 35	5 523 3*	12 549 24	11 420 60	13 100 100
Pa 91	6 060 70	4 320 70	6 205 20*	13 210 120	10 130 120	16 360 60
U 92	7 740 200	4 970 60	6 796 10*	-	8 627 48	13 950 110
229 Th 90	5 389 38	6 860 38	5 130 15*	12 546 41	12 330 60	14 264 41
Pa 91	7 140 70	4 306 45	5 780 30*	13 200 60	10 720 50	14 610 50
U 92	6 210 70	5 120 80	6 541 20*	13 950 210	9 440 70	14 900 70
230 Th 90	6 720 50	-	4 773 5*	12 110 60	12 850 70	12 490 70
Pa 91	5 822 49	4 740 43	5 200 100	12 960 60	11 599 42	15 942 25
U 92	7 470 70	5 450 49	5 991 5*	13 677 48	9 755 24	13 480 60
231 Th 90	5 030 70	-	4 216 21	11 746 41	-	-
Pa 91	6 609 43	4 630 70	5 140 3*	12 430 50	-	14 721 41
U 92	5 850 70	5 460 70	5 550 50*	13 300 90	10 200 60	14 790 70
Np 93	-	3 250 70	6 400 50*	-	8 700 80	15 350 90
232 Th 90	6 338 35	-	4 079 5*	11 370 70	-	-
Pa 91	5 674 40	5 278 40	4 412 41	12 284 32	-	15 760 60
U 92	7 290 60	6 142 35	5 416 3*	13 124 25	10 770 60	13 319 25
Np 93	-	-	-	-	-	-
Pu 94	-	4 670 90	6 700 50*	-	7 920 70	-
233 Th 90	5 074 36	-	-	11 413 39	-	-
Pa 91	6 582 44	5 522 37	-	12 257 40	-	14 210 40
U 92	5 900 39	6 368 44	4 904 2*	13 190 60	11 645 40	14 028 40
Np 93	-	4 090 70	5 630 50*	13 960 90	10 230 70	14 690 90
Pu 94	6 490 90	-	6 417 20*	-	8 580 90	14 920 90
234 Th 90	6 070 60	-	-	11 150 90	-	-
Pa 91	5 030 60	5 480 60	-	11 620 80	-	15 510 90
U 92	6 770 50	6 550 50	4 855 4*	12 670 60	12 070 70	12 940 60
Np 93	6 000 130	4 180 110	5 460 120	-	10 550 120	15 990 120
Pu 94	7 590 80	4 780 90	6 300 50*	14 080 90	8 870 60	-

TABLE 3 (Continued)

A El Z	B_n	B_p	Q_α	B_{2n}	B_{2p}	$Q_{d\alpha}$
235 Pa 91	6 150 ± 120	5 560 ± 120	-	11 180 ± 110	-	14 440 ± 110
U 92	5 250 70	6 760 70	4 638 ± 12*	12 012 43	12 244 ± 42	14 273 43
Np 93	6 920 120	4 340 70	5 151 16	12 920 80	10 887 45	14 968 45
Pu 94	6 170 80	4 960 130	5 957 20*	13 760 90	9 140 70	15 110 90
236 U 92	6 394 38	7 010 110	4 582 4*	11 640 70	12 570 90	12 910 90
Np 93	5 691 41	4 782 44	5 134 22	12 610 120	11 540 80	16 040 60
Pu 94	7 380 60	5 424 40	5 869 5*	13 560 60	9 760 60	13 730 120
237 U 92	5 419 38	-	4 237 12	11 814 43	-	13 640 110
Np 93	6 762 40	5 150 38	4 954 3*	12 454 45	12 160 110	14 526 43
Pu 94	6 017 44	5 750 45	5 752 20*	13 300 70	10 531 48	14 629 49
Am 95	-	3 840 80	6 120 50*	-	9 260 90	14 850 100
238 U 92	6 040 60	-	4 269 5*	11 460 90	-	-
Np 93	5 370 50	5 100 50	4 610 50	12 140 60	-	15 550 80
Pu 94	6 910 50	5 900 50	5 609 3+	12 930 60	11 050 70	13 410 60
Am 95	-	-	-	-	-	-
Cm 96	-	4 280 100	6 625 30*	-	8 120 60	-
239 U 92	4 760 90	-	-	10 800 70	-	-
Np 93	6 200 70	5 260 70	4 560 100	11 571 44	-	14 769 42
Pu 94	5 620 70	6 140 70	5 239 3*	12 525 47	11 242 43	14 558 43
Am 95	-	4 070 80	5 870 30*	13 170 100	9 970 50	15 090 60
240 U 92	5 980 90	-	-	10 740 110	-	-
Np 93	5 060 70	5 560 90	-	11 250 100	-	15 750 100
Pu 94	6 382 39	6 324 39	5 251 3*	12 000 70	11 580 90	13 550 80
Am 95	-	-	-	-	-	-
Cm 96	-	4 930 60	6 360 30*	13 820 70	9 010 70	-
241 Np 93	5 940 120	5 520 120	-	11 000 110	-	14 570 120
Pu 94	5 522 38	6 790 70	5 148 4	11 905 44	12 350 70	14 224 45
Am 95	-	4 761 38	5 640 2*	12 680 50	11 084 44	14 927 44
Cm 96	6 200 70	-	6 180 50*	-	9 600 70	14 930 80
242 Pu 94	6 210 60	7 060 120	4 980 5*	11 730 90	12 580 110	13 070 100
Am 95	5 470 50	4 710 50	5 541 10	-	11 500 100	15 840 80
Cm 96	6 870 70	5 320 50	6 213 4*	13 070 70	10 080 70	-
243 Pu 94	5 010 80	-	4 720 60	11 220 50	-	14 000 110
Am 95	6 300 70	4 800 70	5 440 7*	11 771 45	11 860 110	15 061 45
Cm 96	5 670 70	5 520 70	6 159 5*	12 540 70	10 231 44	15 077 44
Bk 97	-	3 450 90	6 840 50*	-	8 780 70	15 750 90
244 Am 95	5 150 110	4 940 110	5 350 120	11 450 130	-	16 120 130
Cm 96	6 644 39	5 867 39	5 897 2*	12 310 70	10 670 90	13 910 80
Bk 97	-	-	-	-	-	-
Cf 98	-	4 480 80	7 290 20*	-	7 930 70	-
245 Am 95	6 300 130	-	4 980 130	11 450 90	-	14 830 100
Cm 96	5 720 90	6 440 130	5 700 80	12 360 90	11 370 100	14 480 90
Bk 97	-	4 188 43	6 470 20*	13 050 80	10 054 49	15 238 48
Cf 98	6 250 80	-	7 240 20*	-	8 510 70	15 340 90
246 Pu 94	-	-	-	-	-	-
Am 95	4 890 110	-	-	11 200 140	-	-
Cm 96	6 270 100	6 400 100	5 642 10*	11 990 90	-	13 370 130
Bk 97	-	-	-	-	-	-
Cf 98	7 240 80	4 930 50	6 868 5*	13 500 70	9 110 70	-

TABLE 3 (Continued)

A El Z	B_n	B_p	Q_α	B_{2n}	B_{2p}	$Q_{d\alpha}$
247 Bk 97	–	4 670 ± 90	5 770 ± 50*	12 470 ± 70	11 070 ± 110	15 130 ± 100
248 Cf 98	–	5 270 70	6 370 30*	12 810 80	9 940 90	–
249 Bk 97	–	–	5 505 15*	11 720 100	–	–
Cf 98	5 790 ± 90	–	6 295 10*	–	–	15 010 100
Es 99	–	3 690 70	6 870 50*	–	8 950 90	–
250 Bk 97	4 760 140	–	5 640 110	–	–	–
Cf 98	6 430 100	5 780 100	6 128 5*	12 230 90	–	–
Es 99	–	–	–	–	–	–
Fm 100	–	4 250 90	7 550 50*	–	7 930 90	–
251 Es 99	–	4 220 100	6 590 50*	12 760 100	9 990 120	15 420 120
252 Fm 100	–	4 690 90	7 165 20*	13 200 90	8 900 90	–
253 Es 99	–	–	6 747 5*	11 560 110	–	–
254 Es 99	4 970 140	–	6 540 10*	–	–	–
Fm 100	–	5 220 100	7 305 15*	12 090 90	–	–

* Alpha decay energies marked thus have been used in the presented adjustment as initial data that did not change (changed initial alpha decay energies are presented in table 2a)

+ Erroneously, this value has been used instead of the correct one 5589. The reported masses of ^{238}Np, ^{238}Pa, ^{242}Am, ^{242}Cm, ^{246}Cf and ^{250}Fm are therefore 20 keV high. This error affects all derived quantities by less than half their reported errors.

1.D.2:
1.E.3

Nuclear Physics **28** (1961) 42—62; © *North-Holland Publishing Co., Amsterdam*
Not to be reproduced by photoprint or microfilm without written permission from the publisher

THE GROUND-STATE EQUILIBRIUM DEFORMATION IN RARE-EARTH NUCLEI

D. R. BÈS † and Z. SZYMAŃSKI ††

Institute for Theoretical Physics, University of Copenhagen, Denmark

Received 13 June 1961

Abstract: The ground-state equilibrium deformation of nuclei has been calculated by Mottelson and Nilsson using Nilsson's single-particle model. It is the aim of the present investigation to study the influence of the pairing correlations on this deformation.

In addition, the values of the deformation obtained when assuming uniform charge distribution are shown to be in good agreement with the corresponding deformation of the potential. The strength of the quadrupole interaction, needed to account for the empirical electric quadrupole moments, is compared with the values used in other investigations.

1. Introduction

It appears that, for many purposes [1]), the most important correlation between the nucleons in a nucleus can be described in terms of competition between the quadrupole and pairing components in the effective nuclear interaction.

The quadrupole force is usually incorporated into a smoothly varying binding field of ellipsoidal shape [2, 3]). This cannot be done with the pairing force, which is analogous to that used in the recent theory of superconductivity [4]) and which is a generalization of the force in terms of which seniority is defined [5]).

Preliminary investigations [6–9]) have shown that this nuclear model contains many qualitative features of the observed nuclear spectra. In addition, a number of quantitative tests have been carried out rather successfully, both in the spherical [10, 11]) and in the deformed region [12–15]).

It is the aim of the present investigation to calculate the values of the equilibrium deformation, using a realistic spacing of the single-particle energy levels [16]), and including the effect of the pairing interaction.

2. Formulation of the Model

As the pairing force problem is easily treated in the formalism of second quantization, it is convenient to express our Hamiltonian in terms of creation and annihilation operators.

† Present address: Facultad de Ciencias Exactas y Naturales, Universidad de Buenos Aires, Argentina.

†† On leave of absence from the Institute for Nuclear Research, Warsaw, Poland.

In this section, we give (1) a discussion of the single-particle Hamiltonian, (2) a brief survey of the results of the coupling between the particles by the pairing force, and (3) a discussion of the different criteria which can be used in order to determine the equilibrium deformation.

2.1. THE SINGLE-PARTICLE HAMILTONIAN

The single-particle Hamiltonian H_{sp} is

$$H_{\mathrm{sp}} = \sum_{\nu} \varepsilon_{\nu}(c_{\nu+}^{\dagger} c_{\nu-} + c_{\nu-}^{\dagger} c_{\nu-}), \tag{1}$$

where $c_{\nu}^{\dagger}$ and c_{ν} are, respectively, the creation and annihilation operators for the single-particle state ν, which obey the usual anti-commutation relations, and ε_{ν} is the eigenvalue of the single-particle Hamiltonian corresponding to the two degenerate states $|\nu+\rangle$ and $|\nu-\rangle$. These are connected by the time-reversal operation.

The single-particle Hamiltonian can be divided into two parts, none of which is necessarily diagonal. The first part $\varepsilon_{\nu\omega}^{0}$ is spherically symmetric. We denote the matrix elements of the deformed part by the product of the single-particle and the total nuclear quadrupole moments,

$$\varepsilon_{\nu\omega} = \varepsilon_{\nu\omega}^{0} - kQq_{\nu\omega} = \varepsilon_{\nu}\delta_{\nu\omega}, \tag{2}$$

where k is a coupling constant ultimately determined by the quadrupole force, and

$$q_{\nu\omega} = 4\sqrt{\tfrac{1}{5}\pi}\,\langle \nu | r^2 Y_{20}(\theta) | \omega \rangle, \tag{3a}$$

$$Q = 4\sqrt{\tfrac{1}{5}\pi}\sum_{j} \langle 0 | r_j^2 Y_{20}(\theta_j) | 0 \rangle, \tag{3b}$$

$|0\rangle$ being the total nuclear ground-state wave function. The summation is to be performed over both neutrons and protons. Eqs. (2) and (3b) imply the self-consistency condition that the quadrupole deformation of the field is the sum of the quadrupole tensors of the orbits determined by that field and the pairing force. This condition can be taken into account [6]) by means of a Lagrange multiplier $\hat{\mu}$. Thus, ε_{ν} has to be replaced by

$$\varepsilon_{\nu\omega} = \varepsilon_{\nu\omega}^{0} - \mu q_{\nu\omega} = \varepsilon_{\nu}\delta_{\nu\omega}, \tag{2'}$$

where

$$\mu = kQ + \hat{\mu}. \tag{4}$$

The value of $\hat{\mu}$ is to be determined from the condition (3b).

The ε_{ν} defined by (2') will be taken from the Nilsson model [16]) which has been successfully used in explaining the properties of odd-particle states in deformed nuclei [19]). The nucleons are supposed to be in the states ν which are very similar to those of a deformed harmonic oscillator. The states are labelled by $(N, n_z, \Lambda, \Lambda+\Sigma)$, where N is the principal quantum number of

the oscillator shell, n_z the number of oscillator quanta along the z-axis, and Λ and Σ are the components, along the symmetry axis, of the orbital and spin angular momenta.

The matrix elements $\varepsilon^0_{\nu\omega}$ are expressed in the Nilsson model by

$$\varepsilon^0_{\nu\omega} = \frac{1}{2M}(\mathbf{p}^2)_{\nu\omega} + \tfrac{1}{2}M\omega_0(r^2)_{\nu\omega} - \hbar\omega_0[2\kappa(\mathbf{l}\cdot\mathbf{s}) + \sigma\mathbf{l}^2]_{\nu\omega}, \tag{5}$$

where M is the nucleon mass, ω_0 is the harmonic oscillator frequency, and κ and σ are constants which are chosen in order to have the correct level-sequence in spherical nuclei.

This model differs from the harmonic oscillator in that — due to the presence of the spin-orbit and $\mathbf{l}^2$ terms — states with the same n_z are not degenerate.

Nilsson's deformation parameter δ is related to the parameter μ defined in (4) by the equation

$$\mu = \tfrac{1}{3}\delta M\omega_0^2. \tag{6}$$

It is important that the single-particle levels ν should diagonalize exactly the single-particle Hamiltonian, including the matrix elements between states belonging to different shells. In order to achieve this result, it is necessary to use the representation described in Nilsson's Appendix A. However, we have neglected any effect arising from the difference between $\mathbf{l}_t$ and $\mathbf{l}$.

An important assumption made in the following is that both neutrons and protons move in fields with the same deformation.

It is an unfortunate consequence of the appproximations needed in order to solve the problem with the inclusion of pairing forces that the wave functions are not eigenstates of the number of particles. In order to ensure that the average particle-number in the ground state has a prescribed value n, a second Lagrange multiplier is introduced. That is, H_{sp} is replaced by H'_{sp}:

$$H'_{\text{sp}} = H_{\text{sp}} - \lambda n_{\text{op}} = \sum_{\nu}(\varepsilon_\nu - \lambda)(c^\dagger_{\nu+}c_{\nu+} + c^\dagger_{\nu-}c_{\nu-}), \tag{1'}$$

where n_{op} is the operator corresponding to the number of particles

$$n_{\text{op}} = \sum_{\nu}(c^\dagger_{\nu+}c_{\nu+} + c^\dagger_{\nu-}c_{\nu-}). \tag{7}$$

We fix λ by the condition

$$n = \langle 0\,|n_{\text{op}}|\,0\rangle. \tag{8}$$

2.2. THE QUASI-PARTICLE APPROXIMATION

The pairing force is given in the formalism of second quantization by†

$$H_{\text{pair}} = -G\sum_{\nu\omega} c^\dagger_{\nu+}c^\dagger_{\nu-}c_{\omega-}c_{\omega+}. \tag{9}$$

† The expression $\Sigma_\nu c^\dagger_{\nu+}c^\dagger_{\nu-}$ remains invariant if we change the single-particle representation, provided that the unitary matrix which connects the new representation with the old one commutes with the time-reversal operator. Therefore G is not a function of the deformation.

In order to solve the problem, we shall use the same formalism that Belyaev [6]) has applied to the nuclear case. We start by introducing two new creation operators for quasi-particles defined by the following canonical transformation:

$$\alpha_\nu^\dagger = u_\nu c_{\nu+}^\dagger - v_\nu c_{\nu-}, \qquad \beta_\nu^\dagger = u_\nu c_{\nu-} + v_\nu c_{\nu+}. \tag{10}$$

By means of the inverse transformation we can express $H = H'_{\mathrm{sp}} + H_{\mathrm{pair}}$ in terms of $\alpha_\nu^\dagger$, $\beta_\nu^\dagger$, β_ν and α_ν, and obtain the following structure:

$$H = U + H_{11} + H_{20} + H_{\mathrm{int}}. \tag{11}$$

The two first terms $U+H_{11}$ describe a system of non-interacting quasi-particles

$$U + H_{11} = \sum_\nu (\varepsilon_\nu - \lambda) 2v_\nu^2 - (\Delta^2/G) + \sum_\nu E_\nu (\alpha_\nu^\dagger \alpha_\nu + \beta_\nu^\dagger \beta_\nu), \tag{12}$$

where $E_\nu = [(\varepsilon_\nu - \lambda)^2 + \Delta^2]^{\frac{1}{2}}$ and $\Delta = G \sum_\nu u_\nu v_\nu$. Thus, if we require that $H_{20} = 0$ and neglect H_{int}, the functions can be characterized by the number of quasi-particles present. In particular, the ground state has no quasi-particles. Expressed in terms of the original particle creation operators, it is given by

$$|0\rangle = \prod_\nu (u_\nu + v_\nu c_{\nu+}^\dagger c_{\nu-}^\dagger) |\text{ vacuum}\rangle. \tag{13}$$

The requirement that $H_{20} = 0$ has to be satisfied simultaneously with the condition (8). This leads to the two equations

$$2/G = \sum_\nu 1/E_\nu, \qquad n = \sum_\nu 2v_\nu^2 = \sum_\nu [1 - (\varepsilon_\nu - \lambda)/E_\nu]. \tag{14}$$

From eq. (13) it is seen that v_ν^2 is the probability that the states $\nu+$ and $\nu-$ are occupied.

Apart from some very exceptional cases, there are no nuclei in the deformed region in which an external neutron and an external proton occupy time-reversed states. Thus, the pairing force (9) we have been using will not couple the neutrons and protons. One has to solve the equations (14) for both kinds of particles separately. In the quasi-particle approximation, eq. (3b) is equivalent to

$$Q = \sum_\nu q_{\nu\nu} 2v_\nu^2. \tag{3b'}$$

2.3. CALCULATION OF THE GROUND-STATE EQUILIBRIUM DEFORMATION

The expectation value

$$\mathscr{E}(Q) = \langle 0|H + \tfrac{1}{2}kQ^2 + \lambda n + \hat{\mu}Q|0\rangle = \langle 0|H_{\mathrm{spher}}|0\rangle + \lambda n - \tfrac{1}{2}kQ^2, \tag{15}$$

regarded as a function of Q, gives the potential energy as a function of the quadrupole deformation. The constants λn and $\hat{\mu}Q$ take care of the two Lagrange multipliers used in ε_ν. The factor $\frac{1}{2}$ in the term $\frac{1}{2}kQ^2$ ensures that we have not counted twice each particle pair.

It can be shown [15]) that

$$\mu = \frac{\partial}{\partial Q}\langle 0|H_{\text{spher}}|0\rangle. \tag{16}$$

Thus, the equilibrium condition $\partial\mathscr{E}/\partial Q = \mu - kQ = 0$ implies that

$$\mu = kQ. \tag{17}$$

The Lagrange multiplier $\hat{\mu}$ vanishes at equilibrium [15, 17]). The energy is minimized when both the single-particle potential and the wave function have the same deformation.

Let us apply this result to the case when the single-particle spherically symmetric potential is of the harmonic oscillator type, and no pairing force is present:

$$\begin{aligned} H_{\text{sp}} &= \frac{1}{2M}\mathbf{p}^2 + \tfrac{1}{2}M\omega_0 r^2 - \mu(2z^2 - x^2 - y^2), \\ \varepsilon_\nu &= \hbar\omega'_0 N - \tfrac{1}{3}\hbar\omega'_0(3n_z - N), \end{aligned} \tag{18}$$

where

$$\omega_z^2 \equiv \omega_0^2 - 4\mu/M \equiv \omega_0'^2(1-\tfrac{2}{3}\varepsilon)^2 \text{ and } \omega_\perp^2 \equiv \omega_0^2 + 2\mu/M \equiv \omega_0'^2(1+\tfrac{1}{3}\varepsilon)^2.$$

The single-particle states ν correspond to the representation used by Nilsson in his Appendix.

The quadrupole moment Q includes a contribution from the occupied shells Q_{in} and a contribution from the unfilled shell Q_{out}, given by

$$Q_{\text{in}} = \tfrac{1}{6}(\hbar/M\omega'_0)\varepsilon N^2, \tag{19a}$$

$$Q_{\text{out}} = (\hbar/M\omega'_0)2n_{\text{out}}(N - \sqrt{n_{\text{out}}}). \tag{19b}$$

We have assumed that both N and n_{out}, the number of particles in the unfilled shell, are large compared to unity. In this case, eq. (17) reads

$$k\left(\frac{\hbar}{M\omega'_0}\cdot\varepsilon_{\text{m}}\frac{N^4}{6} + Q_{\text{out}}\right) = \tfrac{1}{3}\varepsilon_{\text{m}}M\omega_0'^2. \tag{17'}$$

It was pointed out by Mottelson [18]) that the value of k has to be related to the strength of the central field in the following way. For a single particle outside closed shells, the total average field is given by

$$V = \tfrac{1}{2}M\omega_0^2 r^2 - kQ(2z^2 - x^2 - y^2). \tag{20}$$

Thus, the surfaces of equal potential are ellipsoids with the ratio of axes

$$(M\omega_0^2 + 2kQ)/(M\omega_0^2 - 4kQ) = 1 + 6kQ/M\omega_0^2. \tag{21}$$

If we assume that the average field has the same shape as the density distribution, we have

$$\frac{\sum_\nu \langle\nu|z^2|\nu\rangle}{\sum_\nu \langle\nu|x^2|\nu\rangle} = \frac{4\sum_\nu \langle\nu|r^2|\nu\rangle + 2Q}{2\sum_\nu \langle\nu|r^2|\nu\rangle - Q} = 1+\tfrac{3}{4}\frac{Q}{\sum_\nu \langle\nu|r^2|\nu\rangle}. \tag{22}$$

By equating (21) and (22), we get

$$k = \frac{M\omega_0^2}{8\sum_\nu \langle\nu|r^2|\nu\rangle} = \left(\frac{M\omega_0}{\hbar}\right)^2 \frac{\hbar\omega_0}{N^4}. \tag{23}$$

With this value of k we obtain for the equilibrium deformation

$$\varepsilon_m = (6M\omega'_0/\hbar)(Q_{out}/N^4). \tag{24}$$

In addition, we find $Q_{in} = Q_{out}$, which is consistent with the empirical charge renormalization that has been used for quadrupole moments and E2 transition rates.

It is known that the relation $Q_{in} = Q_{out}$, and thus the equilibrium deformation given in (24), can be obtained also if we take as the total energy the sum over all the single-particle energies ε_ν given by (18) and impose the requirement that the product $\omega_\perp^2\omega_z$ should be independent of the deformation. Thus, we neglect the self-consistency condition (3b), but we compensate by a change in the unit length of the system such as to preserve the volume. This is equivalent to putting $\omega'_0 = \mathring{\omega}_0\,(1+\frac{1}{9}\varepsilon^2+O(\varepsilon^3))$, where $\mathring{\omega}_0$ is independent of the deformation.

However, both methods are equivalent only for the value of k given by (23) and for the calculation of the equilibrium deformation. They do not yield, for instance, the same restoring force. This can easily be shown by introducing the pairing force and expanding the energy as a function of ε:

$$\begin{aligned}
\mathscr{E}_{\text{self-cons.}} &= \langle 0|H_{\text{spher}}|0\rangle - \tfrac{1}{2}kQ^2 - \Delta^2/G \\
&= \mathscr{E}_{\text{self-cons.}}(\varepsilon=0) + \varepsilon^2\hbar\omega'_0(\tfrac{1}{72}N^4)[1-(\hbar\omega'_0/G)^2\Theta_n^2], \\
\mathscr{E}_{\text{vol. cons.}} &= \sum_\nu \varepsilon_\nu 2v_\nu^2 - \Delta^2/G \\
&= \mathscr{E}_{\text{vol. cons.}}(\varepsilon=0) + \varepsilon^2\hbar\omega'_0(\tfrac{1}{56}N^4)[1-(\hbar\omega'_0/G)\Theta_n],
\end{aligned} \tag{25}$$

where

$$\Theta_n = \frac{4n_{out}}{N^2}\left(1-\frac{n_{out}}{N^2}\right).$$

Here, $\mathscr{E}_{\text{vol. cons.}}$ is the energy calculated using volume conservation, and $\mathscr{E}_{\text{self-cons.}}$ that determined by the self-consistency requirement.

In spite of the fact that the restoring forces are not the same, the instability-point occurs for the same number of particles in the unfilled shell. This indicates that both criteria continue to give the same result for the ground-state equilibrium deformation, even in the case when the pairing force is present.

Although the self-consistency criterium is probably a more fundamental approach to the problem, calculations with it prove to be very difficult. The equilibrium deformation turns out to be very sensitive to the value of the parameters (a 1 % change in k produces a 15 % change in ε). Therefore, we have chosen the method which uses volume-conservation, in the same way as Mottelson and Nilsson [19]) employed it, but with the addition of pairing forces.

Consequently, the ground-state energy was taken to be

$$\mathscr{E} = \sum_{\nu} \varepsilon_{\nu} 2v_{\nu}^2 - \Delta^2/G + \mathscr{E}_{\mathrm{C}}, \tag{26}$$

where $\mathscr{E}_{\mathrm{C}}$ represents the Coulomb energy.

It has been usual [19]) to include a factor of $\frac{3}{4}$ in front of the first term in eq. (26) †. Indeed such a term should appear when calculating the total energy, since, in the harmonic oscillator, the kinetic and potential energies are equal. The potential energy, being a sum of two-particle interactions, would be counted twice if we simply summed all the single-particle potential energies.

However, if we include the factor $\frac{3}{4}$, we are considering only the sum of the changes in the potential energy of each nucleon. We are neglecting any change in the total energy arising from the fact that a displacement of each nucleon affects the central binding field. Although this is an effect of order $1/A$ in the common field, it is felt by all the nucleons.

On the other hand, it is known that the factor $\frac{3}{4}$ must not be present if we calculate the nuclear excitation energy. In this case, the total change in the potential energy ($\frac{1}{2}$ the sum of individual changes) is increased by an exactly equal quantity which must come from the change in the field.

As we are interested in calculating the change in the total energy due to the deformation, rather than the binding energy itself, and as we can represent the change in deformation as a many-particle excitation, we conclude that no factor $\frac{3}{4}$ should be present in our calculations.

One could arrive at the same conclusion from eqs. (25). It is evident that the self-consistency and volume conservation requirements are only equivalent if we neglect the factor $\frac{3}{4}$. Anyhow, this factor is not very important in deformed nuclei, because Δ does not vary very much in the neighbourhood of the equilibrium deformation.

† We are indebted to Dr. S. G. Nilsson for illuminating comments on this point. See also S. A. Moszkowski, Handbuch der Physik XXXIX (Springer-Verlag, Berlin 1957) p. 511.

The Coulomb interaction between protons $\mathscr{E}_C$ has been taken into account [20,16]) by evaluating the integral

$$\mathscr{E}_C = \tfrac{1}{2}\int \frac{\rho(\mathbf{r}_1)\rho(\mathbf{r}_2)}{|\mathbf{r}_1-\mathbf{r}_2|}\,d\mathbf{r}_1\,d\mathbf{r}_2, \tag{27}$$

where $\rho(\mathbf{r})$ is the density of charge. If we use the new variables

$$x' = (1+\tfrac{1}{3}\bar{\varepsilon})x, \qquad y' = (1+\tfrac{1}{3}\bar{\varepsilon})y, \qquad z' = (1-\tfrac{2}{3}\bar{\varepsilon})z, \tag{28}$$

and assume that $\rho(\mathbf{r}) = \rho(r')$, we easily obtain

$$\mathscr{E}_C = \tfrac{1}{2}(1-\tfrac{4}{45}\bar{\varepsilon}^2-\tfrac{2}{189}\bar{\varepsilon}^3)\int \frac{\rho(r'_1)\rho(r'_2)}{|\mathbf{r}'_1-\mathbf{r}'_2|}\,d\mathbf{r}_1'\,d\mathbf{r}'_2. \tag{29}$$

The deformation parameter $\bar{\varepsilon}$ is defined by (28). It describes the deformation of the nuclear surface and must not be confused with the deformation ε of the single-particle potential. The parameter $\bar{\varepsilon}$ can be expressed by means of the electric quadrupole moment of the system

$$Q_e = \tfrac{4}{5}eZ\bar{\varepsilon}(1+\tfrac{1}{2}\bar{\varepsilon})\int \rho(r')r'^2\,d\mathbf{r}'. \tag{30}$$

In order to evaluate the Coulomb energy as a function of the potential deformation ε, we obtain $Q_e(\varepsilon)$ by means of (3b), and use (29) and (30) in order to derive $\mathscr{E}_C[Q/(\varepsilon)]$.

The integrals in (29) and (30) were calculated with the experimental data available on electron scattering in nuclei [21]). According to these data, the electric charge distribution may be better represented with a trapezoidal function than with a step function. However, the results with a step function

$$\tfrac{1}{2}\int\frac{\rho(r')_1\rho(r'_2)}{|\mathbf{r}_1'-\mathbf{r}'_2|}\,d\mathbf{r}'_1\,d\mathbf{r}'_2 = \tfrac{3}{5}\,\frac{Z^2e^2}{R}. \tag{31}$$

and

$$\int \rho(r')r'^2\,d\mathbf{r}' = \tfrac{3}{5}R^2, \tag{32}$$

with $R = 1.2\cdot A^{\frac{1}{3}}$ fm, overestimate $\mathscr{E}_C$ only by 7 % in the Sm region and underestimate it by 1 % around Os.

By using (26) we have made two implicit assumptions. The first one is that the change in σ for protons does not arise from the deformation-dependent terms in $\mathscr{E}_C$. This is reasonable since this change is independent of ε. The second one is that the self-consistency condition should remain, at least approximately, valid when the equilibrium position is obtained, taking into account the Coulomb energy.

In order to calculate the electric quadrupole moments we must extend the summation in (3b) only over the proton states. The single-particle quadrupole

moments $q_{\nu\nu}$ are obtained when using again the representation described in Nilsson's Appendix 1; we get

$$\begin{aligned} q_{\nu\nu} &= \langle\nu|(2z^2-x^2-y^2)|\nu\rangle \\ &= \langle\nu|[(\hbar/M\omega_z)2\zeta^2-(\hbar/M\omega_\perp)(\xi^2+\eta^2)]|\nu\rangle \\ &= (\hbar/M\mathring{\omega}_0)[\langle\nu|(2\zeta^2-\xi^2-\eta^2)|\nu\rangle(1+\tfrac{1}{3}\varepsilon+\tfrac{1}{9}\varepsilon^2) \\ &\quad +\langle\nu|(\xi^2+\eta^2+\zeta^2)|\nu\rangle\cdot\tfrac{2}{3}\varepsilon(1+\tfrac{1}{3}\varepsilon)+O(\varepsilon^3)], \end{aligned} \tag{33}$$

where

$$\zeta = \sqrt{\hbar/M\omega_z}\,Z \quad \text{and} \quad \omega_z = \mathring{\omega}_0(1-\tfrac{2}{3}\varepsilon+\tfrac{1}{9}\varepsilon^2+O(\varepsilon^3)), \text{ etc.}$$

The operators $(2\zeta^2-\xi^2-\eta^2)$ and $(\xi^2+\eta^2+\zeta^2)$ are diagonal within the shell in the "asymptotic" representation, with matrix elements

$$\begin{aligned} &\langle N\, n_z\, \Lambda\, \Lambda+\Sigma|(2\zeta^2-\xi^2-\eta^2)|Nn_z\Lambda\Lambda+\Sigma\rangle = 3n_z-N, \\ &\langle N\, n_z\, \Lambda\, \Lambda+\Sigma|(\xi^2+\eta^2+\zeta^2)|Nn_z\Lambda\Lambda+\Sigma\rangle = N+\tfrac{3}{2}. \end{aligned} \tag{34}$$

Therefore, it is convenient to use Rassey's eigenfunctions [22]) in order to calculate (33).

3. Discussion of the Parameters used in the Calculations

3.1. SINGLE-PARTICLE ENERGY LEVELS

Nilsson [16]) has chosen the three parameters entering in his model on the following basis. The first one, $\hbar\mathring{\omega}_0 = 41/A^{\frac{1}{3}}$ MeV, is the frequency associated with the harmonic oscillator potential. It fixes the unit of length of the system and, therefore, it is determined from considerations involving the nuclear radius. The second parameter, κ, measures the strength of the spin-orbit potential. It is chosen to be 0.050 in order to reproduce the level sequence in spherical nuclei. This criterium is also used for σ, which depends on the value of the $\mathbf{l}^2$ term. With $\sigma = 0.45$, Mottelson and Nilsson [17]) are able to account very well for the properties of odd-neutron levels in deformed nuclei with $150 < A < 190$ and $A > 220$.

For the odd-proton levels some changes are necessary due to the Coulomb interaction. The spin-sequence of levels in the rare-earth region is well reproduced by choosing the same value κ, and $\sigma = 0.55$. However, Nilsson's calculations with $\sigma = 0.55$ are available only for $N = 4$ particles. Nevertheless, one can use the calculations with $\sigma = 0.45$ for the $N = 5$ protons, and compensate this error in the case of the $h_{\frac{11}{2}}$ protons by shifting them down by $0.20\hbar\mathring{\omega}_0$. This corresponds to an increase in σ of about 0.12.

With these parameters, there is an excellent correspondence between the empirical levels and those predicted within one nuclear shell. However, some predicted levels belonging to other shells do not appear experimentally, thus suggesting that the inter-shell distance has been underestimated. For instance,

the level $(651\frac{1}{2})$ should be seen in the spectra of odd-neutron nuclei with $A-Z > 105$, and the level $(541\frac{1}{2})$ should appear as an intrinsic excitation of odd-proton nuclei with $Z > 71$. These data suggest that the energies in the upper neutron shell should be increased by at least $0.08\hbar\mathring{\omega}_0$ and those in the proton shell by $0.10\hbar\mathring{\omega}_0$.

There is no direct experimental evidence concerning the displacements of the lower shells. We have kept unchanged the position of the $N = 5$ levels belonging to the lower neutron shell, because the equilibrium deformation is a very sensitive function of the difference between the effective Fermi energy λ and the energy ε_ν of the $(505\frac{11}{2})$ level. If $\varepsilon_\nu - \lambda > 0$, the nucleus is likely to be strongly deformed, and vice versa. There is no hope of reproducing the empirical fact that the electrical quadrupole moments Q_e increase with the neutron number for the Gd and Dy isotopes if the $(505\frac{11}{2})$ level is below the Fermi surface. The position of this level in the Nilsson scheme is not in contradiction with the observed order in the spin-sequence of odd-mass nuclei, because, in the vicinity of the $(505\frac{11}{2})$ level, the energy changes so rapidly with the deformation that it is very unlikely to be found as a ground state. In addition, its high spin prevents it from being fed by β- or γ-transitions and, thus, it is rather difficult to see it as an excited state.

The neutron $N = 4$ levels, $(402\frac{3}{2})$, $(400\frac{1}{2})$, $(404\frac{7}{2})$, have also a large negative quadrupole moment and, therefore, the deformation is very sensitive to their position. The corresponding displacements are listed in table 1.

TABLE 1

Shifts of the single-particle energy levels, in units of $\hbar\mathring{\omega}_0$

		$N = 4$	$N = 6 \neq i_{\frac{13}{2}}$	$N = 7$
single-neutron	I	−0.12	+0.25	$+\infty$
	II	−0.37	+0.07	+0.27
	III	−0.37	+0.21	$+\infty$
	N-P[12])	0.00	+0.15	$+\infty$
	G-R[13])	$-\infty$	+0.10	$+\infty$

		$N = 3$	$N = 5 = h_{\frac{11}{2}}$	$N = 5 \neq h_{\frac{11}{2}}$	$N = 6$
single-proton	IV	−0.08	−0.20	+0.20	+0.20
	V	−0.23	−0.20	+0.07	+0.07
	VI	−0.23	−0.20	+0.17	+0.17
	N-P[12])	0.00	−0.20	+0.10	$+\infty$
	G-R[13])	$-\infty$	−0.20	+0.20	$+\infty$

Our results do not depend very much on the position of the $N = 3$ protons. We have shifted them by $0.23\hbar\mathring{\omega}_0$ down. The $N = 4$ $g_{\frac{9}{2}}$ levels are kept in the same position as in the Nilsson scheme.

Nilsson's single-particle energies are given for the values of the deformation parameter † $\eta = 0, 2, 4$ and 6. We have obtained the eigenvalues corresponding to $\eta = 5$ and $\eta = 7$ by means of a quadratic interpolation and extrapolation, respectively.

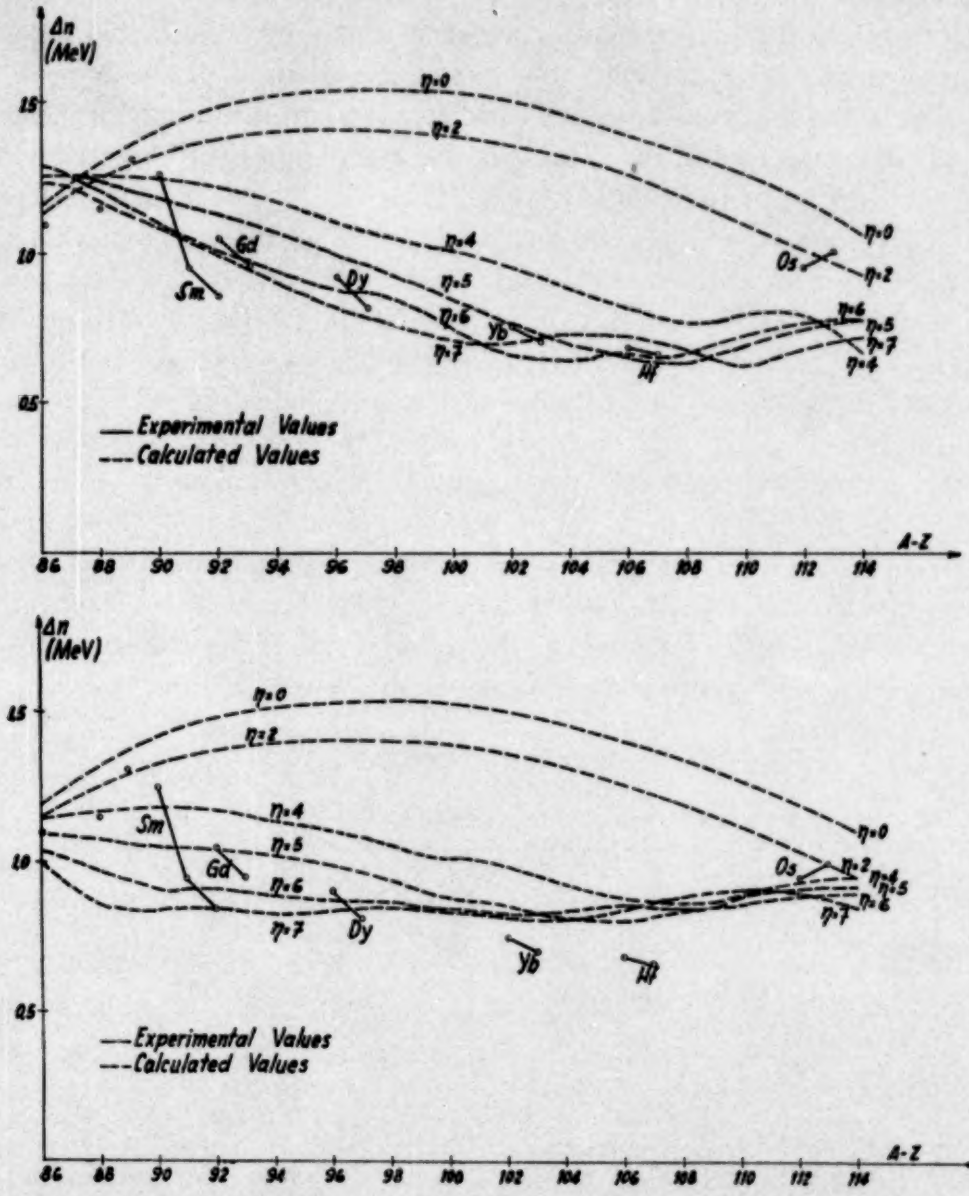

Figs. 1a and 1b. The neutron energy gap Δ_n. The experimental points are taken from refs. [23,24]). The dashed lines represent the theoretical values for single-particle shifts labelled by I and II, respectively, and for $G = 26.5/A$ MeV. The curves corresponding to the case III coincide with those of fig. 1a for the lower neutron numbers and with those of fig. 1b for the upper ones.

3.2. THE STRENGTH OF THE PAIRING FORCE

The effective value of G must be chosen such as to reproduce the increase in the ground-state binding energy in even nuclei. However, the value of G

† The parameter η is related to ε by the equation $\kappa\eta = \varepsilon + \frac{1}{9}\varepsilon^3 + \frac{2}{81}\varepsilon^4 + O(\varepsilon^5)$ (cf. ref. [16])).

depends also on the number of states in which the nucleon pairs are allowed to scatter. In the deformed region, there is no clear-cut distinction between filled and unfilled shells, so there is no obvious prescription how to choose these states. However, states which are far from the Fermi surface contribute to the wave function only [6, 8]) through a renormalization of G. Therefore, we allow the pairing force to scatter only amongst the nearest to the Fermi surface. These states have a total energy spread of about 8 MeV. We take $v_p = 1$ for the states below the 24, and $v_p = 0$ for those above.

From general considerations [8]) about the pairing force it follows that it is a volume interaction, i.e., that it is proportional to A^{-1}. Thus, we must choose

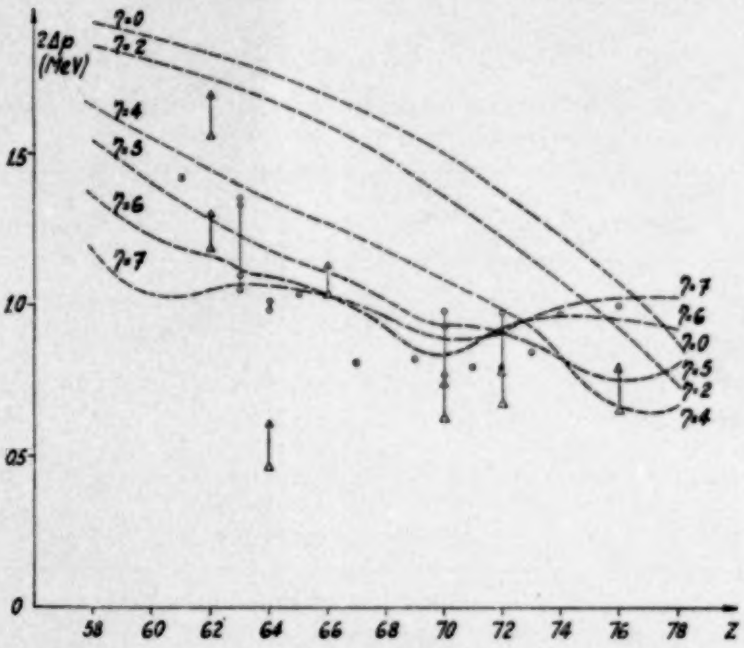

Fig. 1c. The proton energy gap Δ_p. The experimental points are obtained calculating the difference $(\Delta_p - \Delta_n)$ by means of the systematics of β-decay energies and adding to it the date of figs. 1a, b. The dashed lines correspond to the theoretical predictions for the case VI and $G_p = 32.2/A$ MeV.

two constants, viz. AG_n and AG_p, for the neutrons and protons, respectively. After solving equations(14) we should obtain the value of Δ which reproduces the experimental data. The empirical evidence comes mainly from two sources:

1) The average difference between the neutron binding energies of even and odd-mass nuclei is roughly proportional to 2Δ. The experimental data for neutrons were collected by Johnson and Bhanot [22]) and by Kravtzov [23]). A comparisonwith the predicted values is shown in figs. 1a and b ($AG_n = 26.5$ MeV).

There is no direct experimental evidence for the case of protons. However, one can estimate the differenc between Δ_n and Δ_p by considering the energy balance in the β-decay of odd-mass nuclei (fig. 1). The theoretical curves correspond to $AG_p = 32.2$ MeV.

2) A few levels in the deformed region can be attributed unambiguously to quasi-particle excitations, because they have a high spin or a long lifetime. Table 2 contains the experimental energy, spin and parity of the level, the most probable quasi-particle configuration, and the predicted energy. However, the independent quasi-particle method can only be relied upon for a description of the general systematic trends. If we introduce a quasi-particle interaction, or block the states occupied by the particles whose pair is broken, the predicted energy of the lowest quasi-particle state of a certain spin and parity can be lowered substantially [14]). Thus, the excited spectrum of even nuclei provides only a lower limit for the value of G.

TABLE 2

Experimental evidence on the intrinsic excitations in the first deformed region, and the corresponding theoretical interpretations

Nucleus	Experimental energy (MeV)	Character	Ref.	Theoretical interpretation	Theoretical energy (MeV)	Notes
Gd^{156}	1507	4+	[26])	$(413\frac{5}{2})(411\frac{3}{2})_p$	2.16	
				$(505\frac{11}{2})(521\frac{3}{2})_n$	2.44	
Dy^{162}	1520	5−	[27])	$(523\frac{7}{2})(411\frac{3}{2})_p$	2.16	
				$(642\frac{5}{2})(523\frac{7}{2})_n$	2.05	
Er^{166}	1458	0+	[28])	$(411\frac{1}{2})^2_p$	1.92	a)
				$(521\frac{1}{2})^2_n$	1.66	
Hf^{178}	1149	8− or 9−	[28])	$(514\frac{9}{2})(404\frac{7}{2})_p$	1.80	b)
Hf^{180}	1142	8− or 9−	[28])	$(514\frac{9}{2})(404\frac{7}{2})_p$	1.80	b)
Os^{190}	1698	10−	[29])	$(505\frac{9}{2})(615\frac{11}{2})_n$	2.06	

a) If this level is not an intrinsic excitation but a β-vibration, the first column provides only a lower empirical limit for the assumed quasi-particle excitation.

b) We have preferred to assign this level to proton excitations, because it appears in both Hf isotopes. However, the β-transition rate to this level suggests an appreciable admixture of the $(523\frac{7}{2})(624\frac{9}{2})$ neutron excitation [29]).

4. Method of Calculation

Eqs. (14) were solved in the electronic computer SMIL of the University of Lund, Sweden, for values of the deformation parameter $\eta = 0$, 2, 4, 5, 6 and 7, using the single-particle levels previously discussed †.

The total energy (26) was plotted as a function of η. A typical example is shown in fig. 2 for Dy^{164}. In this figure we have also included the calculations made without the pairing force and with the most probable single-particle configurations (similar to the Mottelson-Nilsson calculation). The curves we

† The numerical solutions containing ε_p, λ, Δ^2 and $2v_p^2$ may be obtained on request from either Facultad de Ciencias Exactas y Naturales, Buenos Aires, Argentina or, Institute for Nuclear Research, Warsaw, Poland.

obtained correspond to the envelope of those given by the different single-particle configurations. It is also clear why the Coulomb energy plays a much more important role in our calculation than in theirs; our curves have much less curvature than any of the single-particle ones and, therefore, it is easier to shift the minimum. We obtain the electric quadrupole moments by means of a graphical interpolation.

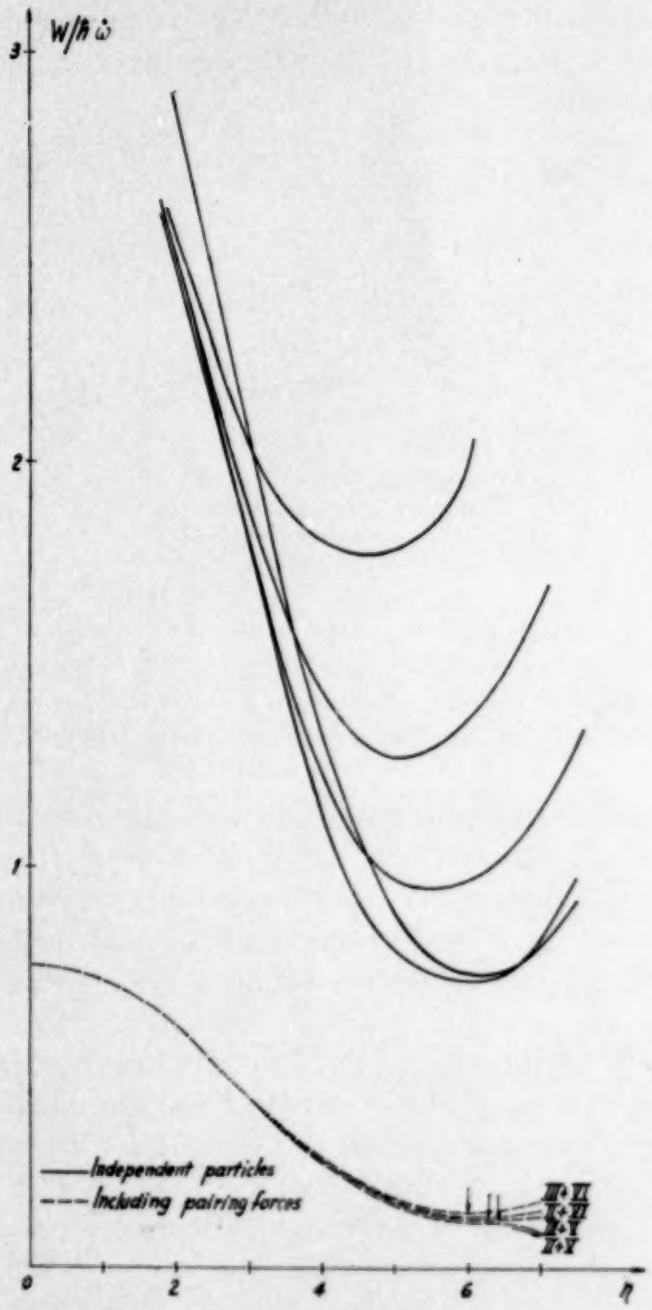

Fig. 2. The ground-state energy of Dy^{164} as a function of the deformation η. The full-drawn lines correspond to the different single-particle configurations in the calculation of Mottelson and Nilsson. The dashed lines include the pairing force effects and correspond to different shifts of the higher shells.

5. Discussion of the Results

5.1. ELECTRIC QUADRUPOLE MOMENT

The results obtained with shifts I+IV are shown in fig. 3, together with the experimental electric quadrupole moments. It is seen that, if we do not shift the $N = 4$ levels and include the Coulomb energy, the deformation becomes very large for the Nd and Sm isotopes. In order to get reasonable values for the deformation we had to use a considerable shift of the neutron $N = 4$ levels ($-0.37\ \hbar\mathring{\omega}_0$). In this way the transition number becomes 86, instead of 90 (fig. 4).

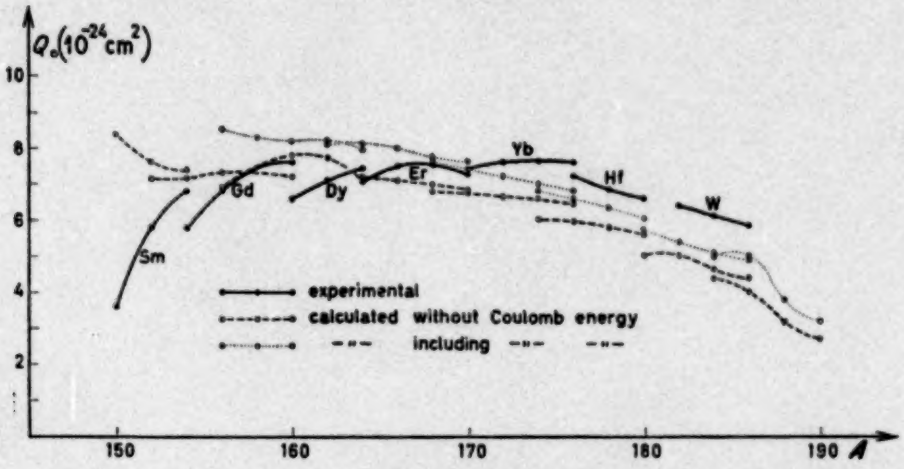

Fig. 3. The electric quadrupole moments for the shifts I+IV. The experimental values are taken from ref. [25]). The Coulomb effects are included in the dotted curve, but not in the dashed curve.

The validity of these results is, however, handicapped because the Coulomb energy produces a major change in the deformation for the Nd and Sm isotopes. This is due to the fact that, in this case, the curves representing energy versus deformation are very flat. Therefore the condition (3b) may not be satisfied and thus the different criteria for the equilibrium deformation may not be equivalent.

In order to study the influence of the position of the higher shells, we have performed the calculations II, III, V and IV. From the experimental data the smallest displacement should be about $0.07\ \hbar\mathring{\omega}_0$ both for neutrons and protons. In this case, we get spherical stability for Ce^{142}, Nd^{144}, Pt^{190} and Pt^{192}. The nuclei Nd^{146}, Nd^{148}, Sm^{146}, Sm^{148}, Gd^{150} and Gd^{152} are deformed with $\eta_{min} \leqq 7$. In all other nuclei, the minimum is outside the region of deformation studied ($0 \leqq \eta \leqq 7$).

The shifts III and VI give better results. The predicted equilibrium deformations are listed in table 3. In fig. 4 we have drawn the electric quadrupole moments as a function of A.

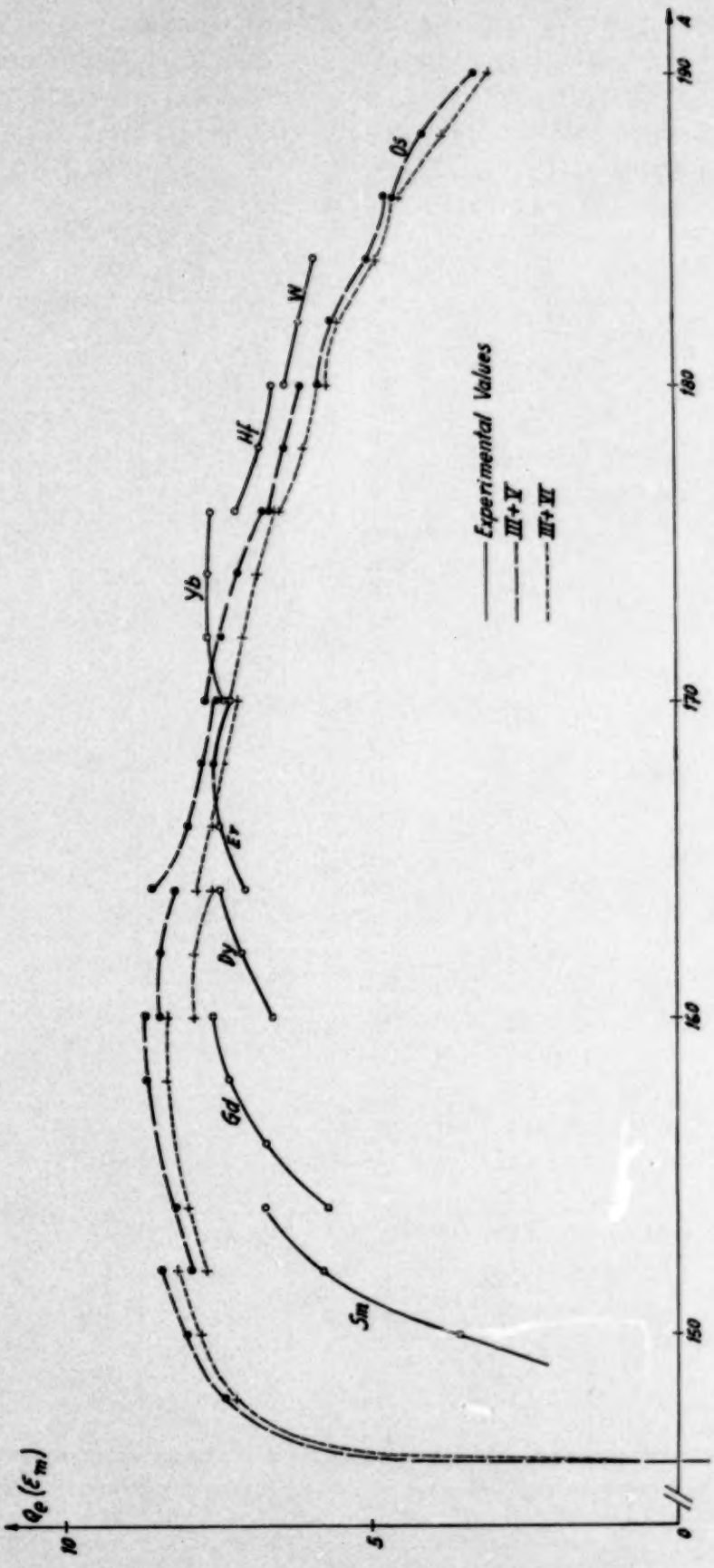

Fig. 4. The electric quadrupole moments for the shifts III + V and III + VI.

It is also easy to perform the calculations combining III with V and II with VI. The corresponding results for the equilibrium deformations and for the electric quadrupole moments are given in table 3 and fig. 4, respectively. They do not show any substantial change with respect to those corresponding to the combination III+VI.

TABLE 3

Predicted equilibrium deformations ε_m. The different columns correspond to different shifts of the higher shells (table 2)

	III+VI	III+V	II+VI	II+V
$_{62}Sm^{146}$	0	0	0	0
Sm^{148}	0.30	0.30	0.31	0.31
Sm^{150}	0.33	0.33	0.33	0.33
Sm^{152}	0.34	[a])	0.35	[a])
Sm^{154}		[a])		[a])
$_{64}Gd^{152}$	0.31	0.31	0.32	0.32
Gd^{154}	0.33	0.33	0.33	0.35
Gd^{156}		0.33		
Gd^{158}	0.34	0.34	0.35	[a])
Gd^{160}	0.34	0.35	0.35	[a])
$_{66}Dy^{160}$	0.31	0.32	0.33	[a])
Dy^{162}	0.31	0.32	0.33	[a])
Dy^{164}	0.30	0.32	0.32	[a])
$_{68}Er^{164}$	0.30	0.30	0.32	[a])
Er^{166}	0.29	0.30	0.30	[a])
Er^{168}	0.28	0.29	0.29	[a])
Er^{170}	0.27	0.28	0.28	[a])
$_{70}Yb^{170}$	0.27	0.27	0.28	[a])
Yb^{172}	0.26	0.27	0.27	[a])
Yb^{174}	0.25	0.26	0.26	[a])
Yb^{176}	0.24		0.24	[a])
$_{72}Hf^{176}$	0.24	0.24	0.24	[a])
Hf^{178}	0.22		0.23	[a])
Hf^{180}	0.21	0.22	0.22	[a])
$_{74}W^{180}$	0.21		0.21	
W^{182}	0.20	0.20	0.20	0.21
W^{184}	0.18	0.19	0.18	0.20
W^{186}	0.17	0.18	0.17	0.18
$_{76}Os^{186}$	0.17	0.17	0.17	0.17
Os^{188}	0.14	0.15	0.15	0.14
Os^{190}	0.11	0.12	0.12	0.12

[a]) The curves do not show any minimum, so that ε_m is probably greater than 0.35. In order to have more reliable results for the equilibrium deformation when $\varepsilon_m < 0.30$, it should be convenient to solve the Nilsson Hamiltonian for higher values of the deformation.

It remains to be seen whether some intermediate position of the higher neutron or proton levels would produce a better agreement with the experimental data. Probably this is not true. In fig. 2 we have represented successive plots of energy versus deformation. As we decrease the shifts of the higher shells we get a shallower minimum, but it is practically always at the same point. Further decrease brings in another minimum and we have a discrete change in the deformation †. This suggests that the reason for the remaining disagreement upon the values of Q_e probably lies beyond the uncertainty of the position of the higher shells.

5.2. DEFORMATIONS

It is interesting to compare the deformation of the potential ε with the value of the deformation $\bar{\varepsilon}$ obtained from the electric quadrupole moment, assuming a uniform charge distribution (32),

$$Q_e = \tfrac{4}{5} Z R^2 \bar{\varepsilon} (1 + \tfrac{1}{2} \bar{\varepsilon}). \tag{35}$$

It is seen †† that $\bar{\varepsilon} \approx \varepsilon$ (Table 4).

TABLE 4

Comparison of the values of the deformation of the potential ε with the values of the deformation $\bar{\varepsilon}$, obtained on the assumption of a uniform charge distribution

Z	$\varepsilon = 0.10$		$\varepsilon = 0.20$		$\varepsilon = 0.30$	
	Q_e	$\bar{\varepsilon}$	Q_e	$\bar{\varepsilon}$	Q_e	$\bar{\varepsilon}$
62	2.30	0.11	4.91	0.22	7.25	0.31
64	2.44	0.11	5.30	0.22	7.47	0.31
66	2.56	0.11	5.42	0.22	7.68	0.30
68	2.67	0.11	5.57	0.21	7.93	0.29
70	2.68	0.10	5.66	0.20	8.21	0.29
72	2.79	0.10	5.64	0.20	8.53	0.29
74	2.79	0.10	5.58	0.19	8.86	0.28
76	2.72	0.09	5.45	0.17	9.10	0.28

The electrical quadrupole moments are given in units 10^{-24} cm^2. The A-dependence in the frequency of the harmonic oscillator potential is taken into account by means of an average over all the corresponding stable isotopes.

5.3. THE STRENGTH OF THE QUADRUPOLE INTERACTION

If we calculate the mass quadrupole moment for the equilibrium deformation, we can determine the value of k by means of (6) and (17). In fig. 5 we have plotted the mass quadrupole moment against the deformation. The slope of the line joining the origin with the point corresponding to the equilibrium deformation measures the value of k. It is clear now why the equilibrium

† The existence of several minima has been discussed in refs. [15, 17]).

†† There appears to be a systematic discrepancy between this result and that obtained recently by Glendenning and Sawicki [30]). They obtain greater quadrupole moments than we do for the same value of η, and thus they have $\bar{\varepsilon} < \varepsilon$.

deformation is so sensitive to the value of k: the curve representing the quadrupole moment is almost a straight line.

Conversely, and for the same reason, we can obtain a fairly reliable value of k, which is almost independent of the displacements of the levels. The mean value of k is

$$k = 102\, A^{-\frac{1}{3}} (M\mathring{\omega}_0/\hbar)^2 \text{ MeV}. \tag{36}$$

The $A^{-\frac{1}{3}}$ dependence predicted by Belyaev [6]) appears very clearly because the mean square deviation of the constant in (36) is only 5.

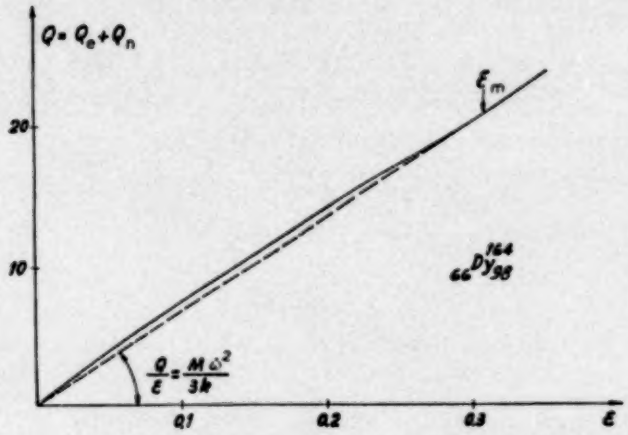

Fig. 5. The total quadrupole moment Q is represented as a function of the deformation for Dy^{164} (full-drawn line). The slope of the straight dotted line measures the value of k.

In order to get the vibrational parameters in nuclei with only one kind of particles outside closed shells, Kisslinger and Sorensen have used the value (in MeV)

$$k = \frac{275}{A}\left(\frac{M\mathring{\omega}_0}{\hbar}\right)^2 \frac{1}{N+\frac{3}{2}} \approx 211\, A^{-\frac{1}{3}}\left(\frac{M\mathring{\omega}_0}{\hbar}\right)^2 \tag{37}$$

(cf. eq. (41) of ref. [10])). The value given by (37) is about twice as large as (36). This is very reasonable, since (37) is renormalized by closed-shell effects, while we have treated explicitly all the neutrons and protons.

6. Conclusions

Fig. 4 shows that the predicted electric quadrupole moments are in good agreement with the experimental values, provided certain shifts in the single-particle energy levels are made. This was to be expected in view of the results of Mottelson and Nilsson [19]) and because, once the nucleus is deformed, the gap does not vary very much with the deformation. However, the gain in energy $\Delta\mathscr{E}$ produced by the deformation is considerably reduced when the pairing force is present. It becomes negative for neutron numbers less than 86. In the cases when the gain is close to zero, the influence of the small Coulomb

force becomes decisive. Therefore, before making a more accurate treatment of the Coulomb force, there is no point in trying to push further down the neutron $N = 4$ shells in order to get $\Delta\mathscr{E} < 0$ for neutron numbers less than 90.

The parameters G and k, which are necessary in order to fit the experimental data examined here, are in agreement with the values used in other calculations. This fact provides a new support to the validity of the model.

The authors wish to express their gratitude to Professors N. Bohr and A. Bohr for the hospitality of the Institute for Theoretical Physics, Copenhagen. Sincere thanks are due Professors A. Bohr and B. Mottelson and Dr. S. G. Nilsson for valuable suggestions. We also wish to acknowledge many discussions with other members of the nuclear-physics group working at Copenhagen during 1959. We are grateful to Mr. J. Bohman for his assistance in the numerical computations at the electronic Computer SMIL, University of Lund, Sweden. Our stay in Copenhagen during 1959 was made possible by stipends granted to D. B. by Professor A. Bohr, and to Z.S. by the International Atomic Energy Agency.

References

1) A. Bohr, Comptes Rendus du Congrès International de Physique Nucléaire, Paris, July 1958 (Dunod, Paris, 1959) p. 203.
2) J. P. Elliot, Proc. Royal Society A **245** (1958) 128, 562;
B. H. Flowers (and subsequent discussion), Proc. of the Rehovoth Conf. on Nuclear Structure, Rehovoth, Israel, September 1957, (North-Holland Publishing Co., Amsterdam, 1958) p. 161;
B. R. Mottelson, to be published
3) B. F. Bayman, Comptes Rendus du Congrès International de Physique Nucléaire, Paris, July 1958 (Dunod, Paris, 1959) p. 741
4) J. Bardeen, L. N. Cooper and J. R. Schrieffer, Phys. Rev. **108** (1957) 1175
5) G. Racah, Proc. of the Rehovoth Conf. on Nuclear Structure, Rehovoth, Israel, September 1957 (North-Holland Publishing Co., Amsterdam, 1958) p. 155
6) S. T. Belyaev, Mat. Fys. Medd. Dan. Vid. Selsk. **31**, No. 11 (1959)
7) B. R. Mottelson, The many-body problem, Lectures given at the École d'Été de Physique Théorique, les Houches, France, (Dunod, Paris, 1959) p. 283
8) B. R. Mottelson, Lectures given at the Institute for Theoretical Physics, Copenhagen, autumn 1958 (unprinted)
9) M. Baranger, Phys. Rev. **120** (1960) 957
10) L. Kisslinger and R. Sorensen, Mat. Fys. Medd. Dan. Vid. Selsk. **32**, No. 9 (1960)
11) J. Bro-Jørgensen and A. Haatuft, to be published
12) S. G. Nilsson and O. Prior, Mat. Fys. Medd. Dan. Vid. Selsk. **32**, No. 16 (1960)
13) J. J. Griffin and M. Rich, Phys. Rev. Letters **3** (1959) 342
14) V. G. Soloviev, Mat. Fys. Skr. Dan. Vid. Selsk. **1**, No. 11 (1961)
15) D. R. Bès, Mat. Fys. Medd. Dan. Vid. Selsk. **33**, No. 2 (1961)
16) S. G. Nilsson, Mat. Fys. Medd. Dan. Vid. Selsk. **29**, No. 16 (1955)
17) A. Kerman, Annals of Physics **12** (1961) 300
18) B. Mottelson, Lectures given at the International School of Physics "Enrico Fermi", Varenna. Italy, 1960
19) B. Mottelson and S. G. Nilsson, Mat. Fys. Skr. Dan. Vid. Selsk. **1**, No. 8 (1959)
20) N. Bohr and J. A. Wheeler, Phys. Rev. **56** (1939) 426
21) D. G. Ravenhall, Revs. Mod. Phys. **30** (1958) 430

22) A. J. Rassey, Phys. Rev. **109** (1958) 949
23) W. H. Johnson and V. B. Bhanet, Phys. Rev. **107** (1957) 1669
24) B. A. Kratsov, JETP (USSR) **36** (1959) 1224
25) B. Elbek, K. O. Nielsen and M. C. Olesen, Phys. Rev. **108** (1957) 406;
V. Ramšak, M. C. Olesen and B. Elbek, Nuclear Physics **6** (1958) 451;
B. Elbek, M. C. Olesen and O. Skilbreid, Nuclear Physics **10** (1959) 294;
M. C. Olesen and B. Elbek, Nuclear Physics **15** (1960) 34
26) P. Gregers Hansen, N. O. Lassen, O. B. Nielsen and R. K. Sheline, Nuclear Physics **12** (1959) 389
27) O. B. Nielsen, private communication
28) D. Strominger, J. M. Hollander and G. T. Seaborg, Revs. Mod. Phys. **30** (1958) 585
29) C. J. Gallagher, Nuclear Physics **16** (1960) 215
30) N. K. Glendenning and J. Sawicki, Nuclear Physics **18** (1960) 596

1.D.2:
1.E.3

Nuclear Physics **28** (1961) 63—80; © *North-Holland Publishing Co., Amsterdam*
Not to be reproduced by photoprint or microfilm without written permission from the publisher

EQUILIBRIUM DEFORMATIONS OF NUCLEI IN THE TRANSURANIC REGION

ZDZISŁAW SZYMAŃSKI

Institute for Nuclear Research, Warsaw, and University of Warsaw, Poland

Received 26 April 1961

Abstract: The equilibrium deformations and quadrupole moments of even deformed nuclei in the transuranic region are calculated on the basis of wave functions that take into account a pairing interaction through the "superconductivity" formalism. The results obtained theoretically are found to be in reasonable agreement with experiment. The relation between the potential and density deformation parameter is also discussed.

1. Introduction

Nuclei with mass number $A \gtrsim 220$ are known as showing large stable deformations. This can be seen from the fact that nuclei of this region exhibit rotational sequences of levels with energies given by the well known formula

$$E = (\hbar^2/2\mathscr{I})I\,(I+1),$$

with $I = 0, 2, 4$ for even nuclei. The nuclear equilibrium deformation can be obtained from determination of the electric quadrupole moment Q_0 of the nucleus. The later quantity is derived either from the observed half-life time $T_{\frac{1}{2}}$ of the E2 gamma transition $(2+ \rightarrow 0+)$ within the rotational band, or from the experimental measurement of the cross section for Coulomb excitation of the 2+ state from the ground state. Recently new experimental results on quadrupole moments have been published [1, 2]). They are much more exact than the previous data so that even a kind of detailed structure for various isotopes can be seen in the plot of Q_0 versus A.

A first estimation of the equilibrium deformations has been given by Mottelson and Nilsson [3]) on the basis of the independent-particle model with a deformed potential field considered by Nilsson [4]). However, the Mottelson-Nilsson calculation concerns only the odd-mass nuclei for which the ground-state configuration has been chosen from the experimental spin assignment. The calculated minimum in the total energy corresponds to this configuration only and the decrease of the Coulomb energy with the deformation has been neglected. Furthermore in the independent-particle treatment a non-zero deformation always results for all nuclei except for those with doubly-closed

shells, because the first order derivative of the total energy with respect to deformation is different from zero at zero deformation. Thus the independent-particle model does not form the appropriate theoretical scheme for the explanation of the existence and position of the transition point from spherical to deformed nuclei.

Therefore in order to account for the right trend of the deformation it is necessary to introduce the residual interactions between the outside nucleons. We shall assume that the long-range part of those interactions has already been included in the deformed field, while the short-range part can be represented by a pairing force with the appropriate strength. In the case of the many-fermion systems interacting via pairing forces a variational method has been developed [5, 6]) in order to account for the superconductivity phenomena. Following the suggestion [7]) that this method can be also applied in the nuclear case Belyaev [8]) has investigated various properties of the nucleus in the "superconducting" state. Further developments and applications of the model both in the spherical [9, 10]) and deformed cases [11–14]) seem to prove that the short-range part of the residual interaction can be successfully represented by pairing forces while the long-range part leads mainly to the quadrupole deformation of the nuclear field [15]).

One of the results of Belyaev [8]) was the conclusion that the first-order derivative of the total nuclear energy with respect to deformation vanishes at the zero deformation. Thus pairing force is in principle able to explain that the transition from spherical to deformed case occurs for nuclei lying somewhere in between the closed-shell nuclei. The model of the particles moving in the spheroidal (Nilsson) field and interacting with pairing forces has been recently applied to the calculation of the equilibrium deformations of nuclei in the rare-earth region [14]). Rather good agreement with the experimental data has been obtained. The present paper aims at extending those calculations to the other well-known deformed region of the transuranic elements ($A \gtrsim 220$).

2. Method of Calculation

The method of calculation of the equilibrium deformation employed in this paper is esentially the same as in ref. [14]), except for the fact that besides the total energy also the first derivative of the energy with respect to deformation has been calculated. Therefore we shall only sketch the general argumentation and quote the main formulae.

Nilsson's [4]) way of calculating the equilibrium deformation has been used. It consists in the minimisation of the total energy with the condition that the total volume of the nucleus should be kept constant as the shape is varied. The condition of constant volume enables one to avoid the more complicated

self-consistent treatment. It has been shown in ref. [14]) that the condition of constant volume is equivalent in a certain sense to the self-consistent treatment as far as the equilibrium deformation is concerned.

The starting point for the calculation is to assume that the Hamiltonian may be expressed as the sum of the idenpendent-particle energies in a deformed Nilsson field and the pairing forces. In the second-quantisation notation it has the form

$$H = \sum \varepsilon_\nu (b^\dagger_{\nu+} b_{\nu+} + b^\dagger_{\nu-} b_{\nu-}) - G \sum_{\nu\nu'} b^\dagger_{\nu+} b^\dagger_{\nu-} b_{\nu'+} b_{\nu'-}, \tag{1}$$

where the index $(\nu\sigma)$ denotes the set of quantum numbers in a deformed field [4]), $\sigma = +$ or $-$ referring to the two possible signs of the angular momentum projection, while the ε_ν are the deformation-dependent single-particle energies and G the pairing force strength.

Next we go over the auxiliary Hamiltonian [8])

$$H' = H - \lambda \hat{N} - \mu' \hat{Q}, \tag{2}$$

where N and Q are the operators of the number of particles and the total quadrupole moment, and λ, μ' the corresponding Lagrangian multipliers.

Now the Bogolubov transformation

$$b_{\nu+} = u_\nu \alpha_\nu + v_\nu \beta^\dagger_\nu, \quad b_{\nu-} = u_\nu \beta_\nu - v_\nu \alpha^\dagger_\nu, \quad \text{with } u_\nu^2 + v_\nu^2 = 1, \tag{3}$$

is performed to the quasi-particle picture described by the operators α_ν, β_ν. Then neglecting the interaction between quasi-particles and choosing u_ν and v_ν so as to minimize the ground-state energy we are led to a set of two equations for λ and Δ^2;

$$\frac{2}{G} = \sum_\nu \frac{1}{\sqrt{(\varepsilon_\nu - \lambda)^2 + \Delta^2}}, \quad N = \sum_\nu \left(1 - \frac{\varepsilon_\nu - \lambda}{\sqrt{(\varepsilon_\nu - \lambda)^2 + \Delta^2}}\right) \equiv \sum_\nu 2 v_\nu^2, \tag{4}$$

where N is the number of neutrons or protons in the actual nucleus. It has been shown [12]) (see also ref. [16])) that for the equilibrium deformation the second Lagrangian multiplier μ' of eq. (2) vanishes. The total energy $\mathscr{E}$ and quadrupole moment Q_0 are given by the formula

$$\mathscr{E} = \sum_\nu 2 v_\nu^2 \, \varepsilon_\nu - \Delta^2/G, \tag{5}$$

$$Q_0 = \sum_{\nu \text{ (protons)}} 2 v_\nu^2 \, q_{\nu\nu}, \tag{6}$$

where $q_{\nu\nu}$ are the single-particle quadrupole moment matrix elements calculated with the Nilsson wave functions.

In order to obtain the equilibrium deformation one has to calculate the sum of the two energies $\mathscr{E}$ for neutrons and protons respectively as a function of

the deformation of the potential † and find the minimum, which will correspond to the equilibrium. Another way to determine the equilibrium deformation is to find the value of deformation for which the first-order derivative of $\mathscr{E}$ with respect to ε vanishes. One can see that all the quantities appearing on the right-hand side of eq. (5) except G depend upon ε. Similarly all the quantities on the right-hand side of eq. (4) are deformation-dependent while $2/G$ and N are not. Thus combining the derivatives of eqs. (5) and (4) one easily gets the simple expression

$$\frac{\partial \mathscr{E}}{\partial \varepsilon} = \sum_{\nu} 2v_{\nu}^2 \frac{\partial \varepsilon_{\nu}}{\partial \varepsilon}, \tag{7}$$

valid for arbitrary ε. The eigenvalues ε_{ν} of the Nilsson Hamiltonian and their dependence on ε are determined in ref. [4]). The derivative of ε_{ν} is simply

$$\frac{\partial \varepsilon_{\nu}}{\partial \varepsilon} = (N_{\nu}+\tfrac{3}{2}) \frac{\partial}{\partial \varepsilon} [\hbar\omega_0(\varepsilon)] - \tfrac{1}{3} \left\{ \varepsilon \hbar\omega_0(\varepsilon) + \frac{\partial}{\partial \varepsilon} [\hbar\omega_0(\varepsilon)] \right\} \langle \nu | 2\zeta^2 - \xi^2 - \eta^2 | \nu \rangle, \tag{8}$$

where N_{ν} is the harmonic oscillator total quantum number, ξ, η, ζ dimensionless coordinates and $\omega_0(\varepsilon)$ is the ε-dependent oscillator frequency defined in ref. [4]),

$$\hbar\omega_0(\varepsilon) = \hbar\mathring{\omega}_0\{1+\tfrac{1}{9}\varepsilon^2+O(\varepsilon^3)\}, \quad \text{with } \hbar\mathring{\omega}_0 = 41/A^{\frac{1}{3}} \text{ MeV}. \tag{9}$$

In the calculation of the total energy of the protons the change of Coulomb energy with deformation must be included. In the first approximation we assume a certain average distribution of the electric charge over the whole nucleus instead of introducing the complicated quantal calculation of the Coulomb energy. According to the data obtained from electron scattering on nuclei [17]) we adopt a trapezoidal shape of the charge-density distribution. Then the decrease of energy with the density deformation $\bar{\varepsilon}$ is given by the expression

$$\mathscr{E}_{\text{Coul}} = -\tfrac{4}{45} \bar{\varepsilon}^2 \tfrac{1}{2} \int \mathrm{d}\mathbf{r} \int \mathrm{d}\mathbf{r}' \frac{\rho(\mathbf{r})\rho(\mathbf{r}')}{|\mathbf{r}-\mathbf{r}'|}, \tag{10}$$

where the density deformation $\bar{\varepsilon}$ can be determined from the expression for

† The deformation parameter ε of the potential has been introduced in the Appendix A of ref. [4]) and is related to the usual Nilsson deformation δ by the formula

$$\varepsilon = \delta + \tfrac{1}{6}\delta^2 + O(\delta^3).$$

Moreover another deformation parameter η will also be used in the present paper. It is related to ε by the equation

$$\eta = (\varepsilon/\kappa)(1 + \tfrac{1}{9}\varepsilon^2 + \tfrac{5}{81}\varepsilon^3),$$

where κ is a measure for the $\mathbf{L}\cdot\mathbf{S}$-term strength in the single-particle Hamiltonian. In the present paper κ will be assumed equal to 0.05.

the quadrupole moment of the average charge distribution

$$Q_0 = \tfrac{4}{5} Z R_0^2 \bar{\varepsilon}(1+\tfrac{1}{2}\bar{\varepsilon}). \tag{11}$$

Here $R_0 = \{\frac{5}{3}\langle r^2\rangle\}^{\frac{1}{2}}$ is the mean-square radius calculated by means of the charge density $\rho(r)$. It turns out that the Coulomb energy change computed from eq. (10) is rather important in the determination of the equilibrium deformation as it appears to be of the same order of magnitude as the energy change coming from nuclear interaction.

3. Discussion of the Numerical Parameters

3.1. SINGLE-PARTICLE ENERGY LEVELS

Nilsson [4]) investigated single-particle motion in a deformed harmonic oscillator field including the spin-orbit coupling term and the $\mathbf{l}^2$ correction which accounts for the deviation of the average nuclear potential from the harmonic oscillator shape. The energy eigenvalues are given by the expression

$$\varepsilon_\nu = (N_\nu+\tfrac{3}{2})\hbar\omega_0(\varepsilon)+\kappa\hbar\mathring{\omega}_0 r_\nu, \tag{12}$$

where κ is related to the strength of the spin-orbit coupling. The values of r_ν are tabulated [4, 3]) for the deformation $\eta = 0, 2, 4, 6$. The distances r_ν also depend on the parameter μ determining the strength of the $\mathbf{l}^2$-term in the Hamiltonian. A numerical value $\kappa = 0.05$ has been adopted both for neutrons and protons. The μ-value 0.45 has been introduced for $N_\nu = 5$ and 6 neutrons [4]), while $\mu = 0.40$ for $N_\nu = 7$ neutrons [3]). The μ-values for protons are somewhat larger, which partly results from the Coulomb repulsion between protons. Thus $\mu = 0.55$ has been assumed for $N_\nu = 4$ protons, $\mu = 0.70$ for $N_\nu = 5$ protons and finally $\mu = 0.45$ for $N_\nu = 6$ protons [4]). The energy of the closed shells comes into consideration only through the sum of eq. (12) over all the closed shell configurations. Then the sum of all quantities r_ν is independent of ε and the whole contribution of the closed shells reduces to the sum of the first terms in eq. (12). The deformation dependence of such a sum comes only from the condition of constant volume and is determined by eq. (9).

As the single-particle energies ε_ν appear to be important parameters in our calculation it is worthwhile to see how well the Nilsson values of ε_ν correspond to the actual situation in nuclei and to what extent they can be treated as free parameters. The experimental data on the ground and excited states of the odd-mass nuclei can provide a verification of the sequence of levels ε_ν within the last unfilled shells both for neutrons ($N_\nu = 6$) and protons ($N_\nu = 5$). Those data have been analysed in ref. [3]) and seem to confirm the adopted set of numerical parameters. Still there exists some freedom in the values of ε_ν which concerns mainly the distances between the major oscillator shells. This distance cannot be determined directly from the experimental data

because the levels coming from the other major shells never appear above the Fermi surface. The only information which can be obtained is that the lower shell for neutrons ($N_\nu = 5$) and protons ($N_\nu = 4$) should be shifted down by an amount approximately equal at least to $0.23\ \hbar\mathring{\omega}_0$ as compared to the original Nilsson level scheme. This conclusion follows from the fact the single-particle configurations corresponding to the lower shells have never been observed among the excited states of the odd-mass nuclei. For example they have not been seen [3]) in the spectra of U^{233} and Pa^{233} or any heavier nuclei. On the other hand it turns out (see Appendix) that the positions of those shells have rather strong influence on the determination of the ground-state deformation. Also the position of the upper neutron shell ($N_\nu = 7$) can have some influence. Therefore several variants with various shifts have been chosen in order to see their influence on the final results. They are listed in table 1.

TABLE 1

Single-particle level shifts employed in the calculations

	Configuration	Variant 1	Variant 2	Variant 3	Variant 4
Neutrons $N > 126$	$N_\nu = 7, \neq j_{\frac{15}{2}}$	0	0	+0.150	+0.150
	$N_\nu = 7, \quad j_{\frac{15}{2}}$	−0.060	−0.060	−0.060	−0.060
	$N_\nu = 6, \quad i_{\frac{13}{2}}$	−0.230	−0.080	−0.080	−0.103
	$N_\nu = 5$	−0.380	−0.230	−0.230	−0.253
Protons $Z > 82$	$N_\nu = 6, \ i_{\frac{13}{2}}$	−0.350	−0.350	−0.350	−0.350
	$N_\nu = 5, \ h_{\frac{11}{2}}$	−0.200	−0.050	−0.050	−0.084
	$N_\nu = 4$	−0.380	−0.230	−0.230	−0.264

All the shifts are given in units of $\hbar\mathring{\omega}_0 = 41/A^{\frac{1}{3}}$ MeV. The sign + or − denotes the direction of shift, upwards or downwards, respectively.

Moreover the positions of the subshells $N_\nu = 7j_{\frac{15}{2}}$, $N_\nu = 6i_{\frac{13}{2}}$ and $N_\nu = 5h_{\frac{11}{2}}$ have been slightly shifted so as to adjust them to the different μ values in major shells (compare refs. [11, 14])). All the shifts introduced in the present paper are in line with the similar shifts assumed in ref. [11]). The upper proton shell ($N_\nu = 6$) lies rather high above the Fermi surface of the actual nuclei, so that its position does not affect the result of the calculation. The numerical values of the energy levels for one of the variants chosen (variant 2 of table 1) have been listed in a separate report †.

3.2. PAIRING FORCE STRENGTH

The pairing force strength comes into the calculation through the first eq. (4). In the detailed analysis of the previous investigations [9–14]) on the pairing interaction in nuclei it has been concluded that the pairing-force strengths G_n and G_p for neutrons and protons are inversely proportional to the mass

† See the footnote to subsect. 4.1.

number A. It has also been established that from the two approximately constant parameters AG_n and AG_p the latter appears to be larger. Numerical values of those two parameters depend on the number of states taken into account in eq. (4). In the case of large stable deformations there is no prominent shell structure in the spectra. Thus one has to cut off the sums (4) in some arbitrary way. The effective value of G depends rather strongly on the cut-off while the other quantities appearing in the formalism remain almost unchanged, if G is properly adjusted to the number of states included in eq. (4). Following ref. [14]) we shall take into account only 24 states nearest to the Fermi surface. The corresponding parameters in ref. [14]) are $AG_n = 26.49$ MeV and $AG_p = 32.20$ MeV. In the present paper the value $AG_n = 26.04$ MeV (i.e. 1.7 % lower) has been assumed while AG_p remained the same as in ref. [14]). On the other hand Nilsson and Prior [11]) include in eq. (4) all the neutron levels belonging to the $N_\nu = 5,6$ and 7 shells and all the proton levels belonging to the $N_\nu = 4$, 5 and 6 shells. Their G values are then considerably lower: $AG_n = 17$—19 MeV $AG_p = 24$—26 MeV. These values cannot be directly compared with the values used in the present calculation; however, the G-value can be renormalised according to the number of levels included in eq. (4). Then one easily gets (compare eq. (41) of ref. [8]))

$$(2/G_{\text{renorm.}}) = (2/G_{24\text{ levels}}) - \sum_{\substack{\text{remaining}\\ \text{levels}}} |\varepsilon_\nu - \lambda|^{-1}. \tag{13}$$

With the use of this equation $G_{\text{renorm.}}$ has been computed for the 136 neutrons and 94 protons (as an example) in the case of zero deformation. In this way the values 16.5 MeV and 23 MeV have been obtained for $(AG_n)_{\text{renorm.}}$ and $(AG_p)_{\text{renorm.}}$ respectively. If we take into account that eq. (13) tends to underestimate the value of $G_{\text{renorm.}}$ we can conclude that the Nilsson-Prior values assumed for G are almost the same as (or lower by 1—3 % than those adopted in the present paper.

3.3. SINGLE-PARTICLE QUADRUPOLE MATRIX ELEMENTS

The values of the matrix elements $q_{\nu\nu}$ have been computed from the formula

$$q_{\nu\nu} = \langle \nu | (2z^2 - x^2 - y^2) | \nu \rangle, \tag{14}$$

where $|\nu\rangle$ denotes the single-particle Nilsson wave function.

4. Calculation and Results

4.1. DETAILS OF CALCULATION

The numerical computations were performed on the Electronic Computer XYZ of the Polish Academy of Sciences in Warsaw. They aimed at solving the two eqs. (4) simultaneously for a given set of single-particle energies ε_ν, G and N. After having found the solutions for λ and Δ the computer went on

to calculate the $2v_\nu^2$ and the total energy according to eq. (5). Moreover the total quadrupole moment has been computed from eq. (6) with the use of the $q_{\nu\nu}$-matrix elements. The calculations were performed in the four cases of different deformations $\eta = 0, 2, 4, 6$ for all even neutron numbers $130 \leqq N \leqq 152$ and proton numbers $84 \leqq Z \leqq 100$. Some parts of the calculation were repeated with various positions of the lower and higher major shells (see table 1). Some additional calculations were also performed for a slightly changed value of G so as to see its influence on the results.

The numerical solution corresponding to the variant 2 of table 1 has been tabulated †. The solutions contain λ, Δ^2 and the set of the 24 values of $2v_\nu^2$ for each deformation. The lists of ε_ν are also given for each deformation. Both λ and Δ as well as ε_ν are given in units of $\hbar\omega_0 = 41/A^{\frac{1}{3}}$ MeV.

4.2. RESULTS ON ENERGY GAP

The solutions of eq. (4) contain the set of Δ in the whole region of N and Z considered. As G has been kept constant for each N or Z with varying deformation, the dependence of Δ on deformation can be seen for each nucleus separately. The energy gap 2Δ corresponding to the equilibrium should in principle be compared with the experimental energy gap determined from nuclear spectra. However, only in very few cases nuclear excited levels can be unambiguously assigned to definite quasi-particle configurations. Besides, even in those few cases of the lowest known excitations it is not quite excluded that there would exist some strong quasi-particle interaction lowering the level below the gap[11,14])

Another way of discussing the magnitude of Δ is the comparison with the odd-even mass difference, a quantity which can be determined from the experimental data. The odd-even mass difference is defined by the following relations:

$$\begin{aligned} P_n &= \tfrac{1}{2}\{E(Z,N) - 2E(Z,N-1) + E(Z,N-2)\}, \\ P_p &= \tfrac{1}{2}\{E(Z,N) - 2E(Z-1,N) + E(Z-2,N)\}, \end{aligned} \tag{15}$$

for neutrons and protons respectively ††, E denoting the total binding energy. The experimental P_n and P_p should in principle be compared with P_n and P_p calculated from (15) with the theoretical $E(Z,N)$ derived from eq. (5). However, this would require the knowledge of solutions of eq. (4) in the case of odd neutron or proton numbers. In the first approximation one can omit this calculation and assume that

$$\Delta_n \approx P_n^{\mathrm{exp}}, \qquad \Delta_p \approx P_p^{\mathrm{exp}}. \tag{16}$$

Similar approximations have already been made in refs. [11,14]), and moreover in ref. [11]) the validity of the approximation (16) has been discussed.

† Those tables have been deposited as a Report nr. 230/VII of the Institute for Nuclear Research, Warsaw, Hoża 69, Poland. They have not been reproduced here because of limitations of space. A copy may be secured on request at the above address.

†† More precise definitions of P_n and P_p have been introduced in ref. [11]).

The extensive analysis of the existing experimental material concerning the P_n and P_p in the transuranic region has been performed in ref. [11]). We can use these data to compare them with our Δ obtained from the solutions of eq. (4). The results are presented in fig. 1 and fig. 2 for neutrons and protons,

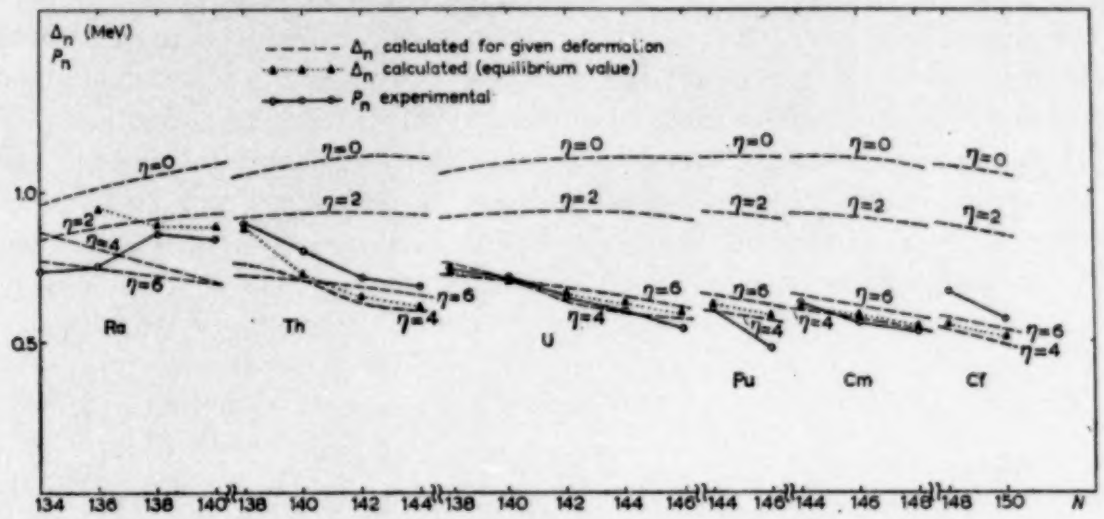

Fig. 1. The odd-even mass difference parameter P_n for neutrons versus the number of neutrons compared with Δ_n. The dashed lines correspond to the calculated Δ_n for various deformations η ($\eta = 0, 2, 4, 6$ as indicated). The equilibrium value of Δ_n is then obtained by interpolation for the actual nuclear deformation (dotted line with triangles). Circles connected with solid line refer to the experimental P_n collected in ref. [11]). The level shifts correspond to the variant 2 of table 1.

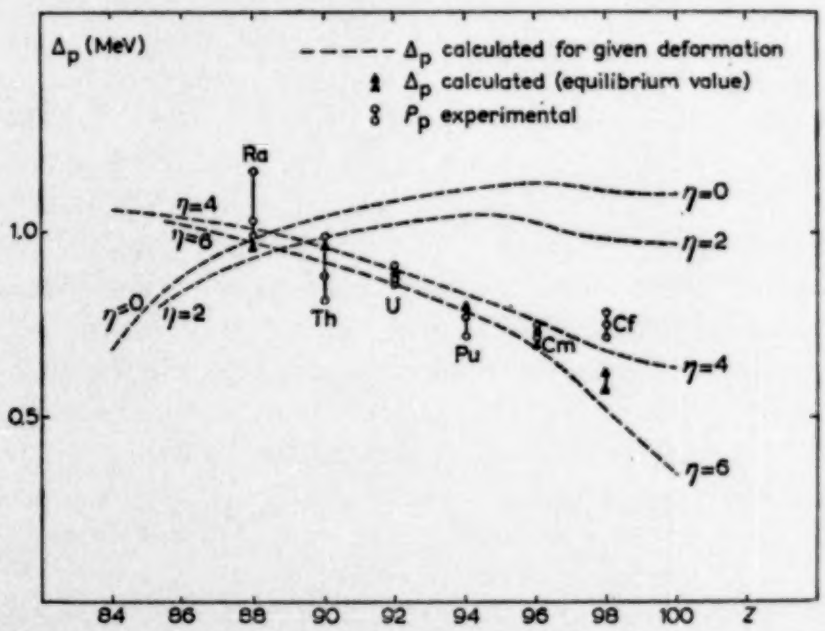

Fig. 2. The odd-even mass difference parameter P_p for protons versus Z, compared with Δ_p. The dashed lines correspond to the calculated Δ_p for various deformations ($\eta = 0, 2, 4, 6$ as indicated). The equilibrium value of Δ_p is then obtained by interpolation for the actual deformation (triangles). Circles connected with solid line refer to the experimental P_p collected in ref. [11]). The level shifts correspond to the variant 2 of table 1.

respectively. The theoretical values of Δ correspond to the variant 2 of table 1. The equilibrium values of Δ have been obtained by interpolation of the Δ-values for the equilibrium value of the deformation ε. One can see from the plots that the agreement of the theory with experiment is rather good apart from some fluctuations. Also the deformation-dependence of Δ can be read from figs. 1 and 2. It turns out that the energy gap in the spherical case $\varepsilon = 0$ is in general larger than in the deformed case (although Δ is not a monotonic function of deformation). This is consistent with the well-known fact that pairing force tends to produce spherical stability. This also supplies the explanation of the increase of Δ in the region of transition from deformed to spherical shape. It seems to be due to the fact that Δ generally increases when the deformation ε drops to zero.

In order to see how sensitive is the dependence of Δ on the pairing-force strength some calculations have been performed for a slightly lower value of G in the case of protons. It turns out that an increase of G by about 4 % causes an increase of Δ of the order of 8 %. On the other hand the Δ values appear not to be very sensitive of the single-particle level shifts, which is consistent with the structure of eq. (4) (see Appendix).

4.3. QUADRUPOLE MOMENTS AND EQUILIBRIUM DEFORMATIONS

The total energy $\mathscr{E}$ computed from eq. (5) can be plotted versus deformation for each nucleus and the position of minimum in the curve is then the resulting equilibrium deformation. The graphical method of determining $\varepsilon_{\text{eq.}}$ is not very exact and has been improved by the calculation of the slope of the curve by means of eq. (7). Still, some errors in the resulting $\varepsilon_{\text{eq.}}$ are possible but it is hoped that the general trend of the variation of $\varepsilon_{\text{eq.}}$ with A has been reproduced correctly. As an example a typical energy curve as a function of deformation is shown in fig. 3 for the U^{230} nucleus. The position of equilibrium has been indicated by an arrow. For the sake of comparison with the independent-particle treatment, the independent-particle energy curves corresponding to the different configurations are also plotted in fig. 3. It can be seen from this example that the existence of pairing forces leads to a lowering the energy curve, while the position of the $\varepsilon_{\text{eq.}}$ is not affected very much for nuclei with large stable deformations. For large deformations ($\eta \approx 6$) the independent particle model shows a sharp increase of the energy which would not exist if the Coulomb energy were included. This accounts for the different behaviour of the two curves in fig. 3 in the region of $\eta \approx 6$.

If the assumption $\bar{\varepsilon} = \varepsilon$ is made for the moment the equilibrium deformation can be determined from the experimental value of Q_0 with use of eq. (11). The results of such a procedure are represented in fig. 4 together with the calculated $\varepsilon_{\text{eq.}}$. We shall discuss those curves together with the corresponding plot of the quadrupole moments.

The electric quadrupole moments of nuclei have been calculated from eq. (6) as a function of deformation η. A typical plot for the U-isotopes is shown in fig. 5. It is seen that the deformation dependence of Q_0 is smooth and almost linear. Now, the equilibrium value of Q_0 can be determined by the interpolation of curves $Q_0 = f(\varepsilon)$ for $\varepsilon = \varepsilon_{eq.}$. The resulting Q_0 (eq.) can be directly

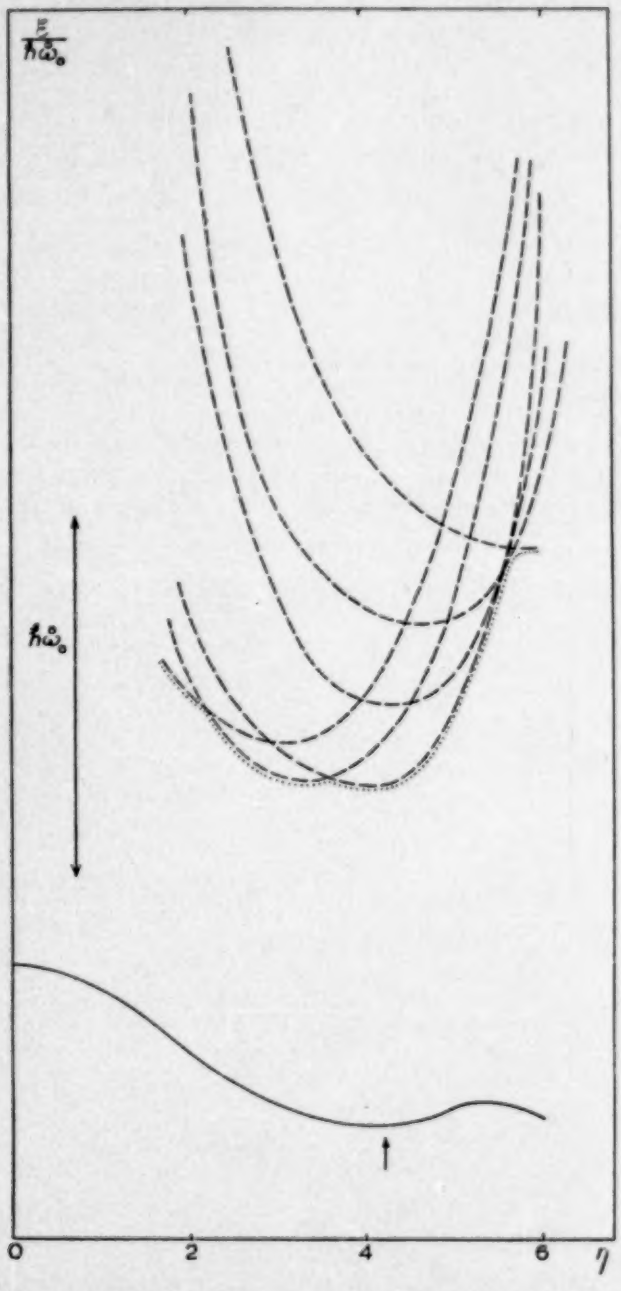

Fig. 3. Example of the total energy plot in terms of deformation for the nucleus U^{230}. The solid line corresponds to the total energy including pairing interaction. Several independent-particle energy curves (according to the Nilsson scheme) corresponding to the various configurations are also plotted for comparison (dashed line). The ground state independent-particle configuration is indicated by the dotted line. The level shifts correspond to the variant 2 of table 1.

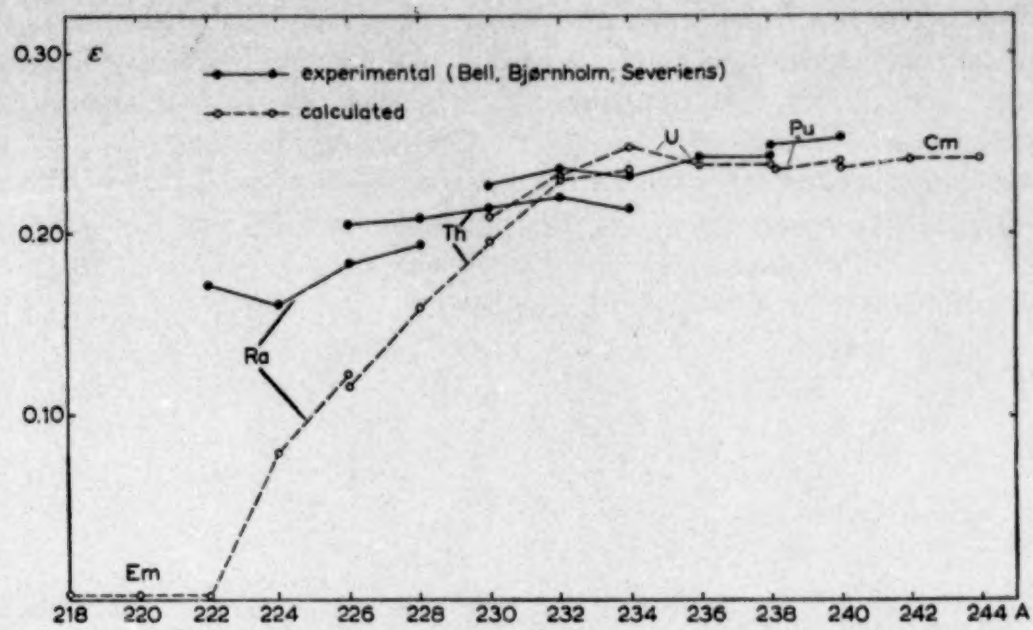

Fig. 4. Equilibrium deformations versus A. The solid line refers to the values of the density deformation parameter $\bar{\varepsilon}$ computed from the experimental quadrupole moments [1]) by means of eq. (11). They are to be compared with the calculated potential deformation ε (dashed line). The level scheme corresponds to the variant 2 of table 1.

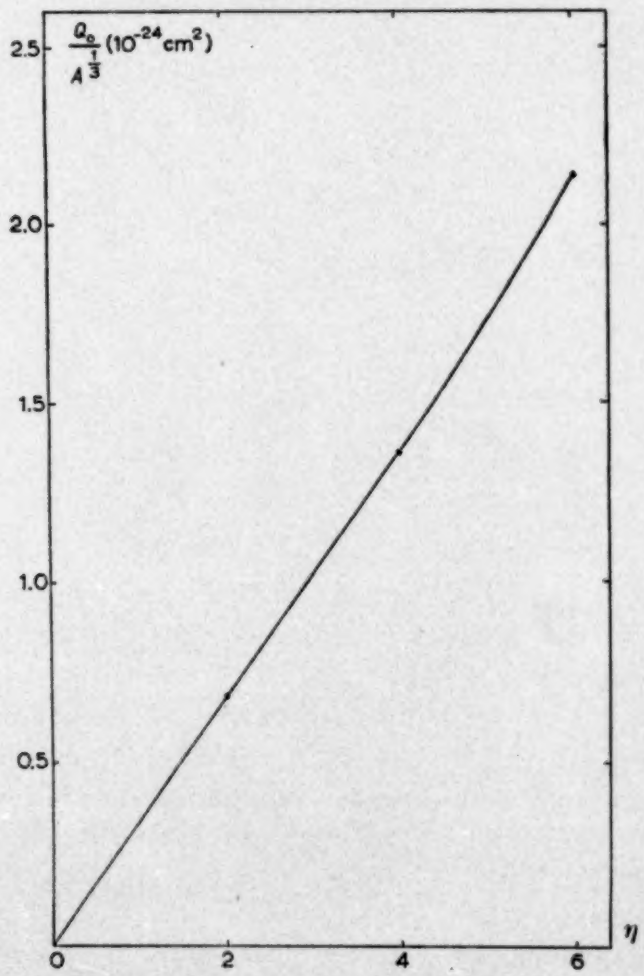

Fig. 5. Example of plot of total quadrupole moment Q_0 (divided by $A^{\frac{1}{3}}$) in terms of deformation for the U isotopes. The level scheme corresponds to the variant 2 of table 1.

compared with the experimental values obtained in refs. [1, 2, 18]). For the variant 2 the plot of Q_0 versus A is presented in fig. 6, while the numerical values of Q_0 are listed in table 2. It is seen that rather good agreement between theory and experiment comes out in the region of the well established deformations. On the other hand in the transition region (i.e. around the Ra isotopes) there appears a striking discrepancy, the theoretical values of Q_0 lying considerably lower. The same discrepancy also appears in the other deformed region [14]) of the rare-earth nuclei near the transition region (around the Hf and W isotopes) but the effect is not so strong there. It is worthwhile to mention that

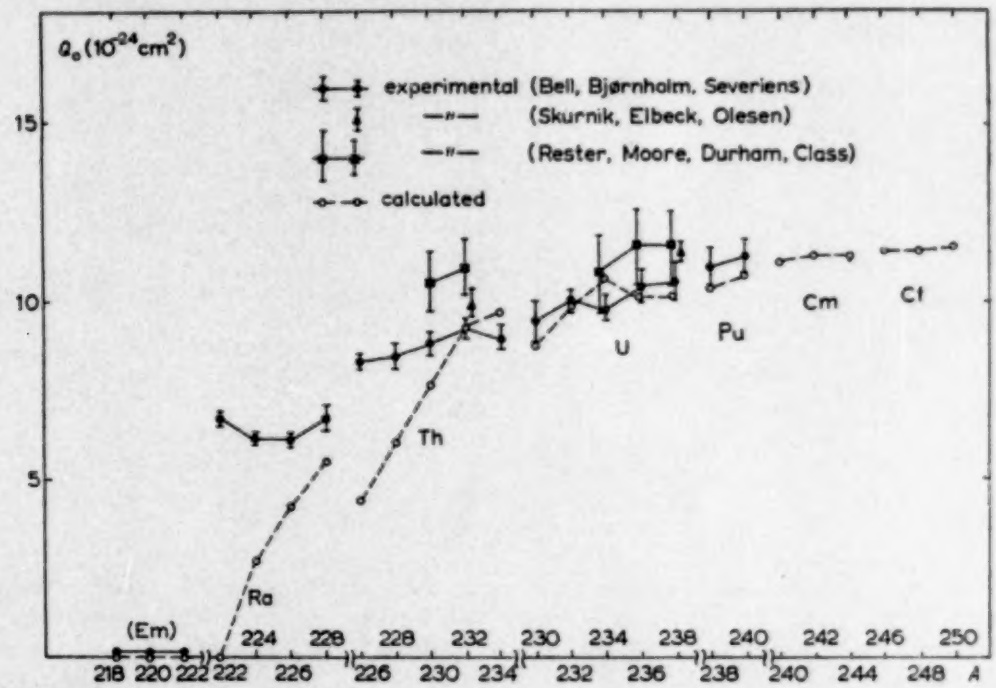

Fig. 6. Equilibrium quadrupole moments versus A. The solid line corresponds to the experimental data found in ref. [1]) (black circles), ref. [2]) (triangles) and ref. [18]) (squares). Experimental errors are indicated. The dashed line with circles refers to the calculated equilibrium quadrupole moments. The level scheme corresponds to the variant 2 of table 1.

the difficulty arises just in the region where the rotational model itself gives a relatively bad approximation. Another possible explanation of the discrepancy between the experiment and theory may be connected with the fact that the solutions of the Bardeen-Cooper-Schrieffer equations do not correspond to a definite number of particles. Indeed the wave function corresponding to the Hamiltonian given by eq. (2) contains an admixture of states of nuclei with Z and N differing by 2, 4, 6 . . . from the original nucleus [8]). This may lead to a smoother A-dependence of the equilibrium deformation than in the case of the exact solution corresponding to the Hamiltonian (1) with definite number of particles.

TABLE 2

Equilibrium quadrupole moments and deformations

Nucleus	Q_0(eq.) (calc) 10^{-24} cm^2	$\varepsilon_{eq.}$ (calc)	Q_0(exp.) 10^{-24} cm^2
Em^{218}	0	0	
Em^{220}	0	0	
Em^{222}	0	0	
Ra^{222}	0	0	6.63±0.26
Ra^{224}	2.75	0.080	6.21±0.13
Ra^{226}	4.25	0.125	7.22±0.12
Ra^{228}	5.55	0.155	7.79±0.28
Th^{226}	4.50	0.115	8.25±0.20
Th^{228}	6.15	0.160	8.47±0.32
Th^{230}	7.66	0.195	8.80±0.35
Th^{232}	9.30	0.230	9.25±0.23
Th^{234}	9.65	0.235	8.93±0.35
U^{230}	8.75	0.210	9.46±0.52
U^{232}	9.80	0.235	9.98±0.28
U^{234}	10.55	0.250	9.77±0.38
U^{236}	10.05	0.240	10.35±0.44
U^{238}	10.05	0.240	10.52±0.48
Pu^{238}	10.35	0.235	10,95±0.45
Pu^{240}	10.55	0.240	11.26±0.48
Cm^{240}	11.10	0.235	
Cm^{242}	11.25	0.240	
Cm^{244}	11.30	0.240	
Cf^{246}	11.40	0.235	
Cf^{248}	11.45	0.235	
Cf^{250}	11.50	0.235	

Column 1 identifies the nucleide, column 2 gives the calculated equilibrium quadrupole moment Q_0, column 3 gives the calculated equilibrium deformation, column 4 lists the experimental data on quadrupole moments taken from ref. [1]). The single-particle level scheme corresponds to the variant 2 of table 1.

In order to see what is the influence of the position of the neighbouring energy shells the calculations have been repeated with various relative shifts of these shells. Fig. 7 illustrates the equilibrium values of Q_0 in the case of variant 4 (table 1) when the proton lower shell has been shifted down by $0.034\ \hbar\mathring{\omega}_0$, and the neutron lower shell by $0.023\ \hbar\mathring{\omega}_0$ with respect to the variant 2. The theoretical values of Q_0 then appear lower than the observed ones. Further lowering of those shells will diminish the calculated values of Q_0 still more (in the case of variant 1 of table 1 the nucleus of Ra^{224} appears to be spherical). In order to see what is the influence of the upper neutron shell ($N_\nu = 7$ levels different from $j^{\frac{15}{2}}$), a shift by an amount $0.15\ \hbar\mathring{\omega}_0$ upward has been performed (variant 3 of table 1). This change was found not to affect the equilibrium deformation very much (the $\varepsilon_{eq.}$ changed only by one or two percent in a few nuclei only). If the major lower shells were shifted higher than in the variant 2, still higher values of the equilibrium deformations

$\varepsilon_{eq.}$ and quadrupole moments Q_0 would be obtained. This would account for the higher experimental values of Q_0 observed recently [18]). This procedure, however, seems to be illegitimate as a shift larger than $0.15\ \hbar\mathring{\omega}_0$ appears to be disallowed by the data concerning the odd-mass nuclei already discussed in subsect. 2.1.

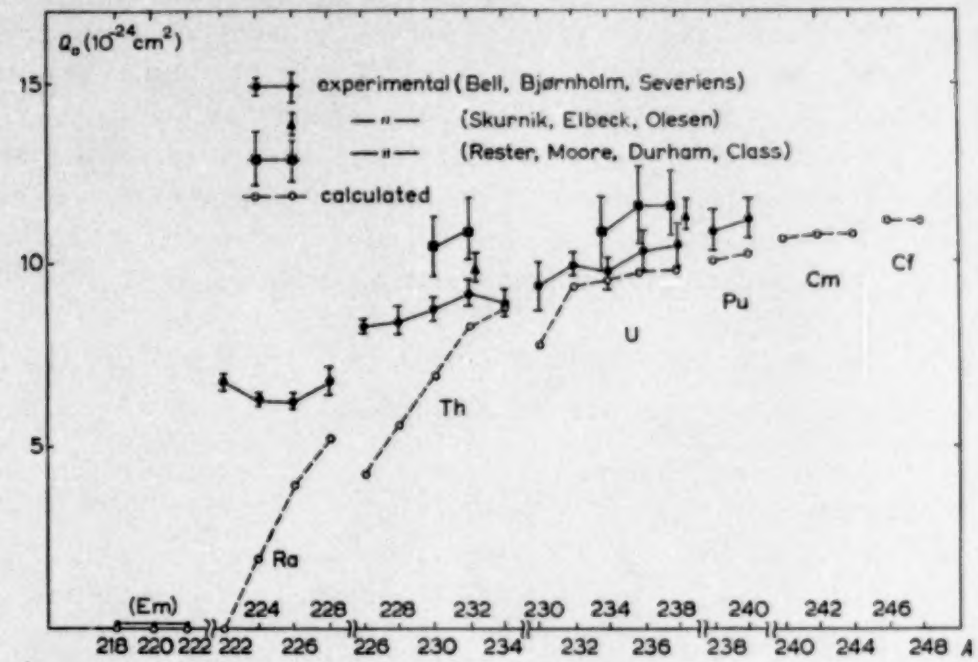

Fig. 7. Equilibrium quadrupole moments versus A. For explanations see fig. 6. The level scheme corresponds to the variant 4 of table 1.

Having the calculated value of the quadrupole moment Q_0 as a function of the deformation ε of the potential, one can use eq. (11) in order to compute the density deformation parameter $\bar{\varepsilon}$. The two deformations ε and $\bar{\varepsilon}$ are compared in table 3. It is seen that the values of $\bar{\varepsilon}$ almost overlap with ε.

TABLE 3

The density deformation parameter $\bar{\varepsilon}$ as a function of the potential deformation ε

Z	$\eta = 2$ $\varepsilon = 0.100$	$\eta = 4$ $\varepsilon = 0.199$	$\eta = 6$ $\varepsilon = 0.297$
86	0.084	0.182	0.305
88	0.091	0.186	0.305
90	0.098	0.193	0.303
92	0.103	0.199	0.300
94	0.108	0.206	0.297
96	0.112	0.211	0.294
98	0.114	0.213	0.291

The density deformation has been calculated from eq. (11) with Q_0 determined from eq. (6) for given ε. The single-particle level scheme corresponds to the variant 2 of table 1.

The relationship between $\bar{\varepsilon}$ and ε has also been discussed by Glendenning and Sawicki [19]). Unlike the above conclusion, they have found a systematical deviation of $\bar{\varepsilon}$ from the potential deformation ε.

The author wishes to express his thanks to Professors A. Bohr and B. R. Mottelson and Drs. S. G. Nilsson and D. Bès whose valuable suggestions and remarks offered him in the course of the work of ref. [14]) have also been taken into account in preparing the present paper. The author is also grateful to Dr. J. Dąbrowski for his valuable suggestions. Thanks are due to Drs. R. E. Bell, S. Bjørnholm and J. C. Severiens as well as Drs. Nilsson and Prior for supplying their results in advance of publication. The cooperation of the Computer Group and especially of Mr. J. Mazurkiewicz and Mrs. H. Mysior for working out the computational program for XYZ is gratefully acknowledged.

Appendix. Small Changes of the Parameters in the Bardeen - Cooper - Schrieffer Equations

It seems to be worthwhile to quote some of the formulae which can be derived from the two B.C.S. (Bardeen-Cooper-Schrieffer) equations (4), when the various parameters of these equations undergo slight changes. Some of the formulae proved to be very useful in predicting the properties of the solutions needed in the present paper.

Let us start with the B.C.S. equations

$$\begin{aligned} 2/G &= \sum_{\nu} 1/E_{\nu}, \\ N &= \sum_{\nu} [1-(\varepsilon_{\nu}-\lambda)/E_{\nu}], \end{aligned} \tag{A.1}$$

where $E_{\nu} = \sqrt{(\varepsilon_{\nu}-\lambda)^2+\Delta^2}$, and adopt the following notation:

$$A = \sum_{\nu} (\varepsilon_{\nu}-\lambda)/E_{\nu}^3, \quad B = \sum_{\nu} 1/E_{\nu}^3. \tag{A.2}$$

As the single-particle energy levels in deformed nuclei are distributed more or less uniformly and the summation in eq. (A. 2) runs over a region approximately symmetric with respect to the Fermi energy λ, it turns out that A is usually a small quantity compared with $B\Delta$:

$$A \ll B\Delta. \tag{A.3}$$

However, in the spherical case ($\eta = 0$) the distribution of the 24 levels nearest to the Fermi surface which determine the region of summation in eqs. (A.1) and (A.2) may be unsymmetrical with respect to λ, owing to the shell structure. Then the inequality (A.3) may be not fulfilled and A cannot be omitted in the calculations. This may be the case especially for neutron or proton numbers not very far from the closed shells.

We shall consider only two different variants of the possible changes in the parameters of eq. (A.1).

A.I. SMALL CHANGES OF THE PAIRING-FORCE STRENGTH AND NUMBER OF PARTICLES

Let us allow small changes in G and N:

$$G' = G+\delta G, \quad N' = N+\delta N.$$

Consequently the solutions of eq. (A.1) will also experience some changes:

$$\lambda' = \lambda+\delta\lambda, \quad (\Delta^2)' = \Delta^2+\delta\Delta^2.$$

Expanding eq. (A.1) in $\delta\lambda$ and $\delta\Delta^2$ up to the first order one easily gets

$$\begin{aligned} \delta\lambda &= \frac{-(2A/G^2)\delta G+B\delta N}{A^2+\Delta^2B^2}, \\ \delta\Delta^2 &= 2\,\frac{A\delta N+(2\Delta^2B/G^2)\delta G}{A^2+\Delta^2B^2}. \end{aligned} \tag{A.4}$$

These formulae (derived together with Daniel Bès in the course of the work of ref. [14])) were very useful in construction of the program for the electronic computer both in ref. [14]) and in the present paper. The variation δN was chosen in such a way as to make N' exactly an integer if N was not.

Taking into account the inequality (A.3) and the actual order of magnitude of δN and δG we get the approximate formulae

$$\delta\lambda = \delta N/\Delta^2B, \quad \delta\Delta^2 = 4\delta G/BG^2. \tag{A.5}$$

It can be seen that λ depends mainly on N while Δ^2 depends on G, which is consistent with the general philosophy of the model.

A.II. SINGLE-PARTICLE ENERGY SHIFTS SIMULTANEOUS WITH THE CHANGE OF THE PAIRING-FORCE STRENGTH

Let us assume that certain energy levels are shifted by a small amount $\delta\varepsilon_\nu$;

$$\varepsilon'_\nu = \varepsilon_\nu+\delta\varepsilon_\nu, \tag{A.6}$$

where

$$\delta\varepsilon_\nu = \begin{cases} \delta\varepsilon & \text{for the levels undergoing the shift,} \\ 0 & \text{for all the other levels.} \end{cases}$$

Let us introduce the following notation:

$$\bar{A} = \sum_\nu{}' (\varepsilon_\nu-\lambda)/E_\nu^3, \quad \bar{B} = \sum_\nu{}' 1/E_\nu^3, \quad \bar{N} = \sum_\nu{}' 2v_\nu^2, \tag{A.7}$$

where the prime denotes that the summations extend only over the shifted levels. If, moreover, a simultaneous change in the pairing-force strength is

allowed,

$$G' = G+\delta G,$$

we get the following relations:

$$\begin{aligned}\delta\lambda &= \frac{-2A}{A^2+B^2\Delta^2}\frac{\delta G}{G^2} + \frac{A\bar{A}+B\bar{B}\Delta^2}{A^2+B^2\Delta^2}\delta\varepsilon,\\ \delta\Delta^2 &= \frac{2\Delta^2(A\bar{B}-\bar{A}B)}{A^2+B^2\Delta^2} + \frac{4B\Delta^2}{A^2+B^2\Delta^2}\frac{\delta G}{G^2}.\end{aligned} \tag{A.8}$$

The increase of the total energy can be easily calculated from eq. (4). One gets

$$\delta\mathscr{E} = \bar{N}\delta\varepsilon-(\Delta^2\delta G/G^2). \tag{A.9}$$

If actual numbers are substituted into eqs. (A.8) and (A.9), it turns out that $\delta\Delta^2$ is not very sensitive to the energy shifts. Therefore $\delta\Delta^2$ is approximately given by the formula

$$\delta\Delta^2 = 4\delta G/BG^2,$$

which overlaps with the second of eqs. (A.5). On the other hand $\delta\mathscr{E}$ appears to be mainly determined by the first term in eq. (A.9). If the steepest energy levels ε_ν (i.e. those changing very strongly with deformation) are the only shifted levels, as is the case with the shifts of the lower major shell, the quantity N depends very strongly on deformation. In this case the position of the lower major shell is of great importance in the determination of the equilibrium deformation.

References

1) R. E. Bell, S. Bjørnholm and J. C. Severiens, Mat. Fys. Medd. Dan. Vid. Selsk. **32**, No. 12 (1960)
2) E. Z. Skurnik, B. Elbeck and M. C. Olesen, Nuclear Physics **22** (1960) 316
3) B. R. Mottelson and S. G. Nilsson, Mat. Fys. Skr. Dan. Vid. Selsk. **1**, No. 8 (1959)
4) S. G. Nilsson, Mat. Fys. Medd. Dan. Vid. Selsk. **29**, No. 16 (1955)
5) J. Bardeen, L. N. Cooper and J. R. Schrieffer, Phys. Rev. **108** (1957) 1175
6) N. N. Bogolubov, JETP (USSR) **34** (1958) 58, **73**, Nuovo Cim. **7** (1958) 794
7) A. Bohr, B. R. Mottelson and D. Pines, Phys. Rev. **110** (1958) 936
8) S. T. Belyaev, Mat. Fys. Medd. Dan. Vid. Selsk. **31**, No. 11 (1959)
9) L. S. Kisslinger and R. A. Sørensen, Mat. Fys. Medd. Dan. Vid. Selsk. **32**, No. 9 (1960)
10) J. Bro-Jørgensen and A. Haatuft, private communication
11) S. G. Nilsson and O. Prior, Mat. Fys. Medd. Dan. Vid. Selsk. **32**, No. 16 (1961)
12) D. Bès, Mat. Fys. Medd. Dan. Vid. Selsk. **33**, No. 2 (1961)
13) V. G. Soloviev, preprint (1960)
14) D. Bès and Z. Szymański, Nuclear Physics (1)
15) A. Bohr, Comp. Rend. Cong. Intern. Phys. Nucl. in Paris (1958) (Dunod, Paris, 1959); B. R. Mottelson, Notes from Cours de l'École d'Été de Physique Théorique des Houches (1958) (Dunod, Paris, 1959)
16) A. K. Kerman, preprint (1960)
17) D. G. Ravenhall, Rev. Mod. Phys. **30** (1958) 430
18) D. H. Rester, M. S. Moore, F. E. Durham and C. M. Class, Nuclear Physics **22**, (1961) 104
19) N. Glendenning and J. Sawicki, Nuclear Physics **18** (1960) 596

8.B

Nuclear Physics **28** (1961) 81—83; © *North-Holland Publishing Co., Amsterdam*

Not to be reproduced by photoprint or microfilm without written permission from the publisher

ON SINGLE-STRANGE MESONS

W. KRÓLIKOWSKI †

Institute for Advanced Study, Princeton, New Jersey

Received 24 March 1961

Abstract: In this note some reactions are pointed out, in which single-strange mesons proposed previously could be observed.

It was recently pointed out by Pais [1]) that experimental data on up-down asymmetries in hyperon decays give us an evidence for the doublet symmetry (DS) of all strong interactions contributing to the hyperon decays. This DS should gain another strong support, if the recently discovered 1385 MeV resonance in $\pi\Lambda$ interaction were a hyperon isobar related to the $\frac{3}{2}\frac{3}{2}$ isobar of the nucleon [2]) (see, however, ref. [3])). In this case the DS called also restricted global symmetry (RGS) would be almost the global symmetry proposed originally by Gell-Mann [4]).

On the other hand, it is well known that the DS is strongly violated in observed K meson processes [1]). It is well known also that K interactions do not appear to be much weaker than π interactions. In this puzzling situation Pais raised the question whether it could be that DS nearly holds in virtual K meson processes and breaks down when real K mesons appear.

In a recent paper [5]) a realization of this possibility was indeed proposed, but it was obtained at a very high price, by postulating some new mesons. Although those mesons could be excluded as real particles by some subsidiary condition imposed on the state vector, only their real existence might give a convincing support for this theory. The aim of the present note is to point out processes in which these mesons could be observed.

The idea of ref. [5]) is that the K meson doublet and a new R meson quartet form together an (isovector) $\times$ (isospinor) tensor $\mathrm{M}_{i\alpha}(i = 1, 2, 3, \alpha = 1,2)$ as the Λ-baryon singlet and Σ-baryon triplet can be gathered in an (isospinor) $\times$ (isospinor) tensor $\mathrm{B}_{A\alpha}$ $((A = 1, 2, \alpha = 1, 2)$, where [6])

$$\mathrm{B}_{A1} = \mathrm{Y}_A = \begin{pmatrix} \Sigma^+ \\ \mathrm{Y}_0 \end{pmatrix}, \qquad \mathrm{B}_{A2} = \mathrm{Z}_A = \begin{pmatrix} \mathrm{Z}^0 \\ \Sigma^- \end{pmatrix}.$$

By the Clebsch-Gordan reduction one gets from $\mathrm{B}_{A\alpha}$ the baryons Λ and

† On leave from Institute for Nuclear Research, Polish Academy of Sciences, Warsaw, and Institute of Theoretical Physics, University of Warsaw.

$\Sigma^+, \Sigma^0, \Sigma^-$ (strangeness $S = -1$), and from $M^*_{i\alpha}$ the mesons

$$K^+, K^0 \text{ and } R^{++}, R^+, R^0, R^- \text{ (strangeness } S = 1).$$

Antiparticles of these mesons are

$$K^-, \bar{K}^0 \text{ and } R^{--}, \bar{R}^+, \bar{R}^0, \bar{R}^- \text{ (strangeness } S = -1).$$

The following analogy holds:

$$N_A \to p, n \text{ corresponding to } \pi_i \to \pi^+, \pi^0, \pi^-,$$

$$B_{A\alpha} \to \begin{cases} \Lambda \\ \Sigma^+, \Sigma^0, \Sigma^- \end{cases} \text{ corresponding to } M_{i\alpha} \to \begin{cases} \bar{K}^0, K^- \\ \bar{R}^-, \bar{R}^0, \bar{R}^+, R^{--} \end{cases}.$$

Now, an interaction is invariant under DS if it is a scalar with respect to A and i indices and independently with respect to α indices [5]). All K mesons and R mesons interactions taken separately *must* violate the DS, but interactions with the M field *can* be invariant under DS. In this case K and R interactions separated from the full M interactions break down the DS, but taken together preserve it. Hence, K meson processes must violate the DS, whereas processes without real K mesons can neraly preserve the DS (modulo $\Lambda-\Sigma$ and K—R mass differences).

A characteristic feature of the $\bar{N}YK$ interaction obtained from the DS-invariant $\bar{N}YM$ interaction is the ratio of coupling constants [5]) $|g_{N\Lambda K}/g_{N\Sigma K}|=3$.

The K and R mesons have both the same zero spin and the same intrinsic parity. Thus processes $R \leftrightarrow K+\pi$ are forbidden and the R meson must not be confused with the possible 880 MeV resonance in πK interaction suspected recently on experimental and theoretical grounds.

Since K and R mesons have the same strangeness, electromagnetic transitions are possible between them. Also strong pionic transitions are possible, if the mass difference $|\mu_R-\mu_K| > 2\mu_\pi$. We must have $\mu_R \geqq \mu_K$, because K mesons are known to be stable with respect to electromagnetic interactions.

The R mesons could be produced beside K mesons in processes like

$$K(\bar{K})+N \to R(\bar{R})+N, \qquad \pi+N \to R+\Lambda, \Sigma.$$

In the case $\mu_R < \mu_K+2\mu_\pi$ the mesons R^+, R^0 and $\bar{R}^+$, $\bar{R}^0$ would transform by electromagnetic processes $R(\bar{R}) \to K(\bar{K})+\gamma$ into K^+, K^0 and $\bar{K}^+$, $\bar{K}^0$ respectively, whereas mesons R^{++} and $\bar{R}^{++}$ would be stable in electromagnetic interactions. These γ transitions would be analogues of the process $\Sigma^0 \to \Lambda+\gamma$. Mesons R^- and $\bar{R}^-$ would be stable in electromagnetic interactions if $\mu_R < \mu_K+\mu_\pi$ and would decay by electromagnetic processes, e.g. $R^- \to K^\circ+\pi^-+2\gamma$ and $\bar{R}^- \to \bar{K}^\circ+\pi^++2\gamma$, if $\mu_R > \mu_K+\mu_\pi$. In the case $\mu_R > \mu_K+2\mu_\pi$ all mesons

R and $\overline{\text{R}}$ would decay by strong transitions $\text{R}(\overline{\text{R}}) \to \text{K}(\overline{\text{K}})+2\pi$. In this case the R and $\overline{\text{R}}$ mesons would give some resonances in $\pi\pi\text{K}$ and $\pi\pi\overline{\text{K}}$ interactions and should manifest by some peaks in CMS momentum spectra of recoil nucleons or hyperons in processes like

$$\text{K}(\overline{\text{K}})+\text{N} \to \text{R}(\overline{\text{R}})+\text{N} \to \text{K}(\overline{\text{K}})+2\pi+\text{N}, \quad \pi+\text{N} \to \text{R}+\Lambda, \Sigma \to \text{K}+2\pi+\Lambda, \Sigma.$$

The author is much indebted to Professor A. Pais for helpful discussions and to Professor J. R. Oppenheimer for his kind hospitality at the Institute for Advanced Study in Princeton.

References

1) A. Pais, Phys. Rev. **110** (1958) 574, 1480, **112** (1958) 624; Nuovo Cim. **18** (1960) 1003; preprint UCRL-9460 (1960)
2) D. Amati, A. Stanghellini and B. Vitale, Nyovo Cim. **13** (1959) 1143; Phys. Rev. Letters **5** (1960) 524
Ph. Mayer, J. Prentki and Y. Yamaguchi, Phys. Rev. Letters **5** (1960) 442;
T. D. Lee and C. N. Yang, preprint IAS (1961) (submitted for publication in Phys. Rev.)
3) R. H. Dalitz, Phys. Rev. Letters **6** (1961) 239
4) M. Gell-Mann, Phys. Rev. **106** (1957) 1296
5) W. Królikowski, Nuclear Physics **26** (1961) 91
6) W. Królikowski, Nuclear Physics **8** (1958) 461, **17** (1960) 421, **23** (1961) 53

4.B

Nuclear Physics **28** (1961) 84—95; © *North-Holland Publishing Co., Amsterdam*

Not to be reproduced by photoprint or microfilm without written permission from the publisher

SEARCH FOR PSEUDOSCALAR INTERACTION IN $\frac{1}{2}+ \rightarrow \frac{1}{2}-$ β-DECAY TRANSITIONS

(I) Measurement of the longitudinal polarization of the β^--particles emitted in the transition $_{81}Tl^{207} \rightarrow {}_{82}Pb^{207}$

SAMI CUPERMAN

Department of Nuclear Physics, The Weizmann Institute of Science, Rehovoth, Israel †

Received 29 April 1961

Abstract: The longitudinal polarization of β-rays emitted in the transition $_{81}Tl^{207} \rightarrow {}_{82}Pb^{207}$ ($\frac{1}{2}+ \rightarrow \frac{1}{2}-$) was measured by double Coulomb scattering. The result obtained was $P_0\{_{81}Tl^{207}\} = (1.04 \pm 0.25)(-v/c)$. Assuming two-component neutrino theory with a left-handed neutrino and $C_S = C_T = 0$, this result indicates that pseudoscalar interaction gives only a small contribution, if any, to β-decay.

1. Introduction

After parity non-conservation in weak interactions was proposed by Lee and Yang [1]) and experimentally demonstrated by various methods, the nature of the β-interaction became the subject of renewed experiments. All the results obtained [2]) suggest that the major contribution in allowed β-decay transitions comes from the vector and axial vector (V, A) interactions and little, if any, comes from scalar and tensor (S, T) interactions. The presence of the pseudoscalar interaction in β-decay cannot be investigated in allowed transitions, to which there is no pseudoscalar contribution. Effect of the pseudoscalar interaction might be observed in a first forbidden transition with $\Delta J = 0$, yes, where a mixture of (V, A) and P contributions of the same order of magnitude might be involved.

A possible way to detect the P interaction in a $\Delta J = 0$, yes transition is by measuring the longitudinal polarization of electrons emitted in this decay. Assuming two-component neutrino theory [3]) it is found that the P interaction gives rise to polarization opposite to that coming from (V, A) interactions. If a left-handed neutrino [4]) is used (V, A) interactions yield negative helicity [5]) and for a (V, A)-P mixture, a polarization different from $-v/c$ is to be expected. The departure of the polarization from $-v/c$ could thus be taken as an indication of the presence of the P interaction.

† Now at Association Euratom-C.E.A., Fontenay-aux-Roses, France

In the present work, the longitudinal polarization of the electrons emitted by $_{81}Tl^{207}(\frac{1}{2}+ \rightarrow \frac{1}{2}-)$ was measured. The decay scheme [6]) of $_{81}Tl^{207}$ is shown in fig. 1. While the spin of $_{82}Pb^{207}(\frac{1}{2}-)$ has been directly measured [7]) there exists only indirect evidence for the assignment $\frac{1}{2}+$ for the ground state spin of $_{81}Tl^{207}$. Nevertheless, this indirect evidence is strong and can be summarized as follows [8]): (1) the measured spins of Tl^{197}, Tl^{199}, Tl^{201}, Tl^{203} and Tl^{205} are all $\frac{1}{2}+$; (2) the β-decay of Tl^{207} populates states in Pb^{207} of $\frac{1}{2}-$ and $\frac{3}{2}-$ (weakly) but not $\frac{5}{2}-$, which argues against spin $\frac{3}{2}+$ for Tl^{207}; (3) the log ft value of this decay is very low (5.2) which indicates a $\Delta J = 0$, yes, transition (of course, an allowed $\Delta J = 0$, no, transition would have such a ft value, but odd parity coupled with low spin is not expected for the ground state of the 81^{st} proton [9])).

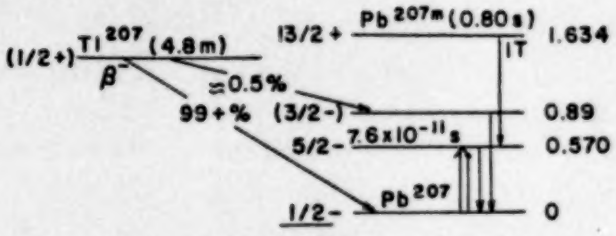

Fig. 1. The decay scheme of $_{81}Tl^{207}$.

Because of its short half-life ($\tau = 4.8$ min), a $_{88}Ra^{223}$ ($\tau = 11.2$ d) source in radioactive equilibrium with its daughters was used; it contained $_{81}Tl^{207}$ as well as $_{82}Pb^{211}$ ($\tau = 36$ min) as β^--emitters. Both these elements emit electrons having roughly the same maximum energy, 1.45 MeV (99 %) and 1.39 MeV (80 %), resp.†. We thus measured the longitudinal polarization of the electrons coming from $_{81}Tl^{207}+_{82}Pb^{211}$, rather than the polarization of the electrons emitted by $_{81}Tl^{207}$ alone. Since the proportion of the electrons coming from $_{81}Tl^{207}$ and $_{82}Pb^{211}$ is known, the longitudinal polarization of the electrons emitted by $_{81}Tl^{207}$ alone may be found, if we assume a $-v/c$ polarization for the $_{82}Pb^{211}$ electrons (fig. 2).

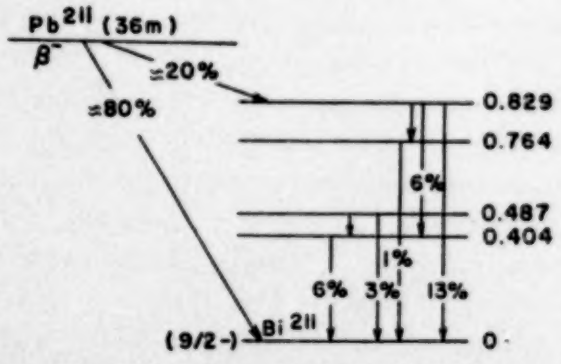

Fig. 2. The decay scheme of $_{82}Pb^{211}$.

† The 20 % decay branch of $_{82}Pb^{211}$ (0.5 MeV) could be easily eliminated by establishing a convenient bias level energy.

The longitudinal polarization was measured by double Coulomb scattering [10]). First, the longitudinal polarized electrons emitted by $_{81}Tl^{207}+_{82}Pb^{211}$ were scattered by 90° in aluminium to transform their longitudinal polarization into polarization with substantial transverse component, then, the electrons were scattered again by a large angle in gold and the resulting azimuthal (left-right) asymmetry was measured. From the experimental value of the azimuthal asymmetry the initial longitudinal polarization for the β-ray was calculated for $_{81}Tl^{207}+_{82}Pb^{211}$, and then for $_{81}Tl^{207}$ alone.

As a check, the longitudinal polarization of P^{32} β-rays (a well-known allowed transition) was measured and the results compared with those obtained by other methods.

2. Experimental Procedure

The detailed description of the double Coulomb scattering method and of the apparatus to measure the longitudinal polarization of electrons emitted in β-decay is given elsewhere [11]). It is well-known [12]) that scattering of transversly polarized electrons through large angles by heavy nuclei results in an azimuthal asymmetry of the scattered electrons. Since this azimuthal asymmetry is related to the transverse component of the polarization, the latter can be determined by measuring the asymmetry.

The electrons emitted in β-decay are longitudinally polarized. However, this polarization may be transformed into one with a substantial transverse component by rotating the direction of the electrons momentum (spin) through 90°, without changing their spin (momentum) direction [13]).

In double Coulomb scattering this rotation is achieved by first scattering the longitudinally polarized electrons through 90° by aluminium. Because of the low atomic number of the scatterer, the spin-orbit interaction and thus the change in the spin direction are small, resulting in a polarization with a substantial transverse component. Then, the transversly polarized electrons are scattered by heavy nuclei, and the azimuthal asymmetry measured. From the result one obtains information on the transverse component of the polarization and from that, on the longitudinal one.

A schematic diagram of the apparatus employed to measure the longitudinal polarization of electrons emitted by $_{81}Tl^{207}$ is shown in fig. 3 (see ref. [11])). β-rays emitted from the source S are first scattered through 90° by the semicircular aluminium foil Σ_1; after a second scattering in the gold foil Σ_2, the doubly scattered electrons are detected by two identical detectors D_1 and D_2, which represent two directions symmetrical with respect to the plane of the first scattering. The semicircular form and the position of the first scatterer provide a large solid angle for the first scattering, assuring at the same time that the direction of any electron reaching the centre of Σ_2 (after being scattered by Σ_1) is turned through 90°.

Special care was taken to avoid any instrumental asymmetry which could mask the true azimuthal asymmetry [11]). As a final general check, the geometrical symmetry of the apparatus was verified by measuring the azimuthal asymmetry with a thick Al($Z = 13$) foil as second scatterer. For the electron energy, scattering angles and thickness of the Al foil used, no azimuthal asymmetry is predicted by the theory. Any asymmetry found under these

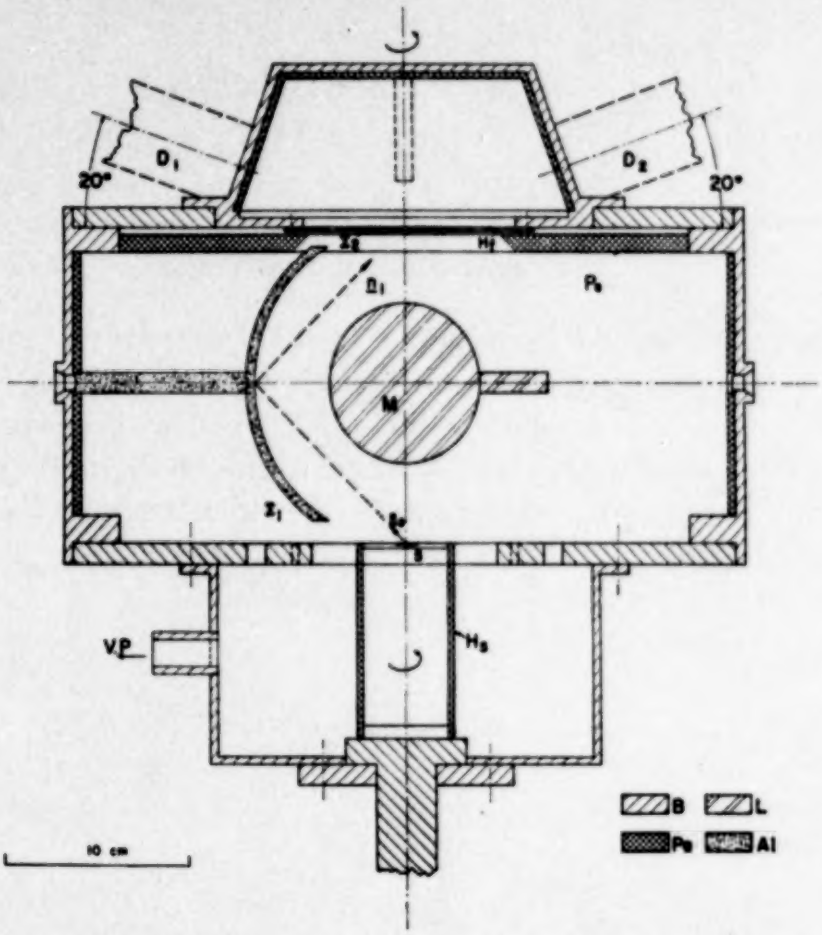

Fig. 3. The scattering apparatus. S-radioactive source; Σ_1- the first scatterer (Al); Σ_2 - the second scatterer; M - lead cylinder covered with aluminium; H_f - foil holder; H_s - source holder; D_1 and D_2 - detectors; $\mathbf{n}_0$ - initial direction of motion of electrons; $\mathbf{n}_1$ - direction of motion of electrons after the first scattering; B - brass; Pe - perspex; L - lead; Al - aluminium. The actual position of the two detectors D_1 and D_2 is in the plane perpendicular to the paper.

conditions would be of instrumental origin. Using the usual definition of the azimuthal asymmetry [12]), the result obtained was

$$A_{\mathrm{Al}}(Z = 13) = \frac{[(I_{\mathrm{L}} - I_{\mathrm{L}}^0) - (I_{\mathrm{R}} - I_{\mathrm{R}}^0)]}{\frac{1}{2}[(I_{\mathrm{L}} - I_{\mathrm{L}}^0) + (I_{\mathrm{R}} - I_{\mathrm{R}}^0)]} = 0.99 \pm 0.005, \qquad (1)$$

indicating a very small asymmetry of the apparatus (in a direction opposite to that expected for the double scattering of β^--particles by heavy nuclei). In this relation, I_{L} and I_{R} represent the intensities of the doubly scattered

electrons in two directions (L and R) symmetrical with respect to the first plane of scattering; I_L^0 and I_R^0 represent the background due to the β-rays scattered by the walls of the apparatus and to the electrons created by the γ-rays emitted by the ${}_{88}Ra^{223}$ source †.

The small geometrical effect given by (1) was taken into account, by calculating the real azimuthal asymmetry as follows:

$$A(Z=79)=\left\{\frac{[(I_L-I_L^0)-(I_R-I_R^0)]}{\frac{1}{2}[(I_L-I_L^0)+(I_R-I_R^0)]}\right\}_{Z=79}\Big/ A_{Al}, \qquad (2)$$

$Z = 79$ being the atomic number of the second scatterer in our experiment.

3. Preparation of Sources

Because of the short half life of ${}_{81}Tl^{207}$ ($\tau = 4.8$ min) we could not study it alone, since the measurements took several weeks. A suitable longer-lived element in radioactive equilibrium with ${}_{81}Tl^{207}$ had to be used. The most convenient one for our experiment was found to be ${}_{88}Ra^{223}$ ($\tau = 11.2$ d) (fig. 4), which was separated from Ac^{227} by cation exchange ††, using $2.5N$

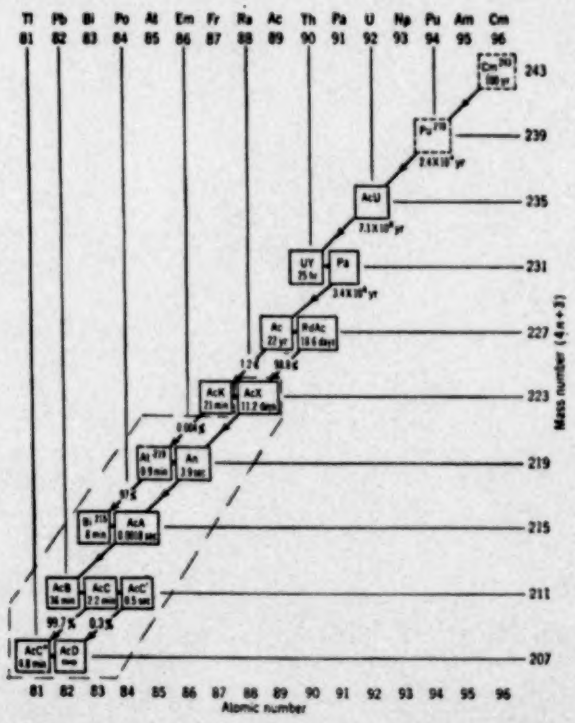

Fig. 4. The actinium series. The dashed line indicates ${}_{88}Ra^{223}$ and its daughters, as used in the experiment.

† Experimentally it was found that the ratio of the electrons created by γ-rays to the β-rays is approximately 1 : 10.

†† The Ac^{227} was supplied by United States Radium Corporation.

HNO_3. The decay of the separated source, as well as the upper end of its spectrum (fig. 5(A)), agreed completely with the characteristics of $_{88}Ra^{223}$ in radioactive equilibrium with its daughters.

Special care was taken to fix the $_{86}Em^{219}$ gas, which is one of the $_{88}Ra^{223}$ daughters, and whose rapid evaporation could lead to the dispersion of the $_{81}Tl^{207}$ parents, and to radioactive contamination of the apparatus. The $_{88}Ra^{223}$ source was deposited together with a suitable quantity of the stable isotope of Ba, on a 2 mg/cm² polyvinyl foil and was covered, after drying, with a 1.5 mg/cm² formvar foil.

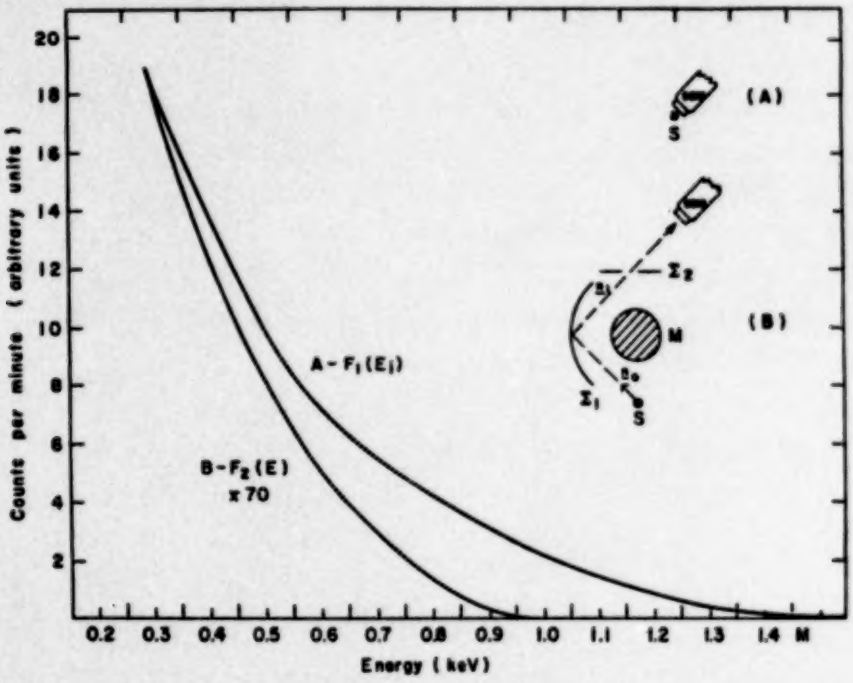

Fig. 5. Comparison of spectra of initial and scattered electrons. (A) Natural β-ray energy spectrum of $_{88}Ra^{223}$ in radioactive equilibrium with its daughters, measured when the source was placed near the detector; this complex spectrum contains the simple spectrum of $_{81}Tl^{207}$ ($E_{max} = 1.45$ MeV) and the two branches of $_{82}Pb^{211}$ ($E^1_{max} = 1.39$ MeV; $E^2_{max} = 0.5$ MeV). (B) β-ray energy spectrum of $_{88}Ra^{223}$ in radioactive equilibrium with its daughters, after the first scattering from Σ_1.

The $_{88}Ra^{223}$ source was approximately 1 mg/cm² thick and 1 cm in diameter, as found by measuring non-radioactive samples, prepared under the same conditions. Its strength was $\approx$ 5 mCur.

The P^{32} source used in our experiment † had an activity of about 20 mCur. It was deposited on a 2 mg/cm² polyvinyl foil and covered, after drying, with another foil of 1.5 mg/cm². Since the P^{32} sample was carrier-free, the source thickness was negligible.

† P^{32} was supplied by the Radiochemical Centre, Amersham.

4. Calculation of Azimuthal Asymmetry

The calculation of the azimuthal asymmetry in a double Coulomb scattering experiment was first given by Mott [12]. Following Tolhoek [13], Gursey [14] presented it in a form which expresses the complete directional and polarization dependence of the scattering. In this form, the azimuthal asymmetry expected in a double Coulomb scattering experiment with initially longitudinally polarized electrons is given by †

$$A = -2P_0(E_1)T(\theta_1, E_1, Z_1)S(\theta_2, E_1, Z_2)(\mathbf{n}\times\mathbf{n}_1)\cdot\mathbf{n}', \tag{3}$$

where

$$\mathbf{n} = (\mathbf{n}_1\times\mathbf{n}_0)/\sin\theta_1, \qquad \mathbf{n}' = (\mathbf{n}_2\times\mathbf{n}_1)/\sin\theta_2.$$

In this formula, E_1 represents the initial kinetic energy of the electron, $P_0(E_1)$ is the amount of the initial longitudinal polarization, $\mathbf{n}_0$, $\mathbf{n}_1$ and $\mathbf{n}_2$ are unit vectors giving the directions of the electron's momenta before the first scattering, after it and after the second scattering, θ_1 and θ_2 the angles of the first and second scattering, Z_1 and Z_2 the atomic numbers of the first and the second scatterer, $T(\theta_1, E_1, Z_1)$ is the transverse component of polarization after the first scattering and $S(\theta_2, E_1, Z_2)$ the asymmetry function calculated by Sherman [15].

Putting

$$P_\perp(E_1) = P_0(E_1)T(\theta_1, E_1, Z_1), \tag{4}$$

$$S'(\theta_2, E_1, Z_2) = S(\theta_2, E_1, Z_2)(\mathbf{n}\times\mathbf{n}_1)\cdot\mathbf{n}', \tag{5}$$

the above formula may be written as

$$A = -2P_\perp(E_1)\cdot S'(\theta_2, E_1, Z_2). \tag{6}$$

The significance of $P_\perp(E_1)$ and $S'(\theta_2, E_1, Z_2)$ is the following: $P_\perp(E_1)$ represents the transverse polarization of an electron with initial kinetic energy E_1 and longitudinal polarization $P_0(E_1)$, after scattering through $\theta_1 = 90°$ (by aluminium); $S'(\theta_2, E_1, Z_2)$ represents the asymmetry coefficient appropiate to the geometry of our apparatus.

As mentioned above, by measuring the azimuthal asymmetry A of eq. (6), the transverse polarization $P_\perp(E_1)$ of eq. (4) and then the initial longitudinal one $P_0(E_1)$ may be found.

However, formula (6) cannot be applied directly to our experiment, because it corresponds to an ideal experiment, namely: first, single Coulomb scattering of initially longitudinally polarized monoenergetic electrons, through an angle $\theta_1(= 90°)$, by aluminium; secondly, single Coulomb scattering through an angle θ_2, by gold. In our experiment a) electrons with kinetic energies between 300 keV and 1450 keV (rather than monoenergetic ones) were accepted by the

† Under the condition $Z_1 \ll Z_2$ (see ref. [11]).

detectors, b) because of the finite thickness of the first scatterer (0.5 cm) mainly multiple scattering (rather than single scattering) was involved, c) the finite scattering solid angles involved different asymmetry factors and scattering cross sections, and d) in spite of the small thickness of the second scatterer ($\approx 10^{-5}$ cm) a supplimentary undesirable process (plural scattering) occurred.

Thus, the formula (3) corresponding to an ideal experiment must be corrected to account for all these effects. For the points a), b) and c), this is achieved by appropriate calculations, as described in ref. [11]). For the mixture of ${}_{81}Tl^{207}+{}_{82}Pb^{211}$ electrons, with $\bar{\theta}_1 \approx 90°$, $\bar{\theta}_2 \approx 73°$, $Z_1 = 13$, $Z_2 = 79$, 300 keV $\leqq E_1 \leqq$ 1450 keV and assuming $P_0(E_1) \approx -(v/c)_1$ (v and c being the velocities of the electron and of light), the value of the azimuthal asymmetry was found to be

$$A({}_{81}Tl^{207}+{}_{82}Pb^{211}) = 14.30\times 10^{-2}. \tag{7}$$

It remains to account for the finite thickness of the second scatterer (point d)), which involves two additional undesirable processes: 1) the so-called plural scattering [16]) which consists of two consecutive scatterings of approximately equal angles φ_1 and φ_2, such that $\varphi_1+\varphi_2 = \theta_2$, and 2) multiple scattering through θ_2. Both these processes mask the asymmetry effect which is predicted for the case when only single scattering is involved, since $S(\varphi_1 = \varphi_2 = \frac{1}{2}\theta_2, E, Z_2) \ll S(\theta_2, E, Z_2)$. While it is possible to reduce multiple scattering to less than 10 % of single scattering when the Wentzel criterion [17]) for the foil thickness is fulfilled, difficulties arise when the same is tried for plural scattering. The latter process becomes very important when the foil thickness is reduced below the value which limits the multiple scattering to 10 %. Further reduction of the thickness would reduce also plural scattering; but, at the same time, a very small yield of singly scattered electrons would be obtained. It is then desirable to choose a not too thin scattering foil and to try to correct the result, taking into account the masking effect of the plural scattering.

The following method [18]) for evaluating the true asymmetry value was used †. Since $S(\frac{1}{2}\theta_2, E, Z) \approx 0$, it is justifiable to assume that the plural scattering results in a symmetric "background" i.e. $I_L{}^p = I_R{}^p$. Thus, instead of A of eq. (6) which gives the single-scattering azimuthal asymmetry ($I_L{}^s \neq I_R{}^s$), we can write

$$A^* = \frac{[I'_L - I'_R]}{\frac{1}{2}[I'_L + I'_R]} \approx 2\frac{(I_L{}^s+I_L{}^p)-(I_R{}^s+I_R{}^p)}{(I_L{}^s+I_L{}^p)+(I_R{}^s+I_R{}^p)} \equiv 2\frac{I_L{}^s - I_R{}^s}{I_L{}^s+I_R{}^s+2I^p}, \tag{8}$$

or

$$\frac{1}{A^*} = \frac{1}{A} + \frac{I^p}{I_L{}^s - I_R{}^s} \equiv \frac{1}{A} + \alpha t, \tag{9}$$

† Unfortunately, no satisfactory theory of plural scattering exists.

where t is the foil's thickness and α a quantity not depending on t. The last step results from I^p being proportional to the square of the foil thickness t, while I^s is proportional to t.

Plotting now $1/A^*$ as function of the thickness t, one obtains a straight line which intersects the ordinate axis at the value $1/A$, corresponding to zero foil thickness (i.e. no plural scattering).

In our experiment, scattering foils of 0.4, 0.8 and 2.8 mg/cm^2 gold were used.

5. Measurement of Longitudinal Polarization of Electrons Emitted by P^{32}

A general check of the above method and assumptions could be carried out by measuring the initial longitudinal polarization of the electrons emitted in a transition in which no pseudoscalar interaction is involved, and which has already been measured by other methods. The β-decay for P^{32} $(1+ \rightarrow 0+)$ provides such an example, for, within an accuracy of about 10 %, all data [19]) are consistent with an initial longitudinal polarization of $-v/c$.

We therefore measured the initial longitudinal polarization of the electrons emitted by P^{32}. We strictly maintained the same geometrical conditions: scattering angles, foils, etc. The only difference with respect to the $_{81}Tl^{207}$ experiment was that electrons with kinetic energies greater than 500 keV were accepted by the detectors. Using the same calculation as in sect. 4, the theoretical value of the azimuthal asymmetry was found to be

$$A(P^{32}) = 10.7 \times 10^{-2}. \tag{10}$$

The experimental data we obtained are given in table 1. The values of $100\, I_L/I_R$ rather than those of $(I_L - I_R)/\frac{1}{2}(I_L + I_R)$ are given, for convenience.

TABLE 1

The azimuthal symmetry $(100\, I_L/I_R)$ in the double Coulomb scattering experiment with β^--particles emitted by P^{32}

Experiment [a])	Second scatterer (mg/cm^2) (gold)			Extrapolated value to zero foil thickness ($t = 0$)
	0.37	0.8	2.8	
The mean of I and II	108.2±0.9	107.8±0 6	103.9±0.6	110.6±1.5

$\bar{\theta}_1 = 90°$, $\bar{\theta}_2 = 73°$, $Z_1 = 13$, $Z_2 = 79$ and $\bar{E}_i = 0.7$ MeV.

[a]) I and II refer to independent measurements of detectors 1 and 2.

As expected, different values for the azimuthal asymmetry were found for various thicknesses of the scattering gold foil, the largest one corresponding to the thinnest foil.

The extrapolated value, corresponding to zero scattering foil thickness, was calculated by the least squares method. This value is to be compared with the theoretical one (10) which corresponds to a deflection of the electron through $\bar{\theta}_1 = 90°$ (in Al) and a single scattering through $\bar{\theta}_2 \approx 73°$ (in Au). Such a comparison then yields the initial longitudinal polarization of the electrons emitted by P^{32}. We get †

$$\frac{P_0(P^{32})}{-v/c} = \frac{A_{exp}(P^{32})}{A_{theor}(P^{32})} \equiv \frac{(10.6 \pm 1.5) \times 10^{-2}}{10.7 \times 10^{-2}},$$

or

$$P_0(P^{32}) = (0.99 \pm 0.14)(-v/c). \tag{11}$$

This result is in good agreement with all other experiments [19]) and indicates therefore the reliability of the method used by us and the validity of the results for ${}_{81}Tl^{207}$.

6. Results and Conclusions

The results obtained for the azimuthal asymmetry of the doubly scattered electrons emitted by ${}_{81}Tl^{207} + {}_{82}Pb^{211}$ are given in table 2.

TABLE 2

The azimuthal asymmetry (100 I_L/I_R) in the double Coulomb scattering experiment with β^--particles emitted by ${}_{81}Tl^{207} + {}_{82}Pb^{211}$.

Experiment	Second scatterer (mg/cm²) (gold)			Extrapolated value to zero thickness ($t = 0$)
	0.48	0.8	2.8	
I	110.8±1	107.4±1	104.0±0.9	
II	110.0±0.9	109.0±0.9	104.6±0.8	
Average on I and II	110.4±0.7	108.2±0.7	104.3±0.6	114.6±2

$\bar{\theta}_1 = 90°$, $\bar{\theta}_2 = 73°$, $Z_1 = 13$, $Z_2 = 79$, $\hat{E}_1 = 0.47$ MeV

Comparison of the extrapolated value (to zero scattering foil thickness) of the asymmetry to the theoretical one (7), yields the initial longitudinal polarization of the electrons emitted by ${}_{81}Tl^{207} + {}_{82}Pb^{211}$:

$$P_0({}_{81}Tl^{207} + {}_{82}Pb^{211}) = (1.02 \pm 0.14)(-v/c). \tag{12}$$

Approximately 56 % of the electrons are emitted by ${}_{81}Tl^{207}$ and 44 % by

† The irrelevant difference between (11), (13) and the corresponding values given in a preliminary note on this experiment [20]) is due to an omission in the earlier calculation.

$_{82}Pb^{211}$. Assuming † a $-v/c$ longitudinal polarization for the electrons emitted by $_{82}Pb^{211}$, the initial longitudinal polarization of the electrons emitted by $_{81}Tl^{207}$ (alone) is found to be

$$P_0(_{81}Tl^{207}) = (1.04 \pm 0.25)(-v/c). \tag{13}$$

As already mentioned, if two component neutrino theory [3]) with left-handed neutrino [4]) are assumed, a $-v/c$ polarization is to be expected for (A, V) interactions and a $+v/c$ one for P interaction. Thus, the result (13) indicates a small contribution, if any, of the pseudoscalar interaction to β-decay, in agreement with the results obtained for $0- \to 0+$ β-decay transitions [21]).

However, the exact interpretation of (13) in terms of the relative contribution of the pseudoscalar interaction to β-decay is possible only after a theoretical formula for the initial longitudinal polarization of the electrons emitted in $\frac{1}{2}+ \to \frac{1}{2}-$ β-decay transition is obtained.

The author wishes to express his appreciation to Professor H. J. Lipkin for suggesting this problem and for guidance during the initial stages of this work. It is a pleasure to thank Professor A. de Shalit for guidance and many valuable suggestions and discussions during the course of this work. The author is also very grateful to Dr. S. Katcoff for his valuable help in carrying out the preparation of the radioactive source of $_{88}Ra^{223}$ and to Mr. G. Kedem for help in preparation of P^{32} sources. The help of Ing. D. Mydansky and Z. Kamil (Electronics Department) and Ing. B. Feldman and I. Choukran is gratefully acknowledged.

† This assumption corresponds to a lowest limit for the longitudinal polarization of $_{81}Tl^{207}$ electrons, in units of $-v/c$, (or to an upper limit of the pseudoscalar contribution to β-decay.)

References

1) T. D. Lee and C. N. Yang, Phys. Rev. **104** (1956) 254
2) M. Goldhaber, 1958 Ann. Int. Conf. on High Energy Physics at CERN, ed. by B. Ferreti
3) T. D. Lee and C. N. Yang, Phys. Rev. **105** (1957) 1671;
A. Salam, Nuovo Cim. **5** (1957) 299;
L. Landau, JETP **32** (1957) 405
4) M. Goldhaber, L. Grodzins and A. W. Sunyar, Phys. Rev. **109** (1958) 1015
5) Jackson, Treiman and Wyld, Phys. Rev. **106** (1957) 517
6) Strominger, Hollander and Seaborg, Rev. Mod. Phys. **30** (1958) 585
7) Strominger, Hollander and Seaborg, as referred in ref. [6])
8) J. M. Hollander, private communication
9) R. W. King and D. C. Peaslee, Phys. Rev. **94** (1954) 1284
10) de Shalit, Cuperman, Lipkin and Rothem, Phys. Rev. **107** (1957), 1459; Proc. Rehovoth Conf. on Nuclear Structure, ed. by H. J. Lipkin (North-Holland Publishing Company, Amsterdam, 1958) p. 400
11) S. Cuperman, Thesis, The Weizman Institute of Science and the Hebrew University of Jerusalem, 1960

12) N. F. Mott, Proc. Roy Soc. **124** (1929) 425, **135** (1932) 429;
N. F. Mott and H. Massey, Theory of atomic collisions
13) H. A. Tolhoek, Rev. Mod. Phys. **28** (1956) 277
14) F. Gürsey, Phys. Rev. **107** (1957) 1734
15) N. Sherman, Phys. Rev. **103** (1956) 1601
16) C. G. Shull, Phys. Rev. **61** (1942) 198;
G. Goertzel and R. T. Cox, Phys. Rev. **61** (1942) 198;
C. G. Shull, C. T. Chase and F. E. Myers, Phys. Rev. **63** (1943) 29
17) G. Wentzel, Ann. Physik **69** (1922) 335
18) Cavenagh, Turner, Coleman, Gard and Ridley, Phil. Mag. **2** (1957) 1105
19) C. S. Wu, Proc. Rehovoth Conf. on Nuclear Structure ed. by H. J. Lipkin (North-Holland Publ. Co., Amsterdam, 1958) p. 346
20) S. Cuperman, Phys. Rev. **117** (1960) 185
21) S. G. Cohen and R. Wiener, Nuclear Physics **15** (1960) 89;
W. Bühring, Z. Phys. **155** (1959) 566;
T. A. Pond, W. A. W. Melhop and E. D. Lambe, Bull. Amer. Phys. Soc., **4** (1959) 77

1.D.1.

Nuclear Physics **28** (1961) 96—121; © *North-Holland Publishing Co., Amsterdam*

Not to be reproduced by photoprint or microfilm without written permission from the publisher

POSITIVE PARITY STATES OF Be^9 AND C^{13}

F. C. BARKER

Research School of Physical Sciences, The Australian National University, Canberra

and

Laboratory for Nuclear Science, Massachusetts Institute of Technology, Cambridge, Massachusetts †

Received 17 April 1961

Abstract: The states produced by weakly coupling a 2s- or 1d-neutron to a core consisting of the ground or first excited state of C^{12} are mixed by means of a two-body central interaction and a one-body spin-orbit interaction of the type normally used in intermediate-coupling calculations, to provide the low-lying positive-parity eigenstates of C^{13}. The positions and neutron widths of the states agree satisfactorily with experimental data, as do the calculated cross sections for photoneutron disintegration of C^{13}; however, in order to obtain agreement with other data involving E1 radiative widths the single-particle shell-model wave functions must be modified so as to have the correct asymptotic form. Similar calculations are performed for the Be^9 positive-parity states, about which little is known experimentally.

1. Introduction

There is considerable experimental support for the main features of the model proposed by Lane [1]) for the states of non-normal parity of light nuclei, especially C^{13} and N^{13}. According to this model, the low-lying positive-parity states of these nuclei are formed by weakly coupling a 2s- or 1d-nucleon to the lowest shell-model states of C^{12}, which are not polarized by the additional nucleon. In the simplified model each state belongs to a unique configuration and has a unique parent.

Lane [1]) considered qualitatively the effects of allowing mixing between these basic states. We calculate this mixing quantitatively by introducing an interaction Hamiltonian of the type normally used in intermediate-coupling calculations. The definition and determination of the parameters occurring in the Hamiltonian and in the shell-model potential well used for the description of the basic states are discussed in sect. 2.

Calculations are performed for both Be^9 and C^{13} positive-parity states; as there is more experimental information on the C^{13} states, we consider this nucleus first and in more detail. Results of the calculations for C^{13} are given in subsects. 3.1—3.5; these include the energies and wave functions of the

† This work is supported in part through AEC Contract At(301-1)2098, by funds provided by the U. S. Atomic Energy Commission, the Office of Naval Research and the Air Force Office of Scientific Research.

eigenstates, their neutron widths and various radiative widths. Among the latter we are particularly interested in the widths of E1 transitions coupling the positive-parity states with the C^{13} ground state, as these are of major importance in the photodisintegration of C^{13}. Difficulties in fitting certain radiative widths are attributed in subsect. 3.6 to a deficiency of shell-model wave functions; when single-particle wave functions with the correct asymptotic forms are used, it seems that almost all the experimental data can be satisfactorily fitted. A comparison is made in subsect. 3.7 with calculations made by other authors on the positive-parity states of C^{13}. Results for Be^9 are given in sect. 4.

2. Weak-Coupling Model for C^{13}

The basic positive-parity states of C^{13} are obtained by coupling a 2s- or 1d-neutron to a core which is either the 0^+ ground or 2^+ first excited state of C^{12} and then antisymmetrizing. These are states of configuration $1s^4\,1p^8\,2s$ or $1s^4\,1p^8\,1d$; states of configuration $1s^3\,1p^{10}$ are omitted. These basic states can be labelled $(Jj)J$ according to the angular momenta J of the core, j of the added neutron and J of the resultant state, giving the set

$$\begin{array}{llll} (0\tfrac{1}{2})\tfrac{1}{2}, & (2\tfrac{3}{2})\tfrac{1}{2}, & (2\tfrac{5}{2})\tfrac{1}{2}, & \\ (0\tfrac{3}{2})\tfrac{3}{2}, & (2\tfrac{1}{2})\tfrac{3}{2}, & (2\tfrac{3}{2})\tfrac{3}{2}, & (2\tfrac{5}{2})\tfrac{3}{2}, \\ (0\tfrac{5}{2})\tfrac{5}{2}, & (2\tfrac{1}{2})\tfrac{5}{2}, & (2\tfrac{3}{2})\tfrac{5}{2}, & (2\tfrac{5}{2})\tfrac{5}{2}, \\ (2\tfrac{3}{2})\tfrac{7}{2}, & (2\tfrac{5}{2})\tfrac{7}{2}, & & \\ (2\tfrac{5}{2})\tfrac{9}{2}. & & & \end{array} \qquad (1)$$

The nuclear Hamiltonian is assumed to be

$$H = K + V^{c} + V^{so} + V^{conf},$$

where

$$K = -(\hbar^2/2M)\sum_i \nabla_i^2,$$

$$V^{c} = \sum_{i<j} [W + MP_{ij}^{x} - HP_{ij}^{\tau} + BP_{ij}^{\sigma}]v(r_{ij}),$$

$$V^{so} = \sum_i \xi_{n_i l_i}(\mathbf{s}_i \cdot \mathbf{l}_i),$$

and V^{conf} is a diagonal operator with matrix elements depending only on the configuration of the state [2]), i.e. on the nl but not the j of the added neutron.

The various contributions of K, V^{c} and V^{so} to the matrix elements of H are treated as follows:

(i) K (core nucleon) $+V^{c}$ (core nucleon — core nucleon) $+V^{so}$ (core nucleon) — this gives just the energies of the C^{12} states, and so contributes 0 or 4.433

MeV to the diagonal matrix elements depending on whether the core is the ground or first excited state of C^{12};

(ii) K (odd neutron) $+V^c$ (odd neutron − closed-shell core nucleon) − this depends only on the configuration of the state and so can be included in the matrix elements of V^{conf};

(iii) V^c (odd neutron − unclosed-shell core nucleon) $+V^{so}$ (odd neutron) − this part is calculated explicitly.

In order to evaluate the matrix elements of V^c, the C^{12} states have to be specified precisely. They are well described by intermediate-coupling wave functions which are far removed from those in the L-S coupling limit [3,4]). The matrix elements we require, however, depend little on the degree of intermediate coupling and for this purpose the C^{12} states are taken in the L-S coupling limit. Elsewhere, as in the calculation of E1 matrix elements, intermediate-coupling wave functions are used.

The matrix elements of H depend on a number of parameters. For the central interaction V^c, we use instead of W, M, H and B, their linear combinations A_{TS} which occur in the interaction between a pair of nucleons with isobaric spin T and ordinary spin S:

$$A_{01} = W+M+H+B,\quad A_{10} = W+M-H-B,\quad A_{00} = W-M+H-B,$$
$$A_{11} = W-M-H+B,$$

normalized by $A_{01} = -1$. Matrix elements of V^c also involve two other parameters, the depth V_0 and the range κ^{-1} of the interaction $v(r)$. The spin-orbit interaction V^{so} only contributes for 1d-neutrons, involving the parameter ξ_{1d}. As only relative energies of the positive-parity states are required, contributions from V^{conf} come only through the parameter $\delta = (V^{conf})_{1d} - (V^{conf})_{2s}$. The single-particle wave functions also introduce a length parameter a; this occurs in the matrix elements of H only in the combination κa.

Numerical values have to be assigned to these parameters before the Hamiltonian can be diagonalized in order to give the C^{13} positive-parity eigenstates and their energies. Most of the calculations are performed using single-particle wave functions for an harmonic oscillator potential well $U(r) = -(\hbar^2/2Ma^4)r^2$; the length parameter a required to fit the mean-square radius of C^{12} as determined by electron scattering [5]) is 1.64 fm; for C^{13} we use $a = 1.67$ fm. Also we use a Yukawa interaction $v(r) = V_0(\kappa r)^{-1}\exp(-\kappa r)$. If κ^{-1} is taken as the π-meson Compton wave length, $\kappa^{-1} = 1.41$ fm, one has $\kappa a = 1.18$, and the correct deuteron binding energy is obtained for $V_0 = 50$ MeV. The exchange parameters A_{TS} occur only in the combinations $A_{01}+A_{10}$ and $A_{00}+9A_{11}$. Values of $A_{01}+A_{10}$ used in previous calculations have always been about -1.6, but values of $A_{00}+9A_{11}$ have varied greatly, including such values as 6.4 (refs. [6,7])), 4.8 (ref. [8])), 1.84 (ref. [9])), -0.86 (ref. [10])) and -4.2 (ref. [11])).

The 1d spin-orbit interaction strength ξ_{1d} has the value -2.03 MeV for O^{17} if the ground and 5.08 MeV states are identified as the $1s^4\,1p^{12}\,1d_{\frac{5}{2}}$ and $1s^4\,1p^{12}\,1d_{\frac{3}{2}}$ states, respectively.

In our calculations we take as plausible starting values

$$\kappa a = 1.2,\ V_0 = 50\ \text{MeV},\quad A_{01}+A_{10} = -1.6,$$
$$A_{00}+9A_{11} = 0,\quad \xi_{1d} = -2\ \text{MeV} \tag{2}$$

and consider the effect of changes in these quantities as indicated in table 1. These changes are performed independently, except that when κa is changed, we keep $V_0(\kappa a)^{-2}$ fixed at 34.72 MeV, as the matrix elements of V^c are more or less proportional to $(\kappa a)^{-2}$. Changes in $A_{01}+A_{10}$ can be absorbed into changes in V_0. The effect of changing the potential well shape from an harmonic oscillator is investigated by using single-particle wave functions for a finite-depth well

$$U(r) = -(\hbar^2/2Ma^2\alpha)[1-\exp\,(-\alpha r^2/a^2)], \tag{3}$$

which reduces to an oscillator potential as $\alpha \to 0$. A self-consistent field type of calculation suggests $\alpha \approx 0.2$ for C^{12}. The mean-square radius of C^{12} is then fitted with $a = 1.29$ fm. We take $\kappa a = 1$ corresponding to $\kappa^{-1} = 1.29$ fm, for which $V_0 = 60$ MeV to fit the deuteron binding energy. Actually we use $V_0 = 85$ MeV as this gives C^{13} levels in closer agreement with those given by the values (2). For each set of parameter values, δ is chosen to fit the observed separation of the two lowest positive-parity states of C^{13} — the $\frac{1}{2}^+$ state at 3.08 MeV and the $\frac{5}{2}^+$ state at 3.85 MeV (ref. [12])) — and their absolute energies fitted by adjusting the zero of the energy scale.

3. The C^{13} Positive-Parity States

3.1. ENERGIES

The energies E_{Jp} of the C^{13} eigenstates, labelled by the values Jp, are given in table 1 for various sets of values of the interaction parameters, together with the measured energies of the known positive-parity states [12]). Among these five observed states, the energies of the $\frac{1}{2}$ 1 and $\frac{5}{2}$ 1 states are fitted for each set of parameters, the energies of the $\frac{3}{2}$ 1 and $\frac{5}{2}$ 2 states do not change significantly with the changes considered in the parameters and agree satisfactorily with the observed energies, while the energy of the $\frac{3}{2}$ 2 state depends essentially only on ξ_{1d}, the best value being obtained for $\xi_{1d} = -2.1$ MeV.

There is some evidence [12]) for other positive-parity states in C^{13} from the reaction Be^9 $(\alpha, n)C^{12}$; these include a $\frac{1}{2}^+$ state of width 70 keV at 11.02 MeV and broad $\frac{3}{2}^+$ and $\frac{5}{2}^+$ states in the region of 13.5 MeV. Such a narrow $\frac{1}{2}^+$ state would probably belong mainly to some other configuration or at any rate be of different structure from the states we are considering, which is not unlikely at 11 MeV excitation. The broad states could be the $\frac{3}{2}$ 3 and $\frac{5}{2}$ 4 states.

There are also positive-parity states known in N^{13}, and apart from effects such as Coulomb energy differences and Thomas shifts, these should have energy separations the same as for the C^{13} states. Then the N^{13} states [12]) observed at excitation energies of 2.36, 3.56, 6.38, 6.91 and 8.08 MeV can be identified as the $\frac{1}{2}1$, $\frac{5}{2}1$, $\frac{5}{2}2$, $\frac{3}{2}1$ and $\frac{3}{2}2$ states, respectively. Also $\frac{1}{2}^+$ and $\frac{5}{2}^+$ states have been suggested at 6.60 and 7.42 MeV, respectively [12]). These

TABLE 1

Calculated and measured values of excitation energies E_{Jp} (in MeV) of C^{13} positive-parity states

Well shape	Harmonic oscillator					Eq. (3) ($\alpha=0.2$)	Measured
κa	1.2	1.0	1.2	1.2	1.2	1.0	
V_0(MeV)	50	34.72	40	50	50	85	
$A_{00}+9A_{11}$	0	0	0	5	0	0	
ξ_{1d}(MeV)	−2	−2	−2	−2	−2.5	−2	
δ (MeV)	5.25	4.97	4.63	7.72	5.75	5.95	
Jp							
$\frac{1}{2}1$	3.08	3.08	3.08	3.08	3.08	3.08	3.08
$\frac{1}{2}2$	13.26	12.96	12.14	14.37	13.31	13.10	
$\frac{1}{2}3$	18.25	17.93	17.04	19.45	19.43	18.10	
$\frac{3}{2}1$	7.52	7.52	7.50	7.52	7.56	7.53	7.64
$\frac{3}{2}2$	8.10	8.13	8.16	8.15	8.92	8.11	8.33
$\frac{3}{2}3$	12.59	12.31	11.62	13.40	13.00	12.51	
$\frac{3}{2}4$	16.38	16.13	15.48	17.16	17.59	16.37	
$\frac{5}{2}1$	3.85	3.85	3.85	3.85	3.85	3.85	3.85
$\frac{5}{2}2$	7.28	7.27	7.29	7.34	7.28	7.17	6.86
$\frac{5}{2}3$	10.32	10.08	9.78	10.49	10.49	9.89	
$\frac{5}{2}4$	13.69	13.46	13.28	14.02	14.75	13.40	
$\frac{7}{2}1$	7.84	7.61	7.78	7.79	7.85	6.89	
$\frac{7}{2}2$	15.04	14.81	14.52	14.81	16.27	15.03	
$\frac{9}{2}1$	10.21	9.99	9.67	9.97	10.21	10.24	

would be an embarrassment to our scheme, although they fitted into the simpler Lane model [1]) which gave eight positive-parity states all in the neighbourhood of 7—8 MeV excitation. Evidence for the $\frac{1}{2}^+$ state is very slight and it is omitted from the summary of N^{13} levels in ref. [12]). The $\frac{5}{2}^+$ assignment [13]) was made on the basis of the angular distribution of the γ-rays in the reaction $C^{12}(p, p')C^{12*}$ (γ) C^{12} proceeding through the 7.42 MeV state of N^{13} and the first excited state of C^{12}; the same angular distribution is calculated, however, for a $\frac{5}{2}^-$ assignment for the N^{13} state and the emission of $p_{\frac{1}{2}}$ protons to C^{12*}. Intermediate-coupling calculations [7]) predict a $\frac{5}{2}^-$ state at 5—6 MeV excitation and its nonappearance has caused some concern. It is not unreasonable that this state is at 7.42 MeV; the width of the state and the magnitude of the

inelastic scattering cross section can be fitted (in the L-S coupling limit) with a single-particle dimensionless reduced width $\theta_0^2(1p) \approx 0.2$ and an f-nucleon impurity of about 1 % intensity. The analogous state in C^{13} could be taken as either of those observed at 7.47 and 7.53 MeV without conflict with the observed properties of these states [12]).

Thus there is no convincing evidence for more positive-parity states in the region up to say 10 MeV excitation than are predicted in the present calculation. There is however a $\frac{7}{2}^+$ state predicted which has not been identified. In C^{13} it should show up in reactions such as [14]) $B^{11}(He^3, p)C^{13}$, but it would appear in $C^{12}(n, n)C^{12}$ and $C^{12}(d, p)C^{13}$ only because of impurities in the wave function belonging to other configurations. It is plausible that the $\frac{7}{2}^+$ state is one of those observed in C^{13} at 7.47 and 7.53 MeV, then the analogous N^{13} state should be at about 7.0 MeV.

A state has recently been observed [15]) in $C^{12}(p, p')C^{12*}(\gamma)C^{12}$ at 7.18 MeV of width about 0.018 MeV. It appears as a small peak on a background due to other states, presumably those at 6.91 and 7.42 MeV and perhaps that at 6.30 MeV. The angular distribution of γ-rays at the energy of the peak is apparently more isotropic than that for the background alone, hence the spin of the 7.18 MeV state has been suggested [15]) as $\frac{1}{2}^{\pm}$. It is not impossible, however, that it is $\frac{7}{2}^+$. The angular distribution for the reaction proceeding through a $\frac{7}{2}^+$ state is $1-1.9\cos^2\theta_{p\gamma}+2.4\cos^4\theta_{p\gamma}$, which could have the observed effect as the background is probably something like $1+6\cos^2\theta_{p\gamma}-5\cos^4\theta_{p\gamma}$. Also the $\frac{7}{2}^+$ state, if at 7.18 MeV, would have a partial proton width for decay to the C^{12} excited state of $\Gamma^0 = 0.008$ MeV, and a ground-state width of the same order if there is a g-wave impurity of 1 % intensity.

Thus the energies given in the first column of table 1 for the parameter values (2) are in good agreement with the energies observed. We now consider the corresponding wave functions in detail.

3.2. WAVE FUNCTIONS

The eigenfunction of the state $J\not{p}$ is written

$$\Psi(J\not{p}) = \sum_{\bar{J}j} C_{J\not{p}}(J_j)\Psi((J_j)J), \tag{4}$$

in terms of the basic states $\Psi(J_j)J)$ taken in the order given in (1). In table 2, values of the coefficients $C_{J\not{p}}(J_j)$ are given corresponding to the parameter values (2) and the first column of table 1.

The basic states used here contain spurious states [16]) and so do the eigenstates. In order to obtain entirely non-spurious eigenstates, we should have to introduce further basic states which would destroy the simplicity of the model (see ref. [17])); instead we calculate the fraction F_s of spurious states in each eigenstate. These are given in table 2 for the C^{12} wave functions taken in the

L-S coupling limit. For the low-lying eigenstates $F_s \lesssim 0.02$, so that elimination of spurious states would probably not change them much, but the eigenstates at higher energies contain more spurious states and matrix elements involving them are therefore less reliable; this would be so in any case as the higher eigenstates are expected to contain contributions from states of other configurations.

TABLE 2

Calculated energies, eigenfunctions, fractions of spurious states and neutron widths of C^{13} positive-parity states

$J\pi$	$E_{J\pi}$ (MeV)	$C_{J\pi}(Jj)$	F_s	$\Gamma_{J\pi}(Jl)$ (MeV)				$\Gamma^0_{J\pi}$ (MeV)
				0s	0d	2s	2d	
$\frac{1}{2}$ 1	3.08	0.985, −0.081, −0.154	0.023	0			0	0
$\frac{1}{2}$ 2	13.26	0.132, −0.234, 0.963	0.164	0.10			2.61	2.16
$\frac{1}{2}$ 3	18.25	0.114, 0.969, 0.220	0.178	0.09			6.49	6.17
$\frac{3}{2}$ 1	7.52	0.206, 0.969, 0.081, −0.110	0.024		0.067	0	0	0.048
$\frac{3}{2}$ 2	8.10	0.758, −0.070, −0.365, 0.536	0.010		1.27	0	0	0.93
$\frac{3}{2}$ 3	12.59	0.505, −0.192, −0.133, −0.831	0.137		1.45	0.13	1.41	2.38
$\frac{3}{2}$ 4	16.38	0.356, −0.141, 0.918, 0.103	0.131		1.02	0.11	4.45	5.06
$\frac{5}{2}$ 1	3.85	0.899, −0.092, −0.090, −0.418	0.008		0	0	0	0
$\frac{5}{2}$ 2	7.28	0.100, −0.905, 0.015, 0.412	0.012		0.0088	0	0	0.0067
$\frac{5}{2}$ 3	10.32	0.344, 0.373, −0.424, 0.750	0.083		0.47	0.27	0.18	0.62
$\frac{5}{2}$ 4	13.69	0.251, 0.181, 0.901, 0.305	0.076		0.40	0.13	2.74	2.70
$\frac{7}{2}$ 1	7.84	0.107, 0.994	0.012				0	0
$\frac{7}{2}$ 2	15.04	0.994, −0.107	0.032				4.20	3.65
$\frac{9}{2}$ 1	10.21	1.000	0.033				0.16	0.10

3.3. NEUTRON WIDTHS

From these eigenfunctions we can easily calculate the partial widths of the states for s- or d-wave neutron emission to the ground or first excited state of C^{12}. We use the notation of Lane [1, 18]) with the state and channel concerned being specified by $\lambda \equiv J\pi$ and $c \equiv Jl$. The total width of the state λ is

$$\Gamma_\lambda = \sum_c \Gamma_{\lambda c}, \tag{5}$$

if we neglect other channels, such as α-emission or neutron emission to higher excited states of C^{12}. Then we have

$$\Gamma_{\lambda c} = 2P_c\gamma^2_{\lambda c}, \tag{6}$$

$$\gamma^2_{\lambda c} = (\hbar^2/M_c a_c^2)\theta^2_{\lambda c}, \tag{7}$$

$$\theta^2_{\lambda c} = A^2_{\lambda c}\theta_0{}^2(c), \tag{8}$$

$$\theta_0{}^2(c) = a_c\,|\phi_c(a_c)|^2/2\int_0^{a_c}|\phi_c(r)|^2 dr. \tag{9}$$

Some authors use a different unit in (7) for extracting a dimensionless reduced width $\theta_{\lambda c}^2$ from the reduced width $\gamma_{\lambda c}^2$; thus in refs. [4, 12]) the values given for θ^2 and for the single-particle dimensionless reduced widths θ_0^2 are $\frac{2}{3}$ of those given by the above convention.

The $\Gamma_{\lambda c}$ are not, however, the partial widths usually obtained from experiment as the cross-section formula which depends on $\Gamma_{\lambda c}$ also involves the energy-dependent level shift

$$\Delta_\lambda = \sum_c \Delta_{\lambda c} = -\sum_c \theta_{\lambda c}^2 [S_c(E) - S_c(E_{res})]. \tag{10}$$

By treating Δ_λ as a linear function of energy, Thomas [19]) has shown that the cross section may be written in a form not involving a level shift (see (20)) by using the "observed" partial widths

$$\Gamma_{\lambda c}^0 = \Gamma_{\lambda c} \left[1 - \frac{\mathrm{d}\Delta_\lambda}{\mathrm{d}E}\right]_{E=E_{res}}^{-1}. \tag{11}$$

We note that $\mathrm{d}\Delta_{\lambda c}/\mathrm{d}E < 0$ for all c. It is the observed width $\Gamma_\lambda^0 = \sum_c \Gamma_{\lambda c}^0$ which is usually given as the width of a level.

In extracting a reduced width $\theta_{\lambda c}^2$ from an observed partial width $\Gamma_{\lambda c}^0$, the contributions to Δ_λ from negative-energy channels are usually neglected, and this could lead to appreciable error for a level which is just below the threshold of a channel for which the reduced width is large [18, 19]). In elastic scattering analyses, the cross section is normally written in terms of the $\Gamma_{\lambda c}$ and Δ_λ, but again negative-energy channels are neglected. Thus it seems safest to compare calculated and experimental values of observed widths $\Gamma_{\lambda c}^0$, unless it is clear that negative-energy channels are not going to contribute appreciably, in which case values of $\theta_{\lambda c}^2$ can be compared.

For the eigenfunction (4) we have

$$A_{\lambda c}^2 \equiv A_{Jp}^2(Jl) = \sum_{j=|l\pm\frac{1}{2}|} C_{Jp}^2(Jj).$$

The usual prescription is assumed for the channel radius $a_c = 1.45\,(A_1^{\frac{1}{3}} + A_2^{\frac{1}{3}})$ fm $= 4.77$ fm. In the shell model treatment we have $\phi_c(r) \equiv \phi_{nl}(r)$, independent of the channel energy, and we can write $\theta_0^2(\mathrm{c}) = \theta_0^2(nl)$. Calculated values for an harmonic oscillator well are $\theta_0^2(2\mathrm{s}) \approx 0.22$, $\theta_0^2(1\mathrm{d}) \approx 0.13$. Lane [1]) has given two reasons why these values are likely to be in error: (a) because an harmonic oscillator is not the best shape for the potential well, (b) because the correct asymptotic wave function should be fitted at the channel radius a_c, and this is not done in shell model treatments. To estimate the effect of (a), we calculate $\theta_0^2(nl)$ for the finite depth well (3); for $\alpha = 0.2$ this gives $\theta_0^2(2\mathrm{s}) \approx 0.60$, $\theta_0^2(1\mathrm{d}) \approx 0.43$. The effect of (b) is considered later in sect. 3.6. For the moment we treat $\theta_0^2(2\mathrm{s})$ and $\theta_0^2(1\mathrm{d})$ as parameters to be fitted empirically. Thus Lane [1]) found that $\theta_0^2(2\mathrm{s}) = \theta_0^2(1\mathrm{d}) = 0.6$, with a possible uncertainty

of the order of 30 %, gave reasonable agreement for the reduced widths of resonance levels in 1p-shell nuclei.

A value of $\theta_0^2(2s)$ is obtainable from the elastic scattering cross section for epithermal neutrons on C^{12}. The measured total cross section [12]) is 4.69b, corresponding to a scattering length $a_s = 6.11$ fm. Assuming the scattering to be due to potential scattering plus a contribution from the C^{13} $\frac{1}{2}1$ state alone, and including the $\frac{1}{2}1$ level shift due to the 0s channel, we have

$$a_s = a_c \left[1 + \frac{\theta_{\lambda c}^2 \hbar^2/M_c a_c^2}{(E-E_\lambda)\left[1+\theta_{\lambda c}^2\left(\frac{2\hbar^2/M_c a_c^2}{E-E_\lambda}\right)^{\frac{1}{2}}\right]}\right], \qquad (13)$$

$$\lambda \equiv J\pi = \tfrac{1}{2}1, \qquad c \equiv Jl = 0s,$$

with $E = 4.95$ MeV and $E_\lambda = 3.08$ MeV. For $a_c = 4.77$ fm, this gives $\theta_{\lambda c}^2 = 0.43$ and $\theta_0^2(2s) = 0.44$. In view of the calculations of subsect. 3.6, we take $\theta_0^2(2s) = 0.5$. The observed widths Γ_λ^0 of three positive-parity states of C^{13} have been measured. These are given [12]) as 0.006 MeV for the $\frac{5}{2}2$ state, (0.055 ± 0.015) MeV for $\frac{3}{2}1$, and (1.00 ± 0.25) MeV for $\frac{3}{2}2$. For each the only positive-energy channel, apart from γ-emission, is d-wave neutron emission to the C^{12} ground state, therefore for each state $\theta_0^2(1d)$ is involved explicitly but $\theta_0^2(2s)$ only through Δ_λ. The best fit is obtained with $\theta_0^2(1d) = 0.8$. In table 2 are given values of the partial widths (column headings are Jl values) and the observed total widths calculated for $\theta_0^2(2s) = 0.5$ and $\theta_0^2(1d) = 0.8$.

Values of reduced widths $\theta_{\lambda c}^2$ obtained for C^{13} states from both resonance and stripping reactions, and for N^{13} states from resonance reactions, are compared with calculated values in table 3. In extracting resonance reduced widths, the usual approximation of neglecting negative-energy channels is made. For $\frac{5}{2}2$, $\frac{3}{2}1$ and $\frac{3}{2}2$ states, inclusion of the effects of neglected channels, using wave functions from table 2, increases the tabulated θ^2 values for C^{13} to 0.0072, 0.038 and 0.49, so that the θ^2 values for N^{13} would probably become about 0.006, 0.029, 0.47 and 0.20. The agreement with the calculated values is satisfactory except for the $\frac{3}{2}2$ state, where the N^{13} experimental observed width $\Gamma^0 = 0.35$ MeV may be inaccurate. Inclusion of effects of negative-energy channels is not expected to change appreciably the θ^2 values for the $\frac{1}{2}1$ and $\frac{5}{2}1$ states of N^{13}, so there is considerable disagreement with the calculated values; the experimental values require $\theta_0^2(2s) = 0.84$, $\theta_0^2(1d) = 0.38$. This difficulty is partly removed by the considerations of subsect. 3.6.

For the stripping reduced widths, we use $\theta_0^2(2s) = 0.25$, $\theta_0^2(1d) = 0.09$, which Macfarlane and French [4]) found gave a good fit to data from 1p-shell nuclei and O^{17}. It is seen from table 3 that improved agreement for the C^{13} states could be obtained by using a somewhat larger value of $\theta_0^2(1d)$; this may

be related so the trend for $\theta_0^2(1d)$ to increase as the binding energy of the d-nucleon decreases [4]).

TABLE 3

Calculated and measured values of dimensionless reduced widths $\theta^2_{Jp}(Jl)$ for positive-parity states of C^{13} and N^{13}

Jp	$E_{Jp}(C^{13})$ (MeV)	Jl	$\theta^2_{Jp}(Jl)$				
			Resonance			Stripping	
			Calculated	Measured		Calculated	Measured C^{13}
				C^{13}	N^{13}		
$\frac{1}{2}1$	3.08	0s	0.48		0.81 [b])	0.24	0.25 [f])
$\frac{3}{2}1$	3.85	0d	0.65		0.31 [b])	0.07	0.11 [f])
$\frac{5}{2}2$	6.86	0d	0.0081	0.0055 [a])	0.0046 [c])	0.001	0.003 [f])
$\frac{1}{2}1$	7.64	0d	0.034	0.028 [a])	0.029 [d])	0.004	0.008 [f])
		2s	0.47		0.47 [d])	0.23	
$\frac{3}{2}2$	8.33	0d	0.46	0.42 [a])	0.17 [e])	0.05	

[a]) From $\Gamma^0 = 0.006$, 0.055 and 1.00 MeV (ref. [13])). From $C^{12}(n, n)C^{12}$ alone [20]), with a slightly different $a_c(4.61$ fm), $\theta^2 = 0.009$, 0.057 and 0.76.

[b]) From [21]) $C^{12}(p, p)C^{12}$; the Γ^0 corresponding to this θ^2 for the $\frac{1}{2}1$ state agrees satisfactorily with Γ^0 values obtained in $C^{12}(p, \gamma)N^{13}$ (see ref. [13])).

[c]) Ref. [22]); neglects contribution to Δ_λ from 2s and 2d channels.

[d]) From $\Gamma^0_{\lambda c} = 0.052$, 0.063 MeV obtained from elastic scattering cross section [22]) and consistent with inelastic scattering cross section [22]); includes contribution to Δ_λ from 0d and 2s channels but not 2d channel. Lane [1]) gives $\theta^2 = 0.02$, 0.5 from somewhat different $\Gamma^0_{\lambda c}$. Other measurements [23, 24]) give $\theta^2 = 0.04$, 0.04.

[e]) Refs. [1, 23]); we calculate $\theta^2 = 0.08$ from observed width $\Gamma^0 = 0.35$ MeV, neglecting contributions to Δ_λ from 2s and 2d channels.

[f]) ref. [4])

3.4. PHOTODISINTEGRATION OF C^{13} BY E1 ABSORPTION

We calculate the cross sections for photodisintegration of C^{13} with neutron emission to either the ground or first excited state of C^{12}, including only E1 absorption and assuming that the positive-parity states we are considering will give the main contributions for γ energies up to order 15 MeV. Contributions from M1, E2,... absorption are expected to be much smaller except perhaps for isolated narrow peaks. The required matrix elements of the E1 operator depend on the wave functions of the $\frac{1}{2}^-$ ground state and of the $\frac{1}{2}^+$ and $\frac{3}{2}^+$ excited states, and therefore on the wave functions taken for the C^{12} core states. It happens that the only dependence on these wave functions, apart from dependence on their T, M_T and J values, is through the reduced widths $\theta_g^2(J)$ of the C^{13} ground state for emission of a 1p neutron to the ground ($J = 0$) or first excited ($J = 2$) state of C^{12}, and these have been determined both experimentally and by calculation in intermediate coupling [4]). We write $A_g(J) = \theta_g(J)/\theta_0(1p)$. The spectroscopic factors of Macfarlane and

French [4]) are $\mathscr{S} = \Lambda^2$. Then without doing further intermediate coupling calculations, we can calculate the E1 matrix elements; they will depend on the $\Lambda_g(J)$ and on single particle radial integrals

$$I_{nl} = \int_0^\infty \phi_{nl}(r) r \phi_{1p}(r) \mathrm{d}r, \tag{14}$$

with

$$\int_0^\infty |\phi_{nl}(r)|^2 \mathrm{d}r = 1. \tag{15}$$

The γ-width of the state $J\pi$ is

$$\Gamma_{J\pi}(\gamma) = (\tfrac{4}{3})(E_\gamma/\hbar c)^3 e^2 |\langle J\pi \,||\mathrm{E1}||\tfrac{1}{2}\rangle|^2, \tag{16}$$

where

$$\langle J\pi||\mathrm{E1}||\tfrac{1}{2}\rangle = \sum_{Jj} C_{J\pi}(Jj)\langle (Jj)J \,||\mathrm{E1}||\tfrac{1}{2}\rangle \tag{17}$$

and the values of $\langle (Jj)J \,||\mathrm{E1}||\,\frac{1}{2}\rangle$ are given in table 4.

TABLE 4

Values of $\langle (Jj)J||\mathrm{E1}||\frac{1}{2}\rangle$

Jj \ J	$\frac{1}{2}$	$\frac{3}{2}$
$0\,\frac{1}{2}$	$-\frac{2}{13}\sqrt{3}\,\Lambda_g(0)I_{2s}$	
$0\,\frac{3}{2}$		$-\frac{2}{13}\sqrt{3}\,\Lambda_g(0)I_{1d}$
$2\,\frac{1}{2}$		$\frac{1}{13}\sqrt{6}\,\Lambda_g(2)I_{2s}$
$2\,\frac{3}{2}$	$\frac{2}{65}\sqrt{3}\,\Lambda_g(2)I_{1d}$	$\frac{2}{65}\sqrt{6}\,\Lambda_g(2)I_{1d}$
$2\,\frac{5}{2}$	$-\frac{12}{65}\sqrt{2}\,\Lambda_g(2)I_{1d}$	$-\frac{3}{65}\sqrt{14}\,\Lambda_g(2)I_{1d}$

Experimentally [4]) $\theta_g^2(2)/\theta_g^2(0) = 0.95$, 0.76 from C^{13}(p, d)C^{12}, C^{13}(d, t)C^{12} respectively, so we take the average value 0.86. Also [4]) $\theta_g^2(0) = 0.063$, 0.047 from C^{12}(d, p)C^{13}, with average 0.055. From fig. 55 of ref. [4]), $\theta_0^2(1p) \approx 0.078$ and 0.066 for neutron binding energies 4.95 and 9.38 MeV, respectively. These values lead to $|\Lambda_g(0)| = 0.84$ and $|\Lambda_g(2)| = 0.85$. Theoretically, most of the data involving the normal parity states of C^{13}, including their reduced widths to the C^{12} ground state, can be fitted [3]) with an intermediate coupling parameter $\zeta = 4.6$, then [4]), $\Lambda_g(0) = -0.83$ and $\Lambda_g(2) = 1.03$. In the calculations we use

$$\Lambda_g(0) = -0.83, \quad \Lambda_g(2) = 0.84 \tag{18}$$

and note the changes produced by taking $\Lambda_g(2) = 1.03$.

The radial integrals I_{nl} can be evaluated easily for harmonic oscillator wave functions, giving

$$I_{2s} = -a = -1.67 \text{ fm}, \quad I_{1d} = (\tfrac{5}{2})^{\frac{1}{2}} a = 2.64 \text{ fm}. \tag{19}$$

For the finite depth well (3), with $\alpha = 0.2$ and a adjusted to give the same mean-square radius of C^{13} as does an oscillator well with parameter 1.67 fm, we get values of I_{2s}, I_{1d} which are respectively 1.17 and 1.02 times the oscillator values.

TABLE 5

Calculated values of E1 matrix elements, γ-widths, integrated (γ, n) cross sections and peak (γ, n) cross sections for transitions from ground state of C^{13} to positive-parity states Jp

Jp	E_{Jp} (MeV)	$\langle Jp \Vert E1 \Vert \frac{1}{2} \rangle$ (fm)	$\Gamma_{Jp}(\gamma)$ (eV)	$\int \sigma_{Jp}(\gamma n) dE_\gamma$ (MeV · mb)	σ_{Jp}^{peak} (mb)
$\frac{1}{2}1$	3.08	−0.284	0.589		
$\frac{1}{2}2$	13.26	−0.634	234	4.08	1.20
$\frac{1}{2}3$	18.25	−0.055	4.6	0.050	0.005
$\frac{3}{2}1$	7.52	−0.080	0.71	0.067	0.89
$\frac{3}{2}2$	8.10	0.195	5.49	0.45	0.31
$\frac{3}{2}3$	12.59	0.642	206	7.95	2.13
$\frac{3}{2}4$	16.38	0.359	142	3.70	0.47

Values of $\langle Jp \Vert E1 \Vert \frac{1}{2} \rangle$ and of $\Gamma_{Jp}(\gamma)$ evaluated at $E_\gamma = E_{Jp}$ are given in table 5 for the values (18) and (19). The total photoneutron cross section due to the state Jp is

$$\begin{aligned} \sigma_{Jp}(\gamma n) &= \frac{2J+1}{4} \pi \left(\frac{\hbar c}{E_\gamma}\right)^2 \frac{\Gamma_{Jp}(\gamma)\Gamma_{Jp}}{(E_\gamma - E_{Jp} - \Delta_{Jp})^2 + \frac{1}{4}(\Gamma_{Jp})^2}, \\ &\approx \frac{2J+1}{4} \pi \left(\frac{\hbar c}{E_\gamma}\right)^2 \frac{\Gamma^0_{Jp}(\gamma)\Gamma^0_{Jp}}{(E_\gamma - E_{Jp})^2 + \frac{1}{4}(\Gamma^0_{Jp})^2}, \end{aligned} \tag{20}$$

where the observed γ-ray width is $\Gamma^0_{Jp}(\gamma) = \Gamma_{Jp}(\gamma)\Gamma^0_{Jp}/\Gamma_{Jp}$. If the variation of $\Gamma^0_{Jp}(\gamma)/E_\gamma^2$ across the level is neglected, and if Γ^0_{Jp} is taken as constant or proportional to $(E_\gamma - E_T)^{\frac{1}{2}}$, where E_T = threshold energy, as is the case for s-wave neutrons, then the integrated cross section for $E_{Jp} > E_T$ is

$$\int \sigma_{Jp}(\gamma n) dE_\gamma = \frac{2J+1}{2} \pi^2 (\hbar c/E_{Jp})^2 \Gamma^0_{Jp}(\gamma) \tag{21}$$

and the peak cross section is

$$\sigma_{Jp}^{peak} = (2/\pi)(\Gamma^0_{Jp})^{-1} \int \sigma_{Jp}(\gamma n) dE_\gamma. \tag{22}$$

Values of $\int \sigma_{J_p}(\gamma n)dE_\gamma$ and $\sigma_{J_p}^{peak}$ are also given in table 5. The cross sections for transitions to the C^{12} ground and first excited states are in the ratio of the partial neutron widths $[\Gamma_{J_p}(0s)+\Gamma_{J_p}(0d)] : [\Gamma_{J_p}(2s)+\Gamma_{J_p}(2d)]$, which are obtained from table 2.

For $\Lambda_g(2) = 1.03$ instead of 0.84, all cross sections are increased by factors ≈ 1.3, except those for states $\frac{3}{2}1$ and $\frac{3}{2}2$ which are multiplied by factors 2.4 and 0.5, respectively. These large changes are due to the large amounts of cancellation taking place in the matrix elements for these states. Use of radial integrals I_{nl} for the finite depth well (3) in place of the values (19) leaves all cross sections more or less unchanged except that for the $\frac{3}{2}1$ state, which is increased by a factor 2.2.

The cross sections given in table 5 may be compared with those measured by Cook [25]), who did not separate neutrons to different C^{12} states. Apart from the "giant resonance" peak at $E_\gamma \approx 22$ MeV, Cook found a "pigmy resonance" peak at $E_\gamma \approx 13.5$ MeV of width 5 MeV and peak height 3.3 mb, and a suggestion of a peak or plateau at $E_\gamma \approx 8$ MeV. The integrated cross section from 5 to 17 MeV was 20 MeV · mb. The calculated cross section, for the values (18) and (19), has a peak at 12.9 MeV of width 3 MeV and peak height 3.2 mb; the integrated cross section from 5 to 17 MeV is 13 MeV · mb. Increasing $\Lambda_g(2)$ to 1.03 increases the integrated cross section to 17 MeV · mb. Contributions from states excited by M1, E2, ... absorption are expected to be of order 1 MeV · mb or less, but some contribution may also come from E1 absorption into states of different structure from those we are considering. There is fair agreement between calculated and measured cross sections, with the former a little low. From table 1, it is seen that the energy of Cook's "pygmy resonance" fixes V_0 at about 50—60 MeV for the values of the other parameters given in (2). It is of interest that few of the neutrons emitted from the C^{13} giant resonance region should leave C^{12} in the ground or first excited state.

Preliminary measurements by the M.I.T. linear accelerator group (see ref. [26])) indicate an integrated cross section of about 0.2 MeV · mb for the $\frac{3}{2}1$ state and about the same or less for the $\frac{3}{2}2$ state. These agree better with the values obtained for $\Lambda_g(2) = 1.03$ rather than 0.84, and for the finite depth well rather than the oscillator well.

The angular distributions of the emitted neutrons may be calculated easily if interference between states is neglected. Then all neutrons from $\frac{1}{2}^+$ states are isotropic, ground state neutrons from $\frac{3}{2}^+$ states have a $1-0.60\cos^2\theta_{\gamma n}$ distribution, while excited state neutrons, assumed to be purely d-wave (see table 2), have distributions $1+0.16\cos^2\theta_{\gamma n}$ and $1+0.58\cos^2\theta_{\gamma n}$ for the $\frac{3}{2}3$ and $\frac{3}{2}4$ states, respectively.

3.5. OTHER ELECTROMAGNETIC TRANSITIONS

There are other experimental data involving E1 matrix elements. These include the E1 widths of the first and second excited states of N^{13}, the branching

ratio of the γ-rays from the second excited state of C^{13} to the ground and first excited states, the thermal-neutron capture cross section for the reaction $C^{12}(n, \gamma)C^{13}$ going to the ground and second excited states of C^{13}, and the $C^{13}(\gamma, n)C^{12}$ cross section for 6—7 MeV γ-rays. We find that the usual shell-model treatment does not give good agreement with any of these.

The measured E1 widths in N^{13} are [12]) $\Gamma^0_{\frac{1}{2}^+\to\frac{1}{2}^-}(\gamma) = 0.67$ eV, $\Gamma^0_{\frac{1}{2}^-\to\frac{1}{2}^+}(\gamma) = 0.04$ eV. In order to calculate the radiative width of the $\frac{3}{2}^-$ state in intermediate coupling we need the value of $\Lambda_e(0) = \theta_e(0)/\theta_0(1p)$, where $\theta_e^2(0)$ is the dimensionless reduced width for emission of a 1p-neutron from the $\frac{3}{2}^-$ state of C^{13} to the ground state of C^{12}; the same wave functions are assumed for C^{13} and N^{13} states. This suffices to calculate the E1 matrix element which connects the $\frac{3}{2}^-$ state with the part of the $\frac{1}{2}^+$ state having C^{12} ground state as core. For the part having C^{12} excited state as core, the matrix element cannot be written in terms of reduced widths and an actual intermediate coupling calculation would be necessary; as this part of the $\frac{1}{2}1$ state is small (table 1), we have evaluated this contribution to the matrix element in the L-S coupling limit. From the C^{12}(d, p)C^{13} reaction [4]), $|\Lambda_e(0)/\Lambda_g(0)|^2 = 0.31$, 0.19 with average 0.25. An intermediate coupling calculation [4]) with $\zeta = 4.6$ also gives $|\Lambda_e(0)/\Lambda_g(0)|^2 = 0.25$, and determines the sign of $\Lambda_e(0)$; then $\Lambda_e(0) = -0.42$. Using also the values (18) and (19), we calculate $\Gamma_{\frac{1}{2}^+\to\frac{1}{2}^-}(\gamma) = 0.27$ eV, $\Gamma_{\frac{1}{2}^-\to\frac{1}{2}^+}(\gamma) = 0.0047$ eV and the observed widths $\Gamma^0_{\frac{1}{2}^+\to\frac{1}{2}^-}(\gamma) = 0.13$ eV, $\Gamma^0_{\frac{1}{2}^-\to\frac{1}{2}^+}(\gamma) = 0.0046$ eV.

The measured branching ratio of the E1 and (M1+E2) transitions from the $\frac{3}{2}^-$ second excited state of C^{13} to the $\frac{1}{2}^+$ first excited state and the $\frac{1}{2}^-$ ground state is [27]) $\Gamma^0_{\frac{3}{2}^-\to\frac{1}{2}^+}(\gamma)/\Gamma^0_{\frac{3}{2}^-\to\frac{1}{2}^-}(\gamma) = (7\pm1)\times10^{-3}$, and this is also the ratio of the true widths Γ. The calculated E2 contribution to the $\frac{3}{2}^- \to \frac{1}{2}^-$ transition vanishes. The M1 width in intermediate coupling is [28]) $\Gamma_{\frac{3}{2}^-\to\frac{1}{2}^-}(\gamma) = 0.60$ eV. The reduced matrix element for the E1 transition is the same as in the corresponding N^{13} transition above, and $\Gamma_{\frac{3}{2}^-\to\frac{1}{2}^+}(\gamma) = 0.00066$ eV, giving $\Gamma^0_{\frac{3}{2}^-\to\frac{1}{2}^+}(\gamma)/\Gamma^0_{\frac{3}{2}^-\to\frac{1}{2}^-}(\gamma) = 1.1\times10^{-3}$.

The capture cross section of C^{12} for thermal neutrons is 3.3 mb, with 0.3 of the γ-rays probably going to the $\frac{3}{2}^-$ second excited state of C^{13} and the remainder to the $\frac{1}{2}^-$ ground state [12]), giving $\sigma_g(n\gamma) = 2.3$ mb, and $\sigma_e(n\gamma) = 1.0$ mb. We can assume that only s-wave neutrons are captured into the tail of the $\frac{1}{2}1$ state. Taking $E_n = 0.025$ eV and allowing for the level shift, we calculate $\sigma_g(n\gamma) = 2.0$ mb and $\sigma_e(n\gamma) = 0.011$ mb.

Edge [29]) measured the cross section for $C^{13}(\gamma, n)C^{12}$ for γ-rays from the F^{19}+p reaction, with γ-energies 6.1 MeV (65 %), 6.9 MeV (24 %) and 7.1 MeV (11 %), and obtained $\sigma(\gamma n) = (94\pm10)\mu$b. At these energies we expect contributions from the $\frac{1}{2}1$ and $\frac{3}{2}2$ states, but not from the $\frac{3}{2}1$ state as it is very narrow. The calculated contributions are 6μb from the $\frac{1}{2}1$ state and 7μb from the $\frac{3}{2}2$ state.

The reason for the discrepancies found between calculated and measured quantities in each of the above cases is discussed in subsect. 3.6. In the case of the branching ratios of the three γ-transitions from the $\frac{5}{2}^+$ state of C^{13} at 3.85 MeV, the calculation also disagrees with measurement, but we attribute this to a different cause. The measured branching ratios of the (M2+E3) transition to the $\frac{1}{2}^-$ ground state, the E1 transition to the $\frac{3}{2}^-$ excited state at 3.68 MeV and the E2 transition to the $\frac{1}{2}^+$ excited state at 3.08 MeV are [30])

$$\Gamma^0_{\frac{1}{2}^+\to\frac{1}{2}^-}(\gamma) : \Gamma^0_{\frac{1}{2}^+\to\frac{3}{2}^-}(\gamma) : \Gamma^0_{\frac{1}{2}^+\to\frac{1}{2}^+}(\gamma) = 0.76 : 0.24 : 0.0093.$$

The true widths Γ are in the same ratio as the observed widths Γ^0. In calculating the widths, centre-of-mass corrections are neglected except for the E1 transition. Then the E3 contribution to the $\frac{5}{2}^+ \to \frac{1}{2}^-$ transition vanishes. The M2 contribution gives $\Gamma_{\frac{1}{2}^+\to\frac{1}{2}^-}(\gamma) = 5.9\times10^{-5}$ eV for the values (18) and (19), corresponding to $|M|^2 = 0.84$ in Weisskopf units [31]). The E1 width cannot be simply obtained in intermediate coupling, as the E1 matrix element cannot be expressed in terms of reduced widths. In the L-S coupling limit, the E1 matrix element for the $\frac{5}{2}^+ \to \frac{3}{2}^-$ transition is a simple multiple of the M2 matrix element for the $\frac{5}{2}^+ \to \frac{1}{2}^-$ transition, giving a ratio $\Gamma_{\frac{1}{2}^+\to\frac{3}{2}^-}(\gamma)/\Gamma_{\frac{1}{2}^+\to\frac{1}{2}^-}(\gamma) = 3.0$, compared with the experimental ratio 0.32. In intermediate coupling, $\Gamma_{\frac{1}{2}^+\to\frac{1}{2}^-}(\gamma)$ is increased by a factor 6, so that to fit experiment $\Gamma_{\frac{1}{2}^+\to\frac{3}{2}^-}(\gamma)$ must be reduced by a factor 0.6. This is not unlikely, but we have not actually calculated $\Gamma_{\frac{1}{2}^+\to\frac{3}{2}^-}(\gamma)$. The calculated $\Gamma_{\frac{1}{2}^+\to\frac{1}{2}^-}(\gamma)$ and the measured branching ratio require $\Gamma_{\frac{1}{2}^+\to\frac{1}{2}^+}(\gamma) = 7.2\times10^{-7}$ eV. The calculated width for the $\frac{5}{2}^+ \to \frac{1}{2}^+$ transition can be expressed in terms of the width of the E2 transition from the first excited state of C^{12} to the ground state and the quadrupole moment of the first excited state. As the latter is not known experimentally, and as the contribution to $\Gamma_{\frac{1}{2}^+\to\frac{1}{2}^+}(\gamma)$ depending on it is probably small, we neglect this contribution and obtain $\Gamma_{\frac{1}{2}^+\to\frac{1}{2}^+}(\gamma) =$ $= 4.5\times10^{-8}$ eV, based on an E2 width of 0.010 eV for the C^{12} transition [32]). This is smaller than the required value by a factor 0.06. Inclusion of the contribution from the quadrupole moment of the C^{12} 2^+ state is not likely to improve the agreement, as in the L-S coupling limit it causes the calculated width to be reduced by a factor 0.55.

Thus we must account for the E2 width in some other way. We note that there are E2 transitions observed between the first excited and ground states of N^{16} and O^{17}, and on a simple picture these states have wave functions similar to those of the states involved in the C^{13} E2 transition. The measured lifetimes [33,34]) give widths $\Gamma^0_{0^-\to2^-}(\gamma) = 8.4\times10^{-11}$ eV, $\Gamma^0_{\frac{1}{2}^+\to\frac{1}{2}^+}(\gamma) = 2.6\times10^{-6}$ eV and reduced matrix elements $[E_\gamma^{-5}\,\Gamma^0(\gamma)]^{\frac{1}{2}} = 1.8\times10^{-6}\,\mathrm{MeV}^{-2}$, $2.3\times10^{-6}\,\mathrm{MeV}^{-2}$ for N^{16}, O^{17}, respectively. The C^{13} width $\Gamma_{\frac{1}{2}^+\to\frac{1}{2}^+}(\gamma) = 7.2\times10^{-7}$ eV corresponds to $\Gamma^0_{\frac{1}{2}^+\to\frac{1}{2}^+}(\gamma) = 5.2\times10^{-7}$ eV and a reduced matrix element, for the $\frac{1}{2}^+ \to \frac{5}{2}^+$ transition, of 2.4×10^{-6} MeV^{-2}. This is very close to the N^{16},

O^{17} values, suggesting that the E2 transitions in all three nuclei are due to the same mechanism. This presumably involves a distortion of the core by the odd neutron [35]), the distortions being comparable for the three cores C^{12}, N^{15} and O^{16}. Such distortions are probably too small to effect nuclear properties other than E2 matrix elements [36]).

3.6. USE OF SINGLE-PARTICLE WAVE FUNCTIONS WITH CORRECT ASYMPTOTIC FORM

The single-particle wave functions used so far have been those for a potential well, either harmonic oscillator or finite-depth (3). These may be suitable when the main contribution to a matrix element comes from the wave function inside the well, as is probably the case for matrix elements of the Hamiltonian, but when the main contributions come from near the edge of the well or outside, say for $r \gtrsim a_c$, then large errors may result. This is because the wave functions in the interior region should smoothly fit on at $r = a_c$ to the asymptotic wave functions, which depend on the type of particle (neutron or proton) and its binding energy in the actual system under consideration. In the shell model, however, the same single-particle wave functions are used for nuclear states at all energies. This difficulty has been discussed by Lane [1]).

The shell model can be modified for certain of the states we have been considering to allow for this difficulty. These are the C^{13} positive-parity states which consist predominately of the neutron in a definite state and the core in a definite state, as for these the core can be replaced fairly accurately by a potential well in which the neutron moves. Thus the lowest $\frac{1}{2}^+$ and $\frac{5}{2}^+$ states, which are mainly C^{12} ground state plus $2s_{\frac{1}{2}}$ or $1d_{\frac{3}{2}}$ nucleons, have been treated in this way by Lane [3, 37]), who fits all data involving these states in C^{13} and N^{13} by use of a square potential well of depth 35 MeV and radius 4.05 fm. Also Frances *et al.*[38]) have calculated the E1 matrix elements involving the $\frac{1}{2}1$ and $\frac{3}{2}2$ states of C^{13} using such wave functions, but for a potential well with a diffuse boundary.

In order to estimate the effect of changing the single-particle wave functions to fit the appropriate boundary conditions, we have calculated $2s_{\frac{1}{2}}$, $1d_{\frac{3}{2}}$ and $1d_{\frac{5}{2}}$ wave functions for neutrons in a square well central potential plus a Thomas type spin-orbit interaction (δ-function at edge of square well). The radius of the well was fixed at $R = 4.05$ fm. For s-neutrons, the depth of the well was adjusted to fit the binding energy of the lowest $\frac{1}{2}^+$ state. For d-neutrons, the depth of the well and the strength of the spin-orbit interaction were adjusted to fit the binding energy of the lowest $\frac{5}{2}^+$ state and to make the $d_{\frac{3}{2}}$ phase shift pass through 90° at a neutron energy [20]) of about 3.7 MeV. For the $\frac{1}{2}^-$ and $\frac{3}{2}^-$ states, we have used p-neutrons in square wells of the same radius, with the depths chosen to fit the observed binding energies; this model is not supposed to be a good description of these states but provides single-particle wave functions with the correct asymptotic form.

The dimensionless single-particle reduced widths calculated with these wave functions for C^{13} are shown † in fig. 1. The notation $\theta_0^2(nl)$ now has to be

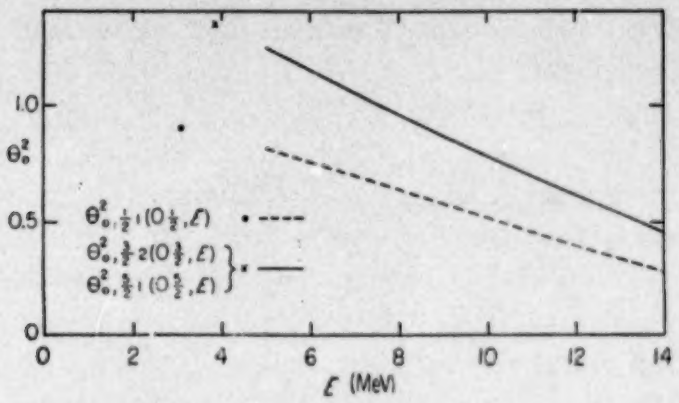

Fig. 1. Dimensionless single-particle reduced widths $\theta^2_{0,Jp}(Jj, E)$ as functions of excitation energy E in C^{13}, for single-particle wave functions with correct asymptotic form.

replaced by $\theta^2_{0,Jp}(Jj, E)$, where E is the excitation energy in C^{13}. For protons from a state of N^{13}, the reduced width is roughly the same as that for neutrons from the corresponding C^{13} state at the same excitation energy. We might similarly estimate the other $\theta^2_{0,Jp}(Jj, E)$ for which $|C_{Jp}(Jj)|^2 \approx 1$, but values cannot be obtained in this way for the $\theta^2_{0,Jp}(Jj, E)$ for which $|C_{Jp}(Jj)|^2 \ll 1$.

The only use we make of these reduced width estimates is to assume that for a given state the reduced width corresponding to the main component decreases as the energy increases across the state. Thus is subsect. 3.3 we assumed that $\theta_0^2(2s)$ which was fitted as 0.44 for the $\frac{1}{2}1$ state at 4.95 MeV excitation had increased to 0.5 at 3.08 MeV excitation. Then for the peak of the $\frac{1}{2}1$ state in N^{13} it would be estimated as 0.53, much less than the value 0.84 required to fit the experimental width. Apparently this discrepancy can be removed by using a channel radius $a_c = R = 4.05$ fm, as was done by Lane [37]), instead of $a_c = 4.77$ fm which we have used. This change in the value of a_c also reconciles to a large extent the values of $\theta_0^2(1d)$ required for the $\frac{5}{2}1$ state of N^{13} and the $\frac{3}{2}2$ state of C^{13}. Thus a channel radius of 4.05 fm seems a better value for the (C^{12}+nucleon) system than that given by the usual formula $1.45(A_1^{\frac{1}{3}}+A_2^{\frac{1}{3}})$ fm.

With these same wave functions, we can also calculate the radial integrals $I_{nl} \equiv I_{Jp}(Jj, J', E)$, where J' is the spin of the negative-parity state. For bound positive-parity states the wave functions are normalized as in (15), for states of the continuum [19])

$$\int_0^R |\phi_{nl}(r)|^2 dr = 1.$$

Apart from the change due to this different normalization, the contributions

† This diagram is of different type from that given by Macfarlane and French [4]) in their fig. 60. There is also a difference as they used $\theta_0^2(c) = a_c|\phi_c(a_c)|^2/2\int_0^\infty|\phi_c(r)|^2dr$ in place of (9).

to the radial integrals from the internal region ($r < R$) are more or less independent of energy, for given initial and final states, whereas the external contributions depend strongly on energy [19]). Values of some of the radial integrals I for C^{13} states are given in fig. 2. It is seen that, at the energies

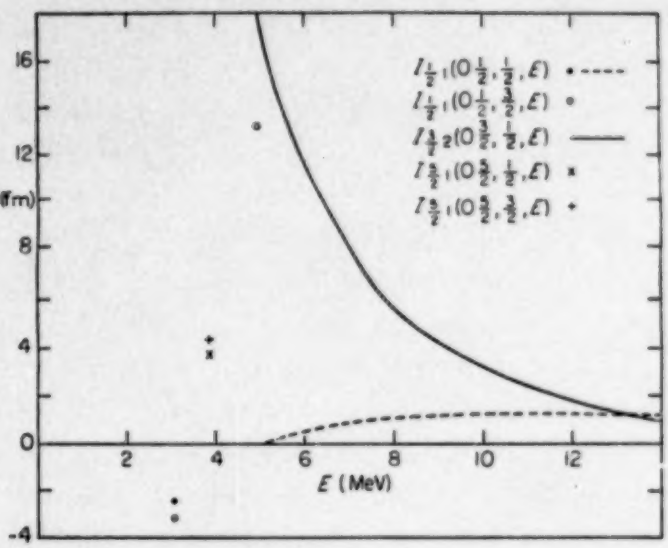

Fig. 2. Radial integrals $I_{Jp}(Jj, J', E)$ occurring in E1 matrix elements as functions of excitation energy E in C^{13}, for single-particle wave functions with correct asymptotic form.

of the $\frac{1}{2}1$, $\frac{5}{2}1$ and $\frac{3}{2}2$ states, the calculated values are respectively about 1.4, 1.4, and 1.9 times the oscillator values (19). Some increase in the latter values might be desirable in order to explain the integrated cross section of Cook's pygmy resonance, but a factor 1.4 is too large. Suppose we use radial integrals which are 1.2 times the oscillator values for calculating widths involving only the C^{13} ground state and the C^{13} positive-parity states at their peaks. Then the γ-widths and cross sections given in subsect. 3.4 and table 5 are increased by a factor 1.44 and approximate agreement is obtained with Cook's integrated cross section.

The E1 widths calculated in subsect. 3.5, which involve N^{13} states or the tails of C^{13} states, should also be altered to allow for the dependence shown in fig. 2 of the radial integrals I on E and on the binding energy of the negative-parity state. Only the values of the I relating to the main component of the positive-parity state are changed, i.e. only the $I_{Jp}(Jj, J', E)$ for which $|C_{Jp}(Jj)|^2 \approx 1$. As we do not take the actual values in fig. 2 too seriously, we mostly calculate the values of I required to fit the experimental data and then see if such values are reasonable; in the comparison the values from fig. 2 are divided by factors 1.2 for bound states and 1.6 for continuum states.

In the first case from subsect. 3.5, involving the E1 widths in N^{13}, the experimental values are fitted with $I_{\frac{1}{2}1}(0\frac{1}{2}, \frac{1}{2}, E) = -3.6$ fm or 2.7 fm and $I_{\frac{1}{2}1}(0\frac{1}{2}, \frac{3}{2}, E) = -3.8$ fm or 2.2 fm (in this paragraph, $E = 2.36$ MeV, the

excitation energy of the $\frac{1}{2}1$ state in N^{13}. We have not calculated any proton wave functions in square well potentials but from the calculations of Thomas [19]) the negative choice for $I_{\frac{1}{2}1}(0\frac{1}{2}, \frac{1}{2}, E)$ seems reasonable. If we take the values corresponding † to Region II of Thomas's fig. 6, then the internal and external contributions to $I_{\frac{1}{2}1}(0\frac{1}{2}, \frac{1}{2}, E)$ are of the same sign and in the ratio 1 : 3.5, which with our calculations implies $I_{\frac{1}{2}1}(0\frac{1}{2}, \frac{1}{2}, E) = -3.2$. $I_{\frac{1}{2}1}(0\frac{1}{2}, \frac{3}{2}, E)$ is expected to be somewhat more negative.

To obtain the experimental branching ratio of γ-transitions from the $\frac{3}{2}^-$ state of C^{13}, we require $I_{\frac{1}{2}1}(0\frac{1}{2}, \frac{3}{2}, 3.08\ \text{MeV}) = -3.3$ fm or 1.8 fm. The expected value from fig. 2 is -2.7 fm.

The thermal neutron capture cross section of C^{12} can be fitted with $I_{\frac{1}{2}1}(0\frac{1}{2}, \frac{1}{2}, 4.95\ \text{MeV}) = -1.8$ fm or 0.9 fm and $I_{\frac{1}{2}1}(0\frac{1}{2}, \frac{3}{2}, 4.95\ \text{MeV}) = -10.6$ fm or 9.0 fm. From fig. 2 the expected values are 0.0 fm and 8.2 fm respectively. A positive value of $I_{\frac{1}{2}1}(0\frac{1}{2}, \frac{1}{2}, 4.95\ \text{MeV})$ corresponds to Region II of Thomas's fig. 6, as the internal and external contributions are of opposite sign with the latter predominating; in our calculation they cancelled almost entirely.

We still assume that there are contributions from both the $\frac{1}{2}1$ and $\frac{3}{2}2$ states to the cross section measured by Edge. From fig. 2 and from the value required at $E = 4.95$ MeV, it seems that $I_{\frac{1}{2}1}(0\frac{1}{2}, \frac{1}{2}, 6\text{—}7\ \text{MeV})$ will be 1—2 fm. Then the contribution of the $\frac{1}{2}1$ state to the cross section is 8—22 μb. Thus we assume that the $\frac{3}{2}2$ state gives a contribution of about 80μb. Assuming $I_{\frac{1}{2}2}(0\frac{3}{2}, \frac{1}{2}, E)$ varies with E as in fig. 2, we then require $I_{\frac{1}{2}2}(0\frac{3}{2}, \frac{1}{2}, E) = \approx -3.9$ fm or 7.4 fm at the mean γ-ray energy $E \approx 6.4$ MeV. From fig. 2 we would expect $I_{\frac{1}{2}2}(0\frac{3}{2}, \frac{1}{2}, 6.4\ \text{MeV}) = 6.3$ fm.

The previous results for the γ-transitions from the $\frac{5}{2}^+$ state of C^{13} will not be changed significantly. The M2 transition is to the ground state, so the oscillator values of I_{nl} are to be multiplied by 1.2 and $\Gamma_{\frac{1}{2}^+ \to \frac{1}{2}^-}(\gamma)$ by 1.44. Then the required value of $\Gamma_{\frac{1}{2}^+ \to \frac{1}{2}^+}(\gamma)$ is also increased by a factor 1.44, and the corresponding reduced matrix element by a factor 1.2 to become 2.9×10^{-6} MeV^{-2}. This is still fairly close to the N^{16} and O^{17} values.

Thus it seems that, when certain of the single-particle wave functions are modified to have the correct asymptotic form, particularly in the calculation of E1 matrix elements, the present model can give agreement with all the experimental data involving the positive-parity states of C^{13} and some of the data on the N^{13} states. In order to obtain this agreement the channel radius may need to be taken smaller than the conventional value.

3.7. COMPARISON WITH OTHER CALCULATIONS

Calculations involving the positive-parity states of C^{13} have been made

† Thomas [19]) chose Region I as giving better results for the level displacement of corresponding N^{13} and C^{13} states, but Region II is required to give $|\Lambda_e(0)/\Lambda_g(0)| < 1$ as observed experimentally (see subsect. 3.5). We note that the absolute value of Thomas's θ_t is then fitted with $\theta_0^2(1\text{p}) \approx 0.22$.

by several authors [1, 19, 28, 37–39]). Some of these have been mentioned already. We now consider the results of some of the other calculations.

Frances *et al.* [38]) used a direct-interaction model to study the photoneutron disintegration of C^{13} up to a few MeV above threshold, including effectively only the $(0\frac{1}{2})\frac{1}{2}$ and $(0\frac{3}{2})\frac{1}{2}$ states. The C^{12} core was replaced by a diffuse-edge potential well plus a spin-orbit interaction. For a diffuseness parameter of 0.4 fm, they obtained cross sections about 3 times greater than those measured for $C^{13}(\gamma, n)\ C^{12}$ by Edge and for thermal neutron capture to the C^{13} ground state, and at the position of the $\frac{3}{2}2$ state ($E = 8.3$ MeV) they obtained a peak cross section for $C^{13}(\gamma, n)C^{12}$ of about 10 mb compared with our value of 0.31 mb (table 5). On the basis of our calculations, the cross sections of Frances *et al.* should be changed because the states involved are not purely of the type they assumed. Thus from the C^{13} ground state comes a factor $\Lambda_g(0)$ in the matrix element, which reduces all cross sections by a factor $|\Lambda_g(0)|^2 = 0.69$. Also the admixture of other components to the $(0\frac{3}{2})\frac{3}{2}$ main component in the $\frac{3}{2}2$ state reduces the E1 matrix element to the ground state by factors 0.58 and 0.33 at $E = 6.4$ and 8.3 MeV, respectively, whereas the similar admixture in the $\frac{1}{2}1$ state increases the E1 matrix element by a factor 1.44 at $E = 4.95$ MeV (assuming $I_{\frac{1}{2}1}(0\frac{1}{2}, \frac{1}{2}, 4.95\ \text{MeV}) > 0$; if $I < 0$, the factor is 0.75). Thus we estimate that the calculated cross sections of Frances *et al.* for $C^{13}(\gamma, n)C^{12}$ at $E = 6.4$ MeV and at $E = 8.3$ MeV, and for $C^{12}(n, \gamma)C^{13}$ for thermal neutrons, should be multiplied by factors 0.23, 0.075 and 1.43, respectively. For a diffuseness parameter 0.6 fm, Edge's measured cross section is then fitted, the cross section at the $\frac{3}{2}2$ peak is in rough agreement with our value, but the thermal-neutron cross section is too large by a factor 2.7. We conclude that the diffuse-edge potential well gives too large a value of $I_{\frac{1}{2}1}(0\frac{1}{2}, \frac{1}{2}, 4.95\ \text{MeV})$, while the square well gave too small a value.

The present model can be taken as a special case of the two-body cluster model of Phillips and Tombrello [39]). In an application of their model to the $\frac{5}{2}^+$ states of C^{13}, they used a restricted group of clusters (effectively the $(0\frac{5}{2})\frac{5}{2}$ and $(2\frac{1}{2})\frac{5}{2}$ basic states) and empirically obtained the mixing between them by fitting the binding energy of the $\frac{5}{2}1$ state and the width and position of the $\frac{5}{2}2$ state. In this way they obtained for the intensity of $(2\frac{1}{2})\frac{5}{2}$ component in the $\frac{5}{2}1$ state the value 0.014. From table 2, however, we see that this does not give a good idea of the part of the $\frac{5}{2}1$ state which has C^{12} excited state as parent, as this is present mainly in the $(2\frac{5}{2})\frac{5}{2}$ component.

We have obtained mixing of the basic states of the simplified Lane model [1]) by introducing a two-particle central interaction V^c and a spin-orbit interaction V^{so}. Kurath and Lawson [28]) have obtained mixing in an alternative way by using a weak coupling of the odd neutron to a deformed C^{12} core. With their coupling strength parameter $\xi \approx -1.0$, there is good agreement between the energies of the C^{13} positive-parity states which they calculate

and those given in table 2. The wave functions are similar but do not agree in detail; this is presumably because our interaction implies a coupling strength ξ depending on the state of the odd neutron.

4. Be^9 Positive Parity States

Similar calculations may be carried out for the positive-parity states of Be^9. The basic states are produced by addition of a 2s- or 1d-neutron to the 0^+ ground or 2^+ first excited state of Be^8, and so are still described by the set (1). A difference from the C^{13} case is that the Be^8 and Be^9 normal-parity states are expected to be close to the L-S coupling limit, as the intermediate-coupling parameter giving best fit to the Be^9 levels is [7, 40]) $\zeta \leqq 2.75$, compared with $\zeta = 4.6$ for C^{13}.

Little is known experimentally about the positive-parity states of Be^9, so the interaction parameters cannot be fitted in the same way as for C^{13}. We therefore use again the values (2) together with harmonic oscillator wave functions, which gave satisfactory results for the C^{13} states. An estimate for the value to be used for δ comes from interpreting the two lowest states of O^{17} as $1s^4\,1p^{12}\,1d_{\frac{5}{2}}$ and $1s^4\,1p^{12}\,2s_{\frac{1}{2}}$ which gives, for the interaction parameters (2), $\xi_{1d}+\delta = 1.28$ MeV. For C^{13} we had $\xi_{1d}+\delta = 3.25$ MeV, and so initially we take $\xi_{1d}+\delta = 5.22$ MeV for Be^9, or $\delta = 7.22$ MeV. With the lowest $\frac{1}{2}^+$ state normalized to 1.75 MeV, as observed [12]), we predict two other states below 6 MeV, a $\frac{3}{2}^+$ state at 4.88 MeV and a $\frac{5}{2}^+$ state at 4.05 MeV. In this energy range one also expects normal-parity states [7, 40]) $\frac{3}{2}^-$ (ground state), $\frac{1}{2}^-$ and $\frac{5}{2}^-$. There are excited states observed [12]) at 3.04 and 4.74 MeV, as well as the 2.43 MeV state which is fairly definitely $\frac{5}{2}^-$. We suggest that the $\frac{3}{2}^+$ state is at 4.74 MeV, while the $\frac{5}{2}^+$ and $\frac{1}{2}^-$ states are both in the neighbourhood of 3.04 MeV and have not been resolved. Actually the widths given for the 3.04 MeV peak vary considerably (see ref. [12])), from (0.425 ± 0.125) MeV (ref. [41])) to (0.161 ± 0.015) MeV (ref. [42])), with some evidence that the peak might be double [41]). Thus we tentatively locate the $\frac{5}{2}^+$ state at 3.04 MeV and adjust δ accordingly; this gives $\delta = 5.16$ MeV.

For this δ, the energies, eigenfunction coefficients, fractions of spurious state, neutron widths and (γ, n) cross sections are given in table 6. We take $a_c = 4.35$ fm and again $\theta_0^2(2s) = 0.5$ and $\theta_0^2(1d) = 0.8$. The effect of the finite width of the 2.9 MeV state of Be^8 on the neutron widths is neglected. Because the $\frac{1}{2}1$ and $\frac{3}{2}1$ states are just above threshold, the neutron widths derived for them are rather meaningless. For states above about 2.5 MeV, there will be contributions to the total widths from α-particle emission. A possibly unreliable estimate of these contributions suggests that they may be appreciable for the $\frac{1}{2}3$, $\frac{3}{2}2$, $\frac{5}{2}2$ and perhaps $\frac{5}{2}1$ states, however we neglect them.

TABLE 6

Calculated energies, eigenfunctions, fractions of spurious states, neutron widths, integrated (γ, n) cross sections and peak (γ, n) cross sections for Be^9 positive-parity states

$J\pi$	$E_{J\pi}$ (MeV)	$C_{J\pi}(Jl)$	F_s	$\Gamma_{J\pi}(Jl)$ (MeV)				$\Gamma^0_{J\pi}$ (MeV)	$\int\sigma_{J\pi}(\gamma n)dE_\gamma$ (MeV · mb)	$\sigma^{peak}_{J\pi}$ (mb)
				0s	0d	2s	2d			
$\frac{1}{2}$ 1	1.75	0.906, 0.162, 0.390	0.044	(0.56)			0	(0.53)	0.75	(0.91)
$\frac{1}{2}$ 2	6.63	0.401, −0.042, −0.915	0.225	0.80			0.69	1.03	1.04	0.64
$\frac{1}{2}$ 3	11.53	0.132, −0.986, 0.102	0.175	0.12			5.12	4.55	1.22	0.17
$\frac{3}{2}$ 1	4.84	0.320, −0.876, 0.149, −0.328	0.063		0.18	(0.94)	0.00	(1.00)	0.001	(0.001)
$\frac{3}{2}$ 2	7.33	0.249, 0.398, −0.116, −0.875	0.189		0.25	0.59	1.13	1.44	0.89	0.39
$\frac{3}{2}$ 3	9.57	0.785, 0.264, 0.485, 0.280	0.161		3.69	0.35	1.11	4.46	0.02	0.003
$\frac{3}{2}$ 4	15.17	0.467, −0.057, −0.854, 0.220	0.262		2.11	0.02	6.13	7.71	0.61	0.05
$\frac{5}{2}$ 1	3.04	0.769, 0.486, 0.117, 0.399	0.030		0.23	0	0	0.15	0.14	0.59
$\frac{5}{2}$ 2	6.30	0.489, −0.865, 0.023, 0.106	0.207		0.75	2.17	0.01	2.73	3.38	0.79
$\frac{5}{2}$ 3	10.65	0.393, 0.112, 0.056, −0.911	0.259		1.05	0.07	3.70	4.11	3.66	0.57
$\frac{5}{2}$ 4	15.10	0.124, 0.043, −0.991, −0.001	0.218		0.15	0.01	7.66	7.24	0.64	0.06
$\frac{7}{2}$ 1	9.30	0.380, −0.925	0.145				3.29	2.59		
$\frac{7}{2}$ 2	12.34	0.925, 0.380	0.124				5.86	5.19		
$\frac{9}{2}$ 1	6.54	1.000	0.063				0.79	0.51		

We consider the widths of the states we are locating at 3.04 MeV. The $\frac{5}{2}^+$ state is calculated to have a width of 0.15 MeV. In the *L-S* coupling limit, the dimensionless reduced width of the $\frac{1}{2}^-$ state for neutron emission to the Be^8 ground state is $\frac{2}{3}\theta_0^2(1p)$, and this does not change much in the intermediate-coupling region of interest [40]). Lane [1]) took $\theta_0^2(1p) = 0.6$. For the finite depth well (3) with $\alpha = 0.2$, $\theta_0^2(1p) = 0.08$, while for neutrons of zero binding energy in the square well used in the C^{13} calculations, $\theta_0^2(1p) = 0.16$. We assume $\theta_0^2(1p) = 0.2$, which we also used for the 7.42 MeV state of N^{13} (subsect. 3.1) and for the ground state of N^{13} (subsect. 3.6), and obtain for the width of the $\frac{1}{2}^-$ state $\Gamma^0 = 0.34$ MeV. Thus both the $\frac{1}{2}^-$ and $\frac{5}{2}^+$ states are calculated to have widths of the order of what is observed for the 3.04 MeV peak, so that either or both may be present in that region.

The photodisintegration cross sections of Be^9 due to E1 absorption may be calculated as for C^{13}. As the ground state of Be^9 has spin $\frac{3}{2}^-$, the E1 matrix elements do not depend on the degree of intermediate coupling only through reduced widths; to avoid an intermediate-coupling calculation we use wave functions in the *L-S* coupling limit which should be fairly accurate. The radial integrals I_{nl} are expected to have different values for Be^9 than for C^{13}, mainly because of the different binding energies of the states. Calculations similar to those in subsect. 3.6, using square well potentials with radius 4.13 fm, lead to the following values of I_{nl} evaluated at the positions of the states (they are taken for $2s_{\frac{1}{2}}$, $1d_{\frac{3}{2}}$ and $1d_{\frac{5}{2}}$ neutrons at 0, 6.2 and 1.4 MeV above the separation energies):

Be^8 ground state core:

$$I_{2s_{\frac{1}{2}}} = -8.80 \text{ fm}, \quad I_{1d_{\frac{3}{2}}} = 3.51 \text{ fm}, \quad I_{1d_{\frac{5}{2}}} = 6.57 \text{ fm},$$

Be^8 excited state core: (23)

$$I_{2s_{\frac{1}{2}}} = -5.22 \text{ fm}, \quad I_{1d_{\frac{3}{2}}} = 4.02 \text{ fm}, \quad I_{1d_{\frac{5}{2}}} = 6.13 \text{ fm}.$$

From the C^{13} calculations, we expect these to be overestimates by factors of order $1.6 \times (4.13/4.05) \times (1.67/1.56) = 1.75$, since these are all continuum states and since the oscillator length parameter for Be^9 determined from electron scattering [5]) is $a = 1.56$ fm. The measured $Be^9(\gamma, n)$ cross section in the neighbourhood of the 1.75 MeV peak [43]) can be fitted with our $\frac{1}{2}1$ state wave function using $I_{2s_{\frac{1}{2}}} = -4.22$ fm or -5.43 fm, corresponding to different choices of $\bar{E}_{\frac{1}{2}1}$ in (20). We take the first choice and use values of I_{nl} which are the values (23) divided by 2.09; for the other choice, all cross sections (except for the $\frac{1}{2}1$ state) are larger by a factor 1.66. Values of $\int \sigma_{Jp}(\gamma n) dE_\gamma$ and σ_{Jp}^{peak} are given in table 6. The cross sections σ_g and σ_e for transitions to the Be^8 ground and first excited states are in the ratio of the partial neutron widths. As α-decay is neglected, the neutron cross sections are overestimates;

there is experimental evidence [44]) that α-decay may contribute neraly half the total cross section for $E_\gamma \approx 6$—7 MeV.

The M.I.T. linear accelerator group [26, 45]) has made measurements of σ_g and σ_e for E_γ from 2.5 to 17 MeV and $\theta_{\gamma n} = 115°$. If isotropy is assumed, σ_g shows a peak at 3 MeV of width 0.2 MeV and $\int \sigma_g dE_\gamma \approx 0.2$ MeV · mb, then a broad hump between 5 and 12 MeV and a shallow minimum at 13 MeV; this gives $\int_{5\ \mathrm{MeV}}^{13\ \mathrm{MeV}} \sigma_g dE_\gamma \approx 3.3$ MeV · mb. The cross section σ_e rises steeply from zero at 6 MeV to a sharp peak of 1.0 mb at 7 MeV, is fairly constant at 0.8 mb up to 10 MeV, has a sharp peak at 12 MeV superimposed on a rapid fall, and rises again above 13 MeV; the integrated cross-section is $\int_{6\ \mathrm{MeV}}^{13\ \mathrm{MeV}} \sigma_e dE_\gamma \approx 4.5$ MeV · mb.

Regarding the 3 MeV peak, the predicted contribution of the $\frac{5}{2}1$ state to $\int \sigma_g dE_\gamma$ is 0.14 MeV · mb, but the E1 matrix element is small because of cancellation and so could be changed appreciably by changes in the values of the I_{nl} and departure from the L-S coupling limit. The $\frac{1}{2}^-$ state at this energy is calculated to give an integrated cross section ≈ 0.17 MeV · mb for the intermediate-coupling region of interest. When allowance is made for the unknown amount of α-decay, either or both of these states could be contributing and giving the observed peak.

The other general features of the measured σ_g are predicted, with the main contributions coming from the $\frac{1}{2}2$, $\frac{5}{2}2$ and $\frac{5}{2}3$ states in the neighbourhoods of 6 and 10 MeV, however $\int_{5\ \mathrm{MeV}}^{13\ \mathrm{MeV}} \sigma_g dE_\gamma \approx 2.3$ MeV · mb, the deficiency being in the 10 MeV region. On the other hand we have $\int_{6\ \mathrm{MeV}}^{13\ \mathrm{MeV}} \sigma_e dE_\gamma \approx 7.5$ MeV · mb, which is reasonable, but we do not get the steep rise at 6 MeV nor the narrow peaks at 7 and 12 MeV. These peaks could well be due to M1 absorption into negative-parity states [12, 26]). The most direct way of increasing the predicted σ_g near 10 MeV, without affecting σ_e, would be by increasing the contribution from the $\frac{3}{2}3$ state, which is mainly Be^8 ground state plus a $d_{\frac{3}{2}}$ neutron, however to make the E1 matrix element large enough would probably require rather drastic changes in the I_{nl} values.

The angular distributions of the emitted neutrons may be calculated if we neglect interference between states. All neutrons from $\frac{1}{2}^+$ states are isotropic. The angular distributions for neutrons to the Be^8 ground state from $\frac{3}{2}^+$, $\frac{5}{2}^+$ states are respectively $1+0.75\cos^2\theta_{\gamma n}$, $1-0.50\cos^2\theta_{\gamma n}$. For neutrons to the Be^8 excited state, the distributions are approximately isotropic for those states ($\frac{3}{2}1$, $\frac{5}{2}2$) which emit mainly s-wave neutrons, while for those ($\frac{3}{2}4$, $\frac{5}{2}3$, $\frac{5}{2}4$) emitting mainly d-wave neutrons we get $1-0.24\cos^2\theta_{\gamma n}$, $1-0.08\cos^2\theta_{\gamma n}$, $1+0.06\cos^2\theta_{\gamma n}$ respectively; for the $\frac{3}{2}2$, $\frac{3}{2}3$ states both s- and d- neutrons are emitted appreciably and the angular distributions depend on relative penetrability and phase factors for s- and d- waves. The angular distribution of neutrons from the 3 MeV peak has an isotropic contribution from the $\frac{1}{2}^-$ state and a $1-0.50\cos^2\theta_{\gamma n}$ contribution from the $\frac{5}{2}^+$ state, with

no contribution due to interference. Measurements of the angular distribution in this region are being made by the M.I.T. linear accelerator group [26]). A measurement at $E_\gamma = 2.76$ MeV gave a $1-0.45\cos^2\theta_{\gamma n}$ distribution [46]).

Note added in proof: M. J. Jacobson [Phys. Rev. **123** (1961) 229] has obtained a $1-0.5\cos^2\theta_{\gamma n}$ distribution for neutrons from the 3 MeV peak, suggesting a $\frac{5}{2}^+$ assignment. Jacobson's 4.6 MeV peak is presumably due to the $\frac{3}{2}1$ state, and is a further indication of the need for change in the I_{nl} values.

The author is indebted to the members of the M.I.T. linear accelerator group [26]) for information on their results, for both C^{13} and Be^9, and for several helpful discussions, to N. M. Nikolic for a discussion on the nature of the 7.18 and 7.42 MeV states of N^{13} and to D. Kurath for making available a preprint of his paper with R. D. Lawson.

References

1) A. M. Lane, Revs. Mod. Phys. **32** (1960) 519
2) E. C. Halbert and J. B. French, Phys. Rev. **105** (1957) 1563
3) A. M. Lane, Proc. Phys. Soc. **68** (1955) 197
4) M. H. Macfarlane and J. B. French, Revs. Mod. Phys. **32** (1960) 567
5) R. Hofstadter, Ann. Rev. Nucl. Sci. **7** (1957) 231
6) D. R. Inglis, Revs. Mod. Phys. **25** (1953) 390
7) D. Kurath, Phys. Rev. **101** (1956) 216
8) J. P. Elliott and B. H. Flowers, Proc. Roy. Soc. **229** (1955) 536
9) J. P. Elliott and B. H. Flowers, Proc. Roy. Soc. **242** (1957) 57
10) J. M. Soper, Phil. Mag. **2** (1957) 1219;
I. S. Grant, Proc. Phys. Soc. **76** (1960) 737
11) F. C. Barker, Phys. Rev. **122** (1961) 572
12) F. Ajzenberg-Selove and T. Lauritsen, Nuclear Physics **11** (1959) 1
13) Lidofsky, Weil, Bent and Jones, Bull. Am. Phys. Soc. **2** (1957) 29
14) Young, Phillips, Spencer and Rao, Phys. Rev. **116** (1959) 962
15) Nikolic, Lidofsky and Kruse, Bull. Am. Phys. Soc. **6** (1961) 25
16) J. P. Elliott and T. H. R. Skyrme, Proc. Roy. Soc. **232** (1955) 561
17) O. M. Bilaniuk and J. B. French, Nuclear Physics **17** (1960) 435
18) A. M. Lane and R. G. Thomas, Revs. Mod. Phys. **30** (1958) 257
19) R. G. Thomas, Phys. Rev. **88** (1952) 1109
20) Wills, Bair, Cohn and Willard, Phys. Rev. **109** (1958) 891
21) H. L. Jackson and A. I. Galonsky, Phys. Rev. **89** (1953) 370
22) Reich, Phillips and Russell, Phys. Rev. **104** (1956) 143
23) H. Schneider, Helv. Phys. Acta **29** (1956) 55
24) Maeder, Martin, Müller and Schneider, Helv. Phys. Acta **27** (1954) 166
25) B. C. Cook, Phys. Rev. **106** (1957) 300
26) W. Bertozzi, P. T. Demos, C. P. Sargent, W. E. Turchinetz, D. B. McConnell and S. B. Kowalski, Contributions to Karlsruhe Photonuclear Conference 1960, R 15
27) D. H. Wilkinson, quoted in ref. [28])
28) D. Kurath and R. D. Lawson, Nuclear Physics **23** (1961) 5
29) R. D. Edge, Phys. Rev. **119** (1960) 1643
30) Pixley, Kane and Wilkinson, Phys. Rev. **120** (1960) 943

31) D. H. Wilkinson, in Nuclear Spectroscopy, ed. by F. Ajzenberg-Selove (Academic Press, New York, 1960) part B, p. 852
32) Rasmussen, Metzger and Swann, Phys. Rev. **110** (1958) 154
33) W. Zimmerman, Phys. Rev. **114** (1959) 867
34) Kane, Pixley, Schwartz and Schwarzschild, Phys. Rev. **120** (1960) 162
35) B. J. Raz, Phys. Rev. **120** (1960) 169 and references given there
36) F. C. Barker, Phil. Mag. **1** (1956) 329
37) A. M. Lane, Phys. Rev. **92** (1953) 839
38) Frances, Goldman and Guth, Phys. Rev. **120** (1960) 2175
39) G. C. Phillips and T. A. Tombrello, Nuclear Physics **19** (1960) 555; **20** (1960) 648
40) French, Halbert and Pandya, Phys. Rev. **99** (1955) 1387
41) Bockelman, Leveque and Buechner, Phys. Rev. **104** (1956) 456
42) R. W. Kavanagh and C. A. Barnes, Phys. Rev. **112** (1958) 503
43) Gibbons, Macklin, Marion and Schmitt, Phys. Rev. **114** (1959) 1319
44) Carver, Kondaiah and McDaniel, Phil. Mag. **45** (1954) 948
45) F. R. Paolini, Ph. D. Thesis, Dept. of Physics, M.I.T., 1960
46) Hamermesh, Hamermesh and Wattenberg, Phys. Rev. **76** (1949) 611

7.C

Nuclear Physics **28** (1961) 122—134; © *North-Holland Publishing Co., Amsterdam*

Not to be reproduced by photoprint or microfilm without written permission from the publisher

ELECTROMAGNETIC INTERACTIONS OF CHARGED PIONS

BIBHUTI BHUSAN DEO

Physics Department, Ravenshaw College, Cuttack-3, India †

Received 3 March 1961

Abstract: Perturbation calculation results of electromagnetic effects involving charged mesons are reported. The pionic vacuum contribution to photon-photon scattering and Delbrück forward scattering are discussed in detail.

1. Introduction

The covariant theory of Tomonaga-Schwinger was first applied to electromagnetic interaction of spinless charged particles by Kanesawa and Tomonaga[1]). A systematic approach was made by Rohrlich [2]). He analysed the problem of divergence in the S-matrix and deduced the rules for obtaining the matrix elements form Feynman diagrams. In spite of the simplicity of the approach sufficient interest has not been attached to the subject and no consistent set of calculations is available in the literature.

We discuss in detail two topics of theoretical interest, the vacuum polarisation tensor leading to photon-photon scattering and Delbrück scattering. The former requires a highly involved calculation of the Karplus-Neumann type. This is reported in sects. 2 and 3. In sect. 4, starting from the result for pion pair production, the method of analytic continuation has been used to deduce the Delbrück forward scattering. In sect. 5, further results obtained for various processes are presented in tabular form.

We shall use a natural system of units, with $\hbar = c = 1$, such that the fine structure constant $\alpha = e^2/4\pi \approx 1/137$.

2. Photon-Photon System

The analytical treatment follows closely the work of Karplus and Neuman [3]). The analysis is much more complicated due to the many more Feynman diagrams and requires an essentially different symmetrisation procedure. The matrix elements can be formally written down using the prescription of Rohrlich [2]). The occurring logarithmic divergences for the single diagrams are eliminated by Rohrlich by means of regulators. It tuns out that this artifice

† Part of the thesis submitted by the author in 1958 to the University of Manchester in partial fulfillment of the requirements for the Ph. D. degree.

is unnecessary; the sum of the divergent contributions from all diagrams is finite as will be shown below. The situation here resembles that in electrodynamics (see, for instance, ref. [4]), p. 390).

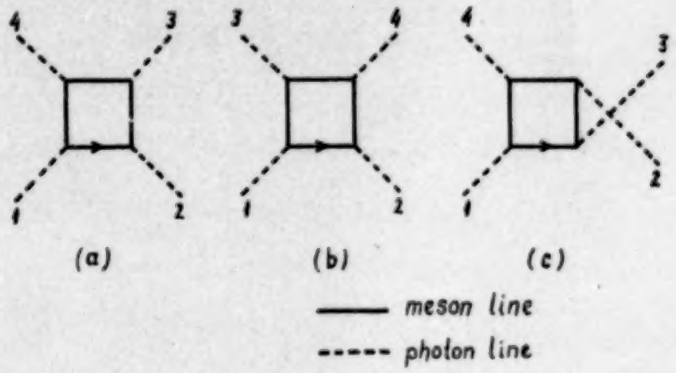

Fig. 1.

The basic Feynman single corner diagrams are shown in fig. 1. For the general case $k^2 \neq 0$, the matrix elements can be cast in the form

$$(e/4\pi)^4 e_\mu(k_1) e_\nu(k_2) e_\gamma(k_3) e_\sigma(k_4) T_{\mu\nu\lambda\sigma}(k_1 k_2 k_3 k_4) \delta(k_1+k_2+k_3+k_4).$$

The diagram of fig. 1(a) gives

$$T^{(a)}_{\mu\nu\lambda\sigma}(1234)$$
$$= \int \mathrm{d}^4 p (2p_\mu - k_{1\mu})(2p_\nu - 2k_{1\nu} - k_{2\nu})(2p_\lambda - 2k_{1\lambda} - 2k_{2\lambda} - k_{3\lambda})(2p_\sigma - k_{1\sigma} - k_{2\sigma} - k_{3\sigma})$$
$$\times [(p^2+\mu^2)((p-k_1)^2+\mu^2)((p-k_1-k_2)^2+\mu^2)((p-k_1-k_2-k_3)^2+\mu^2)]^{-1}.$$

The contributions from figs. 1 (b) and (c) can be obtained by familiar substitutions. Using

$$(abcd)^{-1} = 6 \int \mathrm{d}\tau / (a y_1 + b y_2 + c y_3 + d y_4),$$

where

$$\int \mathrm{d}\tau \ldots \equiv \int\int\int\int_{\substack{y_i > 0 \\ \Sigma y_i = 1}} \mathrm{d}y_1 \mathrm{d}y_2 \mathrm{d}y_3 \mathrm{d}y_4 \ldots,$$

and shifting the origin of p-integration, we get

$$T^{(a)}_{\mu\nu\lambda\sigma}(1234)$$
$$= 6 \int \mathrm{d}\tau \int \mathrm{d}^4 p (2p_\mu + K_{1\mu})(2p_\nu + K_{2\nu})(2p_\lambda + K_{3\lambda})(2p_\sigma + K_{4\sigma}) / (p^2+a^2)^4, \quad (1)$$

where

$$a^2 = \mu^2 + k_1^2 y_1 y_2 + k_4^2 y_2 y_3 + k_3^2 y_3 y_4 + k_4^2 y_1 y_4 - (k_1+k_2)(k_3+k_4) y_3 y_1$$
$$- (k_1+k_4)(k_2+k_3) y_2 y_4,$$

$$K_{1\mu} = +k_{2\mu}(y_2+y_3+y_4-1) + k_{3\mu}(y_3+y_4-y_1-y_2) - k_{4\mu}(y_1+y_2+y_3-y_4),$$
$$K_{2\nu} = -k_{1\nu}(y_2+y_3+y_4-y_1) + k_{3\nu}(y_1+y_3+y_4-y_2) + k_{4\nu}(y_1+y_4-y_2-y_3),$$
$$K_{3\lambda} = k_{1\lambda}(y_1+y_2+y_3-y_4) - k_{2\lambda}(y_1+y_3+y_4-y_2) + k_{4\lambda}(y_1+y_2+y_4-y_3),$$
$$K_{4\sigma} = k_{1\sigma}(y_1+y_2+y_3-y_4) + k_{2\sigma}(y_2+y_3-y_1-y_4) - k_{3\sigma}(y_1+y_2+y_4-y_3).$$

This gives the proper symmetrisation.

From the above expression, we can separate the divergent part

$$\tfrac{2}{3}\varepsilon_{\mu\nu\lambda\sigma}\int \mathrm{d}^4p\,(p^2)^2/(p^2+\mu^2)^4,$$

where

$$\varepsilon_{\mu\nu\lambda\sigma} = g_{\mu\nu}g_{\lambda\sigma}+g_{\mu\lambda}g_{\nu\sigma}+g_{\mu\sigma}g_{\nu\lambda}.$$

Figs. 1 (b) and (c) give the same divergence so that the total divergent integral from single corner diagrams is

$$D^1 = 2\varepsilon_{\mu\nu\lambda\sigma}\int \mathrm{d}^4p\,(p^2)^2/(p^2+\mu^2)^4.$$

Using Rohrlich rules for single-double and double-double corner diagrams, the divergences are found to be contained in

$$D^{1,2} = -4\varepsilon_{\mu\nu\lambda\sigma}\int \mathrm{d}^4p\,p^2/(p^2+\mu^2)^3, \qquad D^{2,2} = +2\varepsilon_{\mu\nu\lambda\sigma}\int \mathrm{d}^4p/(p^2+\mu^2)^2.$$

Adding up the divergent integrals we get

$$D^1+D^{1,2}+D^{2,2} = 2\varepsilon_{\mu\nu\lambda\sigma}\mu^4\int \mathrm{d}^4p/(p^2+\mu^2)^4 = \tfrac{1}{3}i\pi^2\,\varepsilon_{\mu\nu\lambda\sigma}.$$

Thus, there is no inherent divergence in the photon-photon process.

The polarisation tensor can be cast into the form

$$\Pi_{\mu\nu\lambda\sigma} = \sum_{ijlm} A^{ijlm}k_\mu{}^i k_\nu{}^j k_\lambda{}^l k_\sigma{}^m + \sum_{lm} B_1{}^{lm}g_{\mu\nu}k_\lambda{}^l k_\sigma{}^m + \sum_{jm} B_2{}^{jm}g_{\mu\lambda}k_\nu{}^j k_\sigma{}^m + C_1 g_{\mu\nu}g_{\lambda\sigma}+C_2 g_{\nu\lambda}g_{\nu\sigma}+C_3 g_{\mu\sigma}g_{\nu\lambda},$$

where $i = (1, 2, 3, 4)$, $j = (1, 3, 4)$, $l = (1, 2, 4)$ and $m = (1, 2, 3)$ and the A, B, C are scalars independent of the k. The tensor $\Pi_{\mu\nu\lambda\sigma}$ satisfies the gauge-invariance requirements

$$k_{1\mu}\Pi_{\mu\nu\lambda\sigma} = k_{2\nu}\Pi_{\mu\nu\lambda\sigma} = \ldots = 0$$

and the k satisfy

$$\sum_{i=1}^{4} k_i = 0.$$

Because of gauge invariance the coefficients B and C are uniquely determined once the A are known. Thus the determination of the coefficients of

the product of four momenta will be sufficient for our purpose, and these come entirely from single-corner diagrams of which eq. (1) gives a typical element. We supply a factor 2 to take into account the charge conjugate diagram and note that its 'head terms' are entirely contained in

$$T^{(a)}_{\mu\nu\lambda\sigma}(1234) = 12\int d\tau \int d^4p K_{1\mu}K_{2\nu}K_{3\lambda}K_{4\sigma}/(p^2+a^2)^4.$$

The p-integration is now trivial and we get

$$T^{(a)}_{\mu\nu\lambda\sigma}(1234) = 2i\pi^2\mu^{-4}\int d\tau K_{1\mu}K_{2\nu}K_{3\lambda}K_{4\sigma}D(1234), \tag{2}$$

where $D(1234) = (a^2/\mu^2)^{-2}$.

Since each K is the sum of three different momenta, there will be in all 81 coefficients. But there are only six different A to be evaluated for $\Pi_{\mu\nu\lambda\sigma}$, because of the relations between them, given by Karplus and Neumann (eq. (19) in the first paper of ref. [3])).

To evaluate these six basic A we need to know at least 15 integrals of the form (2). They can be written down as in ref. [3]) and are given in ref. [6]). In terms of the $g^{(n)}$ tensors of Karplus and Neuman we have

$$\begin{aligned}\Pi_{\mu\nu\lambda\sigma} = \sum_{24\text{ perm}} \tfrac{1}{8}[A^{2143}(1234)\, g^{(1)}_{\mu\nu\lambda\sigma}(1234)+A^{2341}(1234)g^{(2)}_{\mu\nu\lambda\sigma}(1234)] \\ + \frac{1}{2k_3k_4}[A^{2111}(1234)g^{(3)}_{\mu\nu\lambda\sigma}(1234)+A^{2121}(1234)g^{(4)}_{\mu\nu\lambda\sigma}(1234)] \\ + \frac{1}{2k_2k_4}A^{2311}(1234)g^{(5)}_{\mu\nu\lambda\sigma}(1234).\end{aligned}$$

Thus we conclude that $\Pi_{\mu\nu\lambda\sigma}$ is of the same form as for charged spinors, the values of the A being entirely different.

For small momenta $\mathbf{k}^2 \ll \mu^2$ the function $D(1234)$ can be approximated by unity so that the integrations can be easily performed. The six basic A are given by

$$A^{2111} = A^{2121} = A^{2311} = A^{2143} = 0,$$

$$A^{2143} = A^{3412} = A^{4312} = 1/9\mu^4, \qquad A^{2341} = A^{2413} = A^{3421} = 1/45\mu^4.$$

Thus in the low energy limit we get

$$\begin{aligned}-G_{\mu\nu\lambda\sigma}(1234) = \frac{1}{36\mu^4}(g^{(1)}_{\mu\nu\lambda\sigma}(1234)+g^{(1)}_{\mu\lambda\nu\sigma}(1324)+g^{(1)}_{\mu\sigma\nu\lambda}(1423)) \\ + \frac{1}{180\mu^4}(g^{(2)}_{\mu\nu\lambda\sigma}(1234)+g^{(2)}_{\mu\lambda\nu\sigma}(1324)+g^{(2)}_{\mu\sigma\nu\lambda}(1423)),\end{aligned}$$

where $\alpha = e^2/4\pi$ and $\Pi_{\mu\nu\lambda\sigma} = -(i\alpha^2/4\pi^4)G_{\mu\nu\lambda\sigma}$.

The tensors $g^{(1)}$ and $g^{(2)}$ can be constructed from the symmetric tensors $f_{\mu\nu}$

of the electromagnetic field. Defining

$$I_1 = \tfrac{1}{2} f_{\mu\nu} f_{\mu\nu}, \qquad I_2 = \tfrac{1}{4} \varepsilon_{\mu\nu\lambda\sigma} f_{\mu\nu} f_{\lambda\sigma},$$

we see that the electric and magnetic field strengths

$$\mathbf{E} = (f_{10}, f_{20}, f_{30}), \qquad \mathbf{H} = (f_{23}, f_{31}, f_{13})$$

are related to those quantities by $I_1 = H^2 - E^2$ and $I_2 = \mathbf{H} \cdot \mathbf{E}$.
Further defining

$$I_3 = \tfrac{1}{4} f_{\mu\nu} f_{\nu\lambda} f_{\lambda\sigma} f_{\sigma\mu} = \tfrac{1}{2} I_1^2 + I_2^2,$$

we can write the S-matrix elements as

$$S^{(4)} = \frac{i\alpha^2}{45\mu^4} \int \mathrm{d}^4x (\tfrac{5}{4} I_1^2 + I_3) = \frac{i\alpha^2}{45\mu^4} \int \mathrm{d}^4x [\tfrac{7}{4} (H^2 - E^2)^2 + (\mathbf{H} \cdot \mathbf{E})^2].$$

This expression formally agrees with the derivation of Schwinger [5]) for the case of constant fields, the interaction Lagrangian density being given by

$$\mathscr{L}'(x) = (\alpha^2/45\mu^4) [\tfrac{7}{4} (H^2 - E^2)^2 + (\mathbf{H} \cdot \mathbf{E})^2],$$

which expresses the non-relativistic non-linearity of electromagnetic interaction with charged scalar bosons.

3. Photon-Photon Scattering

We assume the existence of charged spin zero virtual states only. The differential scattering cross-section in the centre-of-mass system for the scattering, is then

$$\frac{\mathrm{d}\sigma}{\mathrm{d}\Omega} = \frac{\alpha^2 R_0^2}{64\pi^2} \left(\frac{\mu}{\omega}\right)^2 \sum |e_\mu(k_1) e_\nu(k_2) e_\lambda(k_3) e_\sigma(k_4) G_{\mu\nu\lambda\sigma}(1234)|^2, \qquad R_0 = e^2/4\pi\mu.$$

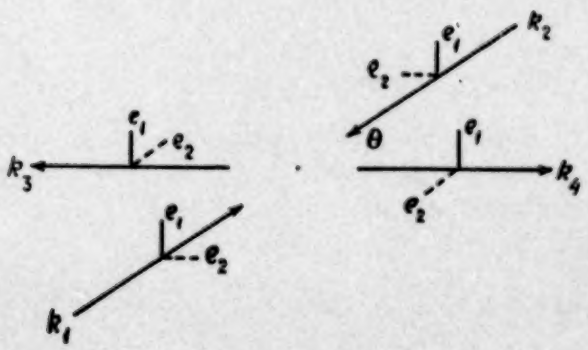

Fig. 2

It has been shown by Karplus and Neuman (2nd paper of ref. [3])) that there are five distinct scattering configurations denoted by M_{1111}, M_{2222}, M_{1212},

M_{1221}, M_{1122} for linear polarisations with weights 2, 2, 4, 4 and 4 respectively. According to our notations we have

$$\sum_{\text{pol}} |\quad\quad|^2 = 16(|M_{1111}|^2+|M_{2222}|^2+2|M_{1122}|^2+2|M_{1212}|^2+2|M_{1221}|^2),$$

where μ, ν, λ, σ take the values corresponding to the particular polarisations considered.

We choose the representation of the e shown in fig. 2. We then get

$$\begin{aligned}
M_{1111} &= M_{2222} = \tfrac{7}{90} a^4(3+\cos^2\theta),\\
M_{1122} &= M_{2211} = \tfrac{1}{90} \omega^4(13-\cos^2\theta),\\
M_{1212} &= M_{2121} = \tfrac{1}{90} \omega^4(1-8\cos\theta+3\cos^2\theta),\\
M_{1221} &= M_{2112} = \tfrac{1}{90} \omega^4(1+8\cos\theta+3\cos^2\theta).
\end{aligned}$$

For non-relatistivistic energies, the differential scattering cross-section is

$$\frac{\mathrm{d}\sigma}{\mathrm{d}\Omega} = \frac{34}{8100}\left(\frac{\alpha}{2\pi}\right)^2 R_0^2(\omega/\mu)^6(3+\cos^2\theta)^2$$

and the total scattering cross section is

$$\sigma = \frac{338}{10125}\,\frac{\alpha^2}{\pi}\,R_0^2\left(\frac{\omega}{\mu}\right)^6.$$

Thus except for numerical factors, the scattering is similar to that for fermion virtual states.

4. Delbrück Scattering

To calculate the Delbrück scattering cross section in the forward direction by the method of analytic continuation, one has to know the total cross section of charged boson pair production. Using Rohrlich rules, in the notation of ref. [4]), the differential pair production cross section for an unpolarised beam of photons is

$$\mathrm{d}\sigma = \alpha Z^2 R_0^2 \frac{p_+ + p_-}{\omega^3}\,\mathrm{d}\varepsilon_- \tfrac{4}{3}\left[-1+\frac{2}{\beta_+\beta_-}\log\{(\mu^2+\varepsilon_+\varepsilon_- + p_+p_-)/\mu\omega\}\right].$$

The total cross section is obtained by integrating over the energies. This can be expressed in terms of complete elliptic functions F and E of the first and second kind of argument $(\eta-1)/(\eta+1)$, where $\eta = \omega/2\mu$,

$$\sigma(\eta) = \alpha Z^2 R_0^2 \frac{2}{27\eta^2}\left[(12\eta^2-6+2\eta)\frac{\eta+1}{\eta}F + (-13\eta^2+5)E\right].$$

A more convenient form is obtained by using the following identities:

$$F\left(\frac{\eta-1}{\eta+1}\right)=\frac{\eta+1}{2\eta}F\left(\left(1-\frac{1}{\eta^2}\right)^{\frac{1}{2}}\right),$$

$$E\left(\frac{\eta-1}{\eta+1}\right)=\frac{\eta}{\eta+1}E\left(\left(1-\frac{1}{\eta^2}\right)^{\frac{1}{2}}\right)+\frac{1}{\eta+1}F\left(\left(1-\frac{1}{\eta^2}\right)^{\frac{1}{2}}\right),$$

whence

$$\sigma(\eta)=\alpha Z^2R_0^2\frac{2}{27\eta^2}\left[\left(5+6\eta^2-\frac{3}{\eta^2}\right)F\left(\left(1-\frac{1}{\eta^2}\right)^{\frac{1}{2}}\right)+(5-13\eta^2)E\left(\left(1-\frac{1}{\eta^2}\right)^{\frac{1}{2}}\right)\right].$$

This result can be inserted in the Bohr-Peierls-Placzek [7]) relation. This well known theorem in optics relates the total absorption cross section $\sigma_{\mathrm{abs}}(\omega)$ and the forward scattering amplitude $a(\omega)$. Writing

$$a(\omega)=a_1(\omega)+ia_2(\omega),$$

we have

$$\sigma_{\mathrm{abs}}(\omega)=\frac{4\pi}{\omega}a_2(\omega).$$

The absorption process related to Delbrück scattering is the pair production. Thus, in units of αZ^2R_0 and with $p=2\mu/\omega$, we have

$$a_2(\omega)=\begin{cases}0 \quad \text{for} \quad p\geqq 1,\\ \dfrac{1}{27\pi p}[(5p^2-13)E((1-p^2)^{\frac{1}{2}})+(6+5p^2-3p^4)F((1-p^2)^{\frac{1}{2}})] \quad \text{for} \quad p<1.\end{cases}$$

To deduce $a_1(\omega)$ we use the method of analytic continuation. Noting that $\sigma_{\mathrm{abs}}(\omega)$ is an even function of ω, we have

$$a_1(\omega)=\frac{\omega^2}{4\pi^2}\mathrm{P}\int_{-\infty}^{+\infty}\frac{\sigma_{\mathrm{abs}}(\omega')}{\omega'(\omega'-\omega)}\mathrm{d}\omega'=\frac{\omega^2}{2\pi^2}\mathrm{P}\int_{2\mu}^{\infty}\frac{\sigma_{\mathrm{abs}}(\omega')}{\omega'^2-\omega^2}\mathrm{d}\omega',$$

where P denotes the principal value. Letting $p'=2\mu/\omega'$ and using the value of $\sigma_{\mathrm{abs}}(\omega)$, we have

$$a_1(p)=\frac{2}{27\pi^2}\mathrm{P}\int_0^1(p^2-p'^2)^{-1}((5p'^2-13)E+(6+5p'^2-3p'^4)F).$$

The integrations can be performed by noting that

$$\int_0^1\mathrm{d}pF((1-p^2)^{\frac{1}{2}})=\tfrac{1}{4}\pi^2, \quad \int_0^1p^2\mathrm{d}pF=\tfrac{1}{16}\pi^2, \quad \mathrm{P}\int_0^1\frac{F}{p^2-p'^2}\mathrm{d}p'=\frac{\pi}{2p}F_1(p),$$

$$\int_0^1E\mathrm{d}p=\tfrac{1}{8}\pi^2, \quad \mathrm{P}\int_0^1\frac{E\mathrm{d}p'}{p^2-p'^2}=\frac{\pi}{2p}[F_1(p)-E_1(p)],$$

where

$$F_1(p) = \mathrm{Re}\int_0^{1/p} \mathrm{d}x/(1-x^2)^{\frac{1}{2}}(1-p^2x^2)^{\frac{1}{2}}, \quad E_1(p) = \mathrm{Re}\int_0^{1/p} (1-p^2x^2)^{\frac{1}{2}}\mathrm{d}x/(1-x^2))^{\frac{1}{2}}.$$

Thus we get the final result

$$a_1(p) = \frac{2}{27\pi p}[(13-5p^2)E_1(p)+(-7+10p^2-3p^4)F_1(p)] + \frac{p^2}{18} - \frac{1}{8}.$$

The Delbruck scattering is obtained from

$$\frac{\mathrm{d}\sigma(\omega, 0)}{\mathrm{d}\Omega} = |a_1(\omega)+ia_2(\omega)|^2.$$

We note that in the non-relativistic limit

$$a_2(\omega) = 0 \qquad \text{for} \qquad p > 1,$$

so that

$$a(\omega) = a_1(\omega) = \frac{5}{128}\frac{\omega^2}{4\mu^2}.$$

Thus $a(\omega)$ is proportional to ω^2, a result which would have been anticipated from classical dimensional considerations.

In the extreme relativistic limit we have

$$a_1(\omega) = \omega/18\mu, \qquad a_2(\omega) = \frac{2}{27\mu}\frac{\omega}{4\pi}(-13+6\log(2\omega/\mu)),$$

which is $\omega/4\pi$ times the extreme relativistic limit of pair production.

5. Tables of Results

The tables 1, 2 and 3 give results of calculations for electron and pion electromagnetic interactions. Most of the results for the case of the electron are taken from ref. [4]). The details of the calculation for the boson case are given in ref. [6]). We hope that the tables may provide an accurate estimate of the electromagnetic effects in high energy meson physics.

The author wishes to record his heartfelt gratitude to Professor L. Rosenfeld under whose guidance this programme was carried out. Special thanks are due to Dr. P. Roman for constant and unfailing supervision. The author is thankful to the theoretical physics group at Manchester in 1956—1958, specially to Dr. Naqvi and Dr. Khan, for many useful discussions and also to Dr. Edwards for some valuable comments. The author acknowledges with due thanks the award of a central Overseas Scholarship by the Government of India and the University of Utkal.

TABLE 1

Renormalisation constants

(a) Modified matter propagator

Meson: $\Delta'(p) = \Delta(p)+\Delta(p)\Sigma(p)\Delta(p)$ (mass $= \mu$)	Electron: $S'(p) = S(p)+S(p)\Sigma(p)S(p)$ (mass $= m$)
$\Sigma(p) = A+(p^2+\mu^2)B+(p^2+\mu^2)^2\Sigma_t(p)$	$\Sigma(p) = A+(i\gamma p+m)B+(i\gamma p+m)^2\Sigma_t(p)$,
$A = -\frac{\alpha}{4\pi}\left(3D_1+6D_2\mu^2+\frac{21}{2}\mu^2\right)$, $B = -\frac{\alpha}{4\pi}\left(\frac{1}{2}+4\int\frac{dx}{x}+2D_1\right)$	$A = \frac{\alpha}{2\pi}m\left(\frac{3}{2}D+\frac{9}{4}\right)$, $B = \frac{\alpha}{4\pi}\left(D-4\int\frac{dx}{x}+\frac{11}{2}\right)$
$\Sigma_t(p) = -\frac{\alpha}{2\pi\mu^2}\left[\frac{1}{\rho}\left(I_1+\int\frac{dx}{x}-\frac{1}{2}\right)-\frac{I_2}{\rho^2}\right]$, $\rho = (p^2+\mu^2)/\mu^2$	$\Sigma_t(p) = \frac{\alpha}{2\pi m}\left\{\frac{1}{2(1-\rho)}\left(1-\frac{2-3\rho}{1-\rho}\log\rho\right)\right.$
	$\left.+\frac{i\gamma p-m}{m}\left[\frac{1}{2\rho(1-\rho)}\left(-2-\rho+\frac{4-8\rho+\rho^2}{1-\rho}\log\rho\right)+\frac{2}{\rho}\int_0^1 dx\left(\frac{1}{x}-x\right)\right]\right\}$
$D_1 = \frac{1}{i\pi^2}\int d^4k/(k^2+\mu^2)$, $D_2 = \frac{1}{i\pi^2}\int d^4k/(k^2+\mu^2)^2$	
$I_1 = \frac{\rho}{1-\rho}\left(1+\frac{2\rho}{1-\rho}\log\rho\right)$, $I_2 = \frac{\rho}{1-\rho}\left(1-\frac{2-3\rho}{1-\rho}\log\rho\right)$	$\rho = (p^2+m^2)/m^2$, $D = \frac{1}{i\pi^2}\int d^4k/(k^2+m^2)^2$

(b) Modified photon propagator

$$\mathscr{D}'_{\mu\nu}(k) = g_{\mu\nu}\mathscr{D}(k)+\mathscr{D}(k)\Pi_{\mu\nu}(k)\mathscr{D}(k), \quad \Pi_{\mu\nu}(k) = [k_\mu k_\nu-k^2g_{\mu\nu}][C-k^2\Pi_t(k^2)]$$

Meson	Electron
$C = \frac{\alpha}{12\pi}\left(D_2+\frac{1}{3}\right)$	$C = -\frac{\alpha}{3\pi}\left(D+\frac{5}{6}\right)$
$\Pi_t(k^2) = -\frac{\alpha}{\pi k^2}\left[V_1\left(\frac{k^2}{\mu^2}\right)-\frac{1}{4}V_0\left(\frac{k^2}{\mu^2}\right)\right]$	$\Pi_t(k^2) = -\frac{2\alpha}{\pi k^2}V_1\left(\frac{k^2}{m^2}\right)$
$\Pi_t(0) = \frac{\alpha}{120\pi\mu^2}$	$\Pi_t(0) = -\alpha/15\pi m^2$

$$V_n(a) = \lim_{\varepsilon\to 0}\int_0^1 dx[x(1-x)]^n\ln[1-i\varepsilon+ax(1-x)]$$

TABLE 1 (continued)

Correction to Coulomb's law $V(r) = \frac{qq'}{4\pi r}(1+\delta(r))$

Meson	Electron
$\delta(r) = -\frac{\alpha}{6\pi}\int_1^\infty e^{-2\mu r t}\left(1-\frac{1}{t^2}\right)\frac{(t^2-1)^{\frac{1}{2}}}{t^2}dt$	$\delta(r) = \frac{2\alpha}{3\pi}\int_1^\infty e^{-2mrt}\left(1+\frac{1}{2t^2}\right)\frac{(t^2-1)^{\frac{1}{2}}}{t^2}dt$
$\approx -\frac{\alpha}{6\pi}\left(\log(\mu r)^{-1}-\gamma-\frac{1}{3}\right)$ $(\mu r \ll 1)$	$\approx \frac{2\alpha}{3\pi}\left(\log(mr)^{-1}-\gamma-\frac{5}{6}\right)$ $(mr \ll 1)$
$\sim -\frac{\alpha}{(2\pi)^{\frac{1}{2}}}\frac{11}{32}\frac{e^{-2\mu r}}{(2\mu r)^{\frac{1}{2}}}$ $(\mu r \gg 1)$	$\sim -\frac{\alpha}{(2\pi)^{\frac{1}{2}}}\frac{e^{-2mr}}{(2mr)^{\frac{1}{2}}}$ $(mr \ll 1)$

(c) Vertex renormalisation

Meson: $\Gamma_\mu = (p_\mu+p'_\mu)+\Lambda_\mu(p',p)$, $\Lambda_\mu(p',p) = (p'_\mu+p_\mu)L+\Lambda_{\mu t}(p',p)$	Electron: $\Gamma_\mu = \gamma_\mu+\Lambda_\mu(p',p)$, $\Lambda_\mu(p',p) = L\gamma_\mu+\Lambda_{\mu t}(p',p)$
$L = -B$	$L = B$
$\Lambda_{\mu t}(p',p) = \frac{\alpha}{4\pi}\left[\frac{1}{2}\int_0^1 dx\int_0^\infty dy\left\{\frac{K_\mu}{a^2}-3\int_0^1 dz\frac{(a^2-\mu^2x^2)[p_\mu(x-2)+k_\mu(1-y)]}{\mu^2x^2+(a^2-\mu^2x^2)z}\right.\right.$ $\left.\left.-\frac{1}{2}\mu^2(2p_\mu(x^2-3x+4)-k_\mu(2x^2y-3x^2+4x-8y+4))\frac{a^2-\mu^2x^2}{a^2\mu^2x^2}\right\}$	$\Lambda_{\mu t}(p',p) = -\frac{\alpha}{2\pi}\int_0^1 dx\int_0^\infty dy\left\{\frac{K_\mu}{a^2}+\gamma_\mu\int_0^1 dz\frac{a^2-m^2x^2}{m^2x^2+(a^2-m^2x^2)z}\right.$ $\left.-2m^2\gamma_\mu\left(1-x-\frac{1}{2}x^2\right)\frac{a^2-m^2x^2}{a^2m^2x^2}\right\}$
$a^2 = \mu^2x^2+k^2y(x-y)+(p^2+\mu^2)(1-x)(x-y)+(p'^2+\mu^2)y(1-x)$	$a^2 = m^2x^2+k^2y(x-y)+(p^2+m^2)(1-x)(x-y)+(p'^2+m^2)(1-x)y$
$K_\mu = k^2(2p_\mu A_k-k_\mu B_k)+(p^2+\mu^2)(2p_\mu A_p-k_\mu B_p)+(p'^2+\mu^2)(2p_\mu A_{p'}-k_\mu B_{p'})$	$K_\mu = (1-x)(i\gamma p'+m)\gamma_\mu(i\gamma p+m)+\gamma_\mu C-(i\gamma p'+m)M'_\mu-M_\mu(i\gamma p+m)+ik_\mu m(1+x)(x-2y)-mx(1-x)\sigma_{\mu\nu}k^\nu$
$A_k = y(y-x)(x-3)+x-2$, $B_k = y(y-x)(2y-3)+x-2$	$C = k^2(1-x+y)(1-y)-(1-x)[(p^2+m^2)(1-x+y)+(p'^2+m^2)(1-y)]$
$A_p = (x-1)(x-2)(x-y)$, $B_p = x(x-y)(2y-3)+5x+4y+2$	$M_\mu = \gamma_\mu m(1-x^2)+iP_\mu(1-x)(1-x+y)+ik_\mu(1+x-2y)(1-x+y)$
$A_{p'} = y(x-1)(x-2)$, $B_{p'} = xy(2y-3)+(x-2)$	$M'_\mu = \gamma_\mu m(1-x^2)+iP_\mu(1-x)(1-y)+ik_\mu(1-x+2y)(1-y)$
$k = p-p'$	$\sigma_{\mu\nu} = \frac{1}{2i}(\gamma_\mu\gamma_\nu-\gamma_\nu\gamma_\mu)$, $P = p+p'$

TABLE 2

Scattering processes

Process	Boson, spin 0	Fermion, spin $\frac{1}{2}$
Compton scattering	$\frac{d\sigma}{d\Omega} = \frac{1}{2}R_0^2\left(\frac{\omega'}{\omega}\right)^2(1+\cos^2\theta)$ $\sigma = 2\pi R_0^2\frac{1+\omega}{\omega^3}[2\omega(1+\omega)/(1+2\omega)-\log(1+2\omega)]$ ω in units of μ (L-system)	$\frac{d\sigma}{d\Omega} = \frac{1}{2}r_0^2\left(\frac{\omega'}{\omega}\right)^2\left(\frac{\omega}{\omega'}+\frac{\omega'}{\omega}-\sin^2\theta\right)$ $\sigma = 2\pi r_0^2\left\{\frac{1+\omega}{\omega^3}\left[\frac{2\omega(1+\omega)}{1+2\omega}-\log(1+2\omega)\right]+\frac{1}{2\omega}\log(1+2\omega)-\frac{1+3\omega}{(1+2\omega)^2}\right\}$ ω in units of m (L-system)
Pair annihilation	$d\sigma = R_0^2\frac{2\pi}{(B\gamma)^2}\frac{d\omega_1}{\mu}\left[2\frac{\mu^2(1+\gamma)}{\omega_1\omega_2}-\frac{\mu^4(1+\gamma)^2}{\omega_1^2\omega_2^2}-2\right]$ $\sigma = (\pi R_0^2/\beta^2\gamma(1+\gamma))[2\log(\gamma+(\gamma^2-1)^{\frac{1}{2}})+\beta(\gamma-1)]$ $\omega_1+\omega_2 = m(1+\gamma)$ (L-system)	$d\sigma = r_0^2\pi\frac{d\omega_1}{m}\frac{1}{(\beta\gamma)^2}\left[\frac{\omega_1}{\omega_2}+\frac{\omega_2}{\omega_1}+2\frac{m^2}{\omega_1\omega_2}(1+\gamma)-\left(\frac{m^2(1+\gamma)}{\omega_1\omega_2}\right)^2\right]$; $\omega_1+\omega_2 = m(1+\gamma)$ $\sigma = r_0^2\pi\frac{1}{\beta^2\gamma(\gamma+1)}\left[\left(\gamma+4+\frac{1}{\gamma}\right)\log(\gamma+(\gamma^2-1)^{\frac{1}{2}})-\beta(\gamma+3)\right]$ (L-system)
Pair production	$d\sigma = \frac{1}{2}\pi R_0^2\beta\left(\frac{\mu}{\omega}\right)^2\frac{(1-2\beta^2-\beta^4\cos\theta+2\beta^4\sin^2\theta)}{(1-\beta^2\cos^2\theta)^2}\sin\theta\,d\theta$ $\sigma = \frac{1}{2}\pi R_0^2(1-\beta^2)\left[(\beta^4-1)\log\frac{1+\beta}{1-\beta}+2\beta(2-\beta^2)\right]$ (C.M. system)	$d\sigma = \frac{\pi r_0^2}{2}\beta\left(\frac{m}{\omega}\right)^2\frac{1-\beta^4\cos^4\theta+2(m/\omega)^2\beta^2\sin^2\theta}{(1-\beta^2\cos^2\theta)^2}\sin\theta\,d\theta$ $\sigma = \frac{1}{2}\pi r_0^2(1-\beta^2)\left[(3-\beta^4)\log\frac{1+\beta}{1-\beta}-2\beta(2-\beta^2)\right]$ (C.M. system)
Møller scattering	$\frac{d\sigma}{d\Omega} = 4R_0^2\left(4\frac{\gamma+1}{\beta^2\gamma}\right)^2\frac{\cos\theta}{[2+(\gamma-1)\sin^2\theta]^2}$ $\times\left[\frac{4}{(1-x)^2}-\frac{\gamma-1}{\gamma}\frac{2}{1-x^2}+\left(\frac{\gamma-1}{2\gamma}\right)^2\right]x = \cos\theta$ (L-system)	$\frac{d\sigma}{d\Omega} = r_0^2\left(4\frac{\gamma+1}{\beta^2\gamma}\right)^2\frac{\cos\theta}{[2+(\gamma-1)\sin^2\theta]^2}$ $\times\left[\frac{4}{(1-x^2)^2}-\frac{3}{1-x^2}+\left(\frac{\gamma-1}{2\gamma}\right)^2\left(1+\frac{4}{1-zx}\right)\right]; x = \cos\theta$ (L-system)
Bhabha scattering	$\frac{d\sigma}{d\Omega} = \frac{R_0^2}{16\gamma^2}\left[\frac{\gamma^2+(\gamma^2-1)\cos^2\frac{1}{2}\theta}{(\gamma^2-1)\sin^2\frac{1}{2}\theta}-\frac{\gamma^2-1}{\gamma^2}\cos\theta\right]^2$ (C.M. system)	$\frac{d\sigma}{d\Omega} = \frac{r_0^2}{16\gamma^2}\left\{\frac{1}{(\beta\gamma\sin\frac{1}{2}\theta)^4}[1+(2\beta\gamma\cos\frac{1}{2}\theta)^2+2(\beta\gamma)^4(1+\cos^4\frac{1}{2}\theta)]\right.$ $-\frac{1}{\gamma^2(\beta\gamma\sin\frac{1}{2}\theta)^2}[3+2(2\beta\gamma\cos\frac{1}{2}\theta)^2+\frac{1}{2}(2\beta\gamma\cos\frac{1}{2}\theta)^4]$ $\left.+\frac{1}{\gamma^4}[3+4(\beta\gamma)^2+(\beta\gamma)^4(1+\cos^2\theta)]\right\}$ (C.M. system)
Photon-photon scattering Non-linear Lagrangian	$\frac{d\sigma}{d\Omega} = \frac{34}{8100}\left(\frac{\alpha}{2\pi}\right)^2R_0^2\left(\frac{\omega}{\mu}\right)^6(3+\cos^2\theta)^2$ (N.R., C.M. System) $\mathscr{L}'(x) = \frac{\alpha^2}{45\mu^4}\left[\frac{7}{4}(H^2-E^2)^2+(\mathbf{H}\cdot\mathbf{E})^2\right]$ (N.R.)	$\frac{d\sigma}{d\Omega} = \frac{139}{8100}\left(\frac{\alpha}{2\pi}\right)^2r_0^2\left(\frac{\omega}{m}\right)^6(3+\cos^2\theta)^2$ (N.R., C.M. system) $\mathscr{L}'(x) = \frac{2\alpha^2}{45m^4}[(H^2-E^2)^2+7(\mathbf{H}\cdot\mathbf{E})^2]$ (N.R.)

grangian	(N.R.)	(N.R.)

TABLE 3 External field problems

Process	Boson	Fermion
Coulomb scattering	$\frac{d\sigma}{d\Omega} = \frac{1}{4}Z^2R_0^2\frac{1}{(\beta\sin\frac{1}{2}\theta)^4}$	$\frac{d\sigma}{d\Omega} = \frac{1}{4}Z^2r_0^2\frac{1-\beta^2\sin^2\frac{1}{2}\theta}{(\beta^2\gamma)^2\sin^4\frac{1}{2}\theta}$
Radiative corrections	$\frac{d\sigma'}{d\Omega} = (1-\delta)\frac{d\sigma}{d\Omega}$ $\delta = \frac{8\alpha}{3\pi}\beta^2\sin^2\frac{1}{2}\theta\left(\log(\mu/\Delta E)+\frac{7}{80}\right)$	$\frac{d\sigma'}{d\Omega} = (1-\delta)\frac{d\sigma}{d\Omega}$ $\delta = \frac{8\alpha}{3\pi}\beta^2\sin^2\frac{1}{2}\theta\left(\log(m/\Delta E)+\frac{19}{30}\right)$
Bremsstrahlung	$d\sigma = \alpha^2Z^2R_0^2\frac{\lvert\mathbf{p}'\rvert}{\lvert\mathbf{p}\rvert}\frac{d\omega}{\omega}\frac{8}{3}\times\left[-1+\frac{2}{\beta\beta'}\log\frac{\varepsilon\varepsilon'+pp'-\mu^2}{\omega\mu}\right]$	$d\sigma = \alpha^2Z^2r_0^2\frac{\lvert\mathbf{p}'\rvert}{\lvert\mathbf{p}\rvert}\frac{d\omega}{\omega}\left\{\frac{4}{3}-\frac{2}{(\beta\beta')^2}\left(\frac{\gamma}{\gamma'}+\frac{\gamma'}{\gamma}-\frac{2}{\gamma'\gamma}\right)+\left(l\frac{\gamma'}{\gamma^2-1}+l'\frac{\gamma}{\gamma'^2-1}-ll'\right)\right.$ $\left.+L\left[\frac{8}{3}\gamma'\gamma+\frac{\omega^2}{m^2}\left(\frac{1}{(\beta'\beta)^2}+1\right)+\frac{\omega}{2m}\left(l\left(1+\frac{\gamma'}{\beta^2\gamma}\right)-l'\left(1+\frac{\gamma}{\beta'^2\gamma'}\right)+2\frac{\omega/m}{\beta^2\beta'^2\gamma\gamma'}\right)\right]\right\}$ $l=\frac{1}{\beta\gamma}\log\frac{1+\beta}{1-\beta},\quad l'=\frac{1}{\beta'\gamma'}\log\frac{1+\beta'}{1-\beta'},\quad L=\frac{1}{\beta\beta'\gamma\gamma'}\log\frac{\gamma\gamma'(1+\beta\beta')-1}{\omega/m}$
Pair production	$\omega = 2\mu\eta$ $\sigma(\eta) = \alpha Z^2R_0^2\frac{2}{27\eta^2}\times\left[\left(5+6\eta^2-\frac{3}{\eta^2}\right)F\left(\left(1-\frac{1}{\eta^2}\right)^{\frac{1}{2}}\right)+(5-13\eta^2)E\left(\left(1-\frac{1}{\eta^2}\right)^{\frac{1}{2}}\right)\right]\quad\eta\geqq1$	$\omega = 2m\eta$ $\sigma(\eta) = \alpha Z^2r_0^2\left\{\frac{2}{\eta^2}[2_2C(\eta)-D_2(\eta)]-\frac{2}{27\eta^2}\left[(109\eta^2+64)E_2(\eta)-(67\eta^2+6)\times\left(1-\frac{1}{\eta^2}\right)F_2(\eta)\right]\right\}$ $C_2(\eta)=\int_1^\eta\cosh^{-1}\times\cosh^{-1}\frac{\eta}{x}\frac{dx}{x},\quad\eta\geqq1\qquad D_2(\eta)=\int_1^\eta\cosh^{-1}\frac{\eta}{x}dx/(x^2-1)^{\frac{1}{2}}$ $E_2(\eta)=F\left(\left(1-\frac{1}{\eta^2}\right)^{\frac{1}{2}}\right)-E\left(\left(1-\frac{1}{\eta^2}\right)^{\frac{1}{2}}\right),\qquad F_2(\eta)=F\left(\left(1-\frac{1}{\eta^2}\right)^{\frac{1}{2}}\right),\quad\eta\geqq1$
Forward Delbrück scattering $\frac{d\sigma}{d\Omega} = \lvert a_1(\omega)+ia_2(\omega)\rvert^2$	$a_2(\omega) = \frac{\omega}{4\pi}\sigma_{\text{patr}}(\omega),\quad\eta = 2\mu/\omega$ $a_1(\omega) = (\alpha Z)^2\frac{2R_0}{27\pi\eta}[(13-5\eta^2)E_1(\eta)+(-7+10\eta^2-3\eta^4)F_1(\eta)]+(\alpha Z)^2R_0\left[\frac{\eta^2}{18}-\frac{1}{8}\right]$	$a_2(\omega) = \frac{\omega}{4\pi}\sigma_{\text{patr}}(\omega),\quad\eta = 2m/\omega$ $a_1(\omega) = (\alpha Z)^2r_0\left\{\frac{\eta}{\pi}[2C_1(\eta)-D_1(\eta)]+\frac{1}{27\pi\eta}[(109+64\eta^2)E_1(\eta)-(67+6\eta^2)(1-\eta^2)F_1(\eta)]-\frac{\eta^2}{9}-\frac{9}{4}\right\}$ $C_1(\eta)=\operatorname{Re}\int_0^{1/\eta}\sin^{-1}x\cosh^{-1}\frac{1}{\eta x}dx/x,\quad\eta>0$ $D_1(\eta)=\operatorname{Re}\int_0^{1/\eta}\cosh^{-1}\frac{1}{\eta x}dx/(1-x^2)^{\frac{1}{2}},\quad\eta>0$ $E_1(\eta)=\begin{cases}E(\eta), & \eta\leqq1\\ \eta E\left(\frac{1}{\eta}\right)+\left(\frac{1}{\eta}-\eta\right)F\left(\frac{1}{\eta}\right), & \eta\geqq1\end{cases}\qquad F_1(\eta)=\begin{cases}F(\eta), & \eta\leqq1\\ \frac{1}{\eta}F\left(\frac{1}{\eta}\right), & \eta\geqq1\end{cases}$

References

1) S. Kanesawa and S. Tomonaga, Progr. Theor. Phys. (Japan) **3** (1948) 1
2) F. Rohrlich, Phys. Rev. **80** (1949) 666
3) R. Karplus and M. Neuman, Phys. Rev. **80** (1950) 380, **83** (1951) 776
4) J. M. Jauch and F. Rohrlich, The theory of photons and electrons (Addison-Wiley, Cambridge, Mass., 1955)
5) J. Schwinger, Phys. Rev. **82** (1951) 664
6) B. B. Deo, Ph. D. Thesis, University of Manchester (1958)
7) N. Bohr, R. Peierls and G. Placzek, Nature **144** (1939) 200

8.B *Nuclear Physics* **28** (1961) 135—139; © *North-Holland Publishing Co., Amsterdam*
Not to be reproduced by photoprint or microfilm without written permission from the publisher

ON MASSES AND MASS-SHIFTS OF ELEMENTARY PARTICLES

BIBHUTI BHUSAN DEO
Physics Department, Ravenshaw College, Cuttack-4, Orissa, India

Received 3 March 1961

Abstract: Solutions have been obtained for two interacting fields, the interaction being a simple product of the two fields operators. It is found that the interacting fields are equivalent to two non-interacting fields of different masses. This is true both for bosons and fermions. The possibility of formation of a massive Fermi particle from interacting neutrinos has also been discussed.

1. Bosons

We wish to solve the following equations of motion for two interacting boson fields:

$$(\Box - m_1^2)\phi_1 = g\phi_2, \tag{1}$$

$$(\Box - m_2^2)\phi_2 = g\phi_1. \tag{2}$$

These equations of motion are deducible from the Lagrangian density

$$\mathscr{L}(\phi_1\phi_2) = -[\tfrac{1}{2}\{(\partial_\mu\phi_1)^2 + m_1^2\phi_1^2\} + \tfrac{1}{2}\{(\partial_\mu\phi_2)^2 + m_2^2\phi_2^2\}] - g\phi_1\phi_2, \tag{A}$$

the last term being the coupling term. From eq. (1) and (2) we deduce the higher order equation

$$[(\Box - m_1^2)(\Box - m_2^2) - g^2]\phi_{1,2} = 0. \tag{3}$$

Eq. (3) gives less information than eq. (1) and (2), but should not give incorrect results. Assuming plane wave solutions like $e^{i\mathbf{k}\cdot\mathbf{x}}$, we have

$$(k^2 + m_1^2)(k^2 + m_2^2) = 0, \tag{4}$$

or

$$(k^2 + M_1^2)(k^2 + M_2^2) = 0, \tag{5}$$

where

$$\begin{aligned} M_1^2 &= \tfrac{1}{2}(m_1^2 + m_2^2 + \sqrt{(m_1^2 - m_2^2)^2 + 4g^2}), \\ M_2^2 &= \tfrac{1}{2}(m_1^2 + m_2^2) - \sqrt{(m_1^2 - m_2^2)^2 + 4g^2}. \end{aligned} \tag{5a}$$

Thus

$$k^2 = -M_1^2 \quad \text{or} \quad k^2 = -M_2^2. \tag{5b}$$

Imposing the restriction that

$$m_1 m_2 > g^2 > 0, \tag{6}$$

we see that there are two stable mass states for the interacting fields different from their original mass values. These shall show up as poles on the real axis of k_0 in the general propagators $\Delta'_F(\phi)_1$ and $\Delta'_F(\phi_2)$.

Thus, we are led to consider the possibility of writing the solutions in terms of two other fields φ_1 and φ_2, the field equations being

$$(\Box - M_1^2)\varphi_1 = 0, \tag{7}$$

$$(\Box - M_2^2)\varphi_2 = 0. \tag{8}$$

By trivial calculations we see that the following relations hold between the $\varphi_{1,2}$ and $\phi_{1,2}$ fields:

$$\varphi_1 = [\phi_1 + \lambda\phi_2]/(1+\lambda^2)^{\frac{1}{2}}, \tag{9}$$

$$\varphi_2 = [-\lambda\phi_1 + \phi_2]/(1+\lambda^2)^{\frac{1}{2}}, \tag{10}$$

$$\phi_1(x) = [\varphi_1(x) - \lambda\varphi_2(x)]/1+\lambda^2)^{\frac{1}{2}}, \tag{11}$$

$$\phi_2(x) = [\lambda\varphi_1(x) + \varphi_2(x)]/(1+\lambda^2)^{\frac{1}{2}}, \tag{12}$$

where

$$\lambda = (M_1^2 - m_1^2)/g. \tag{13}$$

The solutions for the interacting fields are superpositions of two wave functions describing two different stable mass systems. To see this more clearly we evaluate the Lagrangian density given by eq. (A) in terms of φ_1 and φ_2, with the result

$$\mathscr{L}(\varphi_1\varphi_2) = -\tfrac{1}{2}[(\partial_\mu\varphi_1)^2 + M_1^2\varphi_1^2 + (\partial_\mu\varphi_2)^2 + M_2^2\varphi_2^2]. \tag{14}$$

This Lagrangian density refers to two independent fields corresponding to free scalar bose particles of masses M_1 and M_2. These particles will be stable if the inequality (6) is satisfied. If this is not satisfied M_2^2 will be negative and correspond to a decaying state. Further, if g is imaginary the coupling term will be non-hermitian and there will be ghost states. The occurrence of these ghosts can be easily seen in the case when $M_1 = M_2 = m$, for then we have

$$(m_1^2 - m_2^2)^2 + 4g^2 = 0.$$

Eq. (3) in such a case is

$$(\Box - M^2)^2\phi_{1,2} = 0.$$

This and many other fourth order equations can be tested for the presence of ghost states by suitably transforming them to two field equations of the type (1) and (2) and noting the hermicity property of the coupling term [1]).

A very interesting case arises when $m_1 \approx m_2 = m$ with $m \gg g$, so that

$$M_1^2 \approx m^2+g, \qquad M^2 \approx m^2-g.$$

In that case we have

$$\varphi_1 = \frac{1}{\sqrt{2}}(\phi_1+\phi_2), \quad \varphi_2 += \frac{1}{\sqrt{2}}(\phi_1-\phi_2), \quad \phi_1 = \frac{1}{\sqrt{2}}(\varphi_1-\varphi_2), \quad \phi_2 = \frac{1}{\sqrt{2}}(\varphi_1+\varphi_2). \tag{15}$$

Similar states have been considered by Schwinger [2]) to explain the peculiar behaviour of K-mesons. To bring us in line with his notation, let $\phi_{1,2} = \phi_{K^+}$; the states ϕ_{K^+} and ϕ_{K^-} have definite intrinsic parity. The coupling term is $g\phi_{K^+}\phi_{K^-}$. The effect of this coupling, as has been explained above, is to give mass-shifts and the coupled system is now equivalent to two free-particle systems, having wave functions

$$\phi_{K_1} = \frac{1}{\sqrt{2}}(\phi_{K^+}+\phi_{K^-}), \qquad \phi_{K_2} = \frac{1}{\sqrt{2}}(\phi_{K^+}-\phi_{K^-}).$$

The masses of these K_1 and K_2 particles are $\sqrt{m_K{}^2 \pm g}$. They are likely to exhibit properties entirely different from K^+ and K^-, behaving as though they have no memory of their formation. We may assume that K^+ and K^- are the particles produced by strong interactions, with definite intrinsic parity, while K_1 and K_2 are those which decay subsequently. The strength of the coupling should be intermediate.

2. Fermions

Proceeding as before, the following results are obtained for two fermion fields. The field equations are for spin $\frac{1}{2}$

$$(\gamma^\mu\partial_\mu+m_1)\psi_1 = g\psi_2, \qquad (\gamma^\mu\partial_\mu+m_2)\psi_2 = g\psi_1. \tag{16}$$

The solutions are

$$(\gamma^\mu\partial_\mu+M_1)\phi_1 = 0, \qquad (\gamma^\mu\partial_\mu+M_2)\phi_2 = 0,$$
$$M_1 = \tfrac{1}{2}(m_1+m_2+\sqrt{(m_1-m_2)^2+4g^2}), \quad M_2 = \tfrac{1}{2}(m_1+m_2-\sqrt{(m_1-m_2)^2+4g^2}), \tag{17}$$

$$\phi_1 = (\psi_1+\lambda\psi_2)/(1+\lambda^2)^{\frac{1}{2}}, \quad \phi_2 = (\psi_2-\lambda\psi_1)/(1+\lambda^2)^{\frac{1}{2}}, \quad \lambda = (m_1-M_1)/g, \tag{18}$$

$$\mathscr{L}(\psi_1, \psi_2) = -\bar{\psi}_1(\gamma^\mu\partial_\mu+m_1)\psi_1-\bar{\psi}_2(\gamma^\mu\partial_\mu+m_2)\psi_2+g(\bar{\psi}_2\psi_1+\bar{\psi}_1\psi_2), \tag{19}$$

$$\mathscr{L}(\phi_1, \phi_2) = -\bar{\phi}_1(\gamma^\mu\partial_\mu+M_1)\phi_1-\bar{\phi}_2(\gamma^\mu\partial_\mu+M_2)\phi_2. \tag{20}$$

We therefore conclude that not only bosons, but also fermions can be coupled to behave as fermions having different masses and may exhibit properties similar to those of the K-mesons.

3. Neutrinos

The above considerations encourage one to see if mass can be obtained by interacting neutrino fields. Such an idea was originally proposed by Heisenberg [3]). However, Touschek [4]) has shown that a theory of the Heisenberg type will not yield finite mass particles. We shall use some ideas developed by Touschek. Let the two neutrino fields have the following equations of motion

$$\gamma^\mu \partial_\mu \phi_1 = 0, \qquad \gamma^\mu \partial_\mu \phi_2 = 0. \tag{21}$$

One can conveniently identify ϕ_1 and ϕ_2 as left and right handed four component neutrino spinors, or specify their transformation properties

$$\phi'_1(x) = e^{i\gamma_5 \alpha} \phi_1(x), \qquad \phi'_2(x) = e^{-i\gamma_5 \alpha} \phi_2(x). \tag{22}$$

The free field Lagrangian density

$$\mathscr{L} = -\bar{\phi}_1 \gamma^\mu \partial_\mu \phi_1 - \bar{\phi}_2 \gamma^\mu \partial_\mu \phi_2 \tag{23}$$

is seen to be invariant under the transformations (22). We note that a derivative term like $\bar{\phi}_2 \gamma^\mu \partial_\mu \phi_1$ is not invariant, but the scalar combination $\bar{\phi}_1(x)\phi_2(x)$ is. Thus, the following Lagrangian density for the interacting fields is a possible choice:

$$\mathscr{L} = -\bar{\phi}_1 \gamma^\mu \partial_\mu \phi_1 - \bar{\phi}_2 \gamma^\mu \partial_\mu \phi_2 - g(\bar{\phi}_2 \phi_1 + \bar{\phi}_1 \phi_2).$$

The field equations are now

$$\gamma^\mu \partial_\mu \phi_1 = g\phi_2, \qquad \gamma^\mu \partial_\mu \phi_2 = g\phi_1. \tag{24}$$

In complete analogy to what has been done before, the two new field functions are

$$\psi_1 = \frac{1}{\sqrt{2}}(\phi_1 + \phi_2), \qquad \psi_2 = \frac{1}{\sqrt{2}}(\phi_1 - \phi_2),$$

obeying the field equations

$$(\gamma^\mu \partial_\mu + g)\psi_1 = 0, \qquad (\gamma^\mu \partial_\mu - g)\psi_2 = 0.$$

The transformed Lagrangian density is

$$\mathscr{L}(\psi_1, \psi_2) = -\bar{\psi}_1(\gamma^\mu \partial_\mu + g)\psi_1 - \bar{\psi}_2(\gamma^\mu \partial_\mu - g)\psi_2.$$

Neither the transformed Lagrangian nor the new field equations are any longer invariant under γ_5 transformations and therefore the ψ can be representative of massive particles. It would appear that ψ_2 corresponds to a particle of negative mass. This is not a genuine difficulty. For example, one can write

$$(\gamma^\mu \partial_\mu + g)(\gamma^5 \psi_2) = 0,$$

which gives the standard Dirac form and perhaps represents a particle of opposite chilarity.

In concluding we wish to emphasise that there should be a complete "lapse of memory" of the new particles so that they cannot retransform to the old interacting particles; for the new particles have to exhibit properties quite different from the particles from which they arise.

The idea that a coupling term like $g\phi_{K^+}\phi_{K^-}$ may lead to Schwinger's results for K-mesons was suggested to the author by Dr. P. Roman. The author's sincere thanks are due to him. Thanks are also due to Dr. S. P. Misra and Dr. T. Pradhan for many fruitful discussions. The author is highly indebted to Professor L. Rosenfeld for his encouragement from abroad.

References

1) S. P. Misra, Ind. J. Phys. **33** (1959) 520
2) J. Schwinger, Phys. Rev. **104** (1956) 1164
3) W. Heisenberg, Z. f. Naturf. **12a** (1957) 177
4) B. Touschek, Nuovo Cim. **13** (1959) 394

1.D.2:
1.E.1:
2.L

Nuclear Physics **28** (1961) 140—147; © *North-Holland Publishing Co., Amsterdam*
Not to be reproduced by photoprint or microfilm without written permission from the publisher

ENERGY LEVELS IN THE STABLE ISOTOPES OF TITANIUM

O. HANSEN

Institute for Theoretical Physics, University of Copenhagen, Denmark

Received 27 April 1961

Abstract: The excitation energies of a number of nuclear levels in the stable Ti-isotopes have been determined from inelastic proton and deuteron scattering and from (d, p) reactions. New levels were found in Ti^{47}, Ti^{49} and Ti^{50}. The (d, p) reaction Q-values and the nuclear level schemes derived from the measurements are compared to older data and are discussed briefly in terms of the quasi-particle model.

1. Experimental Procedure and Results

The five stable isotopes of titanium were bombarded with protons and deuterons accelerated to energies between 2.3 MeV and 4.2 MeV in the 4 MV electrostatic generator of this institute. The scattered particles or the protons from (d, p) reactions were detected in a heavy-particle spectrograph at an angle of 145° with respect to the beam [1]). The targets, with the exception of the abundant Ti^{48}, were prepared in the isotope separator of this institute by means of a sputtering technique [2]). The Ti^{48} targets were made by vacuum evaporation of TiO_2 enriched to 99.1 % in Ti^{48}. The target thicknesses varied from 10 $\mu g/cm^2$ to 30 $\mu g/cm^2$, and in all cases thin carbon foils were used as backings.

The heavy-particle spectrograph was calibrated with α-particles from Po^{210}, Po^{212} and Bi^{210}, using the $H\rho$-values of Briggs [3]). A check on the calibration curve and a measurement of the scattering angle were made by detecting protons and deuterons elastically scattered from a very thin target ($\approx$ 1 $\mu g/cm^2$) composed of a mixture of Al, Mn, Ag and W evaporated onto a thin carbon backing. The calibration of the spectrograph is believed to be correct to within 0.1 %.

The results from the (p, p') and the (d, p) experiments are given in table 1. The (d, p) data are listed under the residual nucleus. For each isotope, column 1 gives the excitation energies derived from inelastic proton scattering, column 2 lists the same quantity calculated from the (d, p) reactions and column 3 shows the corresponding Q-values. In order to calculate the excitation energies from the (d, p) data, we have to identify one of the observed proton groups with a transition to a definite state in the residual nucleus. This is done, as illustrated on fig. 1, by identifying the level spacings of the proton spectrum obtained from (d, p) reactions with the spacings obtained from inelastic proton

TABLE 1

Measured excitation energies and Q-values in the Titanium isotopes

Ti^{46}	Ti^{47}			Ti^{48}			Ti^{49}			Ti^{50}		
E (keV) (p, p′)	E (keV) (p, p′)	E (keV) (d, p)	Q (keV) (d, p)	E (keV) (p, p′)	E (keV) (d, p)	Q (keV) (d, p)	E (keV) (p, p′)	E (keV) (d, p)	Q (keV) (d, p)	E (keV) (p, p′)	E (keV) (d, p)	Q (keV) (d, p)
0	0	0	6666±12 [a])	0		9405±15 [b])	0	0	5913±12 [a])	0		8725±15 [b])
887±3	160±3	166±10	6500±12	981±4	960±25	8445±25	1308±5			1549±5	1549	7176±12 [a])
2005±8	1247±5	1257±10	5409±12	2293±8	2293	7112±12 [a])		1373±10	4540±12		2688±15	6037±12
	1441±5	1444±10	5222±12	2420±8	2426±15	6979±12	1538±5				4151±15	4574±12
	1547±5	1553±10	5113±12		3231±15	6174±12	1583±5	1578±10	4335±12		4178±15	4547±12
	1793±5	1797±10	4869±12		3337±15	6068±12	1618±5	1624±10	4289±12			
	1823±5	1826±10	4840±12					1716±10	4197±12			
	2162±8	2171±10	4495±12				1758±5	1755±10	4158±12			
	2258±8	2266±10	4400±12				2259±8	2262±10	3651±12			
	2295±8	2304±10	4362±12									
		2374±10	4292±12									
		2427±10	4239±12									
		2450±10	4216±12									

The values are listed under the residual nucleus. For each isotope, column 1 gives the excitation energies derived from inelastic proton scattering, column 2 shows the same quantity obtained from (d, p) experiments and column 3 gives the corresponding (d, p) Q-values.

[a]) This Q-value has been used for matching the (d, p) excitation energy scale to the (p, p′) excitation energies, as discussed in the text.

[b]) This Q-value has not been measured directly in the present experiment, but has been calculated from the observed Q-values and (p, p′) excitation energies.

scattering, where the intense peak from elastic scattering fixes the zero point of the excitation energy scale. The Q-value corresponding to the (d, p) proton group finally picked out for this matching of the energy scales is marked with an [a]) in the table. In the cases of Ti^{47}, Ti^{48} and Ti^{49}, the correspondence between the (d, p) spectra and the (p, p′) spectra is unique, whereas for Ti^{50} the assignment of the (d, p) groups is more tentative. A search for the ground state transition in the Ti^{49} (d, p) Ti^{50} reaction was performed with a

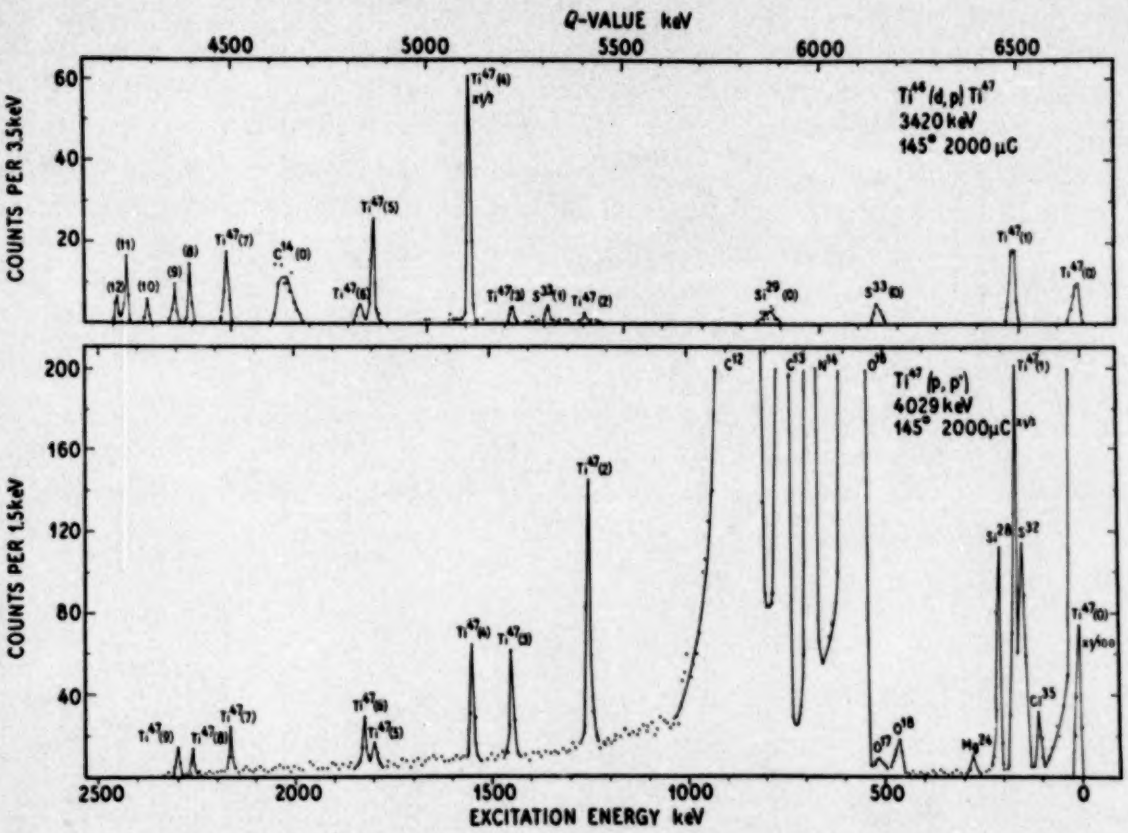

Fig. 1. Comparison between proton spectra obtained from inelastic scattering and from (d, p) reactions. Above: Proton spectrum from Ti^{46}(d, p)Ti^{47}. Below: Proton spectrum from Ti^{47}(p, p′). The energy scales of the two plots have been matched in such a way that the best possible correspondence between the two spectra is obtained.

negative result. However, this is not surprising, since the energy of the deuterons had to be reduced to 2.3 MeV in order to allow us an observation of the corresponding proton group in the spectrograph, employing the highest magnetic field that could be measured accurately (12.7 kG). For the same reason it was impossible to detect the ground-state transition in the Ti^{47}(d, p)Ti^{48} reaction. In these two cases, the Q-values belonging to the ground-state transitions have been calculated from the above mentioned identification of the proton groups.

In the (d, d′) experiments groups were found corresponding to the first excited states in Ti^{46}, Ti^{47} and Ti^{48}, whereas no groups from inelastic scattering

were detected from Ti^{49} and Ti^{50}. The excitation energies agreed in all cases with those obtained from the proton scattering.

The cross sections for inelastic proton scattering are strongly energy-dependent. An excitation function for the Ti^{48}(p, p′) transition to the first excited state was taken from 3.8 MeV to 4.3 MeV in steps of 10 keV. The cross section showed well defined resonances closely spaced over the whole range. Hence, it seems that compound nucleus formation plays a major part in the (p, p′) experiments. The excitation functions for the deuteron induced reactions show a much smoother variation with energy. Preliminary data from angular distribution measurements of the protons from Ti^{48}(d, p)Ti^{49} at 3.8 MeV show that the differential cross sections for the various transitions are smoothly decreasing functions of the angle [4]). Such angular distributions are neither characteristic of compound nucleus formation nor of direct interactions, but rather of a complex situation intermediate between the two. The (d, d′) excitation functions are observed to follow E2 Coulomb excitation rather closely, although the increase with energy is found to be somewhat too fast [5]). However, contributions from nuclear interactions may still be of importance, since the elastic scattering cross section deviates by as much as 25 % from the Rutherford cross section. Thus, a more detailed study of the reaction mechanisms involved is necessary if one wants to derive information on the spins, parities and transition probabilities of the nuclear states from the observed intensities.

2. Level Schemes

Fig. 2 shows the nuclear level schemes corresponding to the data in table 1. The excitation energies from the (p, p′) experiments have been used when

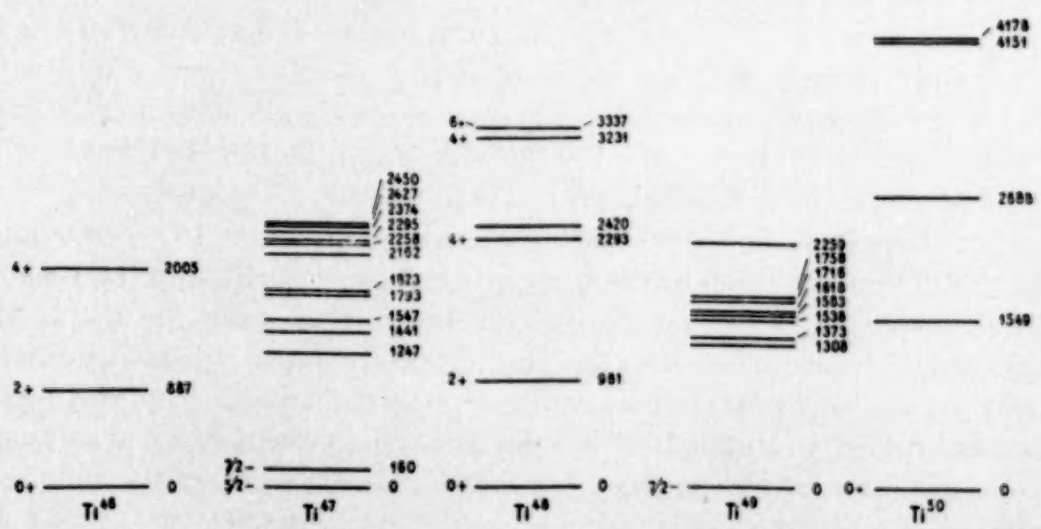

Fig. 2. Level schemes of the stable Ti isotopes. Excitation energies refer to the data contained in table 1. Spin and parity assignments are taken from the tables of Strominger, Hollander and Seaborg.

available. The spin and parity assignments indicated are taken from the tables of Strominger, Hollander and Seaborg [6]).

In Ti^{46} we only observe the two lowest excited states known [6]) from the decay of Sc^{46}. In Ti^{48} three levels are populated by inelastic proton scattering and two more are seen in the (d, p) reactions. With the exception of the state at 2420 keV, all the states are known from the Sc^{48} and V^{48} decays. The 2420 keV level has been suggested by Sinclair [7]) from (n, n'γ) experiments. Under the present conditions, the intensity of the (p, p') group for this level was from 2 to 8 times greater than the intensity of the group corresponding to the lower lying 4+ level at 2293 keV. Considerations of barrier penetrability therefore suggest a lower spin for the 2420 keV level, in agreement with a tentative 2+ assignment made on the basis of the γ-ray intensities observed from inelastic neutron scattering [7]). In Ti^{50} only the first excited state is seen in the (p, p') experiments. The cross section for scattering into this state is lower than the corresponding cross sections for Ti^{46} and Ti^{48} by about two orders of magnitude. This is due partly to the higher excitation energies in Ti^{50} and partly to a strong competition from (p, n) processes. These facts make the identification of the (d, p) groups for Ti^{50} somewhat difficult. The identification suggested gives a state at 2688 keV that fits well into the Ti^{49}(n, γ) data [8, 9]) and two states at 4178 keV and 4151 keV, respectively. The Ti^{49}(d, p)Ti^{50} Q-values in table 1 agree reasonably well with the Q-values obtained by Pieper [10]), but for the transition to the second excited state which, from the data of ref. [10]), should have an excitation energy of 3.0 MeV compared to the 2688 keV found here.

The level schemes for the odd-mass isotopes Ti^{47} and Ti^{49} can be compared to those obtained recently by Rietjens *et al.* [11]) from (d, p) reactions at deuteron energies of about 8 MeV. Inside the present range of excitation energies 9 levels in Ti^{47} and 5 levels in Ti^{49} were found in addition to those reported by Rietjens *et al.* The 0.55 MeV level in Ti^{47} suggested in ref. [11]) was not observed in the present experiment. In Ti^{49} the 1308 keV level and the 1538 keV level are not observed in the (d, p) experiments. These are the only cases where levels observed from inelastic proton scattering are not found from (d, p) reactions as well. As the proton group corresponding to a (d, p) transition to the 1308 keV level coincides with the position of the board peak from the C^{13}(d, p)C^{14} ground state transition on the plates in the spectrograph, a search at different scattering angles was performed, but with negative results. The (d, p) group from the transition to the 1538 keV level may be present in some exposures, but is too weak to be identified beyond doubt. All together the number of levels found in Ti^{47} and Ti^{49} inside the first 2.4 MeV in excitation energy is now comparable to the number of levels found in the same energy range in neighbouring nuclei as Ca^{45}, Mn^{55} and Co^{59} (refs. [12, 13, 14])).

In table 2 we have compared the ground state transition Q-values for the (d, p) reactions obtained in the present experiment with those derived from mass data [15]) and from thermal neutron capture [8, 9]). In all cases the agreement between the different sets of values is satisfactory; thus, the earlier discrepancies between the (d, p) work and the (n, γ) work do not exist any longer. In the case of Ti^{50} this agreement further supports the identification of the (d, p) proton groups discussed above.

TABLE 2

Comparison between ground-state transition (d, p) Q-values derived from different experiments

Nucleus	Ti^{47}	Ti^{48}	Ti^{49}	Ti^{50}
Present exp.	6666±12	9405±15	5913±12	8725±15
Mass data [15])	6660± 3	9394± 3	5922± 3	8713± 2
(n, γ) data [9])	6630±20	9380±30	5900±20	8710±30

All values are in keV and are listed under the residual nucleus in the (d, p) reaction. The errors are those given in the references.

3. Discussion

A striking feature of the results contained in tables 1 and 2 is the pronounced difference between the odd-mass and the even-mass isotopes. The level densities of the odd-mass nuclei are several times greater than those of the even-mass isotopes, and the ground-state transition Q-values for (d, p) reactions leading to an even-mass isotope are considerably higher than those leading to an odd-mass isotope.

In order to discuss these facts one has to take into account the existence of an energy gap between the ground state of an even nucleus and the first intrinsic state, which corresponds to the excitation of one pair of nucleons [16]). In this energy gap only collective excitations of the ground-state configuration occur. The gap can be understood in terms of a pairing correlation between the nucleons. The magnitude of the gap is equal to the neutron or proton pairing energy [17]).

Denoting the Q-value of the (d, p) reaction leading to the ground state of the even nucleus (Z, N) by $Q(Z, N)$ and the mass of this nucleus by $M(Z, N)$, we have

$$P_n(Z,N) = 2M(Z,N-1)-M(Z,N)-M(Z,N-2) = Q(Z,N)-Q(Z,N-1),$$

where $P_n(Z, N)$ is the neutron pairing energy of the nucleus (Z, N) [18]). From the Q-values of table 1 we find $P_n = 2839$ keV for Ti^{48} and $P_n = 2812$ keV for Ti^{50}. This corresponds to an energy gap in these nuclei of roughly 2.82 MeV.

The spectra of the even-mass isotopes appear to be quite similar to those of neighbouring even-mass isotopes. The first excited states in Ti^{46} and Ti^{48} are $2+$ states, and the reduced electric quadrupole transition probabilities are strongly enhanced over the single-particle values [19]), thus supporting a classification as one-phonon states. Dželepow and Peker [20]) give the spin and parity of the first excited state in Ti^{50} as $2+$ and, since the excitation energy is around 50 % of the energy gap, this level probably has also vibrational character; the higher excitation energy as compared to Ti^{46} and Ti^{48} then reflects the smaller deformability of the closed 28-neutron shell. As seen from table 3, the second

TABLE 3

Ratio between the excitation energies of the second and the first excited states

Nucleus	Ti^{46}	Ti^{48}	Ti^{50}
E_2/E_1	2.260	2.337	1.735

excited states in Ti^{46} and Ti^{48} have excitation energies ≈ 2.3 times the excitation energies of the first excited states, but still lower than the energy gap; the spins and parities are $4+$, so that these levels also fit into the surface vibrational scheme [21, 22]). In Ti^{50} the ratio E_2/E_1 is considerably lower than in the two other isotopes and the excitation energy of the second excited state is very close to the energy gap. Kisslinger and Sorensen [17]) suggest that this level corresponds to the lowest two-quasi-particle state. It should be remarked that a similar excitation spectrum is observed in Cr^{52} which also has 28 neutrons [6]).

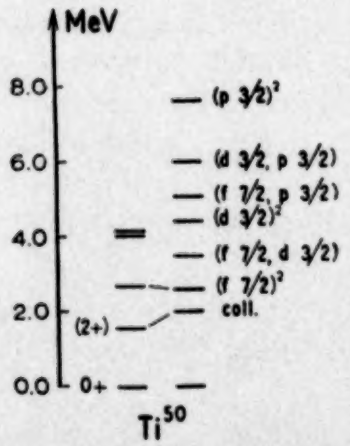

Fig. 3. Comparison between the theoretical and the experimental level schemes of Ti^{50}. The theoretical level scheme as calculated by Kisslinger and Sorensen is indicated to the right, the experimental level scheme to the left. The splitting of the degenerate states, caused by the long-range nuclear force, has not been calculated. For example the $(f_{\frac{7}{2}})^2$ state will generate levels with spins and parities $6+$, $4+$, $2+$ and $0+$; of these the $2+$ and $0+$ levels probably are spurious.

The third excited state in Ti^{48} at 2420 keV appears below the energy gap and as the spin and parity of this state is probably 2+ it would be suggestive to interpret the state as being a member of the collective two-phonon triplet, built on the ground state configuration [23]). This interpretation is, however, wholly tentative.

The energy spectrum of Ti^{50} has been calculated by Kisslinger and Sorensen [17]), using a Hamiltonian which includes a pairing force as well as a long range force. The theoretical spectrum is compared to the experimental spectrum in fig. 3. Taking the splitting of the degenerate quasi-particle states into account, it is seen that the theoretical level density is considerably higher than the experimental one. This might indicate that the calculated $d\frac{3}{2}$ state is placed too low in excitation energy. The fact that Rietjens *et al.* [11]) do not find any even-parity states in Ti^{49} or Ti^{47} inside the first 3.3 MeV in excitation energy (the range covered by their experiment) supports this view, as the d-states are the lowest even parity single-parity states.

The author wishes to thank Professor Niels Bohr for the excellent working conditions at his Institute. I am also grateful to Dr. C. K. Bockelman for many helpful discussions and to Mr. G. Sidenius for making the Ti separations. It is a pleasure to thank Mrs. Ruth Hansen for her accurate track counting.

References

1) B. Elbek, K. O. Nielsen and M. C. Olesen, Phys. Rev. **108** (1957) 406
2) B. Elbek, M. C. Olesen and O. Skilbreid, Nuclear Physics **19** (1960) 523
3) G. H Briggs, Revs. Mod. Phys. **26** (1954) 1
4) P. F. Dahl, private communication
5) B. Elbek and O. Hansen, to be published
6) D. Strominger, J. M. Hollander and G. T. Seaborg, Revs. Mod. Phys. **30** (1958) 585
7) R. M. Sinclair, Phys. Rev. **107** (1957) 1306
8) G. Manning, G. A. Bartholomew, P. J. Champion and J. W. Knowles, Bull. Amer. Phys. Soc. **2** (1957) 218
9) B. B. Kinsey and G. A. Bartholomew, Phys. Rev. **89** (1953) 375
10) G. F. Pieper, Phys. Rev. **88** (1952) 1299
11) L. H. Rietjens, O. M. Bilaniuk and M. H. Macfarlane, Phys. Rev. **120** (1960) 527
12) W. R. Cobb and D. B. Guthe, Phys. Rev. **107** (1957) 181
13) M. Mazari, A. Sperduto and W. W. Buechner, Phys. Rev. **108** (1957) 103
14) M. Mazari, A. Sperduto and W. W. Buechner, Phys. Rev. **107** (1957) 365
15) H. E. Duckworth, Revs. Mod. Phys. **29** (1957) 767
16) A. Bohr, B. R. Mottelson and D. Pines, Phys. Rev. **110** (1958) 936
17) L. S. Kisslinger and R. A. Sorensen, Mat. Fys. Medd. Dan. Vid. Selsk. **32**, No. 9 (1960)
18) V. B. Bahnot, W. H. Johnson, Jr. and A. O. Nier, Phys. Rev. **120** (1960) 235
19) G. M. Temmer and N. P. Heydenburg, Phys. Rev. **104** (1956) 967
20) B. S. Dželepow and L. K. Peker, Decay Schemes of Radioactive Nuclei (Academy of Sciences of the USSR Press, Moscow, 1958)
21) G. Scharff-Goldhaber and J. Weneser, Phys. Rev. **98** (1955) 212
22) L. Wilets and M. Jean, Phys. Rev. **102** (1956) 788
23) K. Alder, A. Bohr, T. Huus, B. Mottelson and A. Winther, Revs. Mod. Phys. **28** (1956) 432

1.E.1:
4.E

Nuclear Physisc **28** (1961) 148—159; © *North-Holland Publishing Co., Amsterdam*
Not to be reproduced by photoprint or microfilm without written permission from the publisher

ON THE DECAY OF I^{132}

H. G. DEVARE

Tata Institute of Fundamental Research, Bombay-5, India

Received 1 May 1961

Abstract: The beta ray spectrum from the decay of I^{132} has been investigated with a magnetic lens and intermediate image type spectrometers. A new beta group with an end point energy of 2920±40 keV landing on the first excited state of Xe^{132} has been detected. The gamma-ray spectrum has been studied with a scintillation spectrometer. The relative intensities of the gamma-rays have been estimated. A ground state transition has been detected from a level at 2630 keV which has been identified as a possible first excited octupole vibrational state. The summing gamma-ray spectrum is investigated with a well type scintillation crystal. Existence of new levels in Xe^{132} at ≈ 3100 keV, ≈ 3400 keV and ≈ 3550 keV is inferred.

1. Introduction

The β^--decay of I^{132} leading to the excited states of Xe^{132} has been investigated in detail by Finston and Bernstein [1]). Our results [2]) on the electron capture decay of Cs^{132} which also leads to excited states of Xe^{132} and the recent developments in the theoretical [3–7]) and experimental [8–10]) investigations of the levels of the near spherical medium-heavy nuclei indicated that a more careful and purposeful study of the radiations from I^{132} may reveal features which were unnoticed in the earlier work.

In this work, a level at 1320 keV has been found which may be, along with the well-known level at 1450 keV, a member of the second vibrational triplet band. A number of levels of higher energy have been found. The one at 2630 keV is perhaps the first member of the octupole vibrational type. In addition, evidence has been gathered to show that the parity of $_{53}I^{132}$ itself is perhaps odd.

2. Preparation of the Source

The source of I^{132} was the chemically separated tellurium fraction of the uranium fission product, supplied by the Radiochemical Centre, Amersham, England, in the form of sodium tellurite. This tellurium source contained Te^{132}, Te^{131}, Te^{129}, I^{132} and I^{131}. Since the half-lives of Te^{131m}, Te^{132} and Te^{129} are 30 h, 77 h and 33.5 days, respectively, the contributions of the impurities could be corrected for. In order to eliminate the contribution of I^{131} produced when Te^{131m} had decayed the original sodium tellurite was reduced to tellurium metal form by passing SO_2 in the hot 3*N* HCl medium. The metallic tellurium

was centrifuged out and washed with 6*N* HCl. The Te^{132}—I^{132} mixture was used as a source for all studies. The presence of Te^{132} did not interfere in the study of I^{132} as the maximum energy of beta-rays from Te^{132} is only about 200 keV and the highest energy gamma-ray has an energy of 230 keV. This point was checked by studying the gamma spectrum from a chemically separated I^{132} source with scintillation spectrometer. For the beta-ray spectrometer studies, a thin layer (< 500 $\mu g/cm^2$) was deposited on a thin mylar film (≈ 700 $\mu g/cm^2$). Tellurium metal in a glass tube served as a source for the study of gamma-rays.

3. Beta-ray Spectrometer Studies

The beta spectrum was studied in a lens type beta-ray spectrometer [11]) with a resolution of ≈ 2.2 %. The electrons were detected in a Geiger counter with a window thickness of ≈ 1 mg/cm². Apart from the K-conversion lines of the 521 keV, 670 keV and 773 KeV gamma-rays and the K and L conversion lines of the 230 keV gamma-ray, no conversion lines were well resolved above the β-continuum. The Fermi-plot of the beta spectrum is reproduced in fig. 1, which shows five groups into which the beta spectrum could be resolved. In the inset is given the Fermi-plot of the highest energy portion of the beta spectrum taken

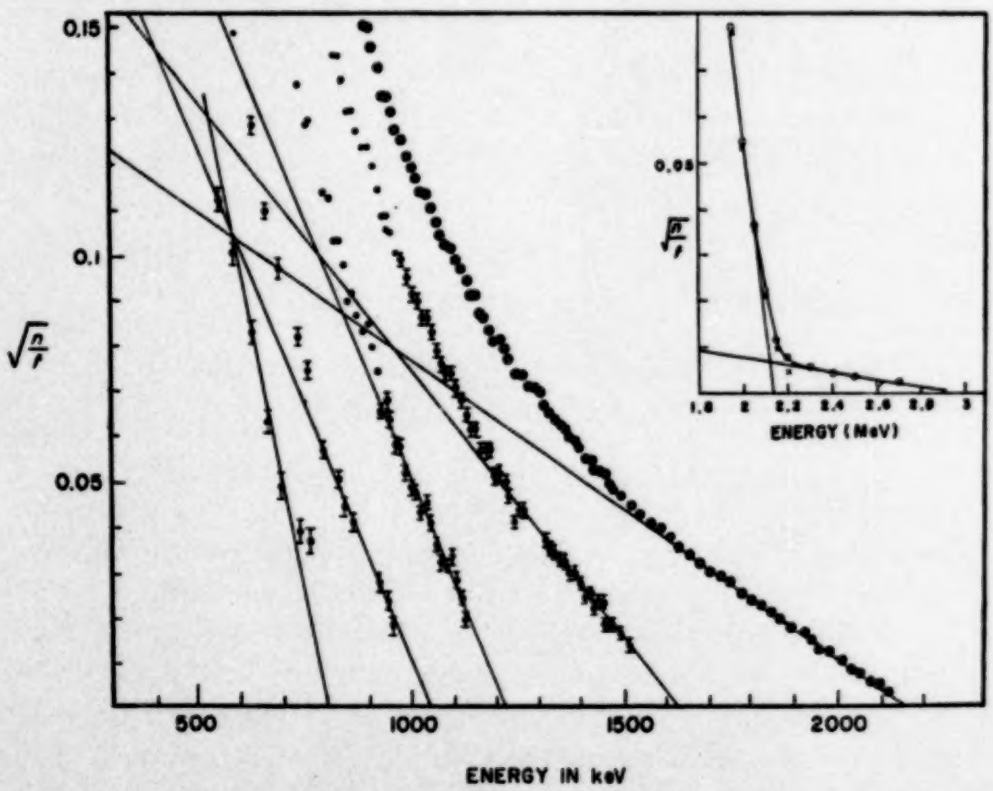

Fig. 1. Fermi plot of the β-spectrum of I^{132}. The inset shows the high energy part of the spectrum; points obtained after subtracting the contribution of the highest energy group are shown by crosses

in an intermediate image type Siegbahn-Slätis spectrometer having a high transmission of $\approx 8\,\%$ at a resolution of $\approx 5\,\%$ which greatly facilitated the detection of the very weak high energy β-group above background. The background itself was considerably reduced by using an anthracene crystal as detector and biasing off all the pulses corresponding to energies < 500 keV. The end point energy, relative intensity and the log ft value of each of the β groups are given in table 1. It may be pointed out that after subtracting the highest energy 2920 keV β-group, the Fermi plot gave an indication of another possible β-group with an end point energy of $\approx$ 2280 keV. However, this cannot be said to have been established beyond doubt as the number of points lying on the Fermi-plot between the energies 2280 keV and 2150 keV where the next β-group ends was too small.

In order to determine the energies of the gamma-rays with some accuracy the external photoelectron spectrum was studied in the lens spectrometer using ≈ 20 mg/cm^2 gold as radiator. Energies of 670 keV, 773 keV and 950 keV γ-rays could be determined from the K and L photoelectron lines. Higher energy γ-rays did not give any distinct photo-electron peaks and so it was not possible to measure their energy with any accuracy.

TABLE 1

Experimental results

End point energies (keV)	Relative intensity (%)	log ft
2920±40	0.03	10
2156±15	18	7.4
1609±25	21	6.7
1218±25	24	6.3
1037±40	15	6.1
802±40	21	5.7

4. Scintillation Spectrometer Studies

The gamma-rays from the decay of I^{132} were studied in a scintillation spectrometer with a NaI(Tl) crystal 7.6 cm × 7.6 cm in size with a well 3.8 cm deep and 0.6 cm in diameter mounted on a DuMont 6363 photomultiplier the integral assembly supplied by Harshaw and Co. The spectrum of the gamma-rays taken with a single channel analyser with the source at 12 cm (solid angle = 0.023) is reproduced in fig. 2. In addition to the strong peak at 230 keV due to Te^{132} well-resolved peaks occur at 670 keV, 773 keV, 950 keV, 1150 keV and a composite peak at about 1400 keV. Higher up in the spectrum, there is a rather broad peak at 1960 keV and humps extend up to 2600 keV. The spectrum was analysed with the help of the profiles of spectra of mono-energetic gamma-rays taken in identical geometry and comparable counting

rate. Thus the contributions of the individual gamma-rays starting from the highest energy could be peeled off. Taking into account the photo-efficiency of the NaI(Tl) crystal, the relative intensities of the gamma-rays were calculated. No correction was made for the contribution from the bremsstrahlung produced

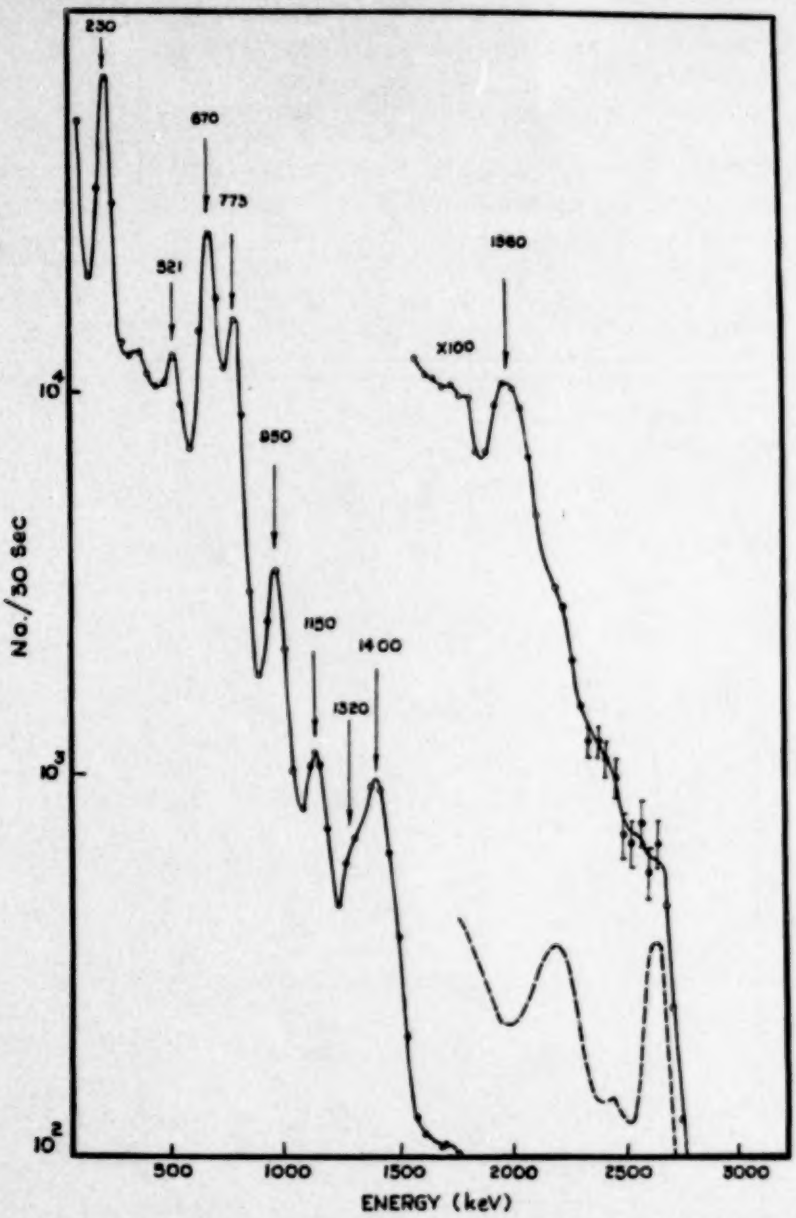

Fig. 2. Gamma spectrum of I^{132} taken with a 7.6 cm × 7.6 cm NaI(Tl) crystal at a distance of 12 cm. Channel width corresponds to ≈ 38 keV. The dashed line represents the background in the high energy region

in the lucite absorber used for stopping β-rays. This hardly affects the results as the bremsstrahlung contribution does not extend in the region above 2100 keV where the γ intensities are low. The relative intensities and the energies of the gamma rays of energy less than 670 keV were obtained from an expanded spectrum, not reproduced here.

TABLE 2

Gamma-ray energies and intensities

Energy of the γ-ray (keV)	Intensity	Energy of the γ-ray (keV)	Intensity
375±20	4.8±1	1500±20	1.80±0.6
460±20	2.2±0.5	1660±20	0.78±0.15
521±3	21 ±2.5	1770±20	1.1 ±0.2
645±20	30 ±7	1960±20	1.6 ±0.3
670±3	100	2050±20	1.3 ±0.3
773±3	86 ±8	2200±20	0.36±0.09
950±5	23 ±2.5	2350±20	0.13±0.04
1150±15	5.8±1.0	2420±20	0.15±0.05
1320±20	5.0±1.0	2540±20	0.09±0.03
1400±20	8.7±1.7	2630±20	0.04±0.02
1450±20	2.2±0.7		

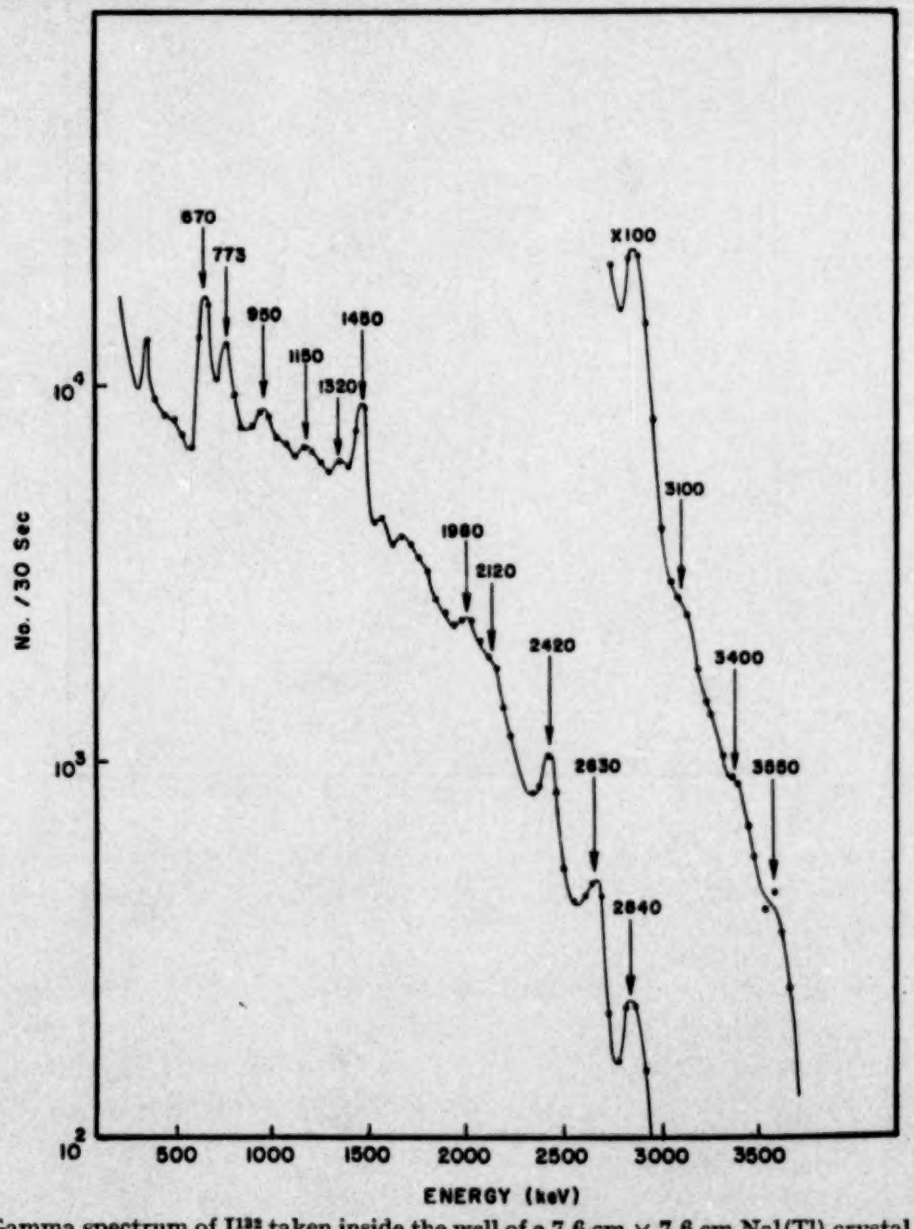

Fig. 3. Gamma spectrum of I^{132} taken inside the well of a 7.6 cm × 7.6 cm NaI(Tl) crystal. Channel width corresponds to ≈ 44 keV.

Of the gamma-rays listed in table 2, the energy values of the 521 keV and 670 keV ones are taken from the conversion-electron peaks and those of the 670 keV, 773 keV and 950 keV ones from the photo-electron peaks observed in the beta-ray spectrometer.

The spectrum of the gamma-rays from I^{132} was also studied with a very weak source placed inside the well of the NaI(Tl) crystal. The spectrum taken with a single channel analyser is reproduced in fig. 3. Clearly formed peaks can be seen at energies 670 keV, 773 keV, 950 keV, 1150 keV, 1320 keV, 1450 keV, 1980 keV, 2120 keV, 2420 keV, 2630 keV and 2840 keV. The spectrum extends up to about 3500 keV with humps occurring at $\approx$ 3100 keV, $\approx$ 3400 keV and $\approx$ 3550 keV. The external bremsstrahlung produced in the copper absorber used for stopping the 2156 keV beta-particles could sum up with the pulses of 670 keV and 773 keV gamma-rays to give pulses corresponding in energy to about 3550 keV. But we figure that the contribution of such triple summing should be much smaller than what is observed. It is well-known that the last few peaks in such spectra taken with the source inside the well of a large crystal correspond to the energy of the levels which are fed in the decay of the source. It is concluded then that there are levels in Xe^{132} at 1450 keV, 1980 keV, 2120 keV, 2420 keV, 2630 keV, 2840 keV and perhaps also at $\approx$3100 keV, $\approx$ 3400 keV and at $\approx$ 3550 keV.

5. Coincidence Studies

In order to fix the position of the gamma-rays in the decay scheme, some gamma-gamma and some beta-gamma coincidence studies were carried out.

TABLE 3
Results of the coincidence studies

Energy of γ-ray in the gate (keV)	Energy of the γ-rays found in coincidence (keV)	Endpoint energy of the β-groups found in coincidence (keV)
670	521, 645 [a]), 773, 950, 1150, 1400, 1960	2100
773	521, 670, 950, 1150, 1400	2150
950	460, 670, 773	1200
1150	670, 773	1000
1400 [b])	670, 773	
1960	670	1000

[a]) This was seen as a hump on the low energy side of the 670 keV line which is also present because of the inclusion of the Compton contribution of the 773 keV γ-ray in the 670 keV gate peak.
[b]) This includes part of the 1320 keV peak also.

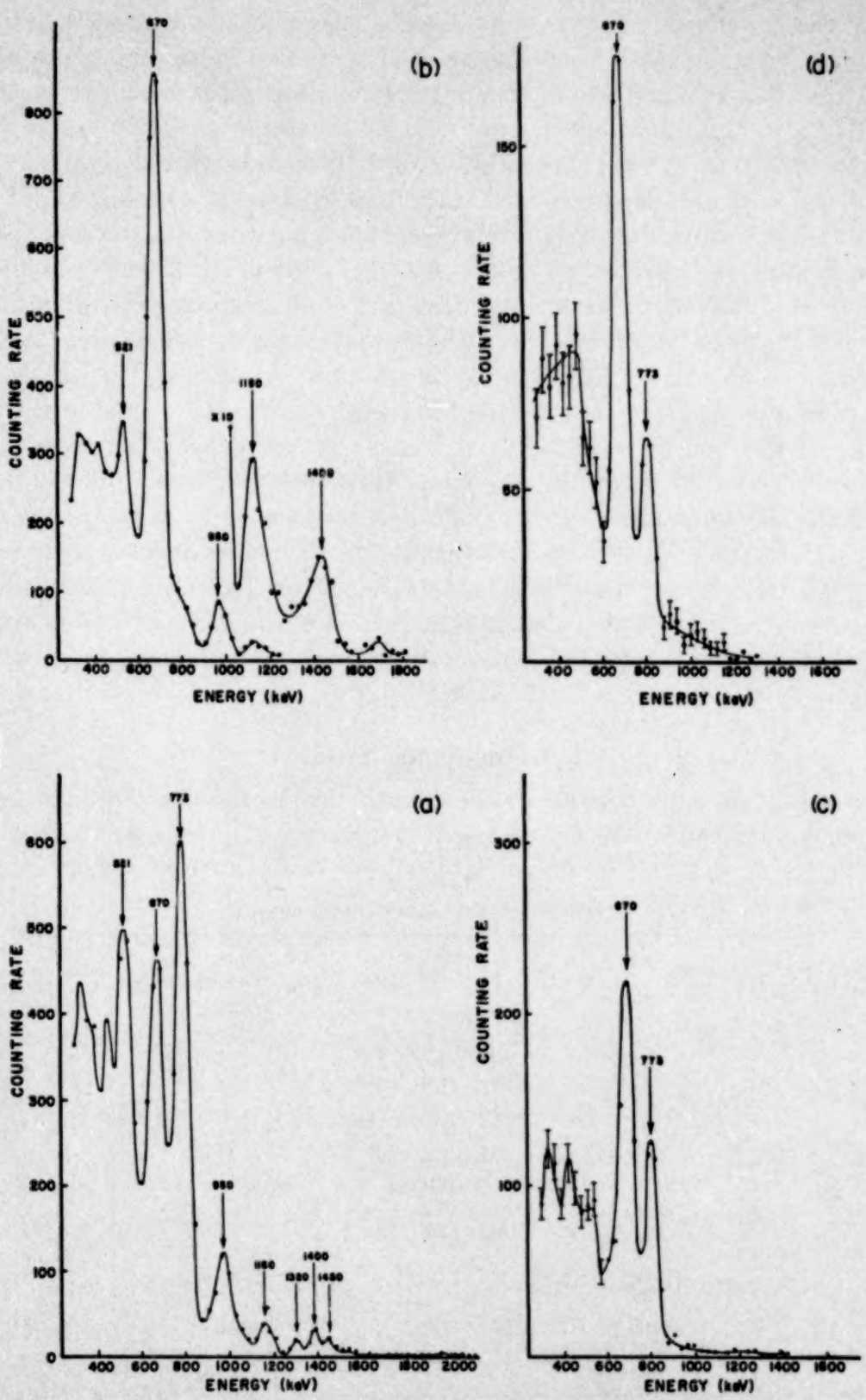

Fig. 4. Gamma spectrum in coincidence with (a) 670 keV gamma (b) 773 keV gamma (c) 950 keV gamma and (d) 1150 keV gamma, taken with 3.8 cm × 5 cm NaI(Tl) detectors at 5 cm from the source.

Two NaI(Tl) crystals, 3.8 cm in diameter and 5 cm high mounted on DuMont 6292 photomultipliers were used along with a coincidence unit with a resolving time of 0.1 μsec for studies of the gamma-gamma coincidences. For thd beta-gamma coincidence studies the NaI(Tl) crystal in one of the units was replaced by an anthracene crystal 3.1 cm in diameter, 1.2 cm high. For the first set of studies, single channel analysers were used. Later, gamma-gamma coincidences were studied with the help of a twenty-channel analyser. Some of the spectra of gamma-rays observed in coincidence, taken with the help of the multi-channel analyser, are reproduced in figs. 4a, 4b, 4c and 4d. The results of the coincidence studies are summarised in table 3.

6. Decay Scheme

Based on these measurements of the beta and the gamma spectra, and gamma-gamma and beta-gamma coincidences a decay scheme is proposed (fig. 5).

The analysis of the gamma spectra revealed several weak gamma-rays. The positions of these gamma-rays in the decay scheme have been inferred only from the energy sum rule and from intensity considerations. As the existence of these gamma-rays has not been conclusively proved by coincidence measurements, such gamma transitions have been indicated in the decay scheme by dashed lines. Shown by dotted lines are those levels and those transitions which arise definitely only in the decay of Cs^{132} to Xe^{132}.

Our decay scheme is similar to that of Finston and Bernstein [1]) except for the levels, proposed by us, at 1320 keV, 2100 keV and the levels above 2840 keV. The levels at 1450 keV, 1980 keV, 2400 keV, 2630 keV and 2840 keV are indicated both by the sum peaks observed with the source inside the well of the scintillation crystal and by the end-point energies of the beta groups. The coincidence measurements confirm the existence of these levels and their decay modes.

The level at 1320 keV, already suspected in the decay of $Cs^{132} \rightarrow Xe^{132}$ is proposed in order to account for the appearance of the 645 keV gamma-ray in coincidence with the 670 keV gamma-ray. The appearance of the 645 keV gamma-ray is not a compelling evidence because this gamma-ray could be coming from a transition from a level at 2100 keV to the 1450 keV level. From the number of coincidences observed between the 670 keV gamma-ray and 1320 keV gamma-ray, it was felt that the intensity of the 1320 keV gamma-ray was more than could be accounted for from its originating entirely in a transition from the 1980 keV state to the 670 keV state; secondly, the peak at 1320 keV shows up more prominently when the source is placed inside the well of the crystal, contrary to what should have happened if this gamma-ray originated entirely from the 1980 keV state. In order to be able to place the evidence for a level at 1320 keV beyond doubt, attempts were made to observe this gamma-

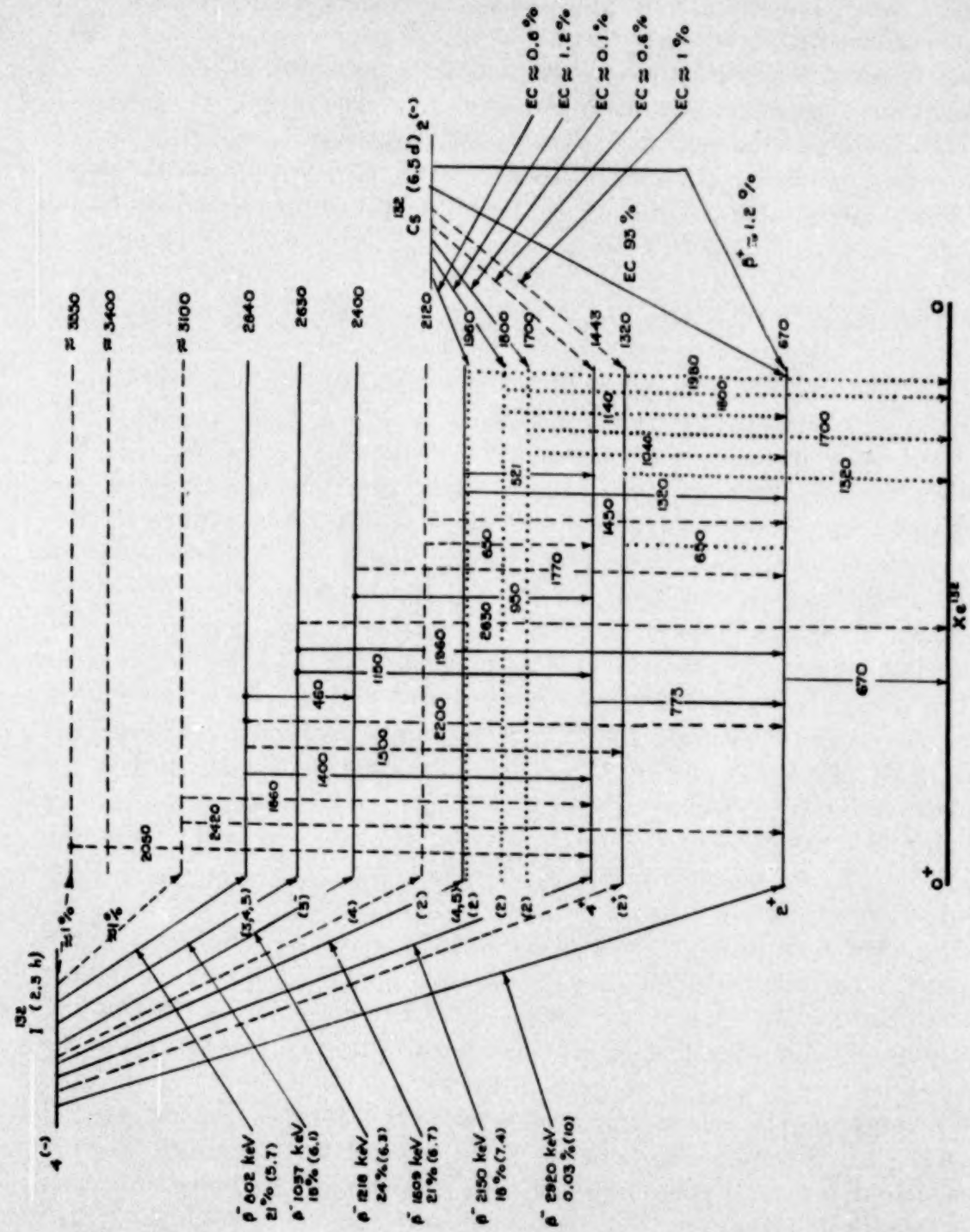

Fig. 5. Decay scheme of I^{132}. Levels and γ-transitions in Xe^{132} known from the decay of Cs^{132} are shown with dotted lines.

ray in coincidence with the betas of energy > 1650 keV in the hope that if there is any beta-group landing at this level then one should be able to detect the 1320 keV gamma-ray. Because of the poor statistics, it cannot be said beyond doubt that this gamma-ray has been observed.

The level at 1443 keV is well established from the 2150 keV beta group being followed by the 670 keV and 773 keV gamma-rays. The levels at 1700 keV and 1800 keV arise presumably only in the decay of Cs^{132} (ref. [2])). A level at 1980 keV is proposed, which must be different from the 1960 keV level found in the decay of Cs^{132} as the two must differ in spin. The occurrence of the beta-group of maximum energy 1609 keV and the coincidence of the 1320 keV gamma-ray with the 670 keV gamma-ray and that of the 521 keV gamma-ray with both 670 keV and 780 keV gamma-rays are the justifications for the proposal. A level at 2120 keV is suggested because a small bump is observed at the energy in the sum spectrum and to accommodate the high-intensity 650 keV gamma-ray which is also in coincidence with the 670 keV gamma-ray. It may be pointed out that this level is also suggested by Robinson *et al* [12]).

The level at 2400 keV is based on the occurrence of the beta group of 1218 keV maximum energy and that of the 950 keV gamma-ray in coincidence with both 670 keV and 773 keV gamma-rays but not in coincidence with any other high intensity gamma-rays. The levels at 2630 keV and 2840 keV are proposed on similar arguments.

For the higher levels at $\approx$ 3100 keV, $\approx$ 3400 keV and at $\approx$ 3550 keV, the only evidence we have are the humps in the sum spectrum and the fact that they can conveniently accommodate the low intensity probably gamma-rays 1660 keV, 2020 keV and 2420 keV.

7. Discussions

The decay scheme proposed in this work has some new features.

The parity of the odd-odd isotope I^{132} contrary to the usual assignment [13]), has been suggested here to be odd. It has been pointed out earlier that all the odd-odd isotopes in this region which have spin more than 1 are assigned odd parity with the exception of Cs^{134} (4^+) I^{132} (4^+) and Cs^{132} (2^+). We have provided [2]) circumstantial evidence for the odd parity of Cs [132].

Since the measured spin of I^{132} is 4, it was expected that the log *ft* of the beta group landing at 1443 keV state, would be either less than 6 or more than 10 depending on whether the spin of the 1443 keV state is 4 or 2. The experimentally found log *ft* value for this group (log *ft* 7.4) suggested that the beta decay could be first-forbidden, and the parity of I^{132} could be odd. If one assigns the spin and partiy 4^- to the ground state of I^{132} one would expect from the normal beta decay selection rules some, though small beta decay branching to the 670 keV level (2^+) also. Our search for such a beta group has

shown that a high energy group does exist. It seems to have the right end-point energy, but the log *ft* value calculated from the intensity, comes out to be ≈ 10, which is rather high for a unique first-forbidden, and rather low for a second-forbidden transition. Therefore, it is hard to come to a definite conclusion about the parity of the parent state from this observation. The beta-gamma directional correlation of the 2150 keV group beta and the following gamma-rays, 670 keV and 773 keV, was found to be isotropic within errors of measurements. This also cannot decide the question of the parity of the ground state of I^{132}.

The assignment of spin and parity 2^+ to the 670 keV state is definite, as this state is observed in the Coulomb excitation. If a state at 1320 keV does exist in Xe^{132} and take s part in the decay of I^{132} in the way we suspect, then the most probable spin assignment for this level is what we assigned in our study of Cs^{132}, that is 2^+. The log *ft* value of the beta group landing at the 1443 keV state and the results of the angular correlation measurements [14]) suggest a spin and parity 4^+ for this state. We have assigned spins and parity 4^+ or 5^+ and 4^+ for the states at 1980 keV and 2400 keV, respectively, consistent with the log *ft* values of the beta groups terminating at these levels, the relative intensities of the gamma-rays emanating from these levels and the results of the angular correlation measurements.

For the 2630 keV state, once the spin value of 3, on the basis of the log *ft* value of the beta branching and the angular correlation results [14]) is assigned, it is most convenient to assign to this level an odd parity and to suggest that this level is presumably the octupole vibrational level [15–18]) of the even-even nucleide Xe^{132}. With such an assignment, the Weisskopf estimate of the intensity ratio of the 2630 keV (E3) and 1960 keV (E1) gamma-rays is 6.3×10^{-6} but the observed value is 2.5×10^{-2}. So if the spin and parity assignment is correct, the transition to the ground state is speeded up by a factor of about 10^4.

The author wishes to thank Dr. S. Jha for suggesting the problem, Mr. R. M. Singru for his help in the early stages of the work, Dr. R. K. Gupta for many helpful suggestions and Mr. K. P. Gopinathan and Mr. R. T. Rane for the chemical separations.

Note added in proof: Recently R. L. Robinson, E. Eichler and N. R. Johnson have published a detailed account of their work on I^{132} (Phys. Rev. **122** (1961) 1863). Most of our conclusions seem to be in good agreement with their results.

References

1) H. L. Finston and W. Bernstein, Phys. Rev. **96** (1954) 71
2) S. Jha, R. K. Gupta, H. G. Devare and G. C. Pramila, to be published

3) G. Scharff-Goldhaber and J. Weneser, Phys. Rev. **98** (1955) 212
4) L. Wilets and M. Jean, Phys. Rev. **102** (1956) 788
5) A. S. Davydov and G. F. Filippov, Nuclear Physics **8** (1958) 237
6) T. Tamura and L. G. Komai, Phys. Rev. Lett. **3** (1959) 344
7) T. Tamura and T. Udagawa, Nuclear Physics **16** (1960) 460
8) D. M. van Patter, Nuclear Physics **14** (1959) 42
9) B. L. Cohen and R. E. Price, Phys. Rev. **118** (1960) 1582
10) P. H. Stelson and F. K. McGowan, Phys. Rev. **110** (1958) 489
11) T. D. Nainan, H. G. Devare and Ambuj Mukerji, Proc. Ind. Acad. Sc. **44** (1956) 111
12) R. L. Robinson, E. Eichler and N. R. Johnson, BAPS **5** (1960) 448
13) Nuclear Data Sheets, NRC 58-8-24, National Research Council, Washington D.C.
14) to be published
15) A. M. Lane and E. D. Pendelbury, Nuclear Physics **15** (1960) 39
16) B. L. Cohen and A. G. Rubin, Phys. Rev. **111** (1958) 1568
17) M. Crut and N. S. Wall, Phys. Rev. lett. **3** (1960) 520
18) C. Ythier, W. Schoo, B. L. Schram, H. L. Polak, R. K. Girgis, R. A. Ricci and R. van Lieshout, Physica **25** (1959) 694

7.C

Nuclear Physics **28** (1961) 160—171; © *North-Holland Publishing Co., Amsterdam*

Not to be reproduced by photoprint or microfilm without written permission from the publisher

HIGHER RESONANCES IN PION-NUCLEON REACTIONS AND THE ISOBAR MODEL

YUKIO TOMOZAWA †

Department of Physics, University College, London

Received 23 January 1961

Abstract: Higher resonances in the pion nucleon reaction are investigated using an isobar model. Introduction of the isobar approximation (Sect. 2) enables us to relate the scattering and one-pion production processes to pion-isobar scattering, which is calculated in the Chew-Low static approximation. If we neglect the crossing terms (except in the Born term), and if the pion-isobar interaction is sufficiently strong, we get resonances in pion-isobar scattering in the four states $(T, J) = (\frac{1}{2}, \frac{1}{2})$, $(\frac{3}{2}, \frac{1}{2})$, $(\frac{1}{2}, \frac{3}{2})$ and $(\frac{3}{2}, \frac{3}{2})$. The first two of these might give resonances in pion-nucleon reactions. Since our model requires positive parity states, they are $p_{\frac{1}{2}}$ for $T = \frac{1}{2}$ and $f_{\frac{3}{2}}$ for $T = \frac{3}{2}$. Comparison with experiments and discussion of Wong and Ross's approximation are presented.

1. Introduction

The following resonances have been observed in pion-nucleon reactions [2, 3]): for $T = \frac{3}{2}$ states at 0.2 GeV and 1.4 GeV pion energy, and for $T = \frac{1}{2}$ states at 0.6 GeV and 0.9 GeV. These are called the A, D, B and C resonances respectively. The first one, A, which has sharp peak of half width $\approx$ 60 MeV and height $\sigma_{res} \approx 200$ mb, is the in $(\frac{3}{2}, \frac{3}{2})$ state [3]) and is explained by the Chew-Low static model [4]). For the other resonances there have been several theoretical approaches [1, 5, 6]), but none as yet completely convincing.

Phenomenologically Sternheimer and Lindenbaum [5]) showed that, near 1 GeV incident pion energy, the isobar model gives a good explanation of the data on the one-pion production process which is the main part of the inelastic processes in this energy region. Their analysis suggests that it may be a reasonable approximation to treat the $(\frac{3}{2}, \frac{3}{2})$ resonance state as a quasi-stable particle (isobar) during the reaction and to assume the probability of isobar formation to be appreciable in this energy region. We make use of this idea to try to explain the details of the pion-nucleon reactions ††). We shall compare our results with experiment and also discuss the Wong-Ross approximation [1]), which used a similar idea, but made a different approximation.

† On leave of absence from the Tokyo University of Education, Tokyo, Japan. This work was done at Cambridge University, 1959—60. (Address of the author from December 1961: Instituto di Fisica, Università di Pisa, Italy)

†† This idea was used by Minami *et al.* [7]) for pion-nucleon scattering.

2. The Isobar Approximation

The isobar approximation implies the following assumptions: (i) the $(\frac{3}{2}, \frac{3}{2})$ resonance state A is treated as a quasi-particle N* which can be regarded as stable during the reaction time, and which decays into one nucleon and one pion in the final stage; (ii) only the intermediate states which include N* contribute appreciably to the reaction. Assumption (i) corresponds to the limiting case of vanishingly small half width for the $(\frac{3}{2}, \frac{3}{2})$ resonance. Actually, this resonance has a finite width of order 60 MeV which corresponds to a life-time $\tau \approx 10^{-23}$ sec. If the reaction goes on for a time $t_r = a \times 10^{-23}$ sec, neglect of the finite half width causes an error of order $t_r/\tau \approx a$. For pion energies in the 1–GeV region the value of a is probably † $a \lesssim \frac{1}{2}$.

We treat the much simplified limiting case of $\tau \to \infty$, which corresponds to the assumption of a stable isobar. Since we are concerned mainly with qualitative arguments about why the higher resonances occur, and about what states they are in, we shall not consider the question of the rigorous validity of this approximation. It should be noted, incidentally, that the assumptions (i) and (ii) do not exclude the existence of elastic processes, because of the shadow scattering.

Assumption (ii) means that in the one-nucleon subspace the states

$$\{n'\} \equiv \{\Psi_{n'}^{(\pm)}\} = \{\Psi_{\mathrm{N}}, \Psi_{\mathrm{N}^*}, \Psi_{\mathrm{N}^*k}^{(\pm)}, \ldots\}$$

approximately form a complete set which will be used when summing over intermediate states. Here Ψ_{N}, Ψ_{N^*}, Ψ_{N^*k}, ... represent eigenstates of the total Hamiltonian which correspond to a one-nucleon state ††, one-isobar state †††, (one isobar + one pion with momentum k) state [4]), ... etc., and the superscript (+) [(−)] means an outgoing [ingoing] state.

Suffixes of other quantum numbers are dropped for simplicity. The dotted part represents the other member of the complete set which will be neglected in this paper.

† The upper limit for a corresponds to $t_r = \hbar/\mu c^2$, where μ is the pion mass. For reactions at extremely high energies the lifetime of the produced isobar is $\tau = 10^{-23}/\sqrt{1-\beta^2}$ sec, where βc is the velocity of the isobar, while the reaction time is not increased with the energy. Thus the ratio t_r/τ is extremely small for extremely high energies. This fact gives the possibility [6]) of direct observation (in principle) of the isobar (or of any strongly unstable particle, e.g. pion-pion isobar etc.) The flight length of the isobar of 1μm (which is the limit of the visibility of the *trace*) corresponds to 4×10^8 GeV of isobar energy.

†† The one-nucleon state is kept for the formal arguments in this section, although in sect 3 it will be neglected according to the assumption (ii).

††† In the usual representation [4]) the one-isobar state would be expanded as $\Psi_{\mathrm{N}^*} = \Sigma_k \rho(k) \Psi_{\mathrm{N}k}^{(\pm)}$, where $|\rho(k)|^2$ represents essentially the resonance formula. We have neglected the other configurations of (one meson + one nucleon) states.

The S matrix for pion-nucleon scattering is

$$\langle k'|S|k\rangle = \langle \Psi^{(-)}_{Nk'}, \Psi^{(+)}_{Nk}\rangle = \sum_{n'} \langle \Psi^{(-)}_{Nk'}, \Psi^{(-)}_{n'}\rangle\langle \Psi^{(-)}_{n'}, \Psi^{(+)}_{Nk}\rangle$$
$$= \langle \Psi^{(-)}_{Nk'}, \Psi^{(-)}_{N^*}\rangle\langle \Psi_{N^*}, \Psi^{(+)}_{Nk'}\rangle + \sum_{p} \langle \Psi^{(-)}_{Nk'}, \Psi^{(-)}_{N^*p}\rangle\langle \Psi^{(-)}_{N^*p}, \Psi^{(+)}_{Nk}\rangle + \ldots, \quad (1)$$

where $\sum_{n'}$ means a sum over the approximate complete set $\{n'\}$ and $\langle \Psi^{(-)}_{Nk'}, \Psi_N\rangle = 0$ is used. We can transform the second term as follows:

$$\langle \Psi^{(-)}_{N^*p}, \Psi_{Nk}\rangle = \sum_{n'} \langle \Psi^{(-)}_{N^*p}, \Psi^{(+)}_{n'}\rangle\langle \Psi^{(+)}_{n'}, \Psi^{(+)}_{Nk}\rangle$$
$$= \sum_{q} \langle \Psi^{(-)}_{N^*p}, \Psi^{(+)}_{N^*q}\rangle\langle \Psi^{(+)}_{N^*q}, \Psi^{(+)}_{Nk}\rangle + \ldots, \quad (2)$$

where $\langle \Psi^{(-)}_{N^*p}, \Psi_{N^*}\rangle = 0$ is used. We confine ourselves to the one-meson approximation, so that

$$\langle k'|S|k\rangle \approx \langle \Psi^{(-)}_{Nk'}, \Psi_{N^*}\rangle\langle \Psi_{N^*}, \Psi^{(+)}_{Nk}\rangle + \sum_{p,q} g_1(k';p)g_1^*(k;q)\langle \Psi^{(-)}_{N^*p}, \Psi^{(+)}_{N^*q}\rangle + \ldots. \quad (3)$$

The first term contributes only to the $(\frac{3}{2}, \frac{3}{2})$ state and gives the $(\frac{3}{2}, \frac{3}{2})$ resonance. In the second term $\langle \Psi^{(-)}_{N^*p}, \Psi^{(+)}_{N^*q}\rangle$ represents *pion-isobar scattering*. The function $g_1(k';p)$ is an overlap integral:

$$g_1(k';p) = \langle \Psi^{(-)}_{Nk'}, \Psi^{(-)}_{N^*p}\rangle = \langle \Psi^{(+)}_{Nk'}, \Psi^{(+)}_{N^*p}\rangle, \quad (4)$$

and therefore non-zero only for states which have the same energy and quantum numbers. (The second equality in eqs. (4) comes from the unitary of the S matrix and the relation $\Psi^{(+)} = S\Psi^{(-)}$).

In a similar way one gets for the S matrix for one-pion production in the pion-nucleon reaction

$$\langle k'_1, k'_2|S|k\rangle = \langle \Psi^{(-)}_{Nk'_1k'_2}, \Psi^{(+)}_{Nk}\rangle$$
$$= \sum_{p} \langle \Psi^{(-)}_{Nk'_1k'_2}, \Psi^{(-)}_{N^*p}\rangle\langle \Psi^{(-)}_{N^*p}, \Psi^{(+)}_{Nk}\rangle + \ldots$$
$$\approx \sum_{p,q} g_2(k'_1, k'_2; p)g_1^*(k;p)\langle \Psi^{(-)}_{N^*p}, \Psi^{(+)}_{N^*q}\rangle, \quad (5)$$

where

$$g_2(k'_1, k'_2; p) = \langle \Psi^{(-)}_{Nk'_1k'_2}, \Psi^{(-)}_{N^*p}\rangle. \quad (6)$$

We have used the fact that according to assumption (i)

$$\langle \Psi^{(-)}_{Nk'_1k'_2}, \Psi_N\rangle = 0, \qquad \langle \Psi^{(-)}_{Nk'_1k'_2}, \Psi_{N^*}\rangle \approx 0.$$

Thus pion-nucleon reactions, up to one-pion production, are related to the *pion-isobar scattering* problem by eqs. (3) and (5). From the energy conserving character of the scattering matrix and the g functions, the summations in eqs. (3) and (5) are reduced to angular integrations only. If we want to take account of the finite width of the isobar, we might also take $|\mathbf{p}|$ and $|\mathbf{q}|$ integra-

tions over a region of the order of this width. The isobar approximation might mean that the isobar is treated as a stable particle for the scattering matrix $\langle \Psi^{(-)}_{N^*p}, \Psi^{(+)}_{N^*q} \rangle$, but the finite width of the isobar is allowed for in the g functions. However, we shall not go further into this effect.

3. Pion-Isobar Scattering

3.1. STATIC APPROXIMATION

We now calculate the pion-isobar scattering matrix. Since the mass of the isobar M_{N^*} ($\approx$ 1.24 GeV) is larger than the mass of the nucleon M_N ($= 0.94$ GeV), we expect to be able to use the static model of Chew Low for *pion-isobar scattering* on a higher energy region than was reasonable in the case of pion-nucleon scattering. For example, for 1 GeV pion kinetic energy in the lab system, the recoil momentum of a nucleon in the C.M.S. is 0.61 GeV/c whereas the recoil momentum of an isobar in the C.M.S. of the corresponding *pion-isobar* system is 0.41 GeV/c. The ratios $(p_N c/M_N)^2$ and $(p_{N^*} c/M_{N^*})^2$ are 0.42 and 0.11, respectively. For 1.5 GeV pion kinetic energy they are 0.68 and 0.24 respectively. Therefore it is not unreasonable to use the static approximation for *pion-isobar scattering* in this energy region.

Following the paper of Chew and Low [4]) we take as our Hamiltonian,

$$H = H_0 + H_I, \qquad H_0 = \sum_k a_k^\dagger a_k \omega_k, \qquad H_I = \sum_k (V_k^{(0)} a_k + V_k^{(0)\dagger} a_k^\dagger),$$
$$V_k^{(0)} = i f^{(0)} \frac{(\sigma \cdot \mathbf{k})}{\sqrt{2\omega_k}} \tau_k v(k), \tag{7}$$

where the notation is the same as in ref. [4]). The *pion-isobar scattering* state is given by

$$\Psi^{(\pm)}_{N^*q} = a_q^\dagger \Psi_{N^*} + \frac{1}{E_q - H \pm i\varepsilon} V_q^{(0)} \Psi_{N^*} \tag{8}$$

and the S matrix is

$$\langle p|S|q \rangle = \langle \Psi^{(-)}_{N^*p}, \Psi^{(+)}_{N^*q} \rangle = \delta_{pq} - 2\pi i \delta(E_p - E_q) T_q(p), \tag{9}$$

where

$$T_q(p) = \langle \Psi^{(-)}_{N^*p}, V_q^{(0)} \Psi_{N^*} \rangle$$
$$= -\sum_{n'} \left[\frac{T_p^\dagger(n') T_q(n')}{E_{n'} - \omega_p - i\varepsilon} + \frac{T_q^\dagger(n') T_p(n')}{E_{n'} + \omega_p} \right], \tag{10}$$

with

$$T_q(n') = \langle \Psi^{(-)}_{n'}, V_q^{(0)} \Psi_{N^*} \rangle. \tag{11}$$

We now neglect the contribution from the one-nucleon state †. This neglect might be called the *hard isobar approximation*, while taking account of this

† Cf. the preceding footnote.

term corresponds to the *soft isobar approximation* because this term corresponds to the breakdown of the isobar state †. We then calculate the contribution from the one-isobar state in the expansion by using the projection theorem for first-rank tensors [8]) (see Appendix 1) which gives

$$T_q(n' = \mathrm{N}^*) \equiv \langle \Psi_{\mathrm{N}^*}, V_q^{(0)} \Psi_{\mathrm{N}^*} \rangle = if \left(\frac{\mathbf{S}^{(\frac{3}{2})} \cdot \mathbf{q}}{\sqrt{2\omega_q}} \right) I_q^{(\frac{3}{2})} v(q). \tag{12}$$

Here $S_i^{(\frac{3}{2})}$ and $I_\alpha^{(\frac{3}{2})}$ are the spin matrix for $j = \frac{3}{2}$ and isobaric spin matrix for $t = \frac{3}{2}$ respectively. The abbreviated notation $I_q^{(\frac{3}{2})}$ means $I_\alpha^{(\frac{3}{2})}$ if a pion with momentum q is in an isobaric spin state α; the coefficient f is the renormalized *pion-isobar coupling constant*. Thus the T matrix for *pion-isobar scattering* has a completely analogous structure to the pion-nucleon scattering matrix and is simply derived from the latter by the replacement

$$\mathrm{N} \to \mathrm{N}^*, \qquad \sigma_i \to S_i^{(\frac{3}{2})}, \qquad \tau_\alpha \to I_\alpha^{(\frac{3}{2})}. \tag{13}$$

3.2. EFFECTIVE RANGE APPROXIMATION.

Making the replacement (13), we can use the results of the Chew-Low calculation [4]). Then for the effective range approximation, we get eventually

$$\begin{aligned} \frac{\lambda_\alpha p^3 v^2(p)}{\omega_p} \cot \delta_\alpha(p) &= 1 - \omega_p \gamma_\alpha, \\ \gamma_\alpha &= \frac{\lambda_\alpha}{\pi} \int_1^\infty \frac{\mathrm{d}\omega_q q^3 v^2(q)}{\omega_q^3}. \end{aligned} \tag{14}$$

Here $\delta_\alpha(p)$ is the *pion-isobar scattering* phase shift in the (T, J) state which is denoted by $\alpha = (2T, 2J)$, and (except in the Born term) we have dropped the crossing term, which may give only a small contribution because of its large energy denominator. The factors λ_α are the numbers which arise from the Born term and are calculated in Appendix 2. They are symmetric with respect to T and J, and are given by

$$\lambda_\alpha = \begin{pmatrix} \lambda_{11} \\ \lambda_{13} \\ \lambda_{15} \\ \lambda_{33} \\ \lambda_{35} \\ \lambda_{55} \end{pmatrix} = \tfrac{1}{3} \frac{f^2}{4\pi} \begin{pmatrix} \frac{25}{4} \\ -\frac{55}{8} \\ -\frac{15}{4} \\ -\frac{13}{2} \\ \frac{33}{8} \\ \frac{9}{4} \end{pmatrix} \tag{15}$$

Thus each positive λ_α gives a resonance, provided the *pion-isobar interaction* is sufficiently strong. The states with positive λ_α are $(\frac{1}{2}, \frac{1}{2})$, $(\frac{3}{2}, \frac{5}{2})$, $(\frac{5}{2}, \frac{3}{2})$ and $(\frac{5}{2}, \frac{5}{2})$. However, the last two of these do not contribute to the pion-nucleon

† R. F. Peierls (preprint) has recently discussed the latter case.

reaction. From $\lambda_{11} = \frac{25}{12} f^2/4\pi$, $\lambda_{35} = \frac{11}{8} f^2/4\pi$ and eq. (14), we estimate the ratio of the resonance energies for $(\frac{1}{2}, \frac{1}{2})$ and $(\frac{3}{2}, \frac{5}{2})$ states to be

$$\frac{\omega_{35}^{\text{res}}}{\omega_{11}^{\text{res}}} \approx \frac{50}{33} = 1.5. \tag{16}$$

This ratio is independent of the *pion-isobar coupling constant* f^2 and the cut-off function $v(q)$ in our approximation.

4. Pion Nucleon Resonances

Pion-nucleon scattering is related to *pion-isobar scattering* by eq. (3). The first term is non-zero only for the $(\frac{3}{2}, \frac{3}{2})$ state and gives the first resonance A as mentioned before. From the second term [provided the overlap integral $g_1(k; p)$ does not change rapidly as a function of energy near the energies of the *pion-isobar resonances* or at least is not small there], we obtain pion-nucleon resonances in the same state as *pion-isobar resonances* and at the corresponding energies. Unfortunately we cannot estimate the energy dependence of the g_1 $(k; p)$, and we shall therefore assume for them a smooth behaviour. The one-pion production matrix element (5) has a similar structure to the scattering matrix element.

Thus for a sufficiently strong *pion-isobar interaction*, our approximation gives resonances in both pion-nucleon scattering and one-pion production in the state $(\frac{1}{2}, \frac{1}{2})$ and $(\frac{3}{2}, \frac{5}{2})$. Since the *pion-isobar system* in a p wave state has positive parity, these states are $p_{\frac{1}{2}}$ and $f_{\frac{5}{2}}$ respectively.

The experimental values of the pion-nucleon resonance energies would correspond to *pion-isobar resonance* energies (in c.m.s.) of

$$\begin{aligned} \omega^{\text{res}}(0.6\ \text{GeV}) &= 0.26\ \text{GeV} \quad \text{(B)}, \\ \omega^{\text{res}}(0.9\ \text{GeV}) &= 0.40\ \text{GeV} \quad \text{(C)}, \\ \omega^{\text{res}}(1.4\ \text{GeV}) &= 0.58\ \text{GeV} \quad \text{(D)}, \end{aligned} \tag{17}$$

respectively. These give the ratios

$$\frac{\omega^{\text{res}}(1.4\ \text{GeV})}{\omega^{\text{res}}(0.9\ \text{GeV})} = 1.5, \qquad \frac{\omega^{\text{res}}(1.4\ \text{GeV})}{\omega^{\text{res}}(0.6\ \text{GeV})} = 2.2. \tag{18}$$

The first value would be in good agreement with the predicted value in (16). Although the approximations used are such that a quantitative estimate is not very reliable, one might hope that the ratio (16) will be insensitive to the approximation. However, we cannot really exclude the second case from this value.

Tentatively, we might suggest the assignments $p_{\frac{1}{2}}$ and $f_{\frac{5}{2}}$ for C and D resonances, respectively. The assignment $f_{\frac{5}{2}}$ for the D resonance might be

sufficient for the explanation of the resonance height. By unitarity at 1.4 GeV we get

$$\sigma_{\text{tot}}(J=\tfrac{5}{2}) \leqq 12\pi\lambda^2 \frac{\sigma_{\text{el}}}{\sigma_{\text{tot}}} = 26\ \text{mb} \times \frac{\sigma_{\text{el}}}{\sigma_{\text{tot}}}. \tag{19a}$$

If we take $\sigma_{\text{el}}/\sigma_{\text{tot}} \approx \frac{1}{2}$ the result is

$$\sigma_{\text{tot}}(J=\tfrac{5}{2}) \lesssim 13\ \text{mb}. \tag{19b}$$

Although the experimental value [2]) is σ_{tot} (1.4 GeV) $\approx$ 40 mb, there seems to exist a large non-resonant part in this experimental value. Thus these two values are not contradictory.

On the other hand, the assignment $p_{\frac{1}{2}}$ for $T=\frac{1}{2}$ resonance (C) does not give a sufficient peak because of the small J value. Also some analysis [9, 10]) of the experiments seems to suggest that the predominant contribution to C is probably $f_{\frac{1}{2}}$ (although this is not conclusive). We shall discuss this point in the next section.

5. Discussion

Wong and Ross [1]) used an approximation (called W–R hereafter) which seems to correspond to the *soft isobar approximation*, since in their model there is a breakdown of the isobar state due to its interaction with the extra pion; but the rigorous correspondence is not clear. They take into account the contribution of the $(\frac{3}{2}, \frac{3}{2})$ resonance in the two-meson approximation in the Chew-Low approach and calculate the probability that both pions are in the $(\frac{3}{2}, \frac{3}{2})$ states with the nucleon. This approximation gives the assignments $f_{\frac{1}{2}}$ for $T=\frac{1}{2}$, and $p_{\frac{3}{2}}$ for $T=\frac{3}{2}$ resonances, both at nearly 1 GeV.

The assignment $f_{\frac{1}{2}}$ for the C resonance seems to be quite promising for the explanation of several experiments [angular distribution and recoil nucleon polarization in photo-pion production [9]), angular distribution of elastic scattering [10]) and height of the resonance peak [2])]. However, this assignment is not by itself sufficient. At 0.9 GeV one has $\sigma_{\text{tot}} \approx 70$ mb for $T=\frac{1}{2}$, and

$$\frac{\sigma_{\text{tot}}}{4\pi\lambda^2} \approx 4.7 \leqq \sum_J (J+\tfrac{1}{2}) \left(\frac{\sigma_{\text{el}}}{\sigma_{\text{tot}}}\right)_J. \tag{20}$$

If we take the experimental value [10]) $\sigma_{\text{el}}/\sigma_{\text{tot}} = \frac{1}{2} \approx \frac{2}{3}$ as a mean value $\overline{(\sigma_{\text{el}}/\sigma_{\text{tot}})_J}$ for $(\sigma_{\text{el}}/\sigma_{\text{tot}})_J$, we need either at least a $J=\frac{7}{2}$ state contribution † or both parity states for some J under $\frac{5}{2}$, because

$$\sum_{J=\frac{1}{2},\frac{1}{2},1} (J+\tfrac{1}{2}) \left(\frac{\sigma_{\text{el}}}{\sigma_{\text{tot}}}\right)_J \lesssim 6 \cdot \tfrac{2}{3} = 4,$$

† This argument was also given by the Saclay group (private communication).

which is less than the experimental value $\sigma_{tot}/4\pi\lambda^2 = 4.7$. Analysis of the angular distributions of elastic scattering in the GeV energy region similarly shows the necessity of such an admixture of several angular momentum states [10]).

Considering the resonant part of the C resonance (whose peak is $\approx$ 40 mb) and the inequality

$$\frac{40\text{ mb}}{4\pi\lambda^2} = 2.7 \lesssim (J+\tfrac{1}{2})\,\frac{\sigma_{el}}{\sigma_{tot}}, \tag{21}$$

we see that a $J = \frac{5}{2}$ resonance is also insufficient to explain the peak unless $\sigma_{el}/\sigma_{tot} \gtrsim 0.9$ which is contradictory to experiment [11]).

Now, since the two approximations give different assignments for the resonance states, we may discuss them as if there were no interference between them in first approximation. A possible explanation for the size of the C resonance peak may then be the coincidence of the two resonances $f_{\frac{5}{2}}$ and $p_{\frac{3}{2}}$ which were derived by the W–R and our approximation respectively †.

The assignment for the D resonance from experimental results has not yet been made. The W–R approximation and the present give a $p_{\frac{3}{2}}$ and $f_{\frac{5}{2}}$ resonance (both $T = \frac{3}{2}$) respectively. This must be checked experimentally. One may point out that the present approximation becomes better for higher energies † (of course within the validity of static approximation). Moreover, this approximation gives a broader width for the $T = \frac{3}{2}$ resonance than for the $T = \frac{1}{2}$ resonance because the width is an increasing function of the resonance energy, while the W–R approximation gives nearly equal widths for both resonances [1]). In this respect the broad width of the D resonance might suggest the possibility of $f_{\frac{5}{2}}$ or the overlapping of the resonances given by the two approximations, i.e. $f_{\frac{5}{2}}$ and $p_{\frac{3}{2}}$.

In conclusion we pose certain questions for experimental analysis which might clarify the validity of the isobar approximations.

For the D resonance:

1) Does the experimental analysis of pion production indicate the validity of the isobar model at this energy (Sternheimer-Lindenbaum analysis)? At present the experimental results are not sufficiently accurate to clarify this point [5]).

2) Is the resonance an $f_{\frac{5}{2}}$ state or a $p_{\frac{3}{2}}$ state or an overlapping of both?

For the C resonance:

3) Is the C resonance a pure $f_{\frac{5}{2}}$ or a coincidence of $f_{\frac{5}{2}}$ and $p_{\frac{3}{2}}$ states or others? At present there is no positive evidence for the existence of a $p_{\frac{3}{2}}$ resonance contribution. However, we must be careful, since even if it exists, it is not large because of the small value of J.

† See the arguments of sect. 2.

For the $T = \frac{3}{2}$ bump at $\approx$ 1 GeV (ref. [2])):

4) Is it a resonance? If so, it may possibly be the $p_{\frac{3}{2}}$ state which is predicted by the W–R approximation.

Both approximations fail to give an explanation of the B resonance which may be a $d_{\frac{3}{2}}$ state with negative parity [9]) (though this is not yet established conclusively). For the explanation of this resonance it might be important to consider the pion-pion interaction [12–14]).

The author is very much indebted to Dr. E. J. Squires for helpful discussions. He wishes to thank Professors J. Hamilton, Y. Yamaguchi, T. H. R. Skyrme, Drs. D. Amati, B. Vitule, Marc Ross, E. Leader and the experimental group at Saclay for critical comments. He is also grateful to Cambridge University for hospitality in 1959—60 and the Department of Scientific and Industrial Research of the United Kingdom for a grant.

Appendix 1. Proof of Eq. (12)

Consider the system of one nucleon and pions. The total angular momentum operator $\mathbf{J}$ is

$$\mathbf{J} = \tfrac{1}{2}\boldsymbol{\sigma} + \mathbf{l}, \tag{A.1}$$

where $\mathbf{l}$ is the angular momentum operator of the pions. Let us denote the eigenstate of total angular momentum J and z-component M as $|J, M\rangle$. We have the relation

$$\langle J, M|\boldsymbol{\sigma}|J, M'\rangle = C_{(J)}\langle J, M|\mathbf{J}|J, M'\rangle, \tag{A.2}$$

where $C_{(J)}$ is a real constant.

This can be proved [15]) by using the commutation relations between J_α and σ_α and the explicit representation of J_α. However, it is shown that this is just the result of the projection theorem for first-rank tensors †. This theorem tells us that for a first-rank tensor

$$\langle J, M|\mathbf{T}_1|J, M'\rangle = \frac{\langle J, M|\mathbf{J}|J, M'\rangle\langle J||(\mathbf{J}\cdot\mathbf{T}_1)||J\rangle}{J(J+1)}. \tag{A.3}$$

We can put $\mathbf{T}_1 \to \frac{1}{2}\boldsymbol{\sigma}$, since $\frac{1}{2}\boldsymbol{\sigma}$ satisfies the criterion for first-rank tensors [see the definition (5.5) of ref. [8]) and also the argument used there about the magnetic moment]. The reduced matrix element $\frac{1}{2}\langle J||\mathbf{J}\cdot\boldsymbol{\sigma}||J\rangle$ is real because $\mathbf{J}\cdot\boldsymbol{\sigma}$ is hermitic. This completes the proof of (A.2).

† For the content of the theorem and the definition of first-rank tensors, see M. E. Rose [8]). There is a mistake in the expression of the decomposition theorem of the first kind [eq. (5.27) in ref. [8])]. It should read $\delta_{jj'}\langle jm'|T_{1M}|jm\rangle = \langle j'm'|J_M(\mathbf{J}\cdot\mathbf{T}_1)|jm\rangle/j(j+1)$.

A similar theorem is valid for isobaric spin space:

$$\langle I, I_3|\boldsymbol{\tau}|I, I'_3\rangle = C_{(I)}\langle I, I_3|\mathbf{T}|I, I'_3\rangle, \tag{A.4}$$

where $\mathbf{T} = \frac{1}{2}\boldsymbol{\tau}+\mathbf{t}$, and $\mathbf{T}$ and $\mathbf{t}$ are the isobaric spin operators of the total system and the pions respectively. Eqs. (A.2) and (A.4) give the proof of eq. (12).

Appendix 2. Evaluation of λ_α

The parameter λ_α in (14) is evaluated by the following eigenvalue problem [15]):

$$-I_\beta I_{\beta'} S_m S_{m'}+I_{\beta'} I_\beta S_{m'} S_m = \sum_{\alpha=(11)}^{(55)} \lambda'_\alpha P_\alpha(\beta, m; \beta' m'), \qquad \lambda_\alpha = \tfrac{1}{3}\frac{f^2}{4\pi}\lambda'_\alpha, \tag{A.5}$$

where

$$P_\alpha(\beta m; \beta', m') = \langle \beta, m|P_\alpha|\beta' m'\rangle;$$

P_α is a projection operator for the state $\alpha = (2T, 2J)$, and β', m' and β, m are the isobaric spin and momentum indices of the initial and final pions [15]).

Let us start from the spin and angular momentum subspace. The total angular momentum is

$$\mathbf{J} = \mathbf{S}+\mathbf{l},$$

where $\mathbf{l}$ is the angular momentum operator of a pion with $l = 1$.
We have

$$\mathbf{J}^2 = S(S+1)+l(l+1)+2\mathbf{S}\cdot\mathbf{l} = \tfrac{23}{4}+2\mathbf{S}\cdot\mathbf{l}$$

and

$$\mathbf{J}^2 = J(J+1) = \begin{cases} \frac{35}{4} & \text{for } J = \frac{5}{2}, \\ \frac{15}{4} & \text{for } J = \frac{3}{2}, \\ \frac{3}{4} & \text{for } J = \frac{1}{2}. \end{cases}$$

Thus the projection operators P_{2J} are

$$\begin{aligned} P_1 &= \frac{(\frac{35}{4}-\mathbf{J}^2)(\frac{15}{4}-\mathbf{J}^2)}{(\frac{35}{4}-\frac{3}{4})(\frac{15}{4}-\frac{3}{4})} = -\tfrac{1}{4}-\tfrac{1}{12}(\mathbf{S}\cdot\mathbf{l})+\tfrac{1}{6}(\mathbf{S}\cdot\mathbf{l})^2, \\ P_3 &= \frac{(\frac{35}{4}-\mathbf{J}^2)(\mathbf{J}^2-\frac{3}{4})}{(\frac{35}{4}-\frac{15}{4})(\frac{15}{4}-\frac{3}{4})} = 1-\tfrac{4}{15}(\mathbf{S}\cdot\mathbf{l})-\tfrac{4}{15}(\mathbf{S}\cdot\mathbf{l})^2, \\ P_5 &= \frac{(\mathbf{J}^2-\frac{15}{4})(\mathbf{J}^2-\frac{3}{4})}{(\frac{35}{4}-\frac{15}{4})(\frac{35}{4}-\frac{3}{4})} = \tfrac{1}{4}+\tfrac{7}{20}(\mathbf{S}\cdot\mathbf{l})+\tfrac{1}{10}(\mathbf{S}\cdot\mathbf{l})^2. \end{aligned} \tag{A.6}$$

Now, the matrix element of $\mathbf{l}$ is given by [15])

$$\langle m|l_j|m'\rangle = i\varepsilon_{mjm'}. \tag{A.7}$$

We also have the relations

$$S_m S_{m'} - S_{m'} S_m = i\varepsilon_{mm'j} S_j, \qquad \varepsilon_{mm'j}\varepsilon_{jkk'} = \delta_{mk}\delta_{m'k'} - \delta_{mk'}\delta_{m'k}. \tag{A.8}$$

From these we can prove the following equations:

$$S_{m'} S_m = \langle m|\mathbf{S}^2 - (\mathbf{S}\cdot\mathbf{1})^2|m'\rangle, \tag{A.9}$$

$$S_m S_{m'} = \langle m|\mathbf{S}^2 - (\mathbf{S}\cdot\mathbf{1}) - (\mathbf{S}\cdot\mathbf{1})^2|m'\rangle \tag{A.10}$$

Eqs. (A.8), (A.9) and (A.10) are valid for any angular momentum operator **S**. We prove this in the following way (using eqs. (A.7) and (A.8)):

$$\begin{aligned}\langle m|(\mathbf{S}\cdot\mathbf{1})^2|m'\rangle &= -\varepsilon_{mjm''}\varepsilon_{m''km'} S_j S_k = -(\delta_{mk}\delta_{jm'} - \delta_{mm'}\delta_{jk}) S_j S_k \\ &= -S_{m'} S_m + \delta_{mm'}\mathbf{S}^2.\end{aligned}$$

This gives eq. (A.9). Eq. (A.10) is obtained as follows:

$$\begin{aligned}S_m S_{m'} &= S_{m'} S_m + i\varepsilon_{mm'j} S_j = S_{m'} S_m - \langle m|\mathbf{S}\cdot\mathbf{1}|m'\rangle \\ &= \langle m|\mathbf{S}^2 - (\mathbf{S}\cdot\mathbf{1}) - (\mathbf{S}\cdot\mathbf{1})^2|m'\rangle.\end{aligned}$$

We finally consider the case of spin $\frac{3}{2}$ and $\mathbf{S}^2 = \frac{15}{4}$. From eqs. (A.6), (A.9) and (A.10) we have

$$\begin{aligned}S_m S_{m'} &= \tfrac{15}{4} P_3^{(J)}(m, m'), \\ S_{m'} S_m &= -\tfrac{5}{2} P_1^{(J)}(m, m') + \tfrac{11}{4} P_3^{(J)}(m, m') + \tfrac{3}{2} P_5^{(J)}(m, m'),\end{aligned}$$

with

$$P_\alpha^{(J)}(m, m') = \langle m|P_\alpha^{(J)}|m'\rangle.$$

For isobaric spin space we have similar relations. Thus we get

$$\begin{aligned}&-I_\beta I_{\beta'} S_m S_{m'} + I_{\beta'} I_\beta S_{m'} S_m \\ &= \langle \beta, m| -(\tfrac{15}{4})^2 P_3^{(T)} P_3^{(J)} + (-\tfrac{5}{2} P_1^{(T)} + \tfrac{11}{4} P_3^{(T)} + \tfrac{3}{2} P_5^{(T)}) \\ &\qquad (-\tfrac{5}{2} P_1^{(J)} + \tfrac{11}{4} P_3^{(J)} + \tfrac{3}{2} P_5^{(J)})|\beta', m'\rangle \qquad \text{(A.11)} \\ &= \langle \beta l m|\tfrac{25}{4} P_{11} - \tfrac{55}{8}(P_{13} + P_{31}) - \tfrac{15}{4}(P_{15} + P_{51}) \\ &\qquad -\tfrac{15}{2} P_{33} + \tfrac{33}{8}(P_{35} + P_{53}) + \tfrac{9}{4} P_{55}|\beta', m'\rangle,\end{aligned}$$

where (T) and (J) refer to isobaric and angular momentum subspace. Use of eqs. (A.5) and (A.11) gives λ_α (eq. (15) in the text).

Note added in proof: The possibility that the C resonance might be a mixture of $f_{\frac{5}{2}}$ and $p_{\frac{1}{2}}$ states was discussed by K. Itabashi *et al.* [14]).

References

1) W. N. Wong and Marc Ross, Phys. Rev. Lett. **3** (1959) 398
2) H. C. Burrowes, D. O. Caldwell, D. H. Frisch, D. A. Hill, D. M. Ritson, R. A. Schluter and M. A. Wahlig, Phys. Rev. Lett. **2** (1959) 119;
J. C. Brisson, J. Detoef, P. Falk-Vairant, L. van Rossum, G. Valladas and Luke C. L. Yuan, Phys. Rev. Lett. **3** (1959) 561;
T. J. Delvin, B. C. Baris, W. N. Hess, V. Perez-Mendez and J. Solomon, Phys. Rev. Lett. **4** (1960) 242
3) Y. Fujimoto and H. Miyazawa, Prog. Theo. Phys. **5** (1950) 1052;
K. A. Brueckner and K. M. Case, Phys. Rev. **83** (1951) 1141;
K. A. Bruckner, Phys. Rev. **86** (1952) 106;
M. Gell-Mann and K. M. Watson, Ann. Rev. Nuc. Sci. **4** (1954)
4) G. F. Chew and F. E. Low, Phys. Rev. **101** (1955) 1570;
G. C. Wick, Rev. Mod. Phys. **27** (1955) 339;
S. Fubini, Nuovo Cim. Supp **14**. (1959) 283
5) R. M. Sternheimer and S. J. Lindenbaum, Phys. Rev. **109** (1958) 1723;
V. Alles-Borelli, S. Bargia, E. Perez Ferreira and P. Waloschek, Nuovo Cim. **14** (1959) 211;
Report of Kiev Conference (1959);
R. F. Peierls, Phys. Rev. **118** (1960) 325
6) S. Bergia, F. Bonsignori and A. Stanghellini, Nuovo Cim. **16** (1960) 1073
7) S. Minami, T. Nakano, K. Nishijima, H. Okonogi and E. Yamada, Prog. Theor. Phys. **8** (1952) 531
8) M. E. Rose, Elementary theory of angular momentum (Wiley, New York, 1959) Ch. V, Sect. 20
9) R. F. Peierls, Phys. Rev. **118** (1960) 325; Phys. Rev. Lett. **1** (1958) 194;
R. Wilson, Phys. Rev. **110** (1958) 1212;
J. J. Sakurai, Phys. Rev. Lett. **1** (1958) 258;
P. C. Stein, Phys. Rev. Lett. **2** (1959) 473
10) A. R. Erwin, Jr., and J. K. Kopp, Phys. Rev. **109** (1958) 1364;
J. Cook and J. Hamilton, Private communication
11) R. R. Crittenden, J. H. Scandrett, W. D. Shephard, W. D. Walker and J. Ballam, Phys. Rev. Lett. **2** (1959) 121;
G. Valladas *et al.*, private communication
12) F. J. Dyson, Phys. Rev. **99** (1955) 1037;
G. Takeda, Phys. Rev. **100** (1955) 440;
V. G. Zinov and S. M. Korenchenko, JETP (Soviet Physics) **34** (1958) 210;
W. A. Perkins, J. C. Caris, R. W. Kenney, E. A. Knapp and V. Perez-Mandez, Phys. Rev. Lett. **3** (1959) 56;
L. S. Rodberg, Phys. Rev. Lett. **3** (1959) 58
13) V. I. Rus'bin, JETP (Soviet Physics) **37** (1960) 74;
F. Bonsignori and F. Selleri, Nuovo Cim. **15** (1960) 465;
I. Derado, Nuovo Cim. **15** (1960) 853;
F. Selleri, Nuovo Cim., **16** (1960) 775;
L. Landovitz and L. Marshall, Phys. Rev. Lett. **4** (1960) 476
14) K. Itabashi, M. Kato, K. Nakagawa and G. Takeda, Prog. Theor. Phys. **24** (1960) 529;
P. Carruthers, preprint;
C. J. Goebel and H. J. Schnitzer, Proc. of the 1960 Annual Conference on High Energy Physics at Rochester (Interscience Publishers, New York, 1960) p. 298;
J. Bowcock, W. N. Cottingham and D. Lurié, Phys. Rev. Lett. **5** (1960) 386
15) G. C. Wick, Rev. Mod. Phys. **27** (1955) 339;
S. Fubini, Nuovo Cim. Supp. **14** (1959) 283 (see especially the appendix)

1.D.2:
1.E.4:
3.B

Nuclear Physics **28** (1961) 172—176; © *North-Holland Publishing Co., Amsterdam*
Not to be reproduced by photoprint or microfilm without written permission from the publisher

DETERMINATION OF THE LIFETIME OF THE 283 keV EXCITED LEVEL OF Dy^{160}

J. BURDE and M. RAKAVY

Department of Physics, The Hebrew University, Jerusalem, Israel

Received 20 May 1961

Abstract: The lifetime of the 4+ level at 283 keV of Dy^{160} was measured by the technique of delayed coincidences between the beta spectrum of Tb^{160} and the appropriate K conversion line following the de-excitation of this state, using a double lens coincidence spectrometer. The mean lifetime of the 283 keV was found to be $\tau = (10.9 \pm 1.1) \times 10^{-11}$ sec. The measured ratio $B(E2;\ 4+ \rightarrow 2+)/B(E2;\ 2+ \rightarrow 0+) = 1.65 \pm 0.33$ agrees fairly well with the value 1.43 predicted by the collective model. An upper limit of $\tau < 2.5 \times 10^{-11}$ sec was also found for the 2^- level of Dy^{160} at 1264 keV using the same method.

1. Introduction

The transition probabilities of many of the first excited 2+ states of even strongly distorted nuclei have been determined by Coulomb excitation and life-time measurements. In view of the collective nature of these E2 transitions, it has been of great interest to compare these results with the predictions of the collective models. However, the transition probabilities from the 4+ second excited states (the second member of the rotational band) have been measured only in a few cases [1,2]). The strong coupling model predicts a unique ratio between the reduced transition probabilities from the second excited state to that of the first .Therefore, the determination of this ratio experimentally might serve as an additional check of the validity of the strong coupling model for various nuclei.

The level structure of Dy^{160} shows characteristics of rotational bands associated with strongly distorted nuclei. The lifetime of the first excited state has already been measured [3]). A measurement of the lifetime of the 4+ second excited state was therefore carried out in order to obtain an experimental value of the ratio of the reduced transition probabilities.

The delayed coincidence measurement between beta particles and conversion electron in a self comparison method [4]) seemed to be the most appropriate for the lifetime measurement of the 283 keV level, provided that the lifetime of the intermediate levels feeding it are sufficiently short in comparison.

Recently the decay scheme of Tb^{160} was reinvestigated by Ewan *et al.* [5]). They have determined the intensities and multipolarities of most recorded transitions. Their work shows the modes of decay populating the 283 keV level

of Dy^{160} from the decay Tb^{160}. Fig. 1 shows the decay scheme given by Ewan *et al* [5]). The intensities in percent per disintegration and multipolarities of the transitions populating the 283 keV level directly or indirectly are indicated.

The 283 keV level is excited in about half of the cases via the 965.8 keV and 1048.8 keV levels that were classified by Nathan [6]) as members of a gamma-vibrational band with $K = 2$. Ewan *et al.* have found quantitative agreement for the reduced E2 transition probability ratios for transitions from these

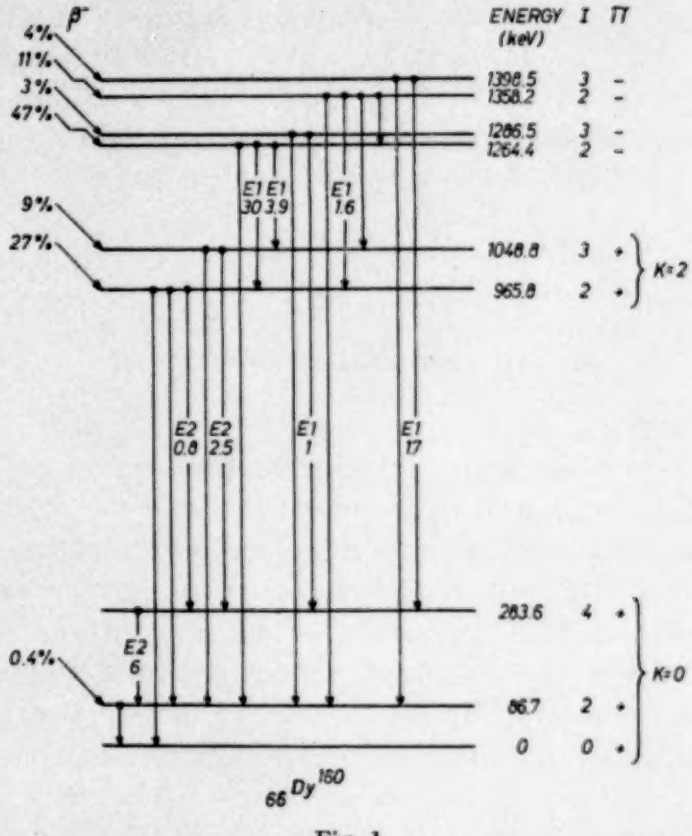

Fig. 1

levels, with the predictions of the unified model with band mixing and also with the prediction of the asymmetric rotor theory according to Davydov and Filippov [7]). The transition probabilities of these levels are expected to be enhanced in comparison with the single proton value and these levels should therefore have a lifetime shorter than 10^{-11} sec. It is interesting to note that the asymmetric rotor theory predicts a unique ratio between the transition probabilities from these levels and the transition probability of the first excited state. The mean lifetime thus computed is about 10^{-12} sec for the 965.8 keV and 1048.8 keV levels.

In the majority of the remaining cases the 283 keV level is fed by E1 transitions from the 1398 keV and the 1286 keV levels. These transitions are probably very fast in view of the large energy of disintegration and are probably not K

forbidden as reflected by the fact that no competing E1 transitions from these levels to the $K = 2$ band has been observed.

In about 20 % the 283 keV level is excited through the 1264 keV level. The latter level is de-excited by three E1 transitions, the high energy transition to the 2+ member of the ground rotational band being hindered by about a factor of 100 in comparison with the transition to the 2+ member of the $K = 2$ band. Thus, of all relevant intermediate levels is seemed less certain to assume that the lifetime of this level could be considered short in comparison with the lifetime of the 283 keV level. Therefore, it was decided to attempt a measurement of the lifetime of the 1264 keV level. It turned out in fact that the lifetime of the level is less than 2.5×10^{-11} sec. Taking into account that only one fifth of the 283 keV level is populated via the 1264 keV state, it was concluded that the uncertainty in the lifetime determination of the 283 keV level arising from the intermediate levels can be ignored in comparison with the experimental error.

2. Experimental Arrangement

The Tb^{160} source was prepared by irradiating Tb_2O_3 in the Saclay reactor for a period of two months at a flux of $2 \times 10^{13} n/cm^2 \cdot sec$. The irradiated oxide was dissolved in diluted hydrochloric acid and the solution was dried. Terbium chloride was dissolved in pyridine and electroplated on a $1 mg/cm^2$ nickel foil. The diameter of the source was about 5 mm.

The lifetime of the 283 keV level was determined by carrying out coincidence measurements between the beta spectrum and the K conversion line of the 197 keV transition using a double lens coincidence spectrometer [8]). The transmission and momentum resolution in both spectrometers were adjusted to about 5 %.

The focused electrons were detected by plastic scintillators coupled to 6810A R.C.A. photomultipliers. The outcoming pulses from the collector were fed into a delay to pulse-height converter similar to that described by Green and Bell [9]). The pulses from the 9th dynodes were introduced into linear amplifiers, and after discrimination against the pulses due to the noise of the photomultipliers, passed to a coincidence circuit having a resolving time of 10^{-7} sec. The full width of the resolution of the differential bias curve of the outcoming pulses from the scintillators at half maximum was about 40 % for electrons of 150 keV. These pulses were channelled with the aid of single channel analyzers to 30 % width of their peak voltage and introduced to a slow triple coincidence circuit having a resolving time of 2×10^{-6} sec, together with the outcoming pulses of the faster coincidence circuit.

The pulses from the linear amplifiers were fed also to a pile up rejector circuit.

The pulses from the time to amplitude converter were fed into an 80-channel pulse-height analyzer gated by the pulses from the fast-slow coincidence. The position of the centroid of the analyzed spectrum, when spectrometer 1 focused the beta spectrum at the lower energetic side of the conversion line and spectrometer 2 focused the conversion electrons, was compared with the position when the role of the spectrometers was inverted by an appropriate increase in energy in both channels [4]). The adjustments of the spectrometers before and after inversion were made in such a way that the average delay between the coincident pulses, due to the small change in energy of the focused electrons and corresponding change in pulse height, was the same. The assumption was made that this delay, to a good approximation, is inversely proportional to the energy of the electrons. The error thus introduced in the lifetime measurement due to the change in the transit time of the electrons in the spectrometers was less than 10^{-12} sec.

The shift between the centroids which corresponds to twice the mean lifetime of the excited state [10, 11]) was calibrated by introducing a 4×10^{-10} sec delay cable between one of the limiters and the 6BN6 coincidence circuit. To eliminate time dependent drifts, many sets of measurements of short duration were made. Every set consisted of 4 measurements of 10 to 15 min each: for two different lengths of cables self comparison measurements were carried out.

The experimental set up was checked by the same self comparison method using the 238 keV transition line of Bi^{212} (Thorium F line). These 148 keV conversion electrons are close in energy to the K conversion line of the 197 keV transition in Dy^{160}. The mean lifetime computed for this excited level of Bi^{212} after analyzing about 50 000 coincidences was $\tau = (-0.5\pm1.5)\times10^{-11}$ sec. The counting rate at the peak of the conversion line was about the same as in the case of the stronger source of Tb^{160}. However, in Pb^{212} source the difference in counting rates, when one spectrometer was set on the line and the second off, was much larger than in the Tb^{160} source. Even under these more stringent conditions, no shift in the centroids was detected as expected for this prompt transition.

3. Experimental Results and Comparison with Theory

The lifetime measurement of the 283 keV level was carried out with two sources of Tb^{160} differing considerably in strength. Using a source of 70 μCur we obtained a mean lifetime of $\tau = (10.5\pm1.4)\times10^{-11}$ sec after analyzing about 100 000 coincidences. Using a weaker source of 25 μCur and analyzing about 45 000 coincidences we obtained a mean lifetime of $\tau = (11.3\pm1.6)\times10^{-11}$ sec. The average value from these two results is $\tau = (10.9\pm1.1)\times10^{-11}$ sec.

The lifetime measurement of the 1264 keV excited state was measured in the same way by making coincidence measurements between the beta spectrum and the K conversion line of the 298 keV transition, using the stronger source of Tb^{160}.

The results obtained by analyzing 55 000 coincidences was $\tau = (0.5 \pm 2) \times 10^{-11}$ sec. The last result justified the assumption as mentioned earlier that the possible error in lifetime determination of the 283 keV state due to partial population via the 1264 keV level can be neglected.

The total conversion coefficients for the 86.7 keV and 196.9 keV transitions, as derived from the work of Ewan *et al.*, are 4.4 and 0.29 respectively, and the half life of the first excited state measured by McCowan and Sunyar [3]) is $T_{\frac{1}{2}} = 1.8 \times 10^{-9}$ sec; using these data and the result of the present measurement, the ratio of the reduced transition probabilities of the 196.9 keV to the 86.7 keV transition is given by

$$\frac{B(\mathrm{E2};\, 4+ \to 2+)}{B(\mathrm{E2};\, 2+ \to 0+)} = \frac{(T_{\frac{1}{2}(86.7)}/\ln 2)(1+\alpha_{86.7}^{\mathrm{tot}})}{\tau_{196.9}(1+\alpha_{196.9}^{\mathrm{tot}})} \left(\frac{86.7}{196.9}\right)^5 = 1.65 \pm 0.33.$$

The error of the ratio was increased to take into account the errors in lifetime determination of the first excited state and of the conversion coefficients. This result agrees fairly well within experimental error with the 1.43 value [12]) as predicted by the theory of the collective model.

We would like to thank Professor S. G. Cohen and Dr. S. Ofer for valuable discussions and interest.

References

1) G. Scharff-Goldhaber, D. E. Alburger, G. Harbottle and M. McKeown, Phys. Rev. **111** (1958) 913
2) S. Ofer, Phys. Rev. **115** (1959) 412
3) F. K. McCowan, Phys. Rev. **85** (1952) 142, 152;
A. W. Sunyar, Phys. Rev. **98** (1955) 653
4) R. E. Bell, R. L. Graham and H. E. Petch, Can. J. Phys. **30** (1952) 35
5) G. T. Ewan, R. L. Graham and J. S. Geiger, Nuclear Physics **22** (1961) 610
6) O. Nathan, Nuclear Physics **4** (1957) 125
7) A. S. Davydov and G. F. Filippov, Nuclear Physics **8** (1958) 237
8) T. R. Gerholm, Rev. Sci. Instr. **26** (1955) 1069
9) R. E. Green and R. E. Bell, Nuclear Inst. **3** (1958) 127
10) T. D. Newton, Phys. Rev. **78** (1950) 490
11) Z. Bay, Phys. Rev. **77** (1950) 419
12) A. Bohr and B. R. Mottelson, Mat. Fys. Medd. Dan. Vid. Selsk. **27**, No. 16 (1953)

NORTH-HOLLAND BOOKS

Just out

Elements of Hamiltonian Mechanics

by D. TER HAAR

University Reader in Theoretical Physics and Fellow of Magdalen College, Oxford

CONTENTS:

1. Newtonian mechanics
2. The Lagrangian equations of motion
3. Small vibrations
4. Dynamics of rigid bodies
5. The canonical equations of motion
6. Hamilton-Jacobi theory
7. Perturbation theory
8. Continuous systems

Bibliography - Problems

This book is based upon a course of lectures given to final year undergraduates and first year graduate students at Oxford University. The emphasis and the selection of subject matter differs in a number of points from those in existing modern text-books. The main differences are in the way constraints are introduced by freezing in of degrees of freedom, and in the discussion of classical perturbation theory.

6 x 9" 196 pp. Gld. 20.— (40s.)

NORTH-HOLLAND PUBLISHING COMPANY

P. O. BOX 103 - AMSTERDAM

Distributor for U.S.A.: Interscience Publishers, Inc. — New York

NORTH-HOLLAND BOOKS

QUANTUM MECHANICS

VOL. I

Just out

by ALBERT MESSIAH (Centre d'Etudes Nucléaires de Saclay)

translated from the French by G. M. Temmer (Florida State University, Tallahassee)

6×9" 520 pp. Gld. 50.- (100s.)

CONTENTS VOL. I. *The formalism and its interpretation.* Origins of the Quantum Theory. Matter waves and the Schrödinger equation. One dimensional quantum systems. Statistical interpretation of the wave-corpuscle duality and uncertainty relations. The development of the formalism of Wave Mechanics and its interpretation. Classical approximation and WKB method. The general formalism of Quantum Theory: A) Mathematical framework. B) Description of physical phenomena. — *Simple systems.* Solution of the Schrödinger equation by separation of variables. Central force field. Scattering problems. Central force field and the method of phase shifts. Coulomb interaction. Harmonic oscillator. — *Appendices:* «δ function» and distributions. Special functions and related formulae.

"... *the reviewer would like to recommend the book to students taking a beginner's course in quantum mechanics, to teachers for broadening the scope of such courses, and also to research workers in understanding the principles and methods of quantum mechanics and for acquiring the necessary knowledge for an understanding of the advanced parts of the field.*"

(PHYSICS TODAY on the original French Edition)

VOLUME II
in preparation

Ask your bookseller or

NORTH-HOLLAND PUBLISHING COMPANY

P.O. BOX 103—AMSTERDAM

Distributor for U.S.A.: Interscience Publishers, Inc. — New York